DATA DRIVEN HYPOTHESIS MODELLING OF *DEHALOCOCCOIDES MCCARTYI* : PREDICTED BIOLOGY AND BIOMARKERS OF STRESS IN TWO MIXED MICROBIAL COMMUNITIES

A Dissertation

Presented to the Faculty of the Graduate School

of Cornell University

in Partial Fulfillment of the Requirements for the Degree of

Doctor of Philosophy

by

Cresten Brant Mansfeldt

January 2013

DATA DRIVEN HYPOTHESIS MODELLING OF *DEHALOCOCCOIDES MCCARTYI* : PREDICTED BIOLOGY AND BIOMARKERS OF STRESS IN TWO MIXED MICROBIAL COMMUNITIES

Cresten Brant Mansfeldt, Ph. D.

Cornell University, 2013

Transcriptomic and proteomic expression levels were examined in two *Dehalococcoides mccartyi* (DMC)-containing mixed community cultures (D2 and the commercially available KB-1®). These reductively organodehalorespiring communities were subjected to a wide range of feeding conditions in regards to electron acceptor type, electron donor type, feeding rate, and additions of known stressors. The electron acceptors included chloroethenes, chlorophenols, and chlorobenzenes. D2- specific and genus-wide (pangenome) microarrays monitored the transcriptional response. Clustering of D2's transcriptome formed distinct groupings of genes responding either positively, negatively, or indifferently to increased chloroethene respiration rate. The transcripts responding positively to respiration potentially participate in DMC's incompletely described electron transport chain. Correlation analysis inferred putative relationships in the regulation of reductive dehalogenases (RDases) and small electron carriers such as glutaredoxin and thioredoxin. Differential expression comparisons across electron acceptor types also highlighted the potential role of the RDases DET1559 and *pceA* (DET0318) in chloro-aromatic respiration.

To comprehend more fully the transcriptomic data, the Reverse Engineering/Forward Simulation™ Bayesian network inference platform predicted a sparse set of confident gene-to-

gene and gene-to-condition relationships. Conditions included metabolite levels, phenotypic respiration rates, or the existence of stressors. Strong interactions were noted across the D2 and KB-1® mixed communities for a positive relationship between the S-Layer cell wall protein and a major RDase (*tceA* in D2 and *vcrA* in KB-1®) as well as a positive interaction between the hydrogenase *hup* and the formate dehydrogenase. Applying a network inference algorithm to the D2 and KB-1® communities' transcriptome behavior created a data-driven predictive tool. This tool allows for hypothesis generation for hundreds of genes in the inferred network. .

Combining the transcriptomic with proteomic data for stress conditions allowed a targeted detection of diagnostic biomarkers. Across the stressful conditions investigated for DMC (electron donor limitation as well as solvent, oxygen, and pH stress) DnaJ and HspR (DET1411-1412) appeared up-regulated. Due to their centrality in the cell and high background noise, they may prove to be difficult in situ biomarkers. Instead, the linking of a methylglyoxal synthase (DET0146) to solvent and the superoxide dismutase operon (DET0954-0965) to oxidative stress should be pursued as potential diagnostic field site indicators.

BIOGRAPHICAL SKETCH

Cresten grew up in the alternatingly frozen and burning state of Minnesota. He stayed transfixed for undergrad and attended the University of Minnesota where he graduated in 2007 with a Bachelors in Civil Engineering. Following the allure of the East Coast, Cresten ended up in the hills of upstate New York, mostly because of his crazy tour guides. Ever since, science and eccentricity have suited him quite well.

"If he was half as good as he thought he was,

He would be twice as good as he was."

- Phyllis Mansfeldt (a.k.a. Grandma)

About Frank Lloyd Wright.

In a museum.

Very loudly.

(…I dedicate this to my mom, for having me).

ACKNOWLEDGEMENTS:

The stoplight outside of my lab window has kept me company through most of the writing process of this thesis. The simple controlled rhythm, the red, the green, the little blinky hand, reminds me of the pace of my graduate career and all of those I have to thank for being here and assisting me along the way.

Green. Go. I am eternally in debt to those who launched me into this world. My parents serve as a great inspiration of how to approach being a human. They sacrificed substantially to ensure that my sister and I were able to lead a comfortable and productive life. Dad, the man of ink, of bass and steel, of electricity and fictional birds, thank you for teaching me how to humbly push against a world set to embarrass and cause harm. Mom, the woman in the yellow shirt, in the car and classroom, in the armor and fiery rage, thank you for teaching me compassion, rebellion, and individuality. My sister, Giliane, my comrade in-arms, my best and oldest friend, thank you for teaching me how to imagine and hope.

Blinking hand. Transition's ahead, plan. I was steered into the world of environmental engineering by numerous incredible teachers. Thank you, Mr. Enderton, for teaching the beauty surrounding mathematics. Newton sits on my shelf to this day. Thank you, Dr. Bill Arnold, for teaching such a great introduction to environmental engineering course that I end up as a dishwasher. Seriously. Thank you, Dr. Tim LaPara, for continuously challenging me and encouraging me to go to grad school. And finally, thank you Dr. Paige Novak. I would not be here without you.

Yellow. Let's be honest, speed up to make it through. I would have mentally crashed years ago were it not for the professional and personal relationships I have here at Cornell University. Often, they blur. To Dr. Ruth Richardson, thank you for taking on a young 21 year-

old. As an advisor, your mentorship and guidance have not only made me (hopefully) a better researcher, but also a better person. I can never thank you enough. To Dr. James Gossett and Dr. Stephen Zinder, thank you for always finding the time to assist me with my small to major research problems. The incredible expertise, talent, and inquisitives both of you display in all areas of life is truly stunning. To Dr. Lorenz Adrian, thank you for the incredible experience and showing me the German side of science. To Dr. Elizabeth Edwards, thank you for always providing input and generally being supportive of our lab. To Boris and Bruce at GNS Healthcare and Mike at EMSL, you guys have continuously saved me.

To the PSS Posse, Annie and Gretchen, to make the complex simple, thank you. You both provided an unmatched collaborator and second family. To Ben Logsdon for his help on the networks, running long distances, and finishing the scotch; to Brian Rahm for coining PSS, mad board game and DJ skills; Laura Hug, without your continued assistance, I would have gone mad; to Jenny Nelson for chlorobenzenes and softball; to Heather Fullerton for trading shop stories of DMC and snarky comments about bands; to Annie O. and the high pitched whining machine; to Garrett, the culturing king; to Ju Khuan and Sage; to all of you, thank you for your help and input on my research.

To my friends, my family away from home, to detail how much you've meant to me would fill far more pages than my thesis. So, in brief as this yellow is about to change, to Ben Heavner, my political ally, thank you for RoboCop. To Mike B, for the hike; Cloe for the walking tour; Sarah Short for always being right; Rick for always being wrong; Pete for the after work beers; Mark J. for the scotch; Howarth for being a pack of flying invisible space bears; Kassie for the Moon; Ross for Mars; Pinshane for space on the couch; Arend for space on the floor; all the micro men and women; the trivia team; the fancy poker crew; the GPSA; and all of

Stewart Little; thank you. Rendina, you are the only one I am not going to thank. You know why. To Punita, thank you for always having space on your couch, whether it was in Ithaca or England. To Madeline, I take back my previous statement: you get no thanks as well. And to those I forgot, I am writing this at four in the morning, so I thank you for your understanding.

The all red. What engineers don't often tell you is that for a brief moment all traffic stops. Everything halts to let the chaos that remains in the intersection to clear before traffic flows again. I have found that brief peace sitting next to you, Melina. I have no idea where the traffic of life will take me next when this light changes, but I will probably figure it out sitting next to you.

TABLE OF CONTENTS

LIST OF TABLES

LIST OF FIGURES

CHAPTER 1:

Introduction and Research Objectives

The underlying motivation for this thesis was to address whether cost-effective high-throughput surveys of an organism crucial to bioremediation applications, *Dehalococcoides mccartyi* (DMC), provide a route to prediction of cellular organization and response. Additionally, this study was concerned with determining if these data-driven hypotheses identified useful biomarkers of cellular stress that could be highlighted for future development and potential field applications. This chapter will connect the research objectives of this thesis investigation to the historical background and current state of the field of anaerobic reductive dehalogenation. As a paper based thesis, each of the subsequent data chapters presented (Chapters 2 – 4) may be considered a complete story unto itself. Each chapter will present the data and discussion required to tie the individual research objectives to the broader narrative existing in the current body of literature. The final chapter (Chapter 5) serves to synthesize the overarching results presented in previous chapters. Additionally, Chapter 5 highlights new hypotheses generated from the described research that could be further tested in future investigations.

1.A. History of Chlorinated Organics

In the United States, the production of mass quantities of chlorinated organics began in response to the outbreak of World War I (62). The supply chain from primarily German organic chemical manufacturers severed and the United States still required this class of organics for their fast evaporation, low flammability, and ability to dissolve most other organic molecules

(16). These compounds found their main applications in degreasing, dry-cleaning, and metal polishing but have moonlighted in a wide range of other applications from adhesives to pharmaceuticals (16). However, the application of chlorinated organics predated full knowledge of human health impacts while proper handling and disposal techniques were lacking. Later, the carcinogenic and bioaccumulative nature of these now commonly used industrial solvents was described (28). Additionally, these compounds began to be detected in the environment. In 1949, Lynne and McMahon documented the first chloroethene contamination of groundwater by noting trichloroethene (TCE) in well-water samples (41). Decades of use of this class of solvents for industrial purposes without stringent disposal requirements have led to chlorinated organics being some of the most prevalent compounds in contaminated properties. In a 2001 survey, TCE was estimated to be present in detectable quantities in 9-34% of all drinking water sources within the United States, underscoring the broad contamination by these chlorinated organics (67).

With the establishment of the Environmental Protection Agency (EPA) in the 1970s, along with the creation of the Clean Air and Water Acts, a push began to restore contaminated lands and minimize human exposure to hazardous compounds (16). Of the organic contaminants, the chlorinated ethene class was of specific concern due to their detection in the majority of contaminated groundwater sites and the toxicity of members of this group (71). Vinyl chloride (VC), dichloroethene (DCE), and trichloroethene (TCE) all to this day populate ASTDR's Priority List of Hazrdous Substances (4). In fact, VC is ranked number four and is the top organic contaminant on this list, just ahead of polychlorinated biphenyls. Therefore, as the field of hazardous waste remediation began, specific attention was paid to finding low cost and effective restorative techniques for prevalent chlorinated organics.

1.B. Discovery of Reductively Dehalogenating Organisms

In initial field studies, researchers observed that groundwaters contaminated with tetrachloroethene (PCE) would display natural attenuation by forming daughter products such as TCE and DCE (56). Mixed methanogenic cultures established from these sites dehalogenated chlorinated organics in addition to producing methane (7,8,22,53,68). Several of the cultures displayed complete dechlorination of PCE to the non-toxic ethene with near zero-order rate kinetics. This indicated that the reductive dechlorination seen was enzyme catalyzed and not mediated by transition metal cofactors alone (23,46,65). The reductive dechlorination noted was additionally linked to the growth of the culture (29). The first reported mixed community that displayed this ability for reducing PCE to ETH was founded from a municipal wastewater treatment plant's anaerobic digester biomass in Ithaca, NY. After several generations passed in this mixed culture, the stable Donna II (D2) mixed community was established. This culture is comprised of a community of organodehalorespirers, methanogens, and fermenters (58). The initial community was fed methanol as the electron donor but was switched to butyrate in D2 to provide a substrate that produces hydrogen (H_2) resulting directly from fermentation (H_2, formate, acetate and glucose all were found to be utilized as electron donors as well) (23). Sustained organochloride respiration of PCE to ETH using butyrate as the electron donor required the amendment of higher levels of cobalamin (vitamin B12) and suggested this vitamin as a possible enzyme cofactor (methanol utilizers produced vitamin B12). Organochloride respiration studies on the D2 and additional lab maintained mixed communities revealed a wide range of chlorinated electron acceptors utilized (including chlorinated -ethenes, -ethanes, -phenols, -benzenes, -dioxins, -dibenzodioxins, -dibenzofurans, -naphthalene, and -biphenyls (1,2,5,6,10,17, 21, 32,39)).

In order to further the study of this organochloride respiring culture, the research community then focused on purifying the organism responsible for reductive dechlorination. The dehalogenating organism from the D2 reactor was successfully isolated after subsequent transfers in media (45). After thorough characterization, this hydrogenotrophic, organochloride-respiring anaerobe was named *Dehalococcoides ethenogenes* strain 195 to denote the fact the culture was successfully dehalorespiring tetrachloroethene to the non-toxic ethene (note: this name was changed to *Dehalococcoides mcccartyi* strain 195 after acceptance to the international culture collection, IJSEM) (45). In addition to *Dehalococcoides mcccartyi* (DMC) 195, six other strains have been isolated and are maintained in purified cultures (CBDB1 (3), BAV1 (34), GT (63), VS (14,15), FL2 (25), and MB (11)). Mixed cultures support higher growth rates and cell densities than any of the various pure cultures.

1.C. Genome Functional Annotation

The genomes of DMC 195 (61), CBDB1 (35), BAV1 (47), GT (63), and VS (47) have been sequenced, annotated, and deposited into national repositories. From their annotations, initial insights into the biochemical organization of key processes in the cell were either discovered or hypothesized. The annotated genomes predicted that electrons from hydrogen enter the cell through a at least one of a number of hydrogenases, (Hup, Hym, Ech, Vhu, and Hyc) with Hup being the enzyme predicted to be the only periplamsic facing hydrogenase (52,61). The Hym and Ech hydrogenases are also predicted to be able to participate in reverse electron flow, potentially providing the cell with an alternative means of producing low energy potential electron carriers for biosynthetic purposes. In addition to the main set of hydrogenases, homologs for a formate dehydrogenase (Fdh) and NADH-ubiquinone oxidoreductase (Nuo) were

predicted to be present on the genome. However, the *fdh* gene contains an authentic point mutation that alters the active site, possibly explaining the cultures inability to oxidize formate. The encoded *nuo* operon lacks the NADH binding subunit, calling into question the final enzyme's *in vivo* electron donor (however, the genes encoding for the missing subunit are located elsewhere on the genome) (61).

The genome sequences for all DMC strains revealed that the combined culture collection contains 90 orthologous clusters of reductive dehalogenases (RDases), the enzymes responsible for the final step of reductive dechlorination through transfer of an electron to the chlorinated organic compound (66). Individual DMC strains' genomes are predicted to contain between 12 and 36 functional RDase catalytic units. For a single strain, multiple RDases are both transcribed (24,69) and translated (48,49,70), even when the cultures were fed a single electron acceptor. Of the complete set of reductive dehalogenases, four (PceA, TceA (42), VcrA (50), and CbrA (2)) have been biochemically characterized while two were additionally linked to specific dehalorespiration activity (MbrA (12) and BvcA (34)). CbrA primarily dehalogenates chlorinated benzenes while the remaining list of described RDases primarily dehalogenate chlorinated ethenes.

1.D. From Biomolecules to Biomarkers

One of the major goals in the DMC research community is finding diagnostic biomarkers of cellular state to monitor the organism's activity and response in field site settings. Research centers on molecules comprising the central dogma of molecular biology (i.e. DNA which is transcribed into RNA which, in turn, is translated into proteins) to connect time-sensitive DMC

specific responses to an environmental condition or rates. DMC's DNA has been used in field-site settings to assess the potential for *in situ* reductive dechlorination (27,40). However, DNA is limited to a presence/absence screen as the molecule is indicative of the potential and not activity of the cell. Specific RNA transcripts, such as genes encoding for RDases and hydrogenases, have been linked to respiration rate providing a potential biomarker for successful reductive dechlorination in the field (13,37,54,55). RNA provides the detection of the initial response of the organism but is difficult to sample without introducing degradation and is not directly representative of the function of the cell. A research push is now underway to uncover diagnostic protein biomarkers as these are more stable in the field and directly connected to the enzymatic process of interest (57). With the availability of high-throughput monitoring techniques, further biomarkers of cellular activity may be detected by monitoring the transcriptomic or proteomic response to defined conditions (38).

1.E. Insights Gained from Analyzing Omic Datasets

Moving from genome annotation to functional prediction and confirmation poses a challenge as we are currently unable to genetically manipulate DMC or overexpress novel enzymes such as RDases in model systems (51,59). The advancement of technologies related to trasncriptomic and proteomic analysis allowed the DMC research community to approach the challenge from a new angle. Initial microarray studies investigated the behavior of a pure strain DMC 195 species as the organism transitioned through growth stages (33). Further studies utilizing microarrays have elucidated the central carbon metabolism network (64) and the stress response of DMC as it is grown under nitrogen limiting conditions (38). Proteomic studies have focused on screening for detectable proteins (48,49,70), linking protein concentration to studied

mRNA biomarkers (49), investigating key metabolic processes (43), and detecting stress-specific peptides (38). Proteomic screens linked the quantification of key peptides to respiration, thus providing key biomarkers of cellular activity (70). The transcripts for the major RDase in DMC 195, TceA, and the Hup hydrogenase were shown to be positively correlated with the respiration rate of the cell (57). The same study also predicted the per enzyme kinetics of the *in vivo* TceA RDase. Marco-Urrea *et al.* (2011) extended proteomic surveys to discover and characterize the missing recitrate synthase, an enzyme central to pathway of amino acid biosynthesis. Combining proteomics with stable isotope mass spectroscopy led to an even more complete description of DMC's biosynthetic pathway of amino acids (44).

1.F. Rationale for Research Initiative

The generation of high-throughput datasets has developed a large repository of information for DMC dominated by studies performed in pure culture. The main focus of this thesis work is to address two important emerging issues for DMC in the fields of microbiology, systems biology, and bioremediation. The first issue is whether high-throughput surveys themselves provide an alternate route to predict gene or protein functions and behaviors for DMC. The second issue is whether this same data-driven hypotheses approach can identify useful biomarkers of active, as well as stressed cellular states.

This dissertation also looks to extend the current proteomic and trasncriptomic data available for DMC in pure culture to the two distinct, mixed-community cultures of D2 and the commercially available KB-1® (18,19). DMC in mixed community cultures more closely resembles the conditions DMC would see in the field by introducing syntrophic producers of and

methanogenic competitors for hydrogen (38). Additionally, KB-1® is a commercial bioaugmentation culture for directly introducing a mixture of dechlorinators, fermenters, and methanogens into the field (26,60). By monitoring these two mixed-community cultures under similar conditions, conserved as well as culture-specific responses may be inferred. Challenging the cultures with non-optimal environmental settings (lower pH, presence of oxygen, lack or excess of respiratory requirements, etc. — see Chapter 4) provides the potential for identifying key biomarkers of stress response in the cell.

Effective assay design as well as management and mining of the generated data are also required to rapidly and efficiently increase our current knowledge of the organism. Previous studies have applied large-scale modeling techniques such as a recent Flux Balance Analysis to predict metabolite flow through and the growth of DMC (31). However, this study was based on genome annotation alone. Our research initiative is the first to use a systems biology approach to comprehend relationships in a broad gene expression dataset for DMC. To discern the highest confidence interactions predicted by the data, we applied one of the most computational intensive and rigorous statistical methods in Bayesian inference (as discussed in Chapter 3 of this text). Rather than preselecting relationships of interest and introducing our preferential biases, the Bayesian inference platform predicts confident interactions based off of the data alone (9). The network inference platform is able to predict substantially more relationships by first assigning a probability score for every possible relationship and then selecting the optimal set of interactions from the current dataset. This essentially collapses the data generated by these high-throughput methods into a sparse arrangement of potentially testable hypotheses.

1.G. Research Objectives

The overarching goal of this research was to analyze high-throughput data to predict mRNA transcript and protein relationships for *Dehalococcoides mccartyi* (DMC). The specific objectives to achieve this data-driven hypotheses inference were to:

1) Design and/or implement microarrays targeting DMC-specific genes across a wide range of experimental conditions to monitor the shifts in the pool of mRNA transcripts (using in-house DMC 195 specific microarrays and the pangenome microarray (30)).
2) Elucidate interaction networks composed of genes, metabolites, and phenotypes by constructing Bayesian inference ensembles on microarray data using the Reverse Engineering/Forward Simulation™ platform.
3) Screen for biomarkers that are diagnostic of stress response by analyzing differential expression patterns in the transcriptomic and available proteomic datasets during stress as well as recovery

REFERENCES:

1. Adrian, L., Hansen, S. K., Fung, J. M., Görisch, H., & Zinder, S. H. (**2007**). Growth of *Dehalococcoides* strains with chlorophenols as electron acceptors. *Environmental Science & Technology*, 41: 2318-2323.

2. Adrian, L., Rahnenführer, J., Gobom, J., & Hölscher, T. (**2007**). Identification of a chlorobenzene reductive dehalogenase in *Dehalococcoides* sp. strain CBDB1. *Applied and Environmental Microbiology*, 73: 7717-7724.

3. Adrian, L., Szewzyk, U., Wecke, J., & Görisch, H. (**2000**). Bacterial dehalorespiration with chlorinated benzenes. *Nature*, 408: 580-583.

4. Agency for Toxic Substances and Disease Registry. (**2011**). *Support Document to the 2011 Priority List of Hazardous Substances that Will Be the Subject of Toxicological Profiles.*

5. Ballerstedt, H., Hantke, J., Bunge, M., Werner, B., Gerritse, J., Andreesen, J. R., & Lechner, U. (**2004**). Properties of a trichlorodibenzo-p-dioxin-dechlorinating mixed culture with a *Dehalococcoides* as putative dechlorinating species. *FEMS Microbiology Ecology*, 47: 223-234.

6. Bedard, D. L., Ritalahti, K. M., & Löffler, F. E. (**2007**). The *Dehalococcoides* population in sediment-free mixed cultures metabolically dechlorinates the commercial polychlorinated biphenyl mixture Aroclor 1260. *Applied and Environmental Microbiology*, 73: 2513-2521.

7. Bouwer, E. J., Rittmann, B. E., & McCarty, P. L. (**1981**). Anaerobic degradation of halogenated 1-and 2-carbon organic compounds. *Environmental Science & Technology*, 15: 596-599.

8. Bouwer, E. J., & McCarty, P. L. (**1983**). Transformations of 1-and 2-carbon halogenated aliphatic organic compounds under methanogenic conditions. *Applied and Environmental Microbiology*, 45: 1286-1294.

9. Box, G. E. (**1980**). Sampling and Bayes' inference in scientific modelling and robustness. *Journal of the Royal Statistical Society*. Series A (General), 383-430.

10. Bunge, M., A. Wagner, M. Fischer, J. R. Andreesen, and U. Lechner. (**2008**). Enrichment of a dioxin-dehalogenating *Dehalococcoides* species in two-liquid phase cultures. *Environmental Microbiology*, 10:2670-2683.

11. Cheng, D., & He, J. (**2009**). Isolation and characterization of "*Dehalococcoides*" sp. strain MB, which dechlorinates tetrachloroethene to trans-1, 2-dichloroethene. *Applied and Environmental Microbiology*, 75: 5910-5918.

12. Chow, W. L., Cheng, D., Wang, S., & He, J. (**2010**). Identification and transcriptional analysis of trans-DCE-producing reductive dehalogenases in *Dehalococcoides* species. *The ISME Journal*, 4: 1020-1030.

13. Cupples, A. M. (**2008**). Real-time PCR quantification of *Dehalococcoides* populations: Methods and applications. *Journal of Microbiological Methods*, 72: 1-11.

14. Cupples, A. M., Spormann, A. M., & McCarty, P. L. (**2003**). Growth of a *Dehalococcoides*-like microorganism on vinyl chloride and cis-dichloroethene as electron acceptors as determined by competitive PCR. *Applied and Environmental Microbiology*, 69: 953-959.

15. Cupples, A. M., Spormann, A. M., & McCarty, P. L. (**2004**). Comparative evaluation of chloroethene dechlorination to ethene by *Dehalococcoides*-like microorganisms. *Environmental Science & Technology*, 38: 4768-4774.

16. Doherty, R. E. (**2000**). A history of the production and use of carbon tetrachloride, tetrachloroethylene, trichloroethylene and 1, 1, 1-trichloroethane in the United States: part 1--historical background; carbon tetrachloride and tetrachloroethylene. *Environmental Forensics*, 1: 69-81.

17. Duhamel, M., Wehr, S. D., Yu, L., Rizvi, H., Seepersad, D., Dworatzek, S., Cox, E., and Edwards, E. A. (**2002**). Comparison of anaerobic dechlorinating enrichment cultures maintained on tetrachloroethene, trichloroethene, cis-dichloroethene and vinyl chloride. *Water Research*, 36: 4193–4202.

18. Duhamel, M., Mo, K., & Edwards, E. A. (**2004**). Characterization of a highly enriched *Dehalococcoides*-containing culture that grows on vinyl chloride and trichloroethene. *Applied and Environmental Microbiology*, 70: 5538-5545.

19. Duhamel, M., & Edwards, E. A. (**2006**). Microbial composition of chlorinated ethene-degrading cultures dominated by *Dehalococcoides*. *FEMS Microbiology Ecology*, 58: 538-549.

20. Fennell, D. E., Gossett, J. M., & Zinder, S. H. (**1997**). Comparison of butyric acid, ethanol, lactic acid, and propionic acid as hydrogen donors for the reductive dechlorination of tetrachloroethene. *Environmental Science & Technology*, 31: 918-926.

21. Fennell, D. E., Nijenhuis, I., Wilson, S. F., Zinder, S. H., & Häggblom, M. M. (**2004**). *Dehalococcoides ethenogenes* strain 195 reductively dechlorinates diverse chlorinated aromatic pollutants. *Environmental Science & Technology*, 38: 2075-2081.

22. Fogel, M. M., Taddeo, A. R., & Fogel, S. (**1986**). Biodegradation of chlorinated ethenes by a methane-utilizing mixed culture. *Applied and Environmental Microbiology*, 51: 720-724.

23. Freedman, D. L., & Gossett, J. M. (**1989**). Biological reductive dechlorination of tetrachloroethylene and trichloroethylene to ethylene under methanogenic conditions. *Applied and Environmental Microbiology*, 55: 2144-2151.

24. Fung, J. M., Morris, R. M., Adrian, L., & Zinder, S. H. (**2007**). Expression of reductive dehalogenase genes in *Dehalococcoides ethenogenes* strain 195 growing on tetrachloroethene, trichloroethene, or 2, 3-dichlorophenol. *Applied and Environmental Microbiology*, 73: 4439-4445.

25. He, J., Sung, Y., Krajmalnik-Brown, R., Ritalahti, K. M., & Löffler, F. E. (**2005**). Isolation and characterization of *Dehalococcoides* sp. strain FL2, a trichloroethene (TCE)-and 1, 2-dichloroethene-respiring anaerobe. *Environmental Microbiology*, 7: 1442-1450.

26. Hood, E. D., Major, D. W., Quinn, J. W., Yoon, W. S., Gavaskar, A., & Edwards, E. A. (**2008**). Demonstration of enhanced bioremediation in a TCE source area at Launch Complex 34, Cape Canaveral Air Force Station. *Ground Water Monitoring & Remediation*, 28: 98-107.

27. Hendrickson, E. R., Payne, J. A., Young, R. M., Starr, M. G., Perry, M. P., Fahnestock, S., ... & Ebersole, R. C. (**2002**). Molecular analysis of *Dehalococcoides* 16S ribosomal DNA from chloroethene-contaminated sites throughout North America and Europe. *Applied and Environmental Microbiology*, 68: 485-495.

28. Henschler, D. (**1994**). Toxicity of chlorinated organic compounds: effects of the introduction of chlorine in organic molecules. *Angewandte Chemie*, 33: 1920-1935.

29. Holliger, C., Schraa, G., Stams, A. J., & Zehnder, A. J. (**1993**). A highly purified enrichment culture couples the reductive dechlorination of tetrachloroethene to growth. *Applied and Environmental Microbiology*, 59: 2991-2997.

30. Hug, L. A., Salehi, M., Nuin, P., Tillier, E. R., & Edwards, E. A. (**2011**). Design and verification of a pangenome microarray oligonucleotide probe set for *Dehalococcoides* spp. *Applied and Environmental Microbiology*, 77: 5361-5369.

31. Islam, M. A., Edwards. E. A., and Mahadevan, R. (**2010**). Characterizing the metabolism of *Dehalococcoides* with a constraint-based model. *PLoS Computational Biology* 6.8:e1000887.

32. Jayachandran, G., Görisch, H., & Adrian, L. (**2003**). Dehalorespiration with hexachlorobenzene and pentachlorobenzene by *Dehalococcoides* sp. strain CBDB1. *Archives of Microbiology*, 180: 411-416.

33. Johnson, D. R., Lee, P. K., Holmes, V. F., Fortin, A. C., & Alvarez-Cohen, L. (**2005**). Transcriptional expression of the tceA gene in a *Dehalococcoides*-containing microbial enrichment. *Applied and Environmental Microbiology*, 71: 7145-7151.

34. Krajmalnik-Brown, R., Hölscher, T., Thomson, I. N., Saunders, F. M., Ritalahti, K. M., & Löffler, F. E. (**2004**). Genetic identification of a putative vinyl chloride reductase in *Dehalococcoides* sp. strain BAV1. *Applied and Environmental Microbiology*, 70: 6347-6351.

35. Kube, M., Beck, A., Zinder, S. H., Kuhl, H., Reinhardt, R., & Adrian, L. (**2005**). Genome sequence of the chlorinated compound–respiring bacterium *Dehalococcoides* species strain CBDB1. *Nature Biotechnology*, 23: 1269-1273.

36. Lee, P. K., Johnson, D. R., Holmes, V. F., He, J., & Alvarez-Cohen, L. (**2006**). Reductive dehalogenase gene expression as a biomarker for physiological activity of *Dehalococcoides* spp. *Applied and Environmental Microbiology*, 72: 6161-6168.

37. Lee, P. K., Macbeth, T. W., Sorenson, K. S., Deeb, R. A., & Alvarez-Cohen, L. (**2008**). Quantifying genes and transcripts to assess the in situ physiology of "*Dehalococcoides*" spp. in a trichloroethene-contaminated groundwater site. Applied and environmental microbiology, 74: 2728-2739.

38. Lee, P. K., Dill, B. D., Louie, T. S., Shah, M., VerBerkmoes, N. C., Andersen, G. L., ... & Alvarez-Cohen, L. (**2012**). Global transcriptomic and proteomic responses of *Dehalococcoides ethenogenes* strain 195 to fixed nitrogen limitation. *Applied and Environmental Microbiology*, 78: 1424-1436.

39. Liu, F. & Fennell, D. E.. (**2008**). Dechlorination and detoxification of 1,2,3,4,7,8-hexachlorodibenzofuran by a mixed culture containing *Dehalococcoides ethenogenes* strain 195. *Environ Science & Technology*. 42: 602–607.

40. Lu, X., Wilson, J. T., & Kampbell, D. H. (**2006**). Relationship between *Dehalococcoides* DNA in ground water and rates of reductive dechlorination at field scale. *Water Research*, 40: 3131-3140.

41. Lyne, F.A. & McLachlan, T. (**1949**). Contamination of water by trichloroethylene, *The Analyst*, 74: 513.

42. Magnuson, J. K., Romine, M. F., Burris, D. R., & Kingsley, M. T. (**2000**). Trichloroethene reductive dehalogenase from *Dehalococcoides ethenogenes*: Sequence of tceA and substrate range characterization. *Applied and Environmental Microbiology*, 66: 5141-5147.

43. Marco-Urrea, E., Paul, S., Khodaverdi, V., Seifert, J., von Bergen, M., Kretzschmar, U., & Adrian, L. (**2011**). Identification and characterization of a Re-citrate synthase in Dehalococcoides strain CBDB1. *Journal of Bacteriology*, 193: 5171-5178.

44. Marco-Urrea, E., Seifert, J., von Bergen, M., & Adrian, L. (**2012**). Stable isotope peptide mass spectrometry to decipher amino acid metabolism in *Dehalococcoides* strain CBDB1. *Journal of Bacteriology*, 194: 4169-4177.

45. Maymo-Gatell, X., Chien, Y. T., Gossett, J. M., & Zinder, S. H. (**1997**). Isolation of a bacterium that reductively dechlorinates tetrachloroethene to ethene. *Science*, 276: 1568-1571.

46. Maymó-Gatell, X., Anguish, T., & Zinder, S. H. (**1999**). Reductive dechlorination of chlorinated ethenes and 1, 2-dichloroethane by "*Dehalococcoides ethenogenes*" 195. *Applied and Environmental Microbiology*, 65: 3108-3113.

47. McMurdie, P. J., Behrens, S. F., Müller, J. A., Göke, J., Ritalahti, K. M., Wagner, R., ... & Spormann, A. M. (**2009**). Localized plasticity in the streamlined genomes of vinyl chloride respiring *Dehalococcoides*. *PLoS Genetics*, 5(11), e1000714.

48. Morris, R. M., Fung, J. M., Rahm, B. G., Zhang, S., Freedman, D. L., Zinder, S. H., & Richardson, R. E. (**2007**). Comparative proteomics of *Dehalococcoides* spp. reveals strain-

specific peptides associated with activity. *Applied and Environmental Microbiology*, 73: 320-326.

49. Morris, R. M., Sowell, S., Barofsky, D., Zinder, S., & Richardson, R. (**2006**). Transcription and mass-spectroscopic proteomic studies of electron transport oxidoreductases in *Dehalococcoides* ethenogenes. *Environmental Microbiology*, 8: 1499-1509.

50. Müller, J. A., Rosner, B. M., Von Abendroth, G., Meshulam-Simon, G., McCarty, P. L., & Spormann, A. M. (**2004**). Molecular identification of the catabolic vinyl chloride reductase from *Dehalococcoides* sp. strain VS and its environmental distribution. *Applied and Environmental Microbiology*, 70: 4880-4888.

51. Neumann, A., Wohlfarth, G., & Diekert, G. (**1998**) Tetrachloroethene dehalogenase from *Dehalospirillum multivorans*: cloning, sequencing of the encoding genes, and expression of the pceA gene in *Escherichia coli*. *Journal of Bacteriology*. 180: 4140–4145.

52. Nijenhuis, I., & Zinder, S. H. (**2005**). Characterization of hydrogenase and reductive dehalogenase activities of *Dehalococcoides ethenogenes* strain 195. *Applied and Environmental Microbiology*, 71: 1664-1667.

53. Quensen 3rd, J. F., Tiedje, J. M., & Boyd, S. A. (**1988**). Reductive dechlorination of polychlorinated biphenyls by anaerobic microorganisms from sediments. *Science*, 242: 752.

54. Rahm, B. G., Morris, R. M., & Richardson, R. E. (**2006**). Temporal expression of respiratory genes in an enrichment culture containing *Dehalococcoides ethenogenes*. *Applied and Environmental Microbiology*, 72: 5486-5491.

55. Rahm, B. G., & Richardson, R. E. (**2007**). Correlation of respiratory gene expression levels and pseudo-steady-state PCE respiration rates in *Dehalococcoides ethenogenes*. *Environmental Science & Technology*, 42: 416-421.

56. Roberts, P. V., Schreiner, J. E., and Hopkins, G. D. (**1982**). Field study of organic water quality changes during ground water recharge in the Palo Alto Baylands. *Water Research*, 16:1025-1035.

57. Rowe, A. R., Heavner, G. L., Mansfeldt, C. B., Werner, J. J., & Richardson, R. E. (**2012**). Relating Chloroethene Respiration Rates in *Dehalococcoides* to Protein and mRNA Biomarkers. *Environmental Science & Technology*.

58. Rowe, A. R., Lazar, B. J., Morris, R. M., & Richardson, R. E. (**2008**). Characterization of the community structure of a dechlorinating mixed culture and comparisons of gene expression in planktonic and biofloc-associated "*Dehalococcoides*" and *Methanospirillum* species. *Applied and Environmental Microbiology*, 74: 6709-6719.

59. Sakaki, T., & Munetsuna, E. (**2010**) Enzyme systems for biodegradation of polychlorinated dibenzo-p-dioxins. *Applied Microbiology and Biotechnology* 88: 23–30.

60. Scheutz, C., Durant, N. D., Dennis, P., Hansen, M. H., Jørgensen, T., Jakobsen, R., ... & Bjerg, P. L. (**2008**). Concurrent ethene generation and growth of *Dehalococcoides* containing vinyl chloride reductive dehalogenase genes during an enhanced reductive dechlorination field demonstration. *Environmental Science & Technology*, 42: 9302-9309.

61. Seshadri, R., Adrian, L., Fouts, D. E., Eisen, J. A., Phillippy, A. M., Methe, B. A., ... & Heidelberg, J. F. (**2005**). Genome sequence of the PCE-dechlorinating bacterium *Dehalococcoides ethenogenes*. *Science*, 307: 105-108.

62. Steen, K. (**1995**). Wartime catalyst and postwar reaction: the making of the U. S. synthetic organic chemicals industry, 1910-1930. Ph.D. Thesis. University of Delaware.

63. Sung, Y., Ritalahti, K. M., Apkarian, R. P., & Löffler, F. E. (**2006**). Quantitative PCR confirms purity of strain GT, a novel trichloroethene-to-ethene-respiring *Dehalococcoides* isolate. *Applied and Environmental Microbiology*, 72: 1980-1987.

64. Tang, Y. J., Yi, S., Zhuang, W. Q., Zinder, S. H., Keasling, J. D., & Alvarez-Cohen, L. (**2009**). Investigation of carbon metabolism in "*Dehalococcoides ethenogenes*" strain 195 by use of isotopomer and transcriptomic analyses. *Journal of Bacteriology*, 191: 5224-5231.

65. Tandoi, V., DiStefano, T. D., Bowser, P. A., Gossett, J. M., & Zinder, S. H. (**1994**). Reductive dehalogenation of chlorinated ethenes and halogenated ethanes by a high-rate anaerobic enrichment culture. *Environmental Science & Technology*, 28: 973-979.

66. Taş, N., Eekert, V., Miriam, H. A., De Vos, W. M., & Smidt, H. (**2010**). The little bacteria that can–diversity, genomics and ecophysiology of '*Dehalococcoides'* spp. in contaminated environments. *Microbial Biotechnology*, 3: 389-402.

67. U.S. Environmental Protection Agency. (**2001**). *Trichloroethylene Health Risk Assessment: Synthesis and Characterization*. Office of Research and Development, Washington, DC.

68. Vogel, T. M., & McCarty, P. L. (**1985**). Biotransformation of tetrachloroethylene to trichloroethylene, dichloroethylene, vinyl chloride, and carbon dioxide under methanogenic conditions. *Applied and Environmental Microbiology*, 49: 1080-1083.

69. Waller, A. S., Krajmalnik-Brown, R., Löffler, F. E., & Edwards, E. A. (**2005**). Multiple reductive-dehalogenase-homologous genes are simultaneously transcribed during dechlorination by *Dehalococcoides*-containing cultures. *Applied and Environmental Microbiology*, 71: 8257-8264.

70. Werner, J. J., Ptak, A. C., Rahm, B. G., Zhang, S., & Richardson, R. E. (**2009**). Absolute quantification of *Dehalococcoides* proteins: enzyme bioindicators of chlorinated ethene dehalorespiration. *Environmental Microbiology*, 11: 2687-2697.

71. Westerick, J. J., Mello, J. W., & Thomas, R. F. (**1984**). The groundwater supply survey. *Journal of American Water Works Association*, 76:52-59.

CHAPTER 2

Dehalococcoides mccartyi strain 195's Genome-wide Transcriptomic Response to a Range of Respiration Rates and Substrate Types with a Focus on the Expression of Reductive Dehalogenases.

2.A. Abstract

Dehalococcoides mccartyi (DMC) strain 195's transcriptomic response to the respiration of the recalcitrant chlorinated organic compounds cis-dichloroethene trichloroethene, tetrachloroethene, 2,3-dichlorophenol, and 1,2,3,4-tetrachlorobenzene under varied conditions was monitored from mixed culture samples by a microarray designed for strain 195. Overall, seven transcripts of strain 195's 17 reductive dehalogenase homologs, the putative enzymes that transfer electrons to a terminal chloroorganic electron acceptor, were detected above 1000 processed fluorescence units in at least one experiment presented. The reductive dehalogenases DET1171 and DET1535 were highly (31 ± 15 and 3.8 ± 0.3 fold) up-regulated in response to 2,3-dichlorophenol being fed as the electron acceptor. This suggests that DET1171 could potentially play a role in chlorophenol respiration. However, DET1559 (27±4.1 fold up-regulated in all 2,3-dichlorophenol experiments) and DET0318 *pceA* (the dominant reductive dehalogenase in fluorescence intensity) in the dechlorination of chlorophenols are more likely to be the dominant enzymes involved, as previously noted. Additionally, DET1559 was highly up-regulated during the dechlorination of 1,2,3,4-tetrachlorobenzene (25 ± 9.5 fold). Investigations into the possible regulation of expression of the reductive dehalogenase *rdhA* catalytic units revealed a very strong negative correlation between the transcripts for *tceA* and two putative regulators (the *marR* type DET1525 and the response regulator *rdhD* DET1531). These enzymes

may serve as repressors for the highly expressed *tceA* transcript or may be negatively regulated by other genes in the *tceA* regulon. Expression relationships between the putative electron carrying redoxin type proteins and *rdhA* subunits was noted with a thioredoxin type (DET0661) negatively correlated with *tceA* and a glutaredoxin type (DET0198) positively correlated to DET1545, tying reductive dehalogenases to enzymes with predicted mechanisms for cellular state redox sensing, electron transport, and regulation.

2.B Introduction

The pervasiveness of recalcitrant halogenated organics in hazardous waste cleanup sites (60) makes bioremediation utilizing populations of *Dehalococcoides* an attractive tool (51). All known *Dehalococcoides* strains are obligate hydrogenotrophs and dehalorespirers (34) that reductively dehalogenate compounds including (but not limited to) chlorinated-ethenes (53,55,59), -ethanes (19,27,59), -phenols (2,22), -benzenes (1,3,22), -dioxins (12,14,23), -dibenzodioxins (22), -dibenzofurans (50), -naphthalene (22), and -biphenyls (8,22,87) suggesting a broad applicability for bioremediation. Additionally, *Dehalococcoides* populations are often found and active at chlorinated-organic contaminated sites (7,8,10,13,15,26,33,37,48,88-89) and, in some cases, need only to be biostimulated to increase the rate of dehalogenating the chlorinated organic compounds. Several case studies focusing on bioaugmentation of DMC at contaminated sites have also showed success (20,49,57,73). To date, this potential has only been demonstrated in tetrachloroethene (PCE) and/or trichloroethene (TCE) contaminated sites with a wider range being actively pursued.

The first strain of *Dehalococcoides* identified, *Dehalococcoides mccartyi* strain 195 (DMC195) (52), was isolated in 1997 (58) and its genome sequenced, assembled, and annotated in 2005 (75). Genomes of additional *Dehalococcoides* strains, such as CBDB1 (45,81), VS (63,82,54), GT (78), and BAV1 (29,42,54), have been sequenced and annotated since, with other members being isolated and/or characterized (e.g. strain FL2 (30); KB1 metagenome (18) and ANAS transcriptome both available through the Joint Genome Institute). From the ensemble of genomes and subsequent analysis, the identified putative enzymes and regulatory elements comprising the electron transport chain include a unique network of reductive dehalogenases (RDases) (75), which reduce halogenated-organics; hydrogenases, which oxidize DHC's sole electron-donor of hydrogen (Hup is the only hydrogenase predicted to face the periplasm (61,75,80)); and other oxidoreductases of unknown function (e.g. Fdh, formate dehydrogenase; Nuo, NADH ubiquinone oxidoreductase; Mod, molybdopterin containing oxidoreductase). Although RDases, Hup, and other membrane-bound oxidoreductase proteins have been documented in several *Dehalococcoides* proteomic studies (62,84), the organization and interaction between these respiration elements are not well characterized (65). Observations of broad expression patterns across many experiments generate hypotheses about which transcripts are working in concert to fulfill specific biological functions.

Dehalococcoides's strain expression patterns of a subset of the 90 overall RDase homologous clusters currently identified across the genus (43) likely imparts capabilities for dehalogenating different chlorinated substrates (35,36,56,86). Of DMC195's set of 17 full-length RDases, the catalytic subunits (*rdhA*s) DET0079 (TceA), DET0318 (PceA), DET1559, and DET1545 are the most investigated across multiple experiments within a mixed community

culture (D2) containing DMC195 as the sole dehalogenator (25,38,39,46,56,66-68,82). Even under standard feeding conditions of a sole chlorinated substrate such as PCE, transcripts for multiple RDases are expressed (25,44,61-62,66-68). Adding PCE is equivalent to adding TCE, DCE, and VC as daughter products are formed which potentially explains the expression of multiple RDases in a single strain. However, the comparison between strains respiring PCE reveals unique subsets of RDases (82).

Previous transcriptomic studies performed on DHC include characterizing strains or cultures (17,46,85) and monitoring both pure and mixed, well-defined cultures (39,83). Microarray studies investigating the entire transcriptome under pure-culture and batch-fed conditions with TCE and hydrogen (as the electron acceptor and electron donor respectively) (39) revealed key insights into the organism's time-dependent response, carbon metabolism (79), corrinoid cofactor uptake and modification (40), predicted nitrogen fixation pathway (46), and characterizing non-isolated strains (46).

To further the biological understanding of *Dehalococcoides*, this study employed microarrays to monitor the transcriptomic response of DMC195 in a mixed community culture to three batch and 18 continuous-fed conditions. A total of 63 cultures were monitored considering biological replicates. These cultures were grown in conditions with varying electron acceptor feed rates (from 0-80.2 μmole/(L-hr)), electron acceptor types (tetrachloroethene (PCE), trichloroethene (TCE), dichloroethene (DCE), 2,3-dichlorophenol (DCP), 1,2,3,4-tetrachlorobenzene (TeCB), or no electron acceptor), electron donor to acceptor ratios (from 0.7 to 17 on a H_2 electron equivalence basis), and electron donor types (butyrate, lactate, yeast

extract, fermented yeast extract, pure hydrogen, or endogenous biomass decay only) as previously described (71). By monitoring the transcriptome, genome-wide responses can be described. Additionally, the growth of DMC195 in a non-pure culture setting allows a fuller insight into the maintained mixed community cultures (Cornell Donna II (58), Pinellas (28), Victoria (32), KB-1 (19) and ANAS cultures (70)) and a better representation of field conditions in which DMC195 will interact with both fermenters and methanogens (21,72,77).

2.C. Materials and Methods:

2.C.1. Continuous feed setup

The continuous feed culture setup (pseudo steady-state (PSS)) has been previously described (66). In brief, 160-mL glass serum bottles were filled with 100 mL of 3-day starved mixed community culture sampled from the main reactor (Donna II). Varying combination of Pressure Lok® syringes (VICI Precision Sampling) were loaded on a Cole Palmer 74900 Syringe Pump to deliver the electron acceptor and donor stocks at an expected rate.

2.C.2. Culture growth conditions

All subcultures studied in this experiment were 100-mL samples from a maintained 6-L mixed community culture (Donna II (D2)) previously described (21,66-68,72) The culture contains a DMC195 population (near 5×10^8 cells/mL; 60% of total population on per cell basis) mixed with methanogens and organisms that ferment organic substrates. The continuous feed experiments were comprised of 54 subcultures with varying electron acceptor feed rates (0-504 μeeq/(L-hr)), electron acceptor types (PCE (99+%, Sigma-Aldrich), TCE (99+% Sigma-Aldrich), DCE (99+% ,TCI America), 2,3-DCP (99+%,Acros Organics), and no electron

acceptor), electron donor to acceptor ratios (0.7 to 17 on an electron equivalence basis), and electron donor type (butyrate (99+%, Acros Organics), lactate (60% v/v, Acros Organics), yeast extract (Mo Bio Laboratories), fermented yeast extract (Mo Bio Laboratories), pure hydrogen (AirGas), or endogenous biomass decay). The complete setup for each of these experiments is listed in Figure 2.2. The three endogenous decay cultures received no electron donor or acceptor.

For the batch-fed chlorobenzene experiments, six 160 mL bottles were established with 100 mL of 3-day starved D2 mixed community culture and were fed with 1 µL neat PCE, 40 µL of 100 mM 1,2,3,4-TeCB (98+%, Sigma Aldrich) in hexadecane (99+%, ACROS Organics), 40 µL of butyric acid, 100 µL of 50 g/L YE, and 100 µL of vitamin solution described previously (76). The PCE was added to provide a starter dose of energy and was completely dehalogenated after 24 hours. Additionally, control bottles that received 40 µL hexadecane phase showed minimal impact on chloroethene dechlorination rates as only 9% of the PCE is calculated to partition into this phase.

2.C.3. Gas chromatography monitoring

Chlorinated-ethenes, ethanes, and methane were assayed utilizing gas chromatography (GC) methods previously described (68). Tetrachlorobenzene daughter products were assayed utilizing a different GC method previously described (64). Both methods sampled the headspace and detected the chlorinated compound using a flame ionization detector (FID).

Chlorinated phenols were assayed utilizing a modified method (41). The chlorinated phenol samples were comprised of 1 mL liquid samples withdrawn from the subcultures and

frozen. The thawed samples were transferred to a 1-mL glass vial, 100 uL of hexane was added to the sample, and the vial was shaken at 300 rpm for six hours. The FID gas chromatography method selected has an injection temperature of 200° C, a constant column temperature of 160° C, and the FID detector temperature of 200° C on a HP-1 column (5m × 0.53 mm with 2.65 μm film, Hewlett Packard). The gas mixture was 200 kPa nitrogen as the carrying gas, 200 kPa air, and 250 kPa hydrogen. 5 μL of the sample in hexane was injected. Chemical standard curves were made in both hexane and media from pure chlorinated phenols (3- and 2-monochlorophenol were from ACROS Organics, 99+%).

2.C.4. Calculation of respiration rates

Complete dehalorespiration is considered to occur for the higher chlorinated ethenes to vinyl-chloride (VC) or ethene (VC dehalogenated to ethene co-metabloically in strain 195) (66) with 6, 4, and 2 electron equivalents (eeqs) required for PCE, TCE, and cDCE, respectively with the specific calculation previously published (67). Extending this analysis to the DCP experiments, MCP is the terminal product (22). Therefore, DMC195 will respire 2 eeqs per mole of DCP. The respiration rate equation for DCP, r_{DCP}, in μeeq/L/hr is:

$$r_{DCP} = 2\frac{\mathrm{d}(MCP)}{\mathrm{d}t}$$

For chlorobenzene respiration, the amount of energy gained per chlorine removed is less clear. Previous work has shown that DMC195 is capable of growth from 1,2,3,4-TeCB dehalorespiration and not any lower congener (22). However, during this growth, dichlorobenzene is produced. Therefore, it is difficult to discern if the 1,2,4-TriCB to DiCB is cometabolic. Therefore, in the consideration of a respiration rate for chlorobenzenes, the rate is actually total eeqs utilized to transform:

$$r_{TeCB} = 2\frac{\mathrm{d}(TriCB)}{\mathrm{d}t} + 4\frac{\mathrm{d}(DiCB)}{\mathrm{d}t}$$

$$r_{TriCB} = 2\frac{\mathrm{d}(DiCB)}{\mathrm{d}t}$$

2.C.5. Microarray design

The microarray designed for this experiment was an Agilent Technologies© two-color, 15k, 60 mer, 8-plex array. The specific designs of the probes utilized a modified method provided by the eArray© software suite (5). The array probe set utilized for the batch chlorinated ethene versus continuous-feed experiment employed a base-composition (BC) technique for designing and scoring the best probe for each transcript (5). The second array probe set for the remainder of the experiments contained all protein encoding transcripts, community members, non-protein encoding RNA transcripts (rRNAs, tRNAs), and a luciferase control was designed using a modified temperature matching (Tm) method (5). If a Base Composition (BC, a quality metric ranging from 1 (good) to 4 (poor)) score of 3,4, or poor was reported for a transcript, multiple probes around the melting temperature of 80° C were designed. The probe with the best base composition score nearest to the 80° C temperature was selected. The designs were searched using the Basic Local Alignment Search Tool (BLAST) (16) against both the National Center for Biotechnology Information (NCBI) non-redundant nucleotide collection for all organisms and the assembled mixed community metagenome of D2 (available through Joint Genome Institute's IMG/MER) to confirm the specificity of all probes. Both microarray platform designs are uploaded and freely available at the NCBI Gene Expression Omnibus (GEO) database (GPL10023, http://www.ncbi.nlm.nih.gov/geo/).

2.C.6. RNA-cDNA handling for microarray monitoring

50-mL of D2-based liquid culture was centrifuged at 14190×*g* for 10 minutes and stored at -80 C for less than one week. Each centrifuged sample was split into eight individual RNA extractions with each sample following the RNeasy© Mini Kit (Qiagen) extraction previously outlined (68). The 8 distinct RNA extractions were recombined on the spin filter before the first RW1 buffer wash. The Superscript I © DNAse RNA cleanup, amino-allyl cDNA formation, cDNA cleanup, and cDNA labeling with Cy3 or Cy5 followed the method outlined previously (83). The quality and quantity of the RNA was determined using the RNA 6000 Nano assay on an Agilent 2100 bioanalyzer (Agilent Technologies). The quantity of resulting cDNA was determined by using the Quant-IT™ OliGreen® ssDNA Assay Kit (Invitrogen) and NanoDrop 2000c (ThermoScientific). A common control RNA pool sampled from the main D2 reactor after 3 days of starvation was labeled with Cy3.

2.C.7. Microarray hybridization and scanning:

For each experiment, Cy5 labeled cDNA from the mixed community mRNA pool was hybridized against an aliquot of common control of Cy3 labeled cDNA from 3-day starved culture. Additionally, each platform also had an associated dye-swap, labeling a common control pool in both the Cy3 and Cy5 channels, array hybridized as well. The hybridization, washing, and scanning of the microarray samples was performed by the Cornell University Microarray Core Facility and followed the methods outlined by the manufacturer (5). The general procedure mixed 25 µl (~400 ng) of the labeled cDNA sample with 25 µl 2x Gene Expression (GEx) Hybridization Buffer HI-RPM (5), hybridized the sample to the microarray slide at 65° C for 17

hours, washed with GEx Wash Buffer 1 and 2 (5) at room and elevated (37° C) temperatures, and scanned with an Agilent Technologies Scanner G2505C with a 5-μm resolution.

2.C.8. Statistical Treatment of the Data Set:

Microarray image analysis was conducted using Agilent Feature Extraction 10.5 Image Analysis Software. The Feature Extraction Software also performed a within array modified LOESS normalization between the Cy5 and Cy3 signals, calculated a log ratio between the Cy5 and Cy3 channels, and calculated a modified Student t-test p-value between the Cy5 and Cy3 signal distributions (90). The more detailed treatment the Agilent Feature Extraction employed can be found in the user manual (4). Replicate spots for the same probe (ranging from 6-20 spots/probe) were geometrically averaged. Dye swap arrays were performed on both platforms to check for probe bias. Hierarchical and K-means clustering were performed in R 2.15.0 (http://www.r-project.org/). The raw and normalized data have been uploaded and are freely available at the NCBI GEO database (reference series ID number GSE26288).

2.D. Results:

2.D.1. Batch feed compared to continuous feed transcriptional responses

The first set of microarrays compared the mixed community culture with similar electron acceptor/donor conditions under batch versus continuous feed. The batch culture dechlorinated 110 μmol/L of PCE to VC/ethene in 6 hours (18.3 μmol/(L-hr)) while the continuous fed experiments received a rate of 8.83±2.17 or 12.7±0.70 μmol/L-hr of PCE or TCE respectively. The main experimental differences are the high initial pulse of electron acceptor and donor seen by the batch cultures to the low concentrations maintained in the continuous-fed setup (the batch

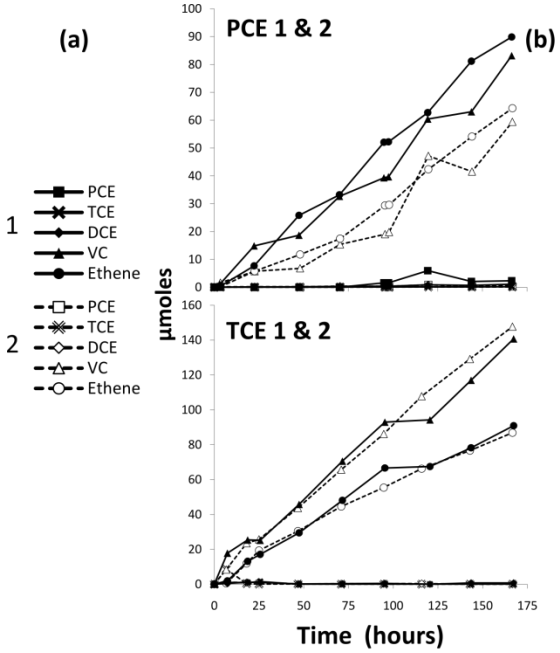

ID	Description	Regulation	Ratio	ID	Description	Regulation	Ratio
DET0036	hypothetical	DOWN	0.43 ± 0.03	DET1038	ileS isoleucyl tRNA synthetase	UP	2.50 ± 0.39
DET0137	mgsA methylglyoxal synthase	DOWN	0.31 ± 0.10	DET1051	hypothetical	UP	3.77 ± 0.61
DET0180	RDase	UP	5.48 ± 4.10	DET1063	LuxR, DNA binding	UP	2.65 ± 0.81
DET0181	RDase anchor	UP	5.12 ± 0.91	DET1092	DNA methylase	DOWN	0.41 ± 0.07
DET0297	hypothetical	UP	4.91 ± 3.03	DET1106	hypothetical	DOWN	0.32 ± 0.06
DET0368	proS prolyl tRNA synthetase	UP	2.73 ± 0.24	DET1107	hypothetical	DOWN	0.28 ± 0.04
DET0423	hypothetical	UP	4.22 ± 5.13	DET1146	hypothetical	DOWN	0.35 ± 0.07
DET0558	atpB ATP synthase	DOWN	0.20 ± 0.04	DET1186	hypothetical	UP	2.89 ± 1.12
DET0560	atpF ATP synthase	DOWN	0.33 ± 0.07	DET1206	metM dehydrogenase	DOWN	0.33 ± 0.09
DET0561	atpH ATP synthase	DOWN	0.33 ± 0.05	DET1224	cobA cobalamin transferase	DOWN	0.43 ± 0.04
DET0562	atpA ATP synthase	DOWN	0.40 ± 0.04	DET1278	nusB N utilization protein B	DOWN	0.25 ± 0.06
DET0673	hypothetical	UP	3.62 ± 1.21	DET1284	hypothetical	DOWN	0.37 ± 0.06
DET0721	hypothetical	DOWN	0.36 ± 0.04	DET1285	serine protease, DegP/HtrA	UP	2.93 ± 0.58
DET0736	oxidoreductase	UP	2.68 ± 0.42	DET1286	serine protease, DegP/HtrA	UP	3.91 ± 1.28
DET0754	hypothetical	UP	2.73 ± 1.12	DET1377	hypothetical	UP	2.95 ± 0.69
DET0755	hypothetical	UP	3.80 ± 0.57	DET1379	auxin responsive GH3 protein	UP	3.73 ± 0.28
DET0864	HymB hydrogenase	DOWN	0.36 ± 0.08	DET1419	AbrB transcriptional regulator	DOWN	0.28 ± 0.15
DET0908	putative arsenical pump	UP	7.84 ± 2.81	DET1511	hypothetical	DOWN	0.13 ± 0.12
DET0909	hypothetical	UP	2.75 ± 0.35	DET1544	RDase anchor	UP	3.49 ± 0.59
DET0945	ABC transporter	DOWN	0.43 ± 0.04	DET1569	hypothetical	UP	2.99 ± 0.65
DET1021	hypothetical	DOWN	0.19 ± 0.08	DET1624	hypothetical	UP	2.58 ± 0.39
DET1035	tryptophan synthase β	UP	3.15 ± 0.39				

Figure 2.1. Comparison of the microarray results for the Batch and Continuous fed cultures. (a) Gas chromatograph results

culture experiences the initial pulse of 110 μmol/L while the continuous-fed cultures maintain a constant level of about 8-12 μmol/L-hr of chlorinated ethenes based on the last 48 hours of GC data) and that the rate of continuous feeding in the PSS cultures was maintained for 7 days. The GC time courses for the continuous fed PCE (1 & 2) and TCE (1 & 2) conditions are shown in Figure 2.1. To determine the transcripts differentially regulated across all four continuous fed experiments, only transcripts where all replicate probe spots (n=6-20) on the microarray recorded a fold ratio between the continuous-fed and batch cultures of greater than two (for up-regulated genes) or less than one-half (for down-regulated genes) and are below a p-value of 0.05 are considered. Using this criterion, PCE 1, PCE 2, TCE 1, and TCE 2 displayed 193, 165, 144, and 275 differentially regulated transcripts as compared to the batch control, respectively. Of these, 43 (23 up- and 20 down-regulated) are shared across all samples (Figure 2.1).

Among the 23 up-regulated transcripts, the *rdhA* DET0180 and its *rdhB* anchoring protein (DET0181) as well as the *rdhB* DET1544 display a 5.5±4.11, 5.1±0.92, and 3.5±0.59 fold increase respectively. The listing of the *rdhB* (DET1544) without the *rdhA* catalytic subunit (DET1545) transcript is surprising as they are predicted to reside on the same polycistronic mRNA and the behavior should be linked on the microarray. All probes for the *rdhA* DET1545 pass the requirement of displaying a p-value below 0.05, but the transcript is excluded from the stringent analysis due to two probe spots (out of 20 replicates) in the PCE1 experiment failing to exceed the ratio cut off of 2. If the stringency of the analysis is relaxed to remove the log ratio cutoff, the number of transcripts shared across all experiments is increased from 43 to 65 (Appendix Table A1.1). DET1545 falls within this category displaying an average ratio across all experiments of 3.3±0.86. The 20 significantly down-regulated transcripts under continuous-

fed conditions in the stringent analysis are populated by many key transcripts encoding for enzymes in respiratory energy conservation. These include transcripts of the *ATPase* operon (DET0558, DET0560, DET0561, DET0562) and subunits of the hydrogenase *ech* (DET0864). Additional members of the *ech* operon (DET0861 and DET0862) are found in the expanded list with 0.37±0.07 and 0.35±0.10 fold down-regulation (Appendix Table A1.1).

2.D.2. Expression profiles comparison across multiple continuously fed experiments

To explore a wide variety of environmental conditions, mRNA pools from 59 additional experiments (performed during 16 separate experimental runs) were analyzed by the microarray technique described above. The parameters and conditions for each experiment are outlined in Figure 2.2. The electron acceptors (none, PCE, TCE, cDCE, DCP, and TeCB) and the electron donors for the PCE experiments were varied (none provided, yeast extract (YE), fermented yeast extract (FYE), butyrate (with YE), lactate (with YE), and hydrogen). The feed rates of electron acceptor and the ratio of electron acceptor to donor were altered as well. DMC195's respiration rates varied between 0 (in cultures not fed electron acceptor) to 170 μeeq/(L-hr).

When the experiments were organized via a hierarchal Ward cluster dendogram based on a Euclidean distance matrix of the log-ratio fold changes between the experimental (Cy5 red) and 3-day starved control (Cy3 green), two distinct groupings developed (Figure 2.2). The two clusters were separated primarily by the respiration rate. However, the High 2 from the High-Low PCE experiment (HLH2_INHIB) plotted with the higher respiration cluster when in fact respiration ceased prior to culture sampling due to the formation of non-aqueous phase PCE. HLH1_INHIB and HLH2_INHIB displayed an unique decay series as both cultures experienced

Figure 2.2. Experimental conditions for the continuous-feed investigations organized by a Ward cluster dendogram based off of Euclidean distance matrix for the log ratio fold change of all gene targets. The experimental title provides a brief description. The culture title designates the electron acceptor (PCE, TCE, DCE, DCP, or none (-)) and electron donor source type (butyrate, lactate, hydrogen, yeast extract (YE), fermented yeast extract (FYE), hydrogen, or none (-)). Note, the experiments that received butyrate and lactate also received YE. The bar graph displays the overall cumulative respiration rate of each experiment. For cultures displaying inhibition, this respiration rate slowed in the last 24-48 hours.

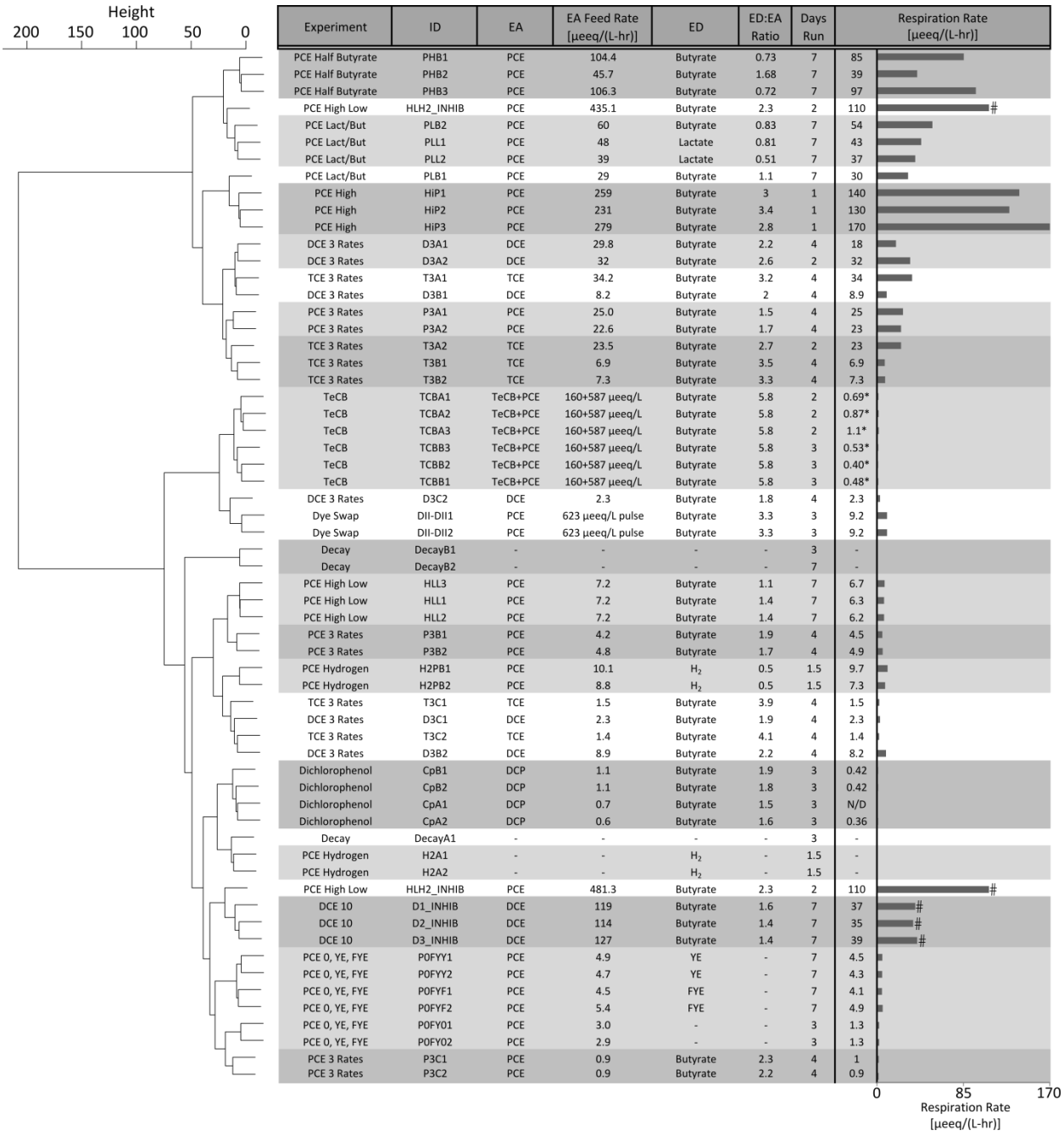

Experiment	ID	EA	EA Feed Rate [µeeq/(L-hr)]	ED	ED:EA Ratio	Days Run	Respiration Rate [µeeq/(L-hr)]
PCE Half Butyrate	PHB1	PCE	104.4	Butyrate	0.73	7	85
PCE Half Butyrate	PHB2	PCE	45.7	Butyrate	1.68	7	39
PCE Half Butyrate	PHB3	PCE	106.3	Butyrate	0.72	7	97
PCE High Low	HLH2_INHIB	PCE	435.1	Butyrate	2.3	2	110 #
PCE Lact/But	PLB2	PCE	60	Butyrate	0.83	7	54
PCE Lact/But	PLL1	PCE	48	Lactate	0.81	7	43
PCE Lact/But	PLL2	PCE	39	Lactate	0.51	7	37
PCE Lact/But	PLB1	PCE	29	Butyrate	1.1	7	30
PCE High	HiP1	PCE	259	Butyrate	3	1	140
PCE High	HiP2	PCE	231	Butyrate	3.4	1	130
PCE High	HiP3	PCE	279	Butyrate	2.8	1	170
DCE 3 Rates	D3A1	DCE	29.8	Butyrate	2.2	4	18
DCE 3 Rates	D3A2	DCE	32	Butyrate	2.6	2	32
TCE 3 Rates	T3A1	TCE	34.2	Butyrate	3.2	4	34
DCE 3 Rates	D3B1	DCE	8.2	Butyrate	2	4	8.9
PCE 3 Rates	P3A1	PCE	25.0	Butyrate	1.5	4	25
PCE 3 Rates	P3A2	PCE	22.6	Butyrate	1.7	4	23
TCE 3 Rates	T3A2	TCE	23.5	Butyrate	2.7	2	23
TCE 3 Rates	T3B1	TCE	6.9	Butyrate	3.5	4	6.9
TCE 3 Rates	T3B2	TCE	7.3	Butyrate	3.3	4	7.3
TeCB	TCBA1	TeCB+PCE	160+587 µeeq/L	Butyrate	5.8	2	0.69*
TeCB	TCBA2	TeCB+PCE	160+587 µeeq/L	Butyrate	5.8	2	0.87*
TeCB	TCBA3	TeCB+PCE	160+587 µeeq/L	Butyrate	5.8	2	1.1*
TeCB	TCBB3	TeCB+PCE	160+587 µeeq/L	Butyrate	5.8	3	0.53*
TeCB	TCBB2	TeCB+PCE	160+587 µeeq/L	Butyrate	5.8	3	0.40*
TeCB	TCBB1	TeCB+PCE	160+587 µeeq/L	Butyrate	5.8	3	0.48*
DCE 3 Rates	D3C2	DCE	2.3	Butyrate	1.8	4	2.3
Dye Swap	DII-DII1	PCE	623 µeeq/L pulse	Butyrate	3.3	3	9.2
Dye Swap	DII-DII2	PCE	623 µeeq/L pulse	Butyrate	3.3	3	9.2
Decay	DecayB1	-	-	-	-	3	-
Decay	DecayB2	-	-	-	-	7	-
PCE High Low	HLL3	PCE	7.2	Butyrate	1.1	7	6.7
PCE High Low	HLL1	PCE	7.2	Butyrate	1.4	7	6.3
PCE High Low	HLL2	PCE	7.2	Butyrate	1.4	7	6.2
PCE 3 Rates	P3B1	PCE	4.2	Butyrate	1.9	4	4.5
PCE 3 Rates	P3B2	PCE	4.8	Butyrate	1.7	4	4.9
PCE Hydrogen	H2PB1	PCE	10.1	H_2	0.5	1.5	9.7
PCE Hydrogen	H2PB2	PCE	8.8	H_2	0.5	1.5	7.3
TCE 3 Rates	T3C1	TCE	1.5	Butyrate	3.9	4	1.5
DCE 3 Rates	D3C1	DCE	2.3	Butyrate	1.9	4	2.3
TCE 3 Rates	T3C2	TCE	1.4	Butyrate	4.1	4	1.4
DCE 3 Rates	D3B2	DCE	8.9	Butyrate	2.2	4	8.2
Dichlorophenol	CpB1	DCP	1.1	Butyrate	1.9	3	0.42
Dichlorophenol	CpB2	DCP	1.1	Butyrate	1.8	3	0.42
Dichlorophenol	CpA1	DCP	0.7	Butyrate	1.5	3	N/D
Dichlorophenol	CpA2	DCP	0.6	Butyrate	1.6	3	0.36
Decay	DecayA1	-	-	-	-	3	-
PCE Hydrogen	H2A1	-	-	H_2	-	1.5	-
PCE Hydrogen	H2A2	-	-	H_2	-	1.5	-
PCE High Low	HLH2_INHIB	PCE	481.3	Butyrate	2.3	2	110 #
DCE 10	D1_INHIB	DCE	119	Butyrate	1.6	7	37 #
DCE 10	D2_INHIB	DCE	114	Butyrate	1.4	7	35 #
DCE 10	D3_INHIB	DCE	127	Butyrate	1.4	7	39 #
PCE 0, YE, FYE	P0FYY1	PCE	4.9	YE	-	7	4.5
PCE 0, YE, FYE	P0FYY2	PCE	4.7	YE	-	7	4.3
PCE 0, YE, FYE	P0FYF1	PCE	4.5	FYE	-	7	4.1
PCE 0, YE, FYE	P0FYF2	PCE	5.4	FYE	-	7	4.9
PCE 0, YE, FYE	P0FY01	PCE	3.0	-	-	3	1.3
PCE 0, YE, FYE	P0FY02	PCE	2.9	-	-	3	1.3
PCE 3 Rates	P3C1	PCE	0.9	Butyrate	2.3	4	1
PCE 3 Rates	P3C2	PCE	0.9	Butyrate	2.2	4	0.9

Figure 2.2 (Continued)

an initial high respiration rate (~100 µeeq/(L-hr)), but PCE built up above its solubility limit at day 2 leading to solvent toxicity inhibiting PCE respiration. Additionally, the DCE "3 rate" mid-range replicates (DCE B1 and B2) did not fall into the same cluster. The remainder of the experiments and biological replicates plotted as expected supporting the reproducibility of the genome-wide transcriptional response captured on microarrays.

2.D.3. Overall redesigned microarray characteristics

Considering the entire microarray set of the 1556 probes specific for DMC195 on the array, in at least one sample 1483, 977, and 219 probes exceeded a value of 100, 1000, and 10000 processed fluorescence units (pfu), respectively. This indicates that the array is effectively capturing 95.3% of all probes above a background level. Of those, 62.7% displayed confident expression above 1000 pfu. Additionally, the current dataset captures 12 and 9 out of the putative 17 RDases at an intensity of 100 and 1000 pfu or greater, respectively. A cutoff of 100 pfu discovers transcripts whose detection was above background signal. The second cutoff of 1000 pfu indicates transcripts that were highly confident and abundant on the microarray.

2.D.4. Gene transcript clusters

After examining the clustering of experiments, genes with similar behavior was explored with a K-means clustering technique. This technique was able to assign all genes into statistically distinct clusters (69). However, the hindrance to employing a K-means clustering technique was that the number of clusters assigned must be set prior to analysis. The general selection technique, $k \approx \sqrt{N=59/2} = 5.43$ clusters, was supported by the elbowed shape of the scree plot of the sum of square of residuals versus the discrete cluster number displaying an inflection point

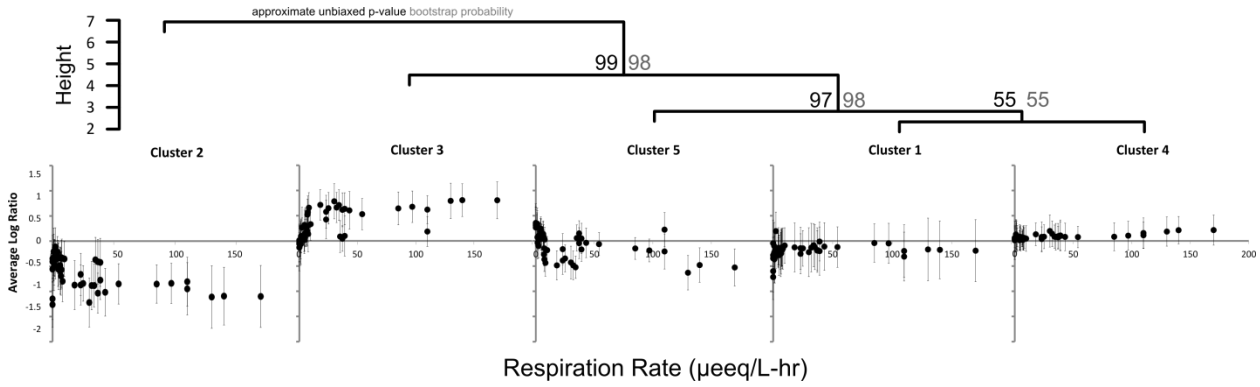

Figure 2.3. Breakdown of the of individual genes' expression patterns into K-means clusters based on log fold change compared to a 3-day starved control. (a) Euclidean distance and Ward hierarchical clustering dendogram comparing the similarities of the 5 selected K-means clusters. The approximated unbiased p-value for each cluster division is presented above the intersection in black with the bootstrap probability presented in grey. (b) Scatterplots plotting the centroid value against the experimental respiration rates (µeeq/L-hr) for all chlorinated ethenes (with standard deviation intervals about the mean of all transcripts in the K-means cluster).

at 5 clusters (not shown). The shape of the scree plot makes selecting between 4, 5, or 6 clusters arbitrary. Therefore, 5 clusters were selected as the general selection criteria indicated this number as a good fit. A hierarchal dendogram displaying the relationship among the five clusters is displayed in Figure 2.3.a. Other clustering techniques, such as the cluster affinity search technique (CAST) (9), gave similar results (data not shown). Selecting 5 K-means clusters as the breakdown, Figure 2.3.b displays the cluster's centroid log ratio expression value versus respiration. Cluster 3 displays a general positive trend in response to respiration rate while Clusters 2 and 5 displays a general negative trend (Clusters 1 and 4 display centroids that remain nearly constant). This bifurcation is important to note as the majority of rapid respiration rate linked RDases (*tceA, pceA,* DET1559), respiration chain elements (*hup* (DET0110-0112), *hym* (DET0145-0148), "*fdh*" (DET0185-0187), *ATPase* (DET0558-0560,0562-0565), *vhu* (DET0614-0615), *ech* (DET0860-0867), *nuo* (DET0924-0926,0928-0929,0931-0932)), ribosomal proteins, and growth and chaperonin related transcripts (*ftsZ* (DET0342-0343), putative S-layer (DET1407), *groES/EL* (DET1427-1428)) are members of Cluster 3 while the slow respiration linked RDases (DET0173, DET1535, DET1538, and DET1545) and three redoxin type electron carrier proteins (glutaredoxin (DET0198), rubrerythrin/rubredoxin (DET0406), thioredoxin (DET0661)) are members of Cluster 2. The remaining predicted redoxin type electron carrier proteins are found in cluster 5 (ferredoxin (DET1150)) and cluster 4 (flavodoxin (DET1501) and desulforedoxin (DET1623)). Hierarchically clustering the subunits of those transcripts identified as putatively involved in the respiration of the cell supported the K-means finding of fast- and slow-respiration linked enzymes clustering together (Appendix Figure A1.1).

Across all clusters, three centroid data points occurring around the 35 μeeq/(L-hr) respiration rate appear to be outliers. These centroids are noteworthy as they represent the DCE_INHIB experiments (respiration rate stalled and DCE concentrations began building in these samples). If the final 48 hours of respiration prior to sampling are considered, the respiration rate was actually around 2.4±1.8 μeeq/(L-hr) which shifts all three centroids to the left in the respiration diagrams of Figure 2.3.b. Following this adjustment, these points do not appear to be outliers and support the overall trend.

2.D.5. Respiration enzymes' transcriptional response to switching the electron acceptor type from chlorinated ethenes to chlorinated aromatics:

Figure 2.4.b displays the natural value differential expression of the individual RDases across a relatively consistent low-rate of respiration (1.4-4.8 μeeq/(L-hr)) with varying electron acceptor type (the electron donor in each case was butyrate). The *tceA* transcript is up-regulated in the DCP (1.8 ± 0.13 and 3.7 ± 0.21, for Mid and Low feeds) and TeCB (2.9 ± 0.71 and 8.0 ± 5.7, for 3 and 2 day experiments) to the same degree as the chlorinated ethenes (PCE, TCE, DCE ranging from 0.69 ± 0.05 to 9.7 ± 8.6) (Figure 2.4.b). DET1559 is up-regulated in all chlorophenol and chlorobenzene fed cultures (18 ± 4.0, 27 ± 4.1, 33 ± 11, 16 ± 2.5 fold for the DCP Low, DCP Mid, TeCB 2 Day, and TeCB 4 day experiments respectively). DET0318 *pceA*, DET1171, and DET1535 are all up-regulated in the chlorophenol fed cultures and not in the chlorobenzene cultures. DET0180 displays up-regulation in the DCE and TCE as well as the TeCB cultures (13 ± 2.3 and 4.9 ± 0.80 fold for the 1.5-Day and 3-Day cultures respectively) while significantly down-regulated in the DCP cultures ($7.9 \times 10^{-2} \pm 6.6 \times 10^{-3}$ and 0.25 ± 0.10 fold for the DCP Low and Mid cultures respectively). The distribution of the absolute intensity

of RDase spots for the varied electron acceptor types (Figure 2.4.b) reveals that for the PCE, TCE, and DCE fed cultures *tceA* dominates the RDase transcriptional pool, the DCP fed culture displays *pceA* as the dominant transcript comprising above 40% of the total summed RDase processed fluorescence, and DET0079 *tceA* is the dominant RDase in the TeCB cultures, but in both the 1.5-Day and 3-Day cultures DET1559 makes up 25% of the total RDase fluorescence. Additionally, the *tceA* transcript is not substantially down-regulated under DCP conditions, contradicting the observations of previous studies (25, 62).

The inclusion of representatives of the other putative respiratory chain enzymes in the analysis revealed that the majority of the transcripts are down-regulated under DCP conditions. However, three of these representative transcripts (*hyc* (DET1571), *vhu* (DET0615), and *ech* (DET0860)) did not display a significant difference between the DCP fed and chlorinated ethene fed cultures in terms of ratio to standard controls.

The analysis for DCP and TeCB specific response was expanded to include all transcripts in a rank-ordered list based on differential expression ratios for the DCP experimental series The highest differentially expressed for the DCP cultures was DET1171 (31 ± 15 fold), as previously indicated in Figure 2.4.b. Besides the two RDases DET1171 and DET1559, response regulators and hypothetical proteins heavily populate the top-responding transcripts following DCP provision. Two histidine kinase sensory boxes flanking RDases (DET0301 and DET1560), *pyrR* (DET1198, putative transcriptional binding protein of pyrimidine nucleotide biosynthesis), and *recX* (DET1607, putative regulatory protein for the DNA recombinase RecA) all displayed an up-regulation greater than ten-fold. Among the most down-regulated transcripts, a number of

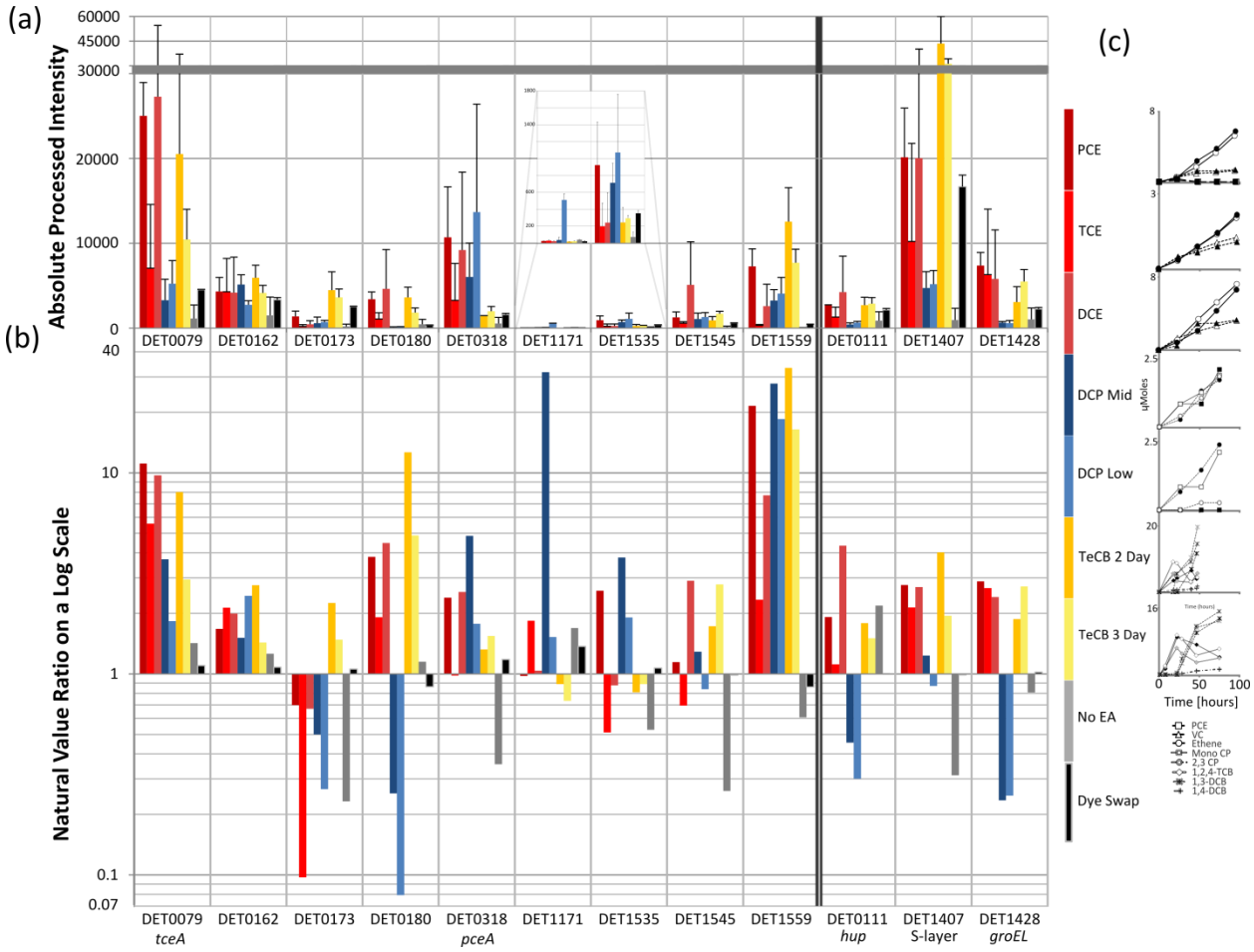

Figure 2.4. RDase distribution across different electron acceptors for the (left to right) PCE, TCE, DCE, DCP, TeCB, and No Acceptor fed conditions. (a) The absolute processed intensity value distribution of the 17 functional RDases, DET0162, and the *hup* (DET0111) transcript is plotted. Error bars represent standard error across biological replicates. The inset highlights the intensities of the *rdhA*s DET1171 and DET1535. (b) The natural value ratio compared to a 3-day starved culture for the transcripts in (a). (c) Chloro-organic concentrations with time for the varied cultures. The dye-swap considered above is a control array comparing a three-day starved pool to itself.

genes related to iron or cobalamin were present. These genes include two ABC transporters (DET0650 -0651 (corrinoid specific) and DET1176), cobalamin 5'-phosphate synthase (DET0658), cob(I)alamin adenosyltransferas (DET1224), and a biotin-Acetyl-CoA-carboxylase ligase (DET0849, also putatively described as a transcriptional repressor).

For the TeCB cultures, the most notable up-regulation in DMC195's genome outside of the mentioned RDases of DET1559, DET0180, and DET0079 was in the transcripts of Nuo (DET0928,0931,0933), ATpase (DET0559-0560), fdh (DET0187) and ftsA/Z cell division protein (DET0342,0343,0636). DET0650 was again down regulated as in the DCP experiments.

2.D.6. Interaction and possible regulation of reductive dehalogenase transcripts

The differential regulation of RDase transcripts under varied electron acceptor feeding rates and types suggests that these enzymes are tightly and specifically regulated. During the annotation of DMC195's genome, it was suggested that the regulation may be dependent on histidine kinase response regulator systems sensing either the halogenated compound of interest or the redox state of the cell as sensed by electron (or redox) carriers (75). Figure 2.5 summarizes the current dataset for putatively identified redox carriers and the regions neighboring the RDase operons. The RDases and surrounding enzymes are presented in cartoon gene position form, where the height of the gene symbol is proportional to 2^($\log_{10}$[average processed intensity across all arrays]) to allow for visual discrimination of abundant transcripts. The connecting lines drawn highlight any log-ratio interaction that exceeds a linear normal correlation score of 0.9 across 56 microarrays (decay sample series is excluded as we are interested in co-expression and not co-decay).

Figure 2.5. Correlation relationship of DMC195's electron carriers and RDase neighborhood genes across the microarray experiments. (a) Gene map plot of the reductive dehalogenase neighborhoods. The color coding highlights genes predicted to be involved in reductive dechlorination. RDase regulation, or RDase maturation. The height of the arrows illustrating transcripts is represented as 2^($\log_{10}$(average processed intensity across all arrays)). Lines connect transcripts that share a correlation value of $|r| \geq 0.9$. Dashed boxes highlight a series of genes (DET0080, 0179, 0234, and 0877) that displayed weak correlation to each other and reside in similar gene position with respect to *rdhAs*. (b) Scatterplot comparing the log ratio of DET0079 *tceA* to 0078 *rdhB*, 1407 the S-layer, and 1525 *rdhR*. (c) Scatterplot comparing the log ratio of DET1559 *rdhA* to 1558 *rdhB*. (d) Scatterplot comparing the log ratio of DET0661 thioredoxin to 0079 *tceA* and 1531 *rdhC*. (e) Scatterplot comparing the log ratio of DET0198 glutaredoxin to 1545 *rdhA*. (f) Average intensity expression of DMC195's putatively described redoxins with 95% confidence intervals.

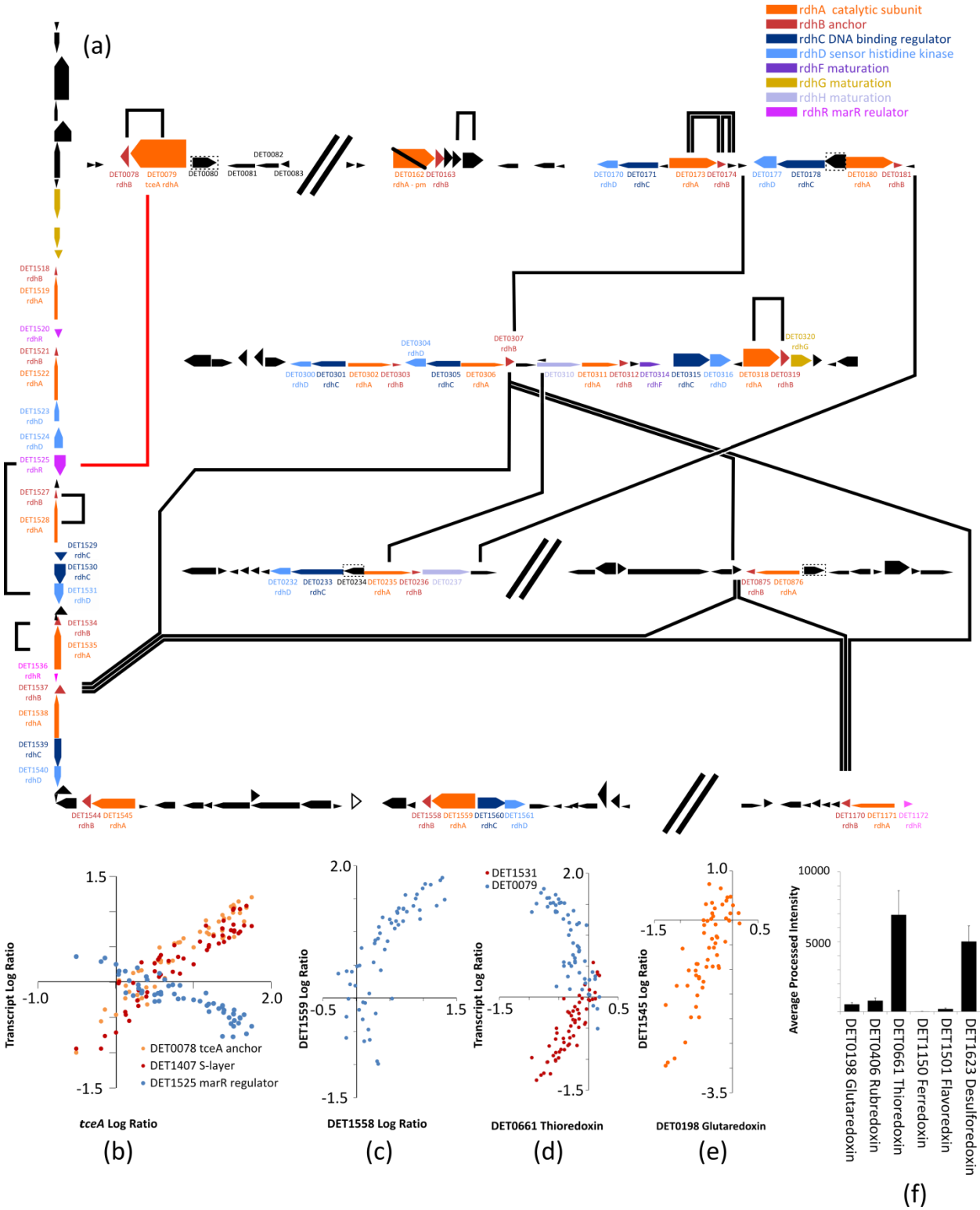

Figure 2.5 (Continued)

The relationships highlighted in this manner support the notion that the *rdhA* (catalytic) and *rdhB* (anchoring) subunits are coexpressed as 4 of the 7 confidently expressed RDases (DET0079-0078 (Figure 2.5.b), 0174-0175, 0318-0319, and 1535-1534; 1528-1527 as well but the pfu never exceeds 1000 on the microarrays) exceed a linear-correlation of r = 0.9. As seen in the scatter plot of DET1559 *rdhA*-1558 *rdhB* log-ratio displayed in Figure 2.5.c, even if the correlation does not meet a r=0.9 cutoff, a linear relationship still exists for the *rdhA-rdhB* subunit series (DET0180-0181, 1538-1537, 1545-1544, and 1559-1558 display an r of 0.78, 0.68, 0.87, and 0.77 respectively). The *rdhB*'s of 3 additional RDase operons (DET0307, 1170, and 1537) are all highly correlated with each other and the transcript DET0874, a hypothetical gene neighboring the *rdhA* DET0876. A surprising relationship was found in the DET1525 *marR –tceA* interaction. Considering all the probes on the microarray, DET1525 displayed the greatest anti-correlation to *tceA* out of any transcript (followed by DET1529 *rdhD*, DET1531 *rdhC*, and DET1532 dinitrogenase iron-molybdenum cofactor with r's of -0.80, -0.85, and -0.85 respectively) and is highlighted in Figure 2.5.b. The strong inverse trend that DET1525 displays to *tceA* was in direct contrast to the positive correlation of DET0078 *rdhB* and DET1407, the S-layer cell wall protein. All three relationships were linear on a log-log scale.

The redox sensors serve as putative electron shuttles and sense the redox state of the cell. Out of the six putative redox carriers, DET0661 (thioredoxin type carrier) and DET1623 (desulforedoxin type carrier) were the highest in average processed intensity across all experiments (Figure 2.5.f). The thioredoxin type carrier displayed an inverse relationship to DET0079 *tceA* and a positive relationship to DET1531 *rdhC* (Figure 2.5.d). The desulforedoxin type carrier did not display a strong relationship to members of the RDase family and appears to

be constitutively on in the cell. The glutaredoxin type carrier displayed a positive relationship with DET1545 (Figure 2.5.e). A list of the top 20 positively and negatively correlated transcripts for 5 of the 6 redoxins (omitting ferredoxi,n DET1150, which was below set detection limits) is displayed in Appendix Table A1.2. The thioredoxin type carrier was correlated negatively to transcripts associated with faster respiration rates and growth (DET0078-0079 *tceA*, DET0110/0112 *hup*, DET0186 *fdh*, DET0559-0560 *ATPase*, DET0652-0653 *cobA*, and DET1407 putative S-layer) and positively to a series of transcripts identified to be involved in regulation (DET1411 dnaJ, DET1505 fur transcriptional regulator, DET1506 ssrA protein tagging for degradation/ribosome rescue, DET1525 *rdhR*, DET1529 *rdhC*, and 1531 *rdhD*). The glutaredoxin electron carrier is correlated positively with DET1545, a transcript that is expressed highly under electron acceptor limiting conditions (Figure 2.5.e). The flavoredoxin electron carrier is correlated positively with several ferredoxin oxidoreductases (DET0199, 0947) (Appendix Table A1.2).

2.E. Discussion:

Focusing on extending the current knowledge of the behavior of DMC195's RDases, the microarray results presented here cover a wide range of electron acceptor types and feeding rates. In the comparison of the batch fed culture to the continuous feed setup, two RDases (DET1545 and DET0180) were highly up-regulated under continuous feed conditions. These two RDases appear to be up-regulated in response to the lower electron acceptor concentrations in the continuously fed cultures as compared to the initial pulse the batch which is in agreement with previous reports (66-68). Although neither transcript is dominant in absolute intensity, the minor RDases potentially may serve as key enzymes when electron acceptor availability is low or, their

regulatory elements are sensitive to external electron acceptor concentrations. Additionally, a methylglyoxyl synthase (*mgsA* DET0137) was noted to be up-regulated in the batch cultures. The *mgsA* transcript will be discussed in more detail in Chapter 4.

In previous work with the mixed community culture D2, qRTPCR was used to monitor transcript levels of selected genes (66-68). The trends from that work with respect to the RDases' relationships to respiration rate are supported here with genome wide profiles. Namely, some highly expressed respiration chain elements and RDases up-regulate sharply in response to increased respiration rate or electron acceptor concentration before plateauing at the highest rates. In contrast, other RDases are up-regulated only at low respiration rates or electron acceptor concentrations while being down-regulated at higher rates. This trend was also supported by batch studies with DMC195 pure cultures where the low-respiration rate linked cluster of RDases is up-regulated upon entry into stationary phase (39). This bifurcation of behavior in the RDase expression profiles between low and high rate of respiration may prove useful as field site biomarkers in determining the respiration state of the organisms *in situ*. However, though the expression patterns of these RDases are remarkably repeatable, their individual enzyme substrate ranges remain unknown, and future functional studies with purified enzymes are needed.

Focusing on responses specific to electron acceptor type, previous studies comparing PCE, TCE, and DCE at similar respiration rates showed changes in relative expression of the RDases (e.g. *pceA* was down-regulated slightly when TCE or DCE was fed when monitored by qRTPCR), but the differential expression was less than two fold (67). Feeding a different set of chloroorganic electron acceptors produced greater differential expression in the RDases

(2,22,25). The current study, in varying the electron acceptor type from chlorinated ethenes to aromatics (DCP, and TeCB) supports the majority of reported findings (25). DET1559 and *pceA* have previously been highlighted as two transcripts potentially involved in chlorophenol dechlorination (25). These two findings are supported in the current study by the dominance of *pceA* in the RDase absolute intensity distribution (Figure 2.4.a), and the high up-regulation of DET1559 (27 ± 4.1 fold for DCP compared to 4.4 ± 1.4 fold for PCE) when fed DCP. PceA has been suggested to be bifunctional, able to dechlorinate both PCE and chlorinated phenols (2).

Expanding these findings in the current study, the RDase DET1171 was highly up-regulated in the duplicate DCP Mid fed cultures (31 ± 15 fold) while not significantly up-regulated in the remaining DCP Low, chloroethene, and chlorobenzene fed cultures (Figure 2.4.b). In Fung *et al.* 2007, the RDase DET1171 was presented as displaying significant up regulation, but was not highlighted due to low overall expression (in this regard, the results of the current microarray study support those previous findings). DET1171 has close ortholog RDases in the CBDB1, BAV1, and VS strains' genomes (95%, 95%, and 97% amino acid identity by BLAST analysis) as previously indicated (54)). Another generally poorly expressed RDase, DET1535 displays a similar but not as exaggerated pattern as DET1171, being expressed at 1.9 ± 0.5 and 3.8 ± 0.3 fold for the DCP Low and Mid experiments respectively. Additionally, the abundance was about two fold higher for DET1535 in the DCP Mid cultures as compared to DET1171 (1072 ± 129 to 510 ± 13.1 pfu respectively). Therefore, both of these enzymes showed a transcriptional recognition to the presence of chlorophenols, albeit at a low level. The translation and activity of these RDases would need to be investigated to confirm whether they

were involved in the reductive dechlorination of chlorophenols or were simply under the same regulation system of other enzymes responding to the electron acceptor switch.

The batch cultures fed 1,2,3,4-tetrachlorobenzene up-regulated the RDases DET1559 and DET0180 (33 ± 12, 16 ± 2.8; 12 ± 2.6, 4.8 ± 0.90 fold per RDase for the 2 and 3 day triplicate culture respectively). Not only were they the most up-regulated RDase transcripts, but were also in the top ten highest up-regulated transcripts for all genes on the arrays. Additionally, DET1559 achieved its highest intensity across all analyzed microarrays in the TeCB fed cultures. Taken in combination with the chlorophenol findings, DET1559 is a likely candidate to be one of the main RDases responsible for aromatic dehalogenation in DMC195 especially for chlorobenzenes. Further functional studies are required to determine if DET1559 is translated and active on the chlorinated aromatics. Literature evidence suggests this as a possibility as the proteomic survey done by Morris *et al.* 2007 found cbdbA80 in 2,3-DCP-grown CBDB1, a close homolog of DMC 195's DET1559.

The diverse transcript levels of the *rdhA* subunits suggest transcriptional regulation. A particular focus is placed on the dominantly expressed *tceA* transcript that contains no previously highlighted proximal putative regulators in the genome but does vary in expression level. The neighboring DET0080 is annotated as a helix-turn-helix transcriptional regulator and is expressed in the dataset. There is weak correlation evidence that it is expressed similarly to genes that are *cis*-regulatory elements of other RDases (DET0179, 0234, and 0877 with an r of 0.68, 0.66, and 0.67 respectively). There was minimal direct relationship of DET0080 to DET0079 (r=-0.3). This may be due to expression of a regulator not necessarily being linked to the actual

mechanism of regulation, or the requirement of a separate regulatory element for *tceA* transcription. Expanding the search of possible regulators to all regions surrounding the RDase transcripts, several strong relationships were highlighted. The *marR* DET1525 displayed the highest negative correlation to *tceA* out of any transcript in the whole genome (Figure 2.5.b) and *rdhD* DET1531 was directly linked to DET1525 (also displaying a high negative correlation r =-0.88 to *tceA*). In addition to the high negative correlation of expression to *tceA*, both of these genes (as well as the *tceA* transcript) are found in regions that are not orthologous with other DMC strains CBDB1, BAV1, GT, and VS (54). The uniqueness of the *tceA*, DET1525, and DET1531 transcripts to DMC195 increases the potential that the relationship these genes show with *tceA* is indicative of a biological process linked either to similar environmental response or direct transcriptional regulation. Therefore, DET1525 and DET1531 are good candidates to explore in future work as potential transcriptional repressors of *tceA*. From this dataset, it appears that the regulation of the *rdhA-B* expression is not limited to *marR* or histidine-kinase response regulators that are located adjacent to the regulated transcript.

Potentially involved in the regulation of the *rdhA* expression are the concentrations and states of electron shuttles (redoxins). The ferroredoxin carrier was not detected in this experimental series. The absence of ferroredoxin-type protein may have been compensated by the presence of a flavoredoxin carrier; both carry low potential electrons and may not need to be expressed simultaneously. A desulforedoxin type carrier transcripts (DET1623) appeared to be at about the same high level across the majority of arrays, indicating that it does not fluctuate significantly with experimental conditions. Thioredoxin transcripts, however, decreased at higher respiration rates. Additionally, thioredoxin transcripts displayed a strong correlation (r = 0.92) to

DET1430, a transcript that maintains the dual annotation of a hydrogenase nickel incorporation protein HypA or a rubredoxin-type Fe(Cys)4 protein. Considering that desulforedoxin type proteins are similar to rubredoxin type proteins in structure, DET1430 may be considered another potential redox carrier, although rubredoxin is predicted to be involved in oxygen stress response of strictly anaerobic organisms (11). Although this experimental data only can speak to the correlation of transcript abundance and not specific states or mechanisms of action of the translated proteins, it was intriguing to find that the expression of redoxin type protein transcripts are correlated with key RDases (DET0079 and DET1545) as well as other predicted respiration linked enzymes. Previous predictions that redox carriers may serve as important cellular sensing components are supported by the current study (75).

2.F. Acknowledgements:

We would like to thank Dr. Laura Hug (University of Toronto) for her input and collaboration in the design of the microarrays, Dr. James Gossett (Cornell University) for his advice in the experimental setup, Jennifer Nelson (Cornell University) for her guidance in the chlorobenzene dechlorination experiments, Heather Fullerton (Cornell University) for her knowledge of DMC195, and the Cornell University Life Sciences Core Facilities Center for their help in developing and running the microarrays. Additionally, we would like to thank our funding sources, the Department of Defense Army Research Office (W911NF-07-1-0249), the National Science Foundation CBET Program (CBET-0731169), and the NSF- IGERT funded Biogeochemistry and Environmental Biocomplexity small grant program (DGE 0221658). Additionally, we would like to thank the NSF Graduate Research Fellowship Program for funding Cresten Mansfeldt in this research.

REFERENCES:

1. Adrian, L., Szewzyk, U., Wecke, J., & Gorisch, H. (**2000**). Bacterial dehalorespiration with chlorinated benzenes. *Nature*, 408: 580–583.

2. Adrian, L., Hansen, S. K., Fung, J. M., Görisch, H., & Zinder, S. H. (**2007**). Growth of *Dehalococcoides* Strains with Chlorophenols as Electron Acceptors. *Environmental Science & Technology*, 41: 2318-2323.

3. Adrian, L., Rahnenfuhrer, J., Gobom, J., & Holscher, T. (**2007**). Identification of a chlorobenzene reductive dehalogenase in *Dehalococcoides* sp. strain CBDB1. *Applied & Environmental Microbiology*, 73: 7717–7724.

4. Agilent Technologies. (**2009**). Agilent Feature Extraction Software (v10.7) Reference Guide. Santa Clara, CA.

5. Agilent Technologies. (**2010**). Agilent Genomic Workbench 6.0 User Guide. Santa Clara, CA.

6. Agilent Technologies. (**2010**). Microarray-Based Gene Low Input Quick Amp Labeling. Gene Expression Analysis Protocol. Santa Clara, CA.

7. Ballerstedt, H., Hantke, J., Bunge, M., Werner, B., Gerritse, J., Andreesen, J. R., & Lechner, U. (**2004**). Properties of a trichlorodibenzo-p-dioxin-dechlorinating mixed culture with a *Dehalococcoides* as putative dechlorinating species. *FEMS Microbiology & Ecology*, 47: 223–234.

8. Bedard, D.L., Ritalahti, K. M., & Loffler, F. E. (**2007**). The *Dehalococcoides* population in sediment-free mixed cultures metabolically dechlorinates the commercial polychlorinated biphenyl mixture Aroclor 1260. *Applied & Environmental Microbiology*, 73: 2513–2521.

9. Ben-Dor, A, Shamir, R., & Yakhini, Z. (**1999**). Clustering gene expression patterns. *Journal of Computational Biology*, 6:281-97.

10. Bowman K. S., Moe, W. M., Rash, B. A., Bae, H., & Rainey, F. A. (**2006**). Bacterial diversity of an acidic Louisiana groundwater contaminated by dense nonaqueous-phase liquid containing chloroethanes and other solvents. *FEMS Microbiology Ecology*, 58:120-33.

11. Brioukhanov, A.L. (**2008**). Nonheme iron proteins as an alternative system of antioxidant defense in the cells of strictly anaerobic microorganism: A review. *Applied Biochemistry and Microbiology*, 44: 335-348.

12. Bunge, M., L. Adrian, A. Kraus, M. Opel, W.G. Lorenz, J.R. Andreesen, H. Görisch, & U. Lechner. (**2003**). Reductive dehalogenation of chlorinated dioxins by an anaerobic bacterium. *Nature*, 421: 357-360.

13. Bunge, M., Kähkönen, M. A., Rämisch, W., Opel, M., Vogler, S., Walkow, F., Salkinoja-Salonen, M., & Lechner, U. (**2007**). Biological activity in a heavily organohalogen-contaminated river sediment. *Environmental Science and Pollution Research,* 14: 3-10.

14. Bunge, M., Wagner, A., Fischer, M., Andreesen, J. R., & Lechner, U. (**2008**). Enrichment of a dioxin-dehalogenating *Dehalococcoides* species in two-liquid phase cultures. *Environmental. Microbiology,* 10: 2670-2683.

15. Bürgmann, H., Kleikemper, J., Duc, L., Bunge, M., Schroth, M., & Zeyer, J.. (**2008**). Detection and quantification of *Dehalococcoides*-related bacteria in a chlorinated ethene-contaminated aquifer undergoing natural attenuation. *Bioremediation Journal,* 12:193–209.

16. Camacho, C., Coulouris, G., Avagyan, V., Ma, N., Papadopoulos, J., Bealer, K., & Madden, T. L. (**2008**). BLAST+: architecture and applications. *BMC Bioinformatics,* 10:421.

17. Cheng, D., & He, J. (**2009**). Isolation and characterization of '*Dehalococcoides*' sp. strain MB that dechlorinates tetrachloroethene to trans-1, 2-dichloroethene. *Applied & Environmental Microbiology,* 75: 5910–5918.

18. Duhamel, M., Mo, K., & Edwards, E. A. (**2004**). Characterization of a Highly Enriched *Dehalococcoides*-Containing Culture that Grows on Vinyl Chloride and Trichloroethene. *Applied & Environmental Microbiology,* 70: 5538-5545.

19. Duhamel, M., Wehr, S. D., Yu, L., Rizvi, H., Seepersad, D., Dworatzek, S., Cox, E., & Edwards, E. A. (**2002**). Comparison of anaerobic dechlorinating enrichment cultures maintained on tetrachloroethene, trichloroethene, cis-dichloroethene and vinyl chloride. *Water Research,* 36: 4193–4202.

20. Ellis, D. E., Lutz, E. J., Odom, J. M., Buchanan, R. J., Bartlett, C. L., Lee, M. D., Harkness, M. R., & DeWeerd, K. A. (**2000**). Bioaugmentation for accelerated in situ anaerobic bioremediation. *Environmental Science and Technology,* 34: 2254–2260.

21. Fennell, D. E., Gossett, J. M., & Zinder, S. H. (**1997**). Comparison of butyric acid, ethanol, lactic acid, and propionic acid as hydrogen donors for the reductive dechlorination of tetrachloroethene. *Environmental Science and Technology,* 31: 918-926.

22. Fennell, D. E., Nijenhuis, I., Wilson, S. F., Zinder, S. H., & Häggblom, M. M. (**2004**). *Dehalococcoides ethenogenes* strain 195 reductively dechlorinates diverse chlorinated aromatic pollutants. *Environmental Science and Technology,* 38: 2075-2081.

23. Field, J. A., & Sierra-Alvarez, R. (**2008**). Microbial degradation of chlorinated dioxins. *Chemosphere,* 71: 1005–1018.

24. Freedman, D.L., & Gossett, J. M. (**1989**). Biological reductive dechlorination of tetrachloroethylene and trichloroethylene under methanogenic conditions. *Applied & Environmental Microbiology,* 55: 2144-2151.

25. Fung, J. M., Morris, R. M., Adrian, L., & Zinder, S. H. (**2007**). Expression of reductive dehalogenase genes in *Dehalococcoides mccartyi* strain 195 growing on tetrachloroethene, trichloroethene, or 2,3-dichlorophenol. *Applied & Environmental Microbiology,* 73: 4439-45.

26. Futamata H., Yoshida, N., Kurogi, T., Kaiya, S., & Hiraishi, A. (**2007**). Reductive dechlorination of chloroethenes by *Dehalococcoides*-containing cultures enriched from a polychlorinated-dioxin-contaminated microcosm. *The ISME Journal,* 1: 471-9.

27. Grostern, A., & Edwards, E. A. (**2006**). Growth of *Dehalobacter* and *Dehalococcoides* spp. during degradation of chlorinated ethanes. *Applied & Environmental Microbiology,* 72: 428–436.

28. Harkness, M.R., Bracco, A. A., Brennan, M. J., DeWeerd, K. A., & Spivack, J. L. (**1999**). Use of bioaugmentation to stimulate complete reductive dechlorination of trichloroethene in Dover soil columns. *Environmental Science & Technology,* 33: 1100–1109.

29. He, J., Ritalahti, K. M., Yang, K. L., Koenigsberg, S. S., & Löffler, F. E. (**2003**). Detoxification of vinyl chloride to ethene coupled to growth of an anaerobic bacterium. *Nature,* 424: 62-65.

30. He, J., Sung, Y., Krajmalnik-Brown, R., Ritalahti, K. M., & Löffler, F. E. (**2005**). Isolation and characterization of *Dehalococcoides* sp. strain FL2, a trichloroethene (TCE)- and 1,2-dichloroethene-respiring anaerobe. *Environmental Microbiology,* 7: 1442-1450.

31. He, J., Holmes, V., Lee, P. K. H., & Alvarez-Cohen, L.. (**2007**). Influence of vitamin B12 and cocultures on the growth of *Dehalococcoides* isolates in defined medium. *Applied & Environmental Microbiology, 73*: 2847–2853.

32. Hendrickson, E. R., Payne, J. A., Young, R. M., Starr, M. G., Perry, M. P., Fahnestock, S., Ellis, D. E., and Ebersole, R. C. (**2002**). Molecular analysis of *Dehalococcoides* 16S ribosomal DNA from chloroethene-contaminated sites throughout North America and Europe. *Applied & Environmental Microbiology,* 68: 485-495.

33. Himmelheber D. W., Pennell, K. D., & Hughes, J. B. (**2007**). Natural attenuation processes during in situ capping. *Environmental Science & Technology,* 41: 5306-13.

34. Holliger, C., Wohlfahrt, G., & Diekert, G. (**1999**). Reductive dechlorination in the energy metabolism of anaerobic bacteria. *FEMS Microbiology Review,* 22:383-398.

35. Holmes, V. F., He, J., Lee, P. K., & Alvarez-Cohen, L. (**2006**). Discrimination of multiple *Dehalococcoides* strains in a trichloroethene enrichment by quantification of

their reductive dehalogenase genes. *Applied & Environmental Microbiology*, 72: 5877–5883.

36. Hölscher, T., Krajmalnik-Brown, R., Ritalahti, K. M., von Wintzingerode, F., Görisch, H., Löffler, F. E., & Adrian, L. (**2004**). Multiple nonidentical reductive-dehalogenase-homologous genes are common in *Dehalococcoides*. *Applied & Environmental Microbiology*, 70: 5290-5297.

37. Imfeld, G., Nijenhuis, I., Nikolausz, M., Zeiger, S., Paschke, H., Drangmeister, J., Grossmann, J., Richnow, H. H., & Weber, S. (**2008**). Assessment of in situ degradation of chlorinated ethenes and bacterial community structure in a complex contaminated groundwater system. *Water Research*, 42: 871–882

38. Johnson, D. R., Lee, P. K., Holmes, V. F., Fortin, A. C., & Alvarez-Cohen, L. (**2005**). Transcriptional expression of the tceA gene in a *Dehalococcoides*-containing microbial enrichment. *Applied & Environmental Microbiology*, 71: 7145-7151.

39. Johnson, D.R., Brodie, E. L., Hubbard, A. E., Andersen, G. L., Zinder, S. H., & Alvarez-Cohen, L. (**2008**). Temporal transcriptomic microarray analysis of '*Dehalococcoides ethenogenes'* strain 195 during the transition into stationary phase. *Applied & Environmental Microbiology*, 74: 2864–2872.

40. Johnson, D.R., Nemir, A., Andersen, G. L., Zinder, S. H., and Alvarez-Cohen, L. (**2009**). Transcriptomic microarray analysis of corrinoid responsive genes in *Dehalococcoides ethenogenes* strain195. *FEMS Letters*, 294: 198-206.

41. Korhonen, I. O. O. (**1983**). Glass-capillary gas chromatography of chlorobenzenes on SE-30 and Carbowax 20M columns: simultaneous determination of chlorobenzenes and chlorophenols. *Chromatographia*, 17: 195-199.

42. Krajmalnik-Brown, R., Hölscher, T., Thomson, I. N., Saunders, F. M., Ritalahti, K. M., & Löffler, F. E. (**2004**). Genetic identification of a putative vinyl chloride reductase in *Dehalococcoides* sp. strain BAV1. *Applied & Environmental Microbiology*, 70: 6347–6351.

43. Krajmalnik-Brown, R., Sung, Y., Ritalahti, K. M., Saunders, F. M., & Löffler, F. E. (**2007**). Environmental distribution of the trichloroethene reductive dehalogenase gene (tceA) suggests lateral gene transfer among *Dehalococcoides*. *FEMS Microbiology Ecology*, 59: 206-14.

44. Krajmalnik-brown, R., Ritalahti, K. M., Wintzingerode, F. V., Lo, F. E., & Adrian, L. (**2004**). Multiple nonidentical reductive-dehalogenase-homologous genes are common in *Dehalococcoides*. *Applied & Environmental Microbiology*, 70: 5290-5297.

45. Kube, M., Beck, A., Zinder, S. H., Kuhl, H., Reinhardt, R., & Adrian, L. (**2005**). Genome sequence of the chlorinated compound-respiring bacterium *Dehalococcoides* species strain CBDB1. *Nature Biotechnology*, 23: 1269-1273.

46. Lee, P. K. H., Cheng, D., Hu, P., West, K. A., Dick, G. J., Brodie, E. L., Andersen, G. L., Zinder, S. H., He, J., & Alvarez-Cohen, L. (**2011**). Comparative genomics of two newly isolated *Dehalococcoides* strains and an enrichment using a genus microarray. *The ISME Journal,* 5: 1014-1024.

47. Lee, P. K., Johnson, D. R., Holmes, V. F., He, J., & Alvarez-Cohen, L. (**2006**). Reductive dehalogenase gene expression as a biomarker for physiological activity of *Dehalococcoides* spp. *Applied & Environmental Microbiology*, 72: 6161-6168.

48. Lee, P. K., Macbeth, T. W., Sorenson, K. S. Jr., Deeb, R. A., & Alvarez-Cohen, L. (**2008**). Quantifying genes and transcripts to assess the in situ physiology of *Dehalococcoides* spp. in a trichloroethene-contaminated groundwater site. *Applied & Environmental Microbiology,* 74: 2728-2739.

49. Lendvay, J. M., Löffler, F. E., Dollhopf, M., Aiello, M. R., Daniels, G., Fathepure, B.Z., Gebhard, M., Heine, R., Helton, R., Shi, J., Krajmalnik-Brown, R., Major, C. L. Jr., Barcelona, M. J., Petrovskis, E., Hickey, R., Tiedje, J. M., & Adriaens, P. (**2003**). Bioreactive barriers: a comparison of bioaugmentation and biostimulation for chlorinated solvent remediation. *Environmental Science Technology*, 37: 1422–1431.

50. Liu, F. & Fennell, D. E. (**2008**). Dechlorination and detoxification of 1,2,3,4,7,8-hexachlorodibenzofuran by a mixed culture containing *Dehalococcoides ethenogenes* strain 195. *Environmental Science Technology*, 42: 602–607.

51. Löffler, F. E. & Edwards, E.A. (**2006**). Harnessing microbial activities for environmental cleanup. *Current Opinion in Biotechnology*, 17: 274–284.

52. Löffler, F. E., Yan, J., Ritalahti, K. M., Adrian, L., Edwards, E. A., Konstantinidis, K. T., Müller, J. A., Fullerton, H., Zinder, S. H., & Sproman, A. M. (**2012**). *Dehalococcoides mccartyi* gen. nov., sp. nov., obligate organohalide-respiring anaerobic bacteria, relevant to halogen cycling and bioremediation, belong to a novel bacterial class, *Dehalococcoidetes* classis nov., within the phylum *Chloroflexi*. *International Journal of Systematic and Evolutionary Microbiology*. Published online ahead of print.

53. McMurdie, P.J., Behrens, S. F., Holmes, S., & Spormann, A. M.. (**2007**). Unusual codon bias in vinyl chloride reductase genes of *Dehalococcoides* species. *Applied & Environmental Microbiology,* 73: 2744–2747.

54. McMurdie, P.J., Behrens, S. F., Müller, J. A., Göke, J., Ritalahti, K. M., Wagner, R., Goltsman, E., Lapidus, A., Holmes, S., Löffler, F. E., & Spormann, A. M. (**2009**). Localized plasticity in the streamlined genomes of vinyl chloride respiring *Dehalococcoides*. *PLoS Genetics*, 5:e1000714.

55. Magnuson, J. K., Stern, R. V., Gossett, J. M., Zinder, S. H., & Burris, D. R. (**1998**). Reductive dechlorination of tetrachloroethene to ethene by two-component enzyme pathway. *Applied & Environmental Microbiology,* 64: 1270-1275.

56. Magnuson, J. K., Romine, M. F., Burris, D. R., & Kingsley, M. T. (**2000**). Trichloroethene reductive dehalogenase from *Dehalococcoides ethenogenes*: Sequence of tceA and substrate range characterization. *Applied & Environmental Microbiology,* 66: 5141-5147.

57. Major, D. W., McMaster, M. L., Cox, E. E., Edwards, E. A., Dworatzek, S. M., Hendrickson, E. R., Starr, M. G., Payne, J. A., & Buonamici, L. W. (**2002**). Field demonstration of successful bioaugmentation to achieve dechlorination of tetrachloroethene to ethene. *Environmental Science &Technology,* 36: 5106–5116.

58. Maymó-Gatell, X., Chien, Y., Gossett, J. M., & Zinder, S. H. (**1997**). Isolation of a bacterium that reductively dechlorinates tetrachloroethene to ethene. *Science,* 276:1568-1571.

59. Maymó-Gatell, X., Anguish, T., and Zinder, S. H. (**1999**). Reductive dechlorination of chlorinated ethenes & 1, 2-dichloroethane by "*Dehalococcoides ethenogenes*" 195. *Applied & Environmental Microbiology,* 65: 3108-13.

60. McCarty, P. L. (**2010**). *In Situ Remediation of Chlorinated Solvent Plumes*. Clean Air. Springer. New York, NY.

61. Morris, R. M., Sowell, S., Barofsky, D., Zinder, S. H., & Richardson, R. E. (**2006**). Transcription and mass-spectroscopic proteomic studies of electron transport oxidoreductases in *Dehalococcoides ethenogenes*. *Environmental Microbiology,* 8: 1499-1509.

62. Morris, R. M., Fung, J. M., Rahm, B. G., Zhang, S., Freedman, D. L., Zinder, S. H., & Richardson, R. E. (**2007**). Comparative proteomics of *Dehalococcoides* spp. reveals strain-specific peptides associated with activity. *Applied & Environmental Microbiology,* 73:320-326.

63. Müller, J. A., Rosner, B. M., von Abendroth, G., Meshulam-Simon, G., McCarty, P. L., & Spormann, A. M. (**2004**). Molecular identification of the catabolic vinyl chloride reductase from *Dehalococcoides* sp. strain VS and its environmental distribution. *Applied & Environmental Microbiology,* 70: 4880-4888.

64. Nelson, J. L, Fung, J. M., Cadillo-Quiroz, H., Cheng, X., & Zinder, S. H. (**2011**). A Role for *Dehalobacter* spp. in the reductive dehalogenation of dichlorobenzenes and monochlorobenzene. *Environmental Science & Technology,* 45: 6806-6813.

65. Nijenhuis, I., & Zinder, S. H. (**2005**). Characterization of Hydrogenase and Reductive Dehalogenase Activities of *Dehalococcoides mccartyi* Strain 195. *Applied & Environmental Microbiology,* 71:1664-1667.

66. Rahm, B.G., & Richardson, R. E. (**2008**). Correlation of respiratory gene expression levels and pseudo-steady state PCE respiration rates in *Dehalococcoides*. *Environmental Science & Technology,* 42: 416–421.

67. Rahm, B.G., & Richardson, R.E. (**2008**). *Dehalococcoides'* gene transcripts as quantitative bioindicators of PCE, TCE and cDCE dehalorespiration rates: trends and limitations. *Environmental Science & Technology,* 42: 5099–5105.

68. Rahm, B.G., Morris, R. M., & Richardson, R. E. (**2006**). Temporal expression of respiratory genes in an enrichment culture containing *Dehalococcoides ethenogenes*. *Applied Environmental. Microbiology,* 72: 5486–5491.

69. Regeard, C., Maillard, J., Dufraigne, C., Deschavanne, P., & Holliger, C. (**2005**). Indications for acquisition of reductive dehalogenase genes through horizontal gene transfer by *Dehalococcoides ethenogenes* strain 195. *Applied & Environmental Microbiology,* 71: 2955-2961.

70. Richardson, R. E., Bhupathiraju, V. K., Song, D. L., Goulet, T. A., & Alvarez-Cohen, L. (**2002**). Phylogenetic characterization of microbial communities that reductively dechlorinate TCE based upon a combination of molecular techniques. *Environmental Science & Technology,* 36: 2652–2662.

71. Rowe, A. R., Heavner, G. L., Mansfeldt, C. B., Werner, J. J., & Richardson, R. E. (**2012**). Relating chloroethene respiration rates in *Dehalococcoides* to protein and mRNA biomarkers. *Environmental Science & Technology*, just accepted manuscript.

72. Rowe, A.R., Lazaar, B. J., Morris, R. M., & Richardson, R. E. (**2008**). Characterization of the community structure of a dechlorinating mixed culture and comparisons of gene expression in planktonic and biofloc-associated *Dehalococcoides* and *Methanospirillum* species. *Applied & Environmental Microbiology*, 74: 6709–6719.

73. Scheutz, C., Durant, N. D., Dennis, P., Hansen, M. H., Jorgensen, T., Jakobsen, R., Cox, E. E., & Bjerg, P. L. (**2008**). Concurrent ethene generation and growth of *Dehalococcoides* containing vinyl chloride reductive dehalogenase genes during an enhanced reductive dechlorination field demonstration. *Environmental Science & Technology,* 42: 9302-9309.

74. Schumacher, W., Holliger, C., Zehnder, A. J., and Hagen, W. R. (**1997**). Redox chemistry of cobalamin and iron-sulfur cofactors in the tetrachloroethene reductase of *Dehalobacter restrictus*. *FEMS Letters,* 409: 421-425.

75. Seshadri, R., Adrian, L., Fouts, D. E., Eisen, J. A., Phillippy, A. M., Methe, B. A., Ward, N. L., Nelson, W. C., Deboy, R. T., Khouri, H. M., Kolonay, J. F., Dodson, R. J., Daugherty, S. C., Brinkac, L. M., Sullivan, S. A., Madupu, R., Nelson, K. E., Kang, K. H., Impraim, M., Tran, K., Robinson, J. M., Forberger, H. A., Fraser, C. M., Zinder, S. H., and Heidelberg, J. F. (**2005**). Genome sequence of the PCE-dechlorinating bacterium *Dehalococcoides ethenogenes*. *Science,* 307: 105-8.

76. Smatlak, C. R., Gossett, J. M., & Zinder, S. H. (**1996**). Comparative kinetics of hydrogen utilization for reductive rechlorination of tetrachloroethene and methanogenesis in an anaerobic enrichment culture. *Environmental Science & Technology,* 30: 2850-2858.

77. Smidt, H., & de Vos, W. M. (**2004**). Anaerobic microbial dehalogenation. *Annual Review of Microbiology,* 58:43-73.

78. Sung, Y., Ritalahti, K. M., Apkarian, R. P., & Loffler, F. E. (**2006**). Quantitative PCR confirms purity of strain GT, a novel trichloroethene-to-ethene-respiring *Dehalococcoides* isolate. *Applied & Environmental Microbiology,* 72: 1980–1987.

79. Tang, Y.J., Yi, S., Zhuang, W., Zinder, S. H., Keasling, J. D., & Alvarez-Cohen, L. (**2009**). Investigation of carbon metabolism in "*Dehalococcoides ethenogenes*" strain 195 by use of isotopomer and transcriptomic analyses. *Journal of Bacteriology,* 191: 5224-31.

80. Vignais, P. M., Billoud, B., & Meyer, J. (**2001**). Classification and phylogeny of hydrogenases. *FEMS Microbiology Review,* 25: 455-501.

81. Wagner, A., Adrian, L, Kleinsteuber, S., Andreesen, J. R., & Lechner, U. (**2009**). Transcription analysis of genes encoding homologues of reductive dehalogenases in *Dehalococcoides* sp. strain CBDB1 using terminal restriction fragment length polymorphism and quantitative PCR. *Applied & Environmental Microbiology,* 75: 1876–1884.

82. Waller, A. S., Krajmalnik-Brown, R., Löffler, F. E., & Edwards, E. A. (**2005**). Multiple reductive-dehalogenase-homologous genes are simultaneously transcribed during dechlorination by *Dehalococcoides*-containing cultures. *Applied & Environmental Microbiology,* 71: 8257-8264.

83. Waller A. S. (**2009**). Molecular Investigation of Chloroethene Reductive Dehalogenation by the Mixed Microbial Community KB1. Ph.D. Thesis. University of Toronto.

84. Werner J. J., Ptak, A. C., Rahm, B. G., Zhang, S., & Richardson, R. E. (**2009**). Absolute quantification of *Dehalococcoides* proteins: enzyme bioindicators of chlorinated ethene dehalorespiration. *Environmental Microbiology,* 11:2687-97.

85. West, K. A., Johnson, D. R., Hu, P., DeSantis, T. Z., Brodie, E. L., Lee, P. K. H., Feil, H., Andersen, G. L., Zinder, S. H., & Alvarez-Cohen, L. (**2008**). Comparative genomics of '*Dehalococcoides ethenogenes*' 195 and an enrichment culture containing unsequenced '*Dehalococcoides*' strains. *Applied & Environmental Microbiology,* 74: 3533–3540.

86. Wohlfarth, G., & Diekert, G. (**1997**). Anaerobic dehalogenases. *Current Opinion Biotechnology,* 8: 290–295.

87. Yan, T., LaPara, T. M., & Novak, P. J. (**2006**). The reductive dechlorination of 2,3,4,5-chlorobiphenyl in three different sediment cultures. Evidence for the involvement of phylogenetically similar *Dehalococcoides*-like bacterial populations. *FEMS Microbiology & Ecology,* 55: 248–261.

88. Yoshida N., Takahashi, N., & Hiraishi, A. (**2005**). Phylogenetic characterization of a polychlorinated-dioxin- dechlorinating microbial community by use of microcosm studies. *Applied & Environmental Microbiology,* 71:4325-4334.

89. Yoshida, N., Asahi, K., Sakakibara, Y., Miyake, K., & Katayama, A. (**2007**). Isolation and quantitative detection of tetrachloroethene (PCE)-dechlorinating bacteria in unsaturated subsurface soils contaminated with chloroethenes. *Journal of Bioscience & Bioengineering* 104:91-97.

90. Zahurak, M., Parmigiani, G., Yu, W., Scharpf, R.B., Berman, D., Schaeffer, E., Shabbeer, S., & Cope, L. (**2007**). Pre-processing Agilent microarray data. *BMC Bioinformatics*, 8:142.

CHAPTER 3

Comparing Gene Expression Network Reconstructions for *Dehalococcoides mccartyi* Strains in Two Dehalorespiring Mixed Communities

3.A. Abstract

In this study, we apply Bayesian algorithms to infer systems-level biology and gene networks for the genetically intractable *Dehalococcoides* species. The metabolic responses and transcriptomes of two chloroethene-respiring mixed community cultures (D2 and the commercially available bioaugmentation agent KB-1®), both containing *Dehalococcoides mccartyi* strains, were monitored using microarrays under various experimental conditions including variations in electron acceptor type, electron donor type, and feeding rate. The D2 and KB-1® cultures were monitored using a *Dehalococcoides mccartyi* strain 195 specific and a pangenome (genus) microarray, respectively. The datasets (n = 48 and 30 culture samples for the D2 and KB-1 cultures, respectively) were applied to the Reverse-Engineering/Forward Simulation (REFS) Bayesian inference platform to develop a sparse network of gene-to-gene and gene-to-condition interactions. Key relationships discovered from this platform included linking the PCE respiration rate in the D2 culture to putative response regulators neighboring RDases (DET0315 and DET1530), positive interaction of respiration linked oxidoreductases *fdh, hup,* and *nuo* in both the D2 and KB-1® cultures, and connection of each that culture's dominant RDase (*tceA* and *vcrA* in the D2 and KB-1® communities, respectively) to the putative S-layer cell-wall protein. Specifically analyzing the RDases revealed high expression of the RDase homolog to DET1545|cbdb1638 in the commercial KB-1® culture, orders of magnitude higher than in the D2 culture. With multiple probes designed for each *Dehalococcoides* genus ortholog,

the pangenome microarray actually discriminated signals for two DET1545 homologs in the KB-1® culture. The probe for the lower abundance DET1545 homolog targeted *Dehalococcoides mccartyi* strains VS and 195. A broader investigation of the pangenome microarray's behavior revealed the successful recapture of two distinct probe-sets targeting different lineages of *Dehalococcoides*, even in core genes. The application of this array, therefore, provided a successful tool to monitor multiple *Dehalococcoides* strains in the commercial KB-1® culture.

3.B. Introduction

Dehalorespiring communities of microrganisms have been utilized at field sites to bioremediate common chlorinated organic pollutants (29,42). These pollutants include pervasive industrial solvents of the chlorinated ethene class (tetrachloroethene (PCE), trichloroethene (TCE), dichloroethene (DCE), and vinyl chloride (VC)). In these communities, the organisms that provide the crucial step of reductively dechlorinating VC to ethene (ETH) (32,33) are strains of *Dehalococcoides mccartyi* (DMC; 27). DMC is an obligate hydrogenotrophic dehalorespiring anaerobe, requiring hydrogen as an electron donor and chlorinated organics as an electron acceptor. The varied strains of DMC (195 (31), CBDB1 (1), VS (5), GT (45), BAV1 (13), FL2 (14), and MB (3)) contain a strain-specific suite of multiple reductive dehalogenases (RDases), enzymes responsible for the replacement of a halogen with a hydrogen which reduces the carbon atom. During dehalorespiration, each strain appears to utilize a unique cluster of RDases in response to environmental conditions (38,47).

The RDases provide an example of the current limitations associated with the biochemical characterization of enzyme behavior in DMC. Currently, only a handful of the

genome-predicted and transcriptionally-expressed RDases have been characterized through assays of enzymes from whole-cell extracts (PceA, TceA (28), CbrA (2), VcrA (36), and MbrA (4)). Successful characterization with whole-cell extracts relied on the fact that RDases are some of the most abundant proteins in the organism (2,35). Without a model organism able to serve as a suitable heterologous host (37), RDases detected at low (or no) abundances in proteomic studies (35) are limited in quantity, complicating biochemical assays.

Each DMC strain also maintains a novel set of predicted protein coding regions of unknown function. A hypothetical designation is applied to 360-520 proteins for each DMC strain, or about 25% of all predicted protein coding regions. The difficulty in investigating these enzymes is that even if they are able to be purified or detected in high abundance, a hypothesis of function would be required to select an appropriate biochemical assay.

A potential path around these issues is screening high-throughput data, such as transcriptomics from microarray analysis, to determine key relationships and hypotheses for functions (30). Previous studies have utilized this approach to discern the organism's behavior as it transitions from exponential growth to stationary phase (21), produces biosynthetic molecules through to the central carbon metabolism pathway (46), acquires and modifies key cofactors required for growth (22), fixes nitrogen (24), or grows under nitrogen limitation (26). These transcriptomic studies, with an experimental link to proteomics (40), have shown success in producing, testing, and confirming a wide range of hypotheses of DMC's behavior.

The main objective of this study was to determine relationships in the expression of transcripts for the DMC populations in two, mixed-community, reductively dechlorinating cultures (D2 Cornell University; Ithaca, NY and the commercially available KB-1® from SiREM Laboratories; Guelph, Ontario Canada). D2 was selected for this study because it is well studied and contains one DMC population (DMC195). In contrast, the KB-1® culture potentially contains multiple DMC populations and was selected for this uncharacterized community makeup as well as its direct field site applications. In detecting the transcript intensities for the KB-1® culture, this study also defined a secondary objective of applying a mixed microbial community with potentially multiple strains of DMC to a newly designed pangenome (genus) type microarray. Two other studies investigated the application of genomic DNA from various strains onto pangenome microarrays (17,26). This is the first study for DMC utilizing a pangenome microarray for transcriptomic analysis.

To achieve the main objective of determining highly confident relationships, this investigation employed a network inference platform. Previous systems biology based DMC reconstructions focused on applying a flux balance analysis to genome annotations (19) and correlations of transcript behavior (Chapter 2). This current study differentiated itself by utilizing a Bayesian network inference platform (Reverse Engineering/Forward Simulation (REFS™) developed by GNS Healthcare; Cambridge, Massachusetts) to investigate datasets containing the transcript abundance of hundreds of DMC genes monitored by microarrays. The resulting Bayesian network is comprised of nodes which are the random variables sampled (in this investigation the microarray gene transcript intensities as well as experimental conditions) and edges which are the conditionally dependent relationships that are established between the two

variables based on the analyzed dataset (10). The Bayesian platform is also designed to provide sparse predictions of relationships, creating a confident set of interactions to speak to the main objective. Separate model reconstructions on two independent datasets were performed for the D2 and KB-1® cultures to begin addressing the question of common DMC species gene networks as well as specific strain behavior in regards to expression and relationships of transcripts.

3.C. Materials and Methods

3.C.1. Culture growth and maintenance

The Donna II (D2) liquid culture maintained at Cornell University under conditions previously described (9,38,39) was used to provide the starter culture for all D2-based experiments. Each culture bottle contained 100 mL of 3-day starved D2 liquid culture and 60 mL of 70/30% $N2/CO_2$ (AIRGas) headspace. The KB-1® commercial culture was provided by SiREM Laboratories (Guelph, Ontario). After receipt, the liquid KB-1® was stored at 4° C under anaerobic conditions for less than one week prior to experimental run. Each experimental series was accompanied by a time-zero sample to account for batch-to-batch KB-1® differences. As similar to the D2 experimental series, each culture bottle contained 100 mL of KB-1® liquid culture and 60 mL of 70/30% $N2/CO_2$ (AIRGas) headspace.

3.C.2. Experimental culture growth

The experimental conditions run on the D2 culture have been summarized in previous publications (40, Chapter 3). The dataset used consists of continuous-feed experiments that were delivered varied rates of electron donor (butyrate (60% w/v ACROS Organics), lactate (99+% ACROS Organics), yeast extract (bacteriological grade, MoBio), fermented yeast extract, and no

donor) and acceptors (PCE (99+% Sigma Aldrich), TCE (99+% Sigma Aldrich), DCE (99+% Sigma Aldrich), 2,3-dichlorophenol (DCP; 99+% ACROS Organics), and no electron acceptor). Electron acceptor feed rates varied from 0 to 507 μeeq/L-hr. Electron donor-to-acceptor ratios varied from 0 to 3.4 in terms of μeeq. In total, 49 continuously fed D2 experiments were considered in the final model. A full summary of experimental conditions utilized in the model is attached in Appendix Table A2.1-2.

The experimental conditions run on the KB-1® culture were, in brief, a batch time-series (13 samples), a batch oxygen stress (7 samples; 1 control, 2 with no stress, 2 sampled six hours after stress, 2 sampled 48 hours after stress), a batch 1,1,1-trichloroethane (TCA) stress (7 samples; 1 control, 2 with no stress, 2 sampled six hours after stress, 2 sampled 48 hours after stress), and a continuous TCE steady-state, three-rate experiment (7 samples; 1 control, 3 sets of duplicates fed TCE at a low, mid, and high rate).

. *KB-1® Culture Batch Time Series.* Twelve 100-mL subcultures of KB-1® were batch-fed TCE (99.5%, Fisher), hydrogen (AIRGas), and acetate (99.7%, Fisher) as previously described (15). At 4.2, 8.3, 13.7, 23.1, 27.9, and 69.7 hours post batch feeding, duplicate 100-mL cultures were sacrificed for protein and nucleic acid extraction. Additional KB-1® experiments considered in the dataset were previously detailed in Appendix 4.

3.C.3. Metabolite monitoring by gas chromatography and ion chromatography

Flame Ionization Detecting (FID) gas chromatography (GC) (Perkin Elmer Autosystems GC, ARNER; SUPELCO 60/80 Carbopak B 1% SP-1000 8’x1/8” column) detected the

chlorinated ethene, ethene, and methane concentration levels for both the D2 and KB-1 culture growth conditions using methods previously detailed (7). Higher concentrations of methane were analyzed by GC total conductivity detection (TCD). Chlorophenols were extracted (l ml of liquid media by 500 µl of hexane) and the hexane extracts were assayed with a GC-FID analysis on a HP-1 column (5m × 0.53 mm with 2.65 µm film, Hewlett Packard) by a previously described method (Chapter 2). Low hydrogen levels were measured by GC with a reduction gas detector (RGD, Trace Analytical; SUPELCO 100/120 Carbosieve G 10'x1/8" column) and for higher concentrations, by GC TCD (41). In addition to gaseous components, the levels of acetate and butyrate in the D2 mixed cultures were monitored by ion chromatography (Dionex AS50; IONPAC AS14A 4x250mm column) as previously described (16).

3.C.4. Nucleic acid extraction and microarray hybridization protocol

In brief, 50 mL of mixed culture was centrifuged for 10 minutes, the supernatant was decanted, and the cell pellet was frozen and stored for less than 1 week at -80° C prior to nucleic acid extraction. RNA was extracted and purified from the cell pellet by a modified RNEasy (Ambion) protocol (39, 40). During the initial lysozyme step of the extraction protocol, 16 µL of 10^8 copies/µL of luciferase RNA (Promega) was added as an internal reference control. Contaminating DNA was then removed by DNAse digestion (TurboDNAse Ambion).

The protocol for transforming the RNA pool into a stable cDNA molecule with a cyanine-3 or -5 (Cy3 or Cy5) dye linker was conducted as previously described in Chapter 2 and adapted from Waller *et al.* 2010. In brief, the extracted RNA was reverse transcribed (Superscript II, Invitrogen) with an amino-allyl dUTP (GE Healthcare) into cDNA. After

purification (base hydrolysis and column cleanup (CyScribe DNA Columns, GE Healthcare)), the cDNA was then labeled by adding Cy3 or Cy5 (GE Healthcare). Either 400 or 800 ng of the labelled cDNA pool was then washed and hybridized by the Cornell University Life Sciences Microarray Division to an Agilent Two-Color 8-plex 15 K (Chapter 2) or 4-plex 30 K (17) microarray, respectively, as described below.

3.C.5. Microarray platform description

The D2 microarray (GEO platform GPL11218) was designed specifically for the genome of DMC195, the only DMC strain in the D2 community. Therefore, a single 60 mer probe was designed for each non-duplicated gene using the Agilent eArray software suite, as previously described (Chapter 2). The final array design consisted of probes for the genome of DMC195, 16S rRNA community member probes, several functional gene community member probes (hydrogenases), and a luciferase internal standard probe. Each probe spot was replicated at least eight times, distributed across the array.

The pangenome microarray used to analyze the commercial KB-1® culture was designed to target each DMC strain that was published at the time of design (DMC strains 195, BAV1, CBDB1, GT, and VS) as well as the DMC strain recovered from the laboratory-maintained KB-1 (KB-1-L) culture's metagenome (17). Therefore, multiple probes per homologous gene were constructed with varied lengths between 49 and 60 nucleotides. Each probe spot was replicated in at least four distributed locations across the array.

3.C.6. Microarray data processing

The microarray data for both the D2 and pangenome arrays was obtained from an Agilent Technologies Scanner G2505C by using Agilent's Feature Extraction Software. The data was background corrected and LOESS internal normalized. Identical probe spots were geometrically averaged. The raw data from the D2 microarray is freely available at the NCBI GEO database (GSE26288). The raw data from the pangenome microarray is freely available at the NCBI GEO database (GSE42136).

3.C.7. Dataset normalization prior to network inference

For both the D2 and pangenome microarrays, spots that did not display an intensity value above 100 pfu in at least one sample were removed from the dataset to select for gene expression values that were confidently detected above background. The list of probes exceeding the 100 pfu cutoff for the pangenome array includes multiple sequences targeting the same homologous gene. These probes often display highly correlated expression patterns. Therefore, the pangenome probe-set was sorted to bin probes that target the same homologous gene. If expression was highly correlated ($r > 0.9$), the probe displaying the higher intensity was kept in the final dataset. The lower intensity probe was masked from further analysis. Further filtering was required to reduce the number of variables analyzed in the model. To this end, instead of applying the filter to remove probes not exceeding 100 pfu in at least one array, the pangenome array was subjected to a more stringent filter of the mean value having to exceed 1000 pfu.

Combining all of the continuous variables together, the data was eighth root transformed (the 8^{th} root rather than log was used to permit for true zeros in the metabolite data, e.g. for a

sample not being fed a specific chlorinated electron acceptor). The dataset for D2 array run with D2 culture and the pangenome array run with KB-1® culture consisted of 49 (previously described, Chapter 3) and 32 samples, respectively. Additionally, three variations of the D2 dataset were analyzed. These included the absolute intensity with no principal components removed (AI nPC), absolute intensity with one principal component removed (AI 1PC; 1 PC was removed to eliminate global biases impacting the current dataset), or the ratio (Ratio) of the red channel to the green channel. The D2 dataset had more samples with fewer variables allowing it to be more sensitive in selecting an appropriate network construction method. The KB-1® model was larger and more computationally hard to solve; therefore only the predicted best network construction method selected in the D2 culture was run. The KB-1® (pangenome array) model was constructed only from the normalized ratio of the red to green channel.

3.C.8. Network inference ensemble construction

Reverse Engineering/Forward Simulation (REFS™) constructed network inference models from the collected data. Figure 3.1 displays a general work-flow of the model construction process. The model components (variables) that were incorporated were binned as continuous and discrete setup conditions established by the investigator as well as continuous (gene expression, respiration rates, and metabolite levels) and discrete experimental response variables (Appendix Figure A2.1-2). Discrete variables were dominated by censoring switches, binary operators that note the presence (1) or absence (0) of a particular state (e.g. when CensINHIB is 0, the culture did not display signs of inhibition; when 1, the culture displayed signs of inhibition). These disparate components were combined in a directed interaction form defined by Bayes theory (Bayesian network reconstruction) as displayed in Formula 3.1.

Figure 3.1. Bayesian network inference platform schematic diagram of transforming variables into a reconstructed network. The model components (a) were continuous experimental conditions set by the investigator, discrete experimental setup conditions set by the investigator, continuous experimental responses such as gene expression and metabolite levels, and discrete experimental responses. The network inference components are used in fragment enumeration (b). The parent may be any continuous experimental response or setup condition (e.g. microarray transcript abundance or metabolite level). The child may be any continuous experimental response. The discrete experimental setup conditions and responses were used to define the type of interaction. The default form is a direct linear relationship. Discrete drivers alter the direct linear to either a switched or conditional form. All possible fragments are scored and placed in a library of fragments. This library of fragments is sampled in the network inference (optimization) step (c) to select for the most likely network due to constraints. Multiple networks are constructed (1 through n) and the occurrence of a specific fragment appearing in a network is counted. The count is divided by the size of the ensemble (n = 1000 for current study) to yield a frequency (discrete/continuous variables are presented in Appendix Figure A2.1-2).

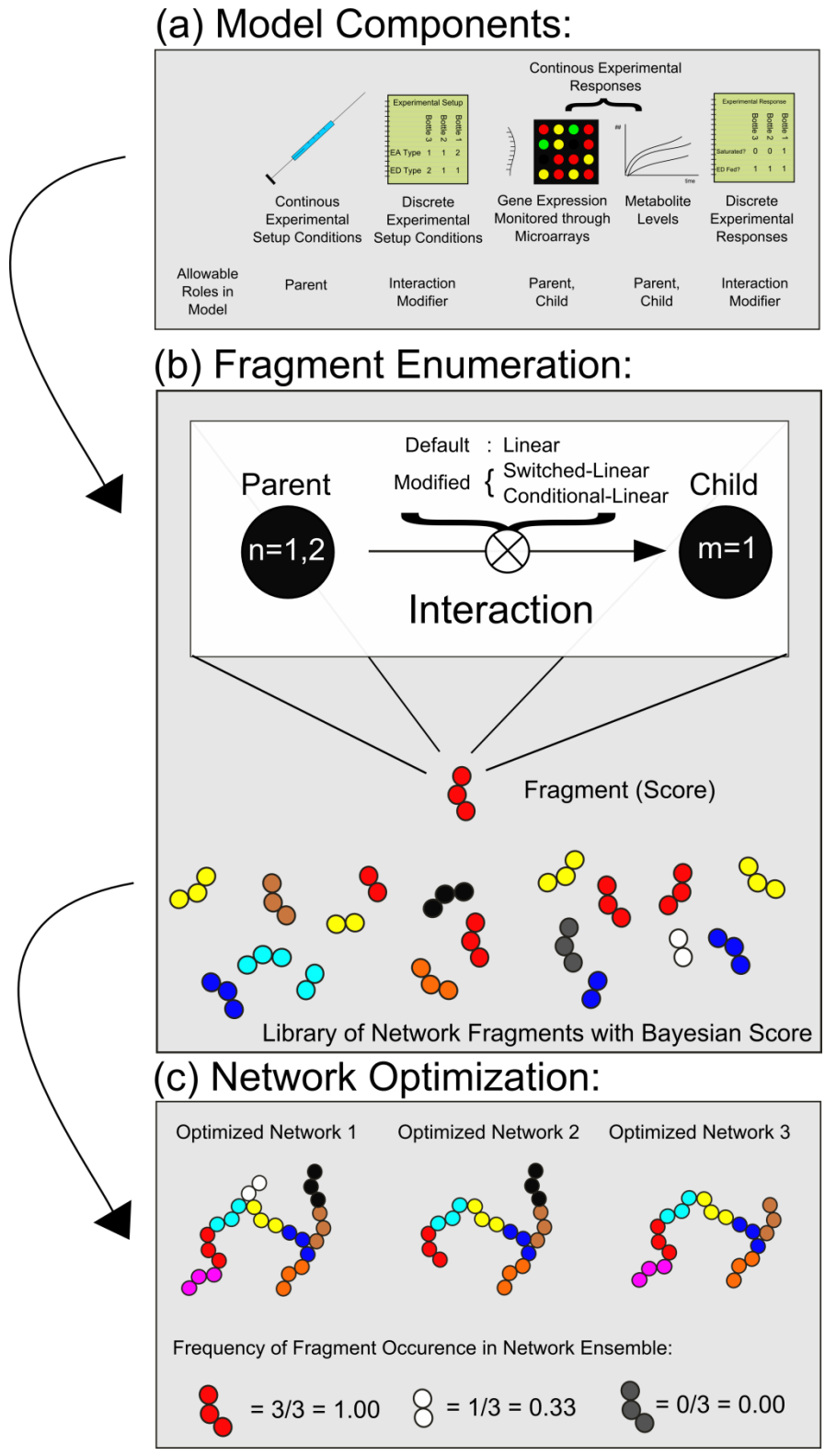

Figure 3.1 (Continued)

Formula 3.1 : $$\Pr(A|B) = \frac{\Pr(B|A)\Pr(A)}{\Pr(B)}$$

Pr(A) is the prior probability assigned to the interaction, Pr(A|B) is the posterior probability, and Pr(B|A)/Pr(B) is the amount of support that B (the data) provides the interaction.

The network inference platform was designed to look for specific variables that can cause (or drive) the expression or level of another variable (this is the posterior) during the fragment enumeration step (Figure 3.1.b). A fragment is defined as a single relationship (i.e. gene 1 was related to gene 2). The default relationship used to define fragments was a direct linear relationship between two variables (following 8^{th} root normalization of the dataset). However, the discrete experimental setup conditions and responses (e.g. electron donor type, electron acceptor type, and saturation) were used to modify the default linear relationships. An experimental parameter-modified relationship was considered a switched or conditional linear relationship. Switched-interactions-forms first bin the dataset by the discrete experimental conditions or responses and determine if a linear relationship exists between two variables in each integer-defined case. Conditional-interaction-forms first bin the dataset by discrete experimental conditions or responses and determine if a linear relationship exists in one of the bins. These fragments, the linear, conditional, and/or switched interactions, are composed of a parent (causing agent or driver) that can be any continuous variable (both setup conditions and responses) and a child (a dependent response) that can only be those variables not dictated by the investigator (continuous experimental responses). Fragments that have one parent driving the level of one child are described as being 1-to-1. More complex combinations of parents to

children are possible. To explore more complex network inference, 2-to-1 interaction forms were included that allowed the combined action of two parents to drive the level of a single child.

Considering the remaining components of Formula 3.1, the prior is a set belief that the interaction occurs. Two variants of priors were employed: the Bayesian Information Criterion (BIC) and the Gull prior (along with global priors that remained the same for both BIC and Gull networks). The Gull prior was the best suited for this dataset to describe the results of the model runs (12). The variation explored in network inference construction is summarized in Appendix Table A2.3.

After all possible fragments have been scored using the method described above during the enumeration step (Figure 3.1.b), the individual interactions comprising the fragment library are then sampled to form a constrained network model. In this case, a group of fragments were strung together in a directed acyclic graph (DAG), which was built and optimized by Monte Carlo sampling. To capture uncertainty in the network structure, this network inference step (optimization, Figure 3.1.c) constructed an ensemble of 1000 networks using the available fragment library. The frequency of occurrence (the f parameter) of a specific fragment in the 1000-network ensemble provided a means to rank interactions that display strong evidence of occurring in the optimized group (as illustrated in Figure 3.1.b). The strongest f values were greater than 900. Confidence is placed in any relationship predicted in over 500 of the 1000 models (f = 500). Values below f = 500 were considered to predict weaker interactions.

3.C.9. D2 operon hypergeometric distribution test:

The list of DMC195's predicted operons was obtained from microbesonline.org and compared to the database available at BioCyc. To determine if the representation of operon structure is over-represented in the final model, a hypergeometric distribution test was performed in R (phyper function of the stats package; (20)). This test samples the dataset without replacement, where the number of successes (total number of interactions described as a result of two genes residing on the same operon displaying a tight relationship) is withdrawn from the total population (all interactions of the model. This is compared against the total number of possible within-operon interactions (2146 possible within operon interactions) against the total possible model (2.33×10^5 possible interactions).

3.C.10. DMC reference dictionary establishment

A dictionary of all DMC genes was developed to streamline the referencing process across multiple strains. The dictionary was created by listing the non-duplicated genes of DMC195 first in ascending order of appearing in the genome. Homologs from the other sequenced DMC strains or unique strains recovered from available metagenome sequences (CBDB1 (1), VS (5), GT (45), BAV1 (14), and KB-1 (18)) were mapped onto DMC195's genome by a MAUVE alignment (6). An 85% nucleotide sequence identity across the entire coding region was used to determine homologous genes. The genes not targeting DMC195's genome, (those that did not display an 85% sequence similarity), were then listed in order for VS, then GT, then CBDB1, then BAV1, and finally KB1 with the same homolog-filtering mechanism as before. The final DMC dictionary is available from the author on request and as an electronic spreadsheet bundled with the microarray data in the NCBI GEO Database.

3.D. Results

The results portion of this text is broken into three main parts. First, we analyzed the performance of the microarrays and network ensembles as well as tested the validity of the models by determining if successful recapture of the known biological operon structure of bacterial mRNA was supported by the predictions. Second, we investigated the D2-based Bayesian inference's data-driven hypothesis with respect to connecting transcripts to experimental conditions, transcripts that encoded putative respiration and growth-linked enzymes to other variables, and RDases to first and second network neighbors. Third, we compared the network ensemble for the D2 mixed community to the network ensemble inferred for the KB-1® mixed community through similar analysis of the RDases and respiration linked enzymes.

3.D.1. Transcripts detected

The number of probes exceeding the 100 pfu filter for the D2 and pangenome arrays were 1503 (1437 DMC-specific) and 7103, respectively. Applying an additional filter to remove probes for homologous genes from the pangenome (KB-1®) dataset resulted in 5103 probes passing the correlation cutoff (linear-linear $r<0.9$). As described in the materials and methods, to further reduce the number of variables prior to network inference, the filter for the pangenome array was raised from exceeding 100 pfu at least once to exceeding a mean value of 1000 pfu. With this filter, 2503 probes remained. Comparing this list against the original design of the pangenome, the probes included 67.3% or 1584 out of 2352 homologous gene bins. Additionally, these probes represented 90.8%, or 917 out of 1009 homologous gene bins, that were predicted to be in all published DMC genomes (referred to as the DMC core genome). Therefore, 87.2% of all DMC195 genes and 67.3% of all DMC genus protein coding genes were

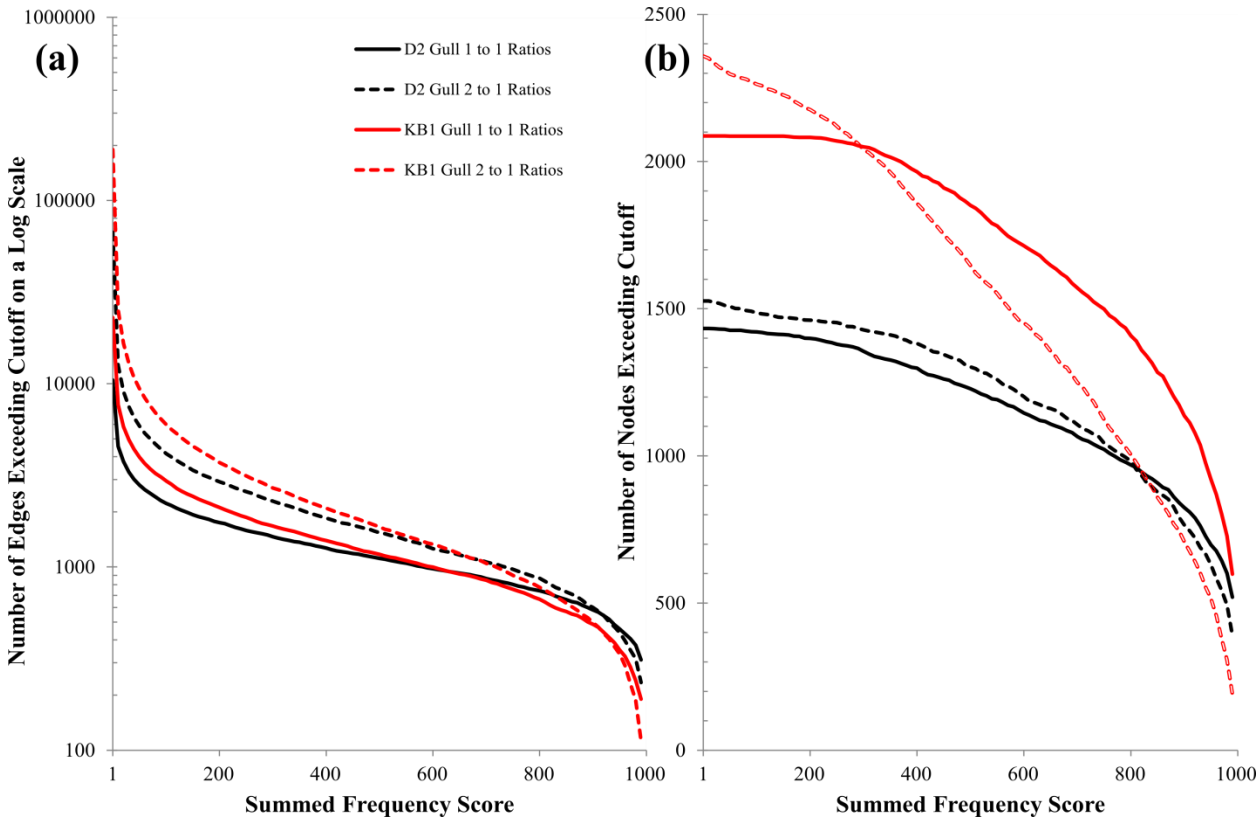

Figure 3.2. Summary of the number of nodes and edges found in each network ensemble at different frequency thresholds. (a) The number of edges and (b) the number of nodes remaining in the ensemble is plotted against the summed frequency score (the number of times the interaction appears in the ensemble) for the D2 and KB-1® cultures.

recaptured successfully and able to be used in REFS analysis of the D2 and KB-1® cultures, respectively.

3.D.2 D2 and KB-1® network ensemble summary and comparison

The two D2 and two KB-1® Gull network ensembles' respective counts of nodes (any variable in the model) and pairwise interactions were plotted against the frequency cutoff (f, the number of networks within the ensemble in which the specific interaction investigated was found which varies from 0 (never observed) to 1000 (in all networks)). This allowed the visualization of the similarity in the size and connectedness (number of edges per node) of the ensembles. Figure 3.2.a presents the cumulative distribution of nodes present as a function of the frequency cutoff and may be considered the size of the ensemble. A node was considered present if it participated in at least one interaction in the network ensemble with a frequency greater than that of the selected cutoff. The corresponding pairwise interaction (variable-to-variable) cumulative distribution is presented in Figure 3.2.b and, if divided by the number of nodes present, may be considered the connectedness of the network. At the f = 500 cutoff, the network ensembles were predicting 1228, 1302, 1851, and 1647 nodes and 1113, 1539, 1171, and 1656 edges for the D2 1-to-1, D2 2-to-1, KB-1® 1-to-1, and KB-1® 2-to-1 network ensembles, respectively.

3.D.3 Operon recovery from the D2 network ensemble

The ensemble of 1000 networks' ability to recover the *in silico* predicted polycistronic nature of the gene operons was tested to validate whether the networks were recovering known biological relationships. The edge frequency between members predicted to reside on the same transcript

Table 3.1. Operon recovery in the D2 ensemble of 1000 networks. The first column for both the 1-to-1 and 2-to-1 model runs displays the number of operons exceeding the summed frequency for all within operon relationships divided by the number of genes present on the operon. The second column displays the number of within operon relationships that exceed the frequency cutoff. The final column displays the hypergeometric p-value.

	1to1			2to1		
Summed Frequency Cutoff	Number of Complete Operons Exceeding Cutoff	Within Operon Interactions Exceeding Cutoff	p-value	Number of Complete Operons Exceeding Cutoff	Within Operon Interactions Exceeding Cutoff	p-value
1	96	315	$< 1 \times 10^{-300}$	148	601	$< 1 \times 10^{-300}$
100	62	160	4.46×10^{-233}	72	198	1.06×10^{-252}
200	54	146	1.71×10^{-221}	63	173	2.23×10^{-235}
300	46	137	2.02×10^{-214}	50	161	1.27×10^{-231}
400	34	123	7.06×10^{-195}	41	145	1.15×10^{-215}
500	26	115	1.08×10^{-185}	35	131	1.22×10^{-199}
600	24	107	1.12×10^{-175}	29	118	1.09×10^{-184}
700	20	96	5.60×10^{-158}	24	112	1.86×10^{-181}
800	17	89	6.06×10^{-150}	20	106	5.01×10^{-179}
900	15	81	2.02×10^{-141}	18	77	2.01×10^{-131}

(operon database available at www.microbesonline.org) was summed and normalized to the number of genes present on the operon to determine the occurrence of operons in the model. The total number of predicted within-operon interactions possible was 2416. Table 3.1 displays the results for the D2 1-to-1 and 2-to-1 Gull prior network ensembles constructed from the ratio dataset. The average frequency across the operon (column 1) identified 15 and 18 operons at the f = 900 cutoff for the 1-to-1 and 2-to-1 model, respectively. In addition, 81 and 77 interactions defined as operon related (column 2) were predicted in the network ensemble. For the 1-to-1 model, 601 total interactions were predicted to exceed f = 900. The hypergeometric test (column 3) compared the percentage of total operon specific interactions at the given cutoff (at f = 900, 81 operon specific interactions divided by the sample population of 601 or 13%) to the percentage of total operon interactions within all possible interactions (2416 total within operon relationships possible for DMC195 to the theoretical maximum 2.33×10^5 interactions possible or 0.1%). This test screens for enrichment in datasets. In this case, significant p-values predicted that the network ensemble was enriched in operons, a known biological organization that should exist.

3.D.4 Behavior of continuous experimental parameters in the D2 network ensemble

The connection of genes to continuous experimental parameters (Table 3.2) highlighted biomarkers of cellular activity and specific catalytic conversion steps in the ensembles. Using the 1-to-1 (f_{11}) and 2-to-1 (f_{21}) ensembles, several biological indicators were noted. Gene transcripts appeared significantly connected to the average levels of chlorinated phenols. The 2-to-1 network ensemble connected the steady-state DCP level (SSDCP_nM) to two RDase catalytic

Table 3.2. Connection of continuous experimental setup and metabolite responses to other variables in the D2 1-to-1 and 2-to-1 ensembles

Table 3.2 (Continued)

Experimental Variable	Variable Response	Description	1-to-1	2-to-1
Steady State DCE nM	DCErespn		-	804
	DET0057	ATP-dependent Clp protease, ClpC	981	-
	DET0132	rhomboid family protein	-	231
	DET0663	DNA-binding response regulator, LuxR	-	685
	DET1433	hydrogenase chaperone HypC/HupF	-	358
	EARATE		-	169
	PCErespn		-	118
	RespnRate		-	177
	SSTCE nM		237	-
Steady State TCE nM	DET0022	hypothetical protein	745	-
	DET0110	Hup hydrogenase large subunit	-	216
	DET0331	cation efflux family protein	-	339
	DET0620	hypothetical protein	-	136
	DET0643	ribose-5-phosphate isomerase B	-	122
	DET0911	aminopeptidase protein	-	140
	DET0997	translation elongation factor Tu	-	410
	DET1325	ribosomal protein L21	-	134
	DET1419	transcriptional regulator, AbrB family	-	648
	SSDCE nM		237	-
Steady State PCE nM	COM59	*Desulfobacter* 16S rRNA	238	148
	COM56	*Syntrophus* 16S rRNA	103	149
	DET1130	glutamine amidotransferase, class II	249	-
	DET1133	iron-sulfur cluster-binding protein	-	967
	DET1233	DNA-binding response regulator	399	-
	EARATE		206	994
Steady State MCP nM	DET0664	hypothetical protein	998	-
	DET1094	HNH endonuclease domain protein	-	424
Steady State DCP nM	DET0302	reductive dehalogenase, putative	-	776
	DET0736	oxidoreductase, short chain	-	224
	DET0991	ribosomal protein L10	998	-
	DET1305	hypothetical protein	-	776
	DET1559	reductive dehalogenase, putative	-	224
θ days	COM01	*Bacteroidetes* 16S rRNA	-	910
	DET tRNA-Phe-1	tRNA	-	803
	DET0027	potassium uptake protein, putative	-	128
	DET0051	hypothetical protein	-	594

Table 3.2 (Continued)

Experimental Variable	Variable Response	Description	1-to-1	2-to-1
DCErespn	EARATE		999	-
	RespnRate		999	1000
	SSDCE nM		-	804
	TCErespn		-	1000
TCErespn	DCErespn		-	1000
	PCErespn		-	1000
	RespnRate		1000	1000
PCErespn	DET0315	sensory box sensor histidine kinase	855	430
	DET0351	hypothetical protein	-	311
	DET0380	pyridoxine biosynthesis protein	-	149
	DET1039	SpoIIIJ-associated protein Jag	-	902
	DET1136	hypothetical protein	-	287
	DET1337	hypothetical protein	-	118
	DET1530	sensor histidine kinase	-	963
	RespnRate		1000	1000
	SSDCE nM		-	118
	TCErespn		-	1000
	ueeq total from YE		-	945
DCPrespn	DET0508	hypothetical protein	1000	-
	DET1094	HNH endonuclease domain protein	-	265
RespnRate last 48 hrs	DET1414	hypothetical protein	-	505
	RespnRate		1000	1000
RespnRate	DCErespn		999	1000
	DET0412	hypothetical protein	-	114
	DET1003	hypothetical protein	-	121
	EARATE		-	229
	PCErespn		1000	1000
	RespnRate last 48 hours		1000	1000
	SSDCE nM		-	177
	TCErespn		1000	1000
	Total eeq respired		1000	1000
Turnover	DET0052	queuine tRNA-ribosyltransferase	-	522
	DET0776	methyltransferase GidB	-	494
	DET1262	ribosomal protein L28	-	490
	DET1443	hypothetical protein	-	933
	DET1480	hypothetical protein	-	333
	DET1573	hydrogenase subunit Hyc	-	124
	DET1622	hypothetical protein	-	290

Table 3.2 (Continued)

Experimental Variable	Variable Response	Description	1-to-1
EARATE	COM43	*Syntrophus/Smithella* 16S rRNA	-
	COM56	*Syntrophus* 16S rRNA	-
	Acetate		-
	DCErespn		999
	DET0111	Hup hydrogenase small subunit	-
	DET0346	hypothetical protein	-
	DET0560	ATP synthase F0, B subunit	175
	DET0954	Hsp20/alpha crystallin family protein	-
	DET1128	glutamate synthase, alpha subunit	-
	RespnRate		-
	SSDCE nM		-
	SSPCE nM		206
EARATE last 48 hrs	DET0666	acetyl-CoA decarbonylase/synthase	-
	DET1337	hypothetical protein	-
	DET1534	RDase anchoring protein	-
ED/EA with YE	DET1005	transcriptional regulator, ArsR family	-
EDRATE total YE and ED	DET0871	transcriptional regulator, MarR family	978
	DET1337	hypothetical protein	-
ueeq total from YE	COM56	*Syntrophus* 16S rRNA	-
	Butyrate		-
	PCErespn		-
H2levelAvg	DET0147	[Fe] hydrogenase, large subunit HymC	248
Acetate	COM11	*Syntrophomonas* 16S rRNA	-
	COM56	*Syntrophus* 16S rRNA	-
	DET0129	hypothetical protein	-
	DET0922	twitching mobility protein	-
	DET1265	degV family protein	172
	DET1278	N utilization substance protein B	120
	DET1345	tagatose 1,6-diphosphate aldolase	296
	EARATE		-
Butyrate	COM43	*Syntrophus/Smithella* 16S rRNA	-
	COM56	*Syntrophus* 16S rRNA	996
	DET0520	daunorubicin resistance ABC transporter	-
	DET1310	hypothetical protein	-
	ueeq total from YE		1000
Methanogenesis	DET1430	hydrogenase nickel insertion HypA	934
	DET1520	transcriptional regulator, MarR family	-

subunits DET0302 (f_{21} = 776) and DET1559 (f_{21} = 224). Additionally, the average MCP level (SSMCP_nM, though steady-state MCP was not achieved as accumulation was noted) was inversely connected to a putative protein (DET0664) in the cobalamin transport operon (f_{11} = 998). Cobalamin is a central cofactor for the formation of functional RDases. Another way to consider the metabolite data was the rate of dehalogenation of the chlorinated organics (i.e. respiration rate). The specific respiration rate of PCE (PCERespnRate) was connected to DET0315 (f_{11} = 855, f_{21} = 430) in both D2 network ensembles. DET0315 is putatively annotated as the sensory box histidine kinase and is genomically located neighboring the PceA reductive dehalogenase (DET0318). Additionally, in the 2-to-1 network ensemble, PCE respiration was connected negatively to DET1530 (f_{21} = 963), another sensory box histidine kinase near several additional RDases. The network ensemble, therefore, directly connected RDase regulators to the respiration of chlorinated organics potentially underscoring regulatory pathways.

Other experimental variables also produced high confidence interactions. Methanogenesis rate was related to a DMC hydrogenase maturation protein, nickel incorporation protein *hypA* DET1430 (f_{11} = 934, f_{21} = 259). The rate of electron donor being fed (EDRATE_Total_YE_and_ED) was tightly connected to a *marR* transcriptional regulator DET0871 in both models (f_{11} = 978, f_{21} = 981). The genomic neighbor and operon member DET0872 was a putative MmpL type protein, potentially involved in fatty acid transport. Acetate was weakly connected to two *Syntrophus* species's 16S rRNA probes on the array (COM11 *Syntroponmonas* 16S rRNA, COM56 *Syntroponmonas* 16S rRNA; f_{12} = 303, 263). Acetate was also weakly connected to several DET genes in the 2-to-1 model including a tagatose 1,6-

diphosphate aldolase (DET1345, f_{21} = 386), a pilus assembly protein (DET0922, f_{21} = 128), and a hypothetical protein (DET0129, f_{21} = 201). Butyrate was connected with COM56 *Syntrophomonas* 16S rRNA (f_{11} = 1, f_{21} = 382) and COM43 *Syntrophus/Smithella* 16S rRNA (f_{21} = 834), community members that are predicted to be capable of fermenting butyrate. The connection was inverse in nature, when butyrate was detected, the *Syntrophus* 16S rRNA sequences signal was lower than when butyrate was absent in the samples. A main end product of butyrate fermentation, hydrogen (H2LevelAvg) was weakly connected to a hydrogenase (*hymC* DET0147 f_{21} = 124). Additional experimental parameters gene interactions are detailed in Table 3.2.

3.D.5. Behavior of discrete experimental parameters in the D2 network

Appendix Table A2.2 displays the discrete variables that modified the relationship of the connected variable for at least 500 interactions in both the 1-to-1 and 2-to-1 network inference ensembles. In this case, frequencies of modification greater than 1000 were expected as the discrete parameters were allowed to modify multiple strong relationships for the same gene. Of note from this, interactions for the oxidoreductase *mod* were modified by the censoring switch for DCE inhibition and interactions for the hydrogenase *hup* were modified by the censoring switch for general inhibition. This linked a discrete variable accounting for stressful conditions during DMC respiration to key hydrogenase transcripts potentially highlighting biomarkers of stress.

Table 3.3. Connection of respiration linked enzyme transcripts of *mod*, *hup*, *hym*, *fdh*, *atpase*, *vhu*, *ech*, *nuo*, and *hyc* in D2. Gray cells highlight within operon relationships. Yellow cells highlight between oxidoreductase relationships. Relationships presented exceed f = 500 in at least one of the 1-to-1 or 2-to-1 REFS D2 ensembles.

	Node1	Node2	Description	1to1	2to1
Mod	DET0103	COM38	*Nitrospira* 16S rRNA	-	917
	DET0103	DET0028	universal stress protein family	-	826
	DET0101	DET0099	*mobA* family protein	974	949
	DET0102	DET0103	*modC*	569	872
	DET0103	DET0342	cell division protein FtsA	-	803
	DET0102	DET0987	acetyltransferase, GNAT family	516	-
	DET0103	DET1504	ferrous iron transport protein	-	908
Hup	DET0112	DET0110	*hupA*	907	579
	DET0112	DET0111	*hupB*	923	965
	DET0112	DET0123	pyridine nucleotide-disulphide	999	1000
	DET0111	DET0187	*fdhA*	1000	883
	DET0112	DET0336	DNA-binding protein, putative	-	657
	DET0111	DET0351	hypothetical protein	448	573
	DET0111	DET0377	30S ribosomal protein S2	-	735
	DET0112	DET0614	*vhuG*	-	526
	DET0112	DET0832	acetolactate synthase, small su	512	-
	DET0110	DET0923	*nuoA*	997	984
	DET0112	DET1146	hypothetical protein	-	738
	DET0112	DET1273	hypothetical protein	986	983
	DET0112	DET1458	*comF* family protein, putative	-	572
Hym	DET0148	DET0001	chromosomal replication initiat	-	631
	DET0145	DET0045	redox family protein	-	642
	DET0145	DET0147	*hymC* large subunit	939	880
	DET0146	DET0148	*hymD* subunit	984	935
	DET0147	DET0148	*hymD* subunit	995	983
	DET0148	DET0648	hypothetical protein	-	996
	DET0148	DET0992	50S ribosomal protein L1	894	476
Fdh	DET0187	DET0111	*hup* small subunit	1000	883
	DET0187	DET0116	(authentic point mutation)	973	690
	DET0187	DET0186	formate dehydrogenase, membrane	1000	997
	DET0186	DET0191	iron-sulfur cluster-binding pro	562	-
	DET0185	DET0402	methyltransferase, UbiE/COQ5	-	528
	DET0185	DET0418	amino acid ABC transporter	829	874
	DET0186	DET0589	GTPase domain, tubulin/FtsZ fam	823	820
	DET0186	DET0636	cell division protein FtsZ	680	-
	DET0185	DET0803	hydroxymethyltransferase	880	233
	DET0185	DET0813	ABC transporter, ATP-binding pr	903	-
	DET0185	DET0864	*ech*	-	658
	DET0185	DET0974	puromycin N-acetyltransferase,	-	506
	DET0186	DET0997	translation elongation factor T	575	143
	DET0186	DET1225	hypothetical protein	775	-
	DET0185	DET1264	degV family protein	993	254
Vhu	DET0616	DET0059	cytidylyltransferase	526	-
	DET0614	DET0112	[Ni/Fe] hydrogenase, *hup*	-	526
	DET0615	DET0831	ketol-acid reductoisomerase	-	554
	DET0614	DET0966	prolipoprotein diacylglyceryl	-	747
	DET0616	DET1002	glycosyl transferase, group 1	998	981
	DET0615	DET1540	DNA-binding response regulator	-	829

	Node1	Node2	Description	1to1	2to1
ATPase	DET0564	DET0137	methylglyoxal synthase	687	-
	DET0563	DET0331	cation efflux family protein	275	625
	DET0564	DET0394	nucleoside diphosphate kinase	999	927
	DET0562	DET0417	amino acid ABC transporter, ATP	-	916
	DET0564	DET0417	amino acid ABC transporter, ATP	877	-
	DET0561	DET0449	isopropylmalate isomerase small	949	558
	DET0564	DET0494	preprotein translocase SecY	864	913
	DET0562	DET0513	S-adenosyl-L-homocysteine hydro	-	933
	DET0560	DET0558	ATP synthase F0, A subunit	-	593
	DET0560	DET0559	ATP synthase F0, C subunit	1000	999
	DET0562	DET0560	ATP synthase F0, B subunit	999	552
	DET0565	DET0563	ATP synthase F1, gamma subunit	1000	988
	DET0565	DET0564	ATP synthase subunit B	1000	939
	DET0560	DET0644	transketolase	801	150
	DET0562	DET0652	cobalamin/Fe3+-siderophores tra	935	374
	DET0560	DET0766	V-type H(+)-translocating pyrop	676	825
	DET0558	DET0788	nuclease SbcCD, D subunit	-	634
	DET0562	DET0801	pyrroline-5-carboxylate reducta	690	143
	DET0564	DET0803	hydroxymethyltransferase	-	707
	DET0565	DET0852	sodium extrusion protein NatB,	757	708
	DET0563	DET1033	long-chain-fatty-acid--CoA liga	629	415
	DET0560	DET1225	hypothetical protein	838	-
	DET0564	DET1225	hypothetical protein	-	599
	DET0564	DET1263	DAK2 domain protein	1000	981
	DET0558	DET1264	*degV* family protein	910	144
	DET0564	DET1264	*degV* family protein	994	845
	DET0565	DET1267	*degV* family protein	-	558
	DET0562	DET1279	acyl carrier protein	-	843
	DET0560	DET1290	NUDIX domain protein	-	728
	DET0559	DET1524	DNA binding response regulator	903	861
	DET0560	DET1595	ApbE/NosX family protein	830	452
	DET0565	DET1608	KH domain/HDIG domain protein	-	516
Hyc	DET1571	DET0122	hypothetical protein	482	816
	DET1573	DET0122	hypothetical protein	450	669
	DET1573	DET0151	hypothetical protein	751	-
	DET1574	DET0151	hypothetical protein	423	995
	DET1570	DET0469	hypothetical protein	750	-
	DET1573	DET0869	lysyl-tRNA synthetase-related	410	692
	DET1571	DET0960	imidazoleglycerol phosphate syn	954	995
	DET1571	DET1082	hypothetical protein	580	-
	DET1570	DET1084	DNA packaging protein, putative	-	988
	DET1575	DET1084	DNA packaging protein, putative	839	189
	DET1570	DET1106	hypothetical protein	1000	649
	DET1570	DET1249	hypothetical protein	815	646
	DET1575	DET1498	*crcB* protein, putative	1000	989
	DET1572	DET1571	*hycE*	930	780
	DET1574	DET1573	*hyc*	824	993
	DET1570	DET1593	hypothetical protein	-	845

	Node1	Node2	Description	1to1	2to1
Ech	DET0861	DET0029	Trk system potassium uptake	924	553
	DET0868	DET0052	queuine tRNA-ribosyltransferase	-	516
	DET0864	DET0185	*fdhE*	-	658
	DET0861	DET0376	elongation factor Ts	758	773
	DET0861	DET0413	cytidine/deoxycytidylate deamin	827	115
	DET0865	DET0413	cytidine/deoxycytidylate deamin	-	992
	DET0864	DET0420	hypothetical protein	992	994
	DET0860	DET0696	(authentic point mutation)	-	549
	DET0862	DET0857	ABC transporter, ATP-binding pr	-	657
	DET0862	DET0861	hydrogenase, *echB* subunit	941	1000
	DET0866	DET0861	hydrogenase, *echB* subunit	954	888
	DET0864	DET0863	hydrogenase subunit *hymA*	946	-
	DET0865	DET0864	hydrogenase subunit *hymB*	-	830
	DET0866	DET0865	hydrogenase subunit *hymC*	967	312
	DET0867	DET0866	hydrogenase subunit, putative	1000	233
	DET0868	DET0866	hydrogenase subunit, putative	109	850
	DET0868	DET0867	hydrogenase, group 4, *echE* subu	886	907
	DET0863	DET0934	hydrolase, TatD family	623	584
	DET0863	DET1114	type III restrict.-modif. endon	701	756
	DET0867	DET1116	sugar fermentation stimulation	510	726
	DET0860	DET1122	glutamine-dependent NAD(+) synt	825	188
	DET0861	DET1138	cobalamin biosynthesis protein	984	284
	DET0862	DET1483	anthranilate phosphoribosyltran	-	577
	DET0868	DET1592	AIR synthase domain protein	533	-
Nuo	DET0926	DET0051	conserved hypothetical protein	-	689
	DET0923	DET0100	hypothetical protein	511	-
	DET0924	DET0109	hydrogenase maturation protease	980	999
	DET0926	DET0109	hydrogenase maturation protease	695	866
	DET0923	DET0110	*hupA*	997	984
	DET0929	DET0321	lipoprotein, putative	-	555
	DET0925	DET0396	conserved hypothetical protein	359	657
	DET0924	DET0431	sensory box sensor histidine ki	-	882
	DET0932	DET0494	preprotein translocase SecY	556	244
	DET0926	DET0595	peptidyl-tRNA hydrolase	674	-
	DET0930	DET0644	transketolase	948	295
	DET0930	DET0789	pseudouridine synthase, RsuA	-	725
	DET0930	DET0837	hypothetical protein	612	-
	DET0931	DET0928	*nuo* I subunit	991	746
	DET0924	DET1011	hypothetical protein	934	-
	DET0927	DET1196	ATP-dependent DNA helicase PcrA	-	927
	DET0933	DET1261	argininosuccinate lyase	997	981
	DET0931	DET1264	degV family protein	996	843
	DET0927	DET1343	tryptophanyl-tRNA synthetase	981	996
	DET0923	DET1364	hypothetical protein	131	868
	DET0926	DET1531	DNA-binding response regulator,	-	563

"=across putative respiration enzymes"

"=within putative respiration enzymes"

3.D.6. D2 network topology highlighted relationships of the putative enzymes involved in respiration

The enzymes predicted to be involved in the respiration pathway as identified by Seshadri *et al* (2005) were analyzed to determine the connection between these enzymes and common nearest neighbors in the network ensemble. Table 3.3 lists the connection of the DMC195 operon subunits for *mod, hup, hym, fdh, vhu, atpase, hyc, ech,* and *nuo* to each other and other variables in the ensemble. Within operon relationships are highlighted in grey (they were assigned to the numerically lowest DET locus tag to remove redundant entries in the Table). Relationships across predicted respiration linked enzymes are highlighted in orange. One of the strongest inter-operon relationships predicted was the interaction between *fdh* and *hup* (DET0111 and DET0187). Inspecting the raw data confirmed that these two transcripts are tightly and positively linearly-correlated (on a linear-linear comparison r = 0.96).

3.D.7. Network nodes connected to reductive dehalogenase transcripts:

The RDase transcripts within the ensemble of 1000 networks were highlighted to analyze the nearest neighbors of the catalytic subunits. Nodes presented in Table 3.4 maintain an interaction with a score of at least f = 500 in either the 1-to-1 or 2-to-1 network ensemble. Of the 17 RDase catalytic subunits encoded on DMC195's genome, the network ensemble predicted interactions for 12. These RDase catalytic subunits (highlighted blue in Table 3.4) were connected to their associated anchoring subunits (highlighted orange) for 7 out of the 12. This was expected as the RDase catalytic and anchoring subunits are predicted to reside on the same polycistronic mRNA. Surprisingly, three RDase anchoring subunits that cluster together

Table 3.4. Reductive dehalogenase nearest neighbors and second nearest neighbors for the D2 1-to-1 and 2-to-1 ensembles cutoff at f = 500. Highlighted blue indicates a nested RDase catalytic unit, highlighted yellow are RDase anchoring proteins, highlighted red are putative regulators.

Table 3.4. (Continued)

Node 1	1-to-1	2-to-1	Node 2	1-to-1	2-to-1	Node 3	1-to-1	2-to-1
DET0079	999	1000	DET0078	RDase anchoring protein				
tceA				921	114	DET1244	iron-sulfur flavoprotein	
				721	-	DET0812	PAP2 family protein	
				517	1	DET1505	transcriptional regulator, Fur	
	1000	974	DET1407	putative S-layer				
				969	99	DET0343	cell division protein FtsZ	
				774	581	DET1531	DNA-binding regulator, LuxR	
				-	528	DET0973	dihydrodipicolinate synthase	
DET0162	7	976	DET0166	IS				
	-	948	DET0318	RDase catalytic unit *pceA*				
				1000	1000	DET0319	RDase anchoring protein	
							933	6 DET0980 hypo.
	820	1	DET0115	ABC transporter, type 2,				
				964	592	DET0451	malate dehydrogenase	
				927	567	DET0365	phenylalanyl-tRNA synthetase	
				-	911	DET1408	transcription termination Rho	
				69	726	DET1375	ribosomal pseudouridine synthase	
	710	-	DET0712	phosphoribosylglycinamide transformylase				
				-	762	DET1279	acyl carrier protein	
				-	759	DET1509	IS	
	596	15	DET0383	hypo.				
				949	274	DET1438	hypo.	
				9	572	DET1247	transcriptional regulator, ArsR	
DET0173	761	985	DET0174	lipoprotein				
				1000	1000	DET0175	RDase anchoring protein	
				651	47	DET1063	DNA-binding regulator, LuxR	
	-	797	DET0390	hypo.				
				909	749	DET1168	hypo.	
				141	672	DET0967	ATP-dependent RNA helicase	
				45	619	DET1068	recombinase, phage integrase	
				550	65	DET1180	ABC transporter	
				527	113	DET0824	nitroreductase family protein	
	63	583	DET1063	DNA-binding regulator, LuxR				
				806	210	DET1586	lemA family protein	
				651	47	DET0174	lipoprotein	
				-	527	DET0409	polyA polymerase	
DET0301	-	972	DET0232	DNA-binding rr				
				877	426	DET0231	hypo.	
				22	816	DET0325	phospholipase family	
	959	669	DET0300	DNA-binding rr				

Table 3.4. (Continued)

Node 1	1-to-1	2-to-1	Node 2	1-to-1	2-to-1	Node 3	1-to-1	2-to-1
DET1545	432	1000	DET1544	RDase anchoring protein				
	964	214	DET0778	thymidylate kinase				
				1	810	DET0987	acetyltransferase	
				-	700	DET0163	RDase anchoring protein	
				27	700	DET1250	hypo.	
	805	414	DET1250	hypo.				
				992	1	DET1307	unknown function DUF1508	
				-	973	DET0980	hypo.	
				871	817	DET0312	RDase anchoring protein	
				746	1	DET0987	acetyltransferase	
				117	741	DET1016	sensory box histidine kinase rr	
				27	700	DET0778	thymidylate kinase	
				4	570	DET1253	hypo.	
				562	286	DET0855	hypo.	
	98	800	DET0181	RDase anchoring protein				
				-	707	DET0649	hypo.	
	25	725	DET0180	RDase catalytic unit				
				753	-	DET1621	hypo.	
							-	981 DET0511 hypo.
							945	- DET0848 SPFH domain
							-	888 DET1233 rr
							-	630 DET0627 hypo.
							537	- DET1301 IS
DET1559	997	1000	DET1558	RDase anchoring protein				
	999	799	DET1556	hypo.				
				-	953	DET1557	lipoprotein	
	898	91	DET1132	imidazole glycerol phosphate synthase				
				906	18	DET1133	iron-sulfur cluster-binding protein	
				65	642	DET1052	translation initiation inhibitor, yjgF	
				545	998	DET1356	hypo.	
	515	-	DET0327	hypo.				
				908	179	DET1417	formyltransferase	
				-	564	DET0328	hypo.	
				25	532	DET0435	pyrophosphokinas	
DET1535	1000	1000	DET1534	RDase anchoring protein				
	981	45	DET0077	hypo.				
				1000	1000	DET0076	resolvase domain protein	
				577	-	DET0433	hypo.	
DET0311	850	448	DET0233	sensory box sensor histidine kinase				
				1000	999	DET0305	sensory box sensor histidine kinase	
				448	981	DET0819	thymidylate synthase	

(DET1170, DET1537, and DET0307, not shown on table) shared the property of being higher in intensity value on the microarray than their associated catalytic subunits despite being predicted to occur later on the mRNA transcript.

Focusing on the *tceA* DET0079 transcript, the model connected it closely to the transcripts encoding for the putative S-layer protein (DET1407) and the *tceA* associated anchoring protein (DET0078). These have been previously identified (Chapter 2) to display a strong and positive linear correlation score. Previous work has also shown that a strong inverse relationship exists between *tceA* and the regulators DET1525 and DET1531 (Chapter 2). However, these relationships are not captured in the model because they are recurringly assigned to DET1407, and due to the acyclic nature of the Bayesian inference model constraints, cannot also be shown to be connected to *tceA* (Appendix Figure A2.1).

3.D.8. Comparison between two mixed communities continuously respiring TCE with evidence of multiple strains in KB1:

The D2 and KB-1® mixed communities expressed a unique set of RDases under similar rates of TCE to ETH dechlorination. DMC195 in D2 has been predicted to gain energy from the reduction of TCE to VC, with the VC to ETH step being co-metabolic (32). Therefore, the DMC population gains 2 µeeq during the reduction of TCE to DCE and 4 µeeq for the reduction of TCE to either VC or ETH. The resulting overall respiration rate (rate of dehalogenation) was 28.9±0.53, 7.1±0.3, and 1.4±0.1µeeq/(L-hr) for the D2 TCE High, Mid, and Low continuous rates, respectively. In KB-1®, at least one DMC population within the community has been predicted to gain energy from the reduction of VC to ETH. However, in addition to DMC strains

in the commercially available KB-1®, a *Geobacter* species capable of reductively dechlorinating TCE to DCE is present (1). Therefore, to account for potential competition of the TCE to DCE step in KB-1®, only the conversions of DCE to VC or ETH were used in calculation of DMC's respiration rate. In this conservative estimate, DMC in KB-1® was assigned to gain 0 µeeq/µmole for the production of DCE, 2 µeeq/µmole for VC, and 4 µeeq/µmole for ETH resulting in respiration rates of 10.5, 11.0; 21.4, 17.5; 14.0, and 29.8 µeeq/(L-hr) for the KB-1® continuous fed TCE Low A1, A2; Mid B1, B2; and High C1, C2; respectively. Due to the variability of ethene generation across duplicates, each culture will be treated independently in all subsequent analysis.

Figure 3.3 displays the average microarray intensity for all RDases across biological duplicate reactors continuously fed TCE at varied rates for the D2 (in blue; leftmost 3 columns) and the individual continuous TCE fed reactors for KB-1® (in yellow to red; middle 6 columns between the black bars). The communities were colored uniquely to highlight the different cultures. Additionally, the batch time series culture (metabolite concentrations across time provided in Appendix Figure A2.2) is presented for the duplicate reactors for the commercially available KB-1® culture (right most 7 columns). The RDases are organized by phylogenetic distance calculated in ClustalW and plotted in Dendoscape.

In the D2 community with DMC195, the RDases DET0079 (*tceA*), 0162 (with an authentic point mutation causing an early stop codon), 0180, 0318 (*pceA*), 1545, and 1559 were all detected at least once with an intensity greater than 1000 pfu (significantly above

Figure 3.3. Comparison of the RDase microarray intensity between the D2 and commercially available KB-1® cultures. (a) The RDases targeted by the pangenome microarray are organized by phylogenetic distance as displayed by the dendogram. (b) The heatmap with the blue scale represents absolute intensity values exceeding 1000 pfu for D2 continuously fed TCE. (c) The first six columns of the yellow-red heatmap represents absolute intensity values greater than 1000 pfu for KB1 continuously fed TCE while the remaining 7 columns (d) plot the absolute intensity values for the batch TCE fed series. Each cell is shaded appropriate to the average intensity.

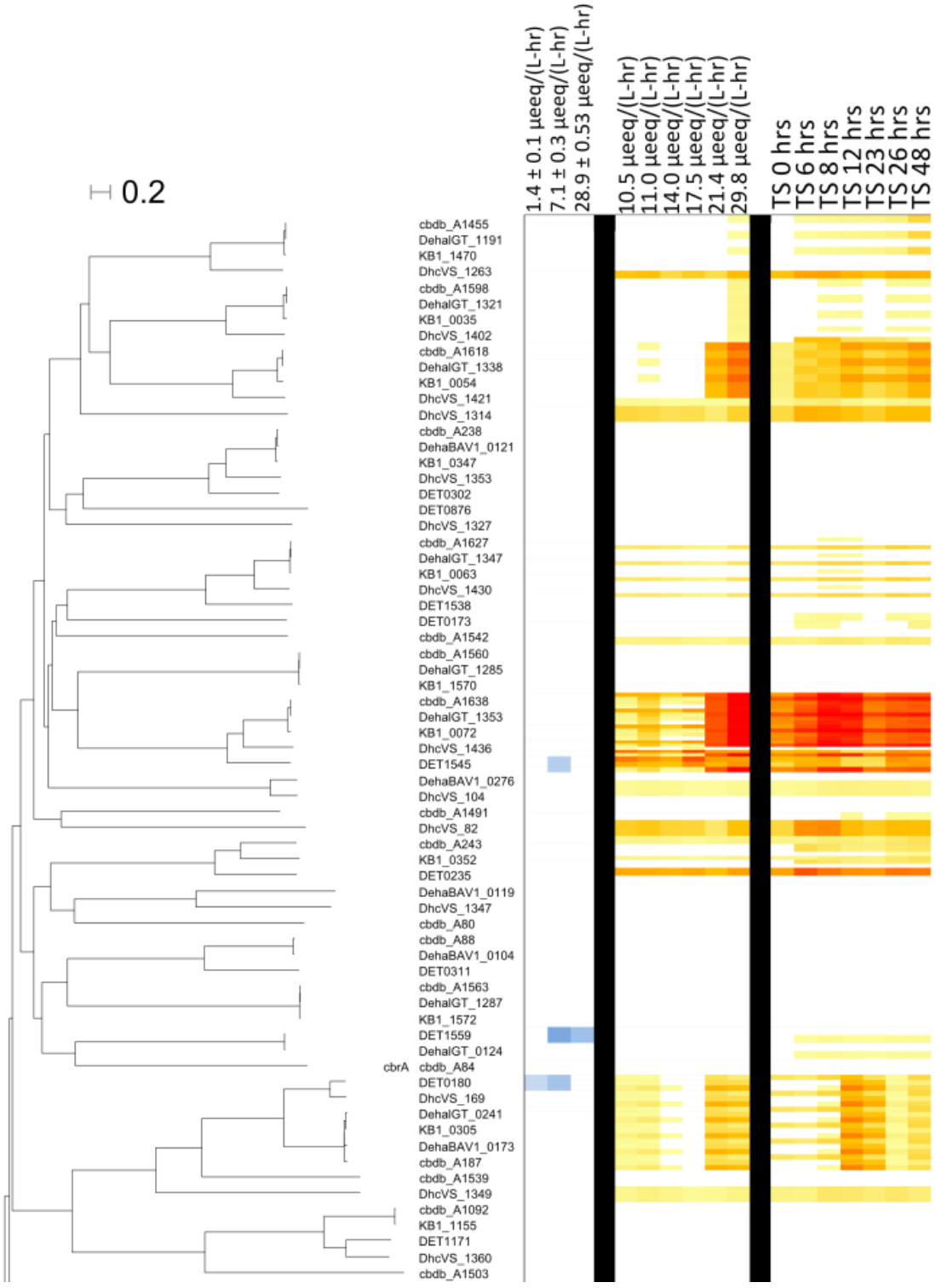

Figure 3.3 (Continued)

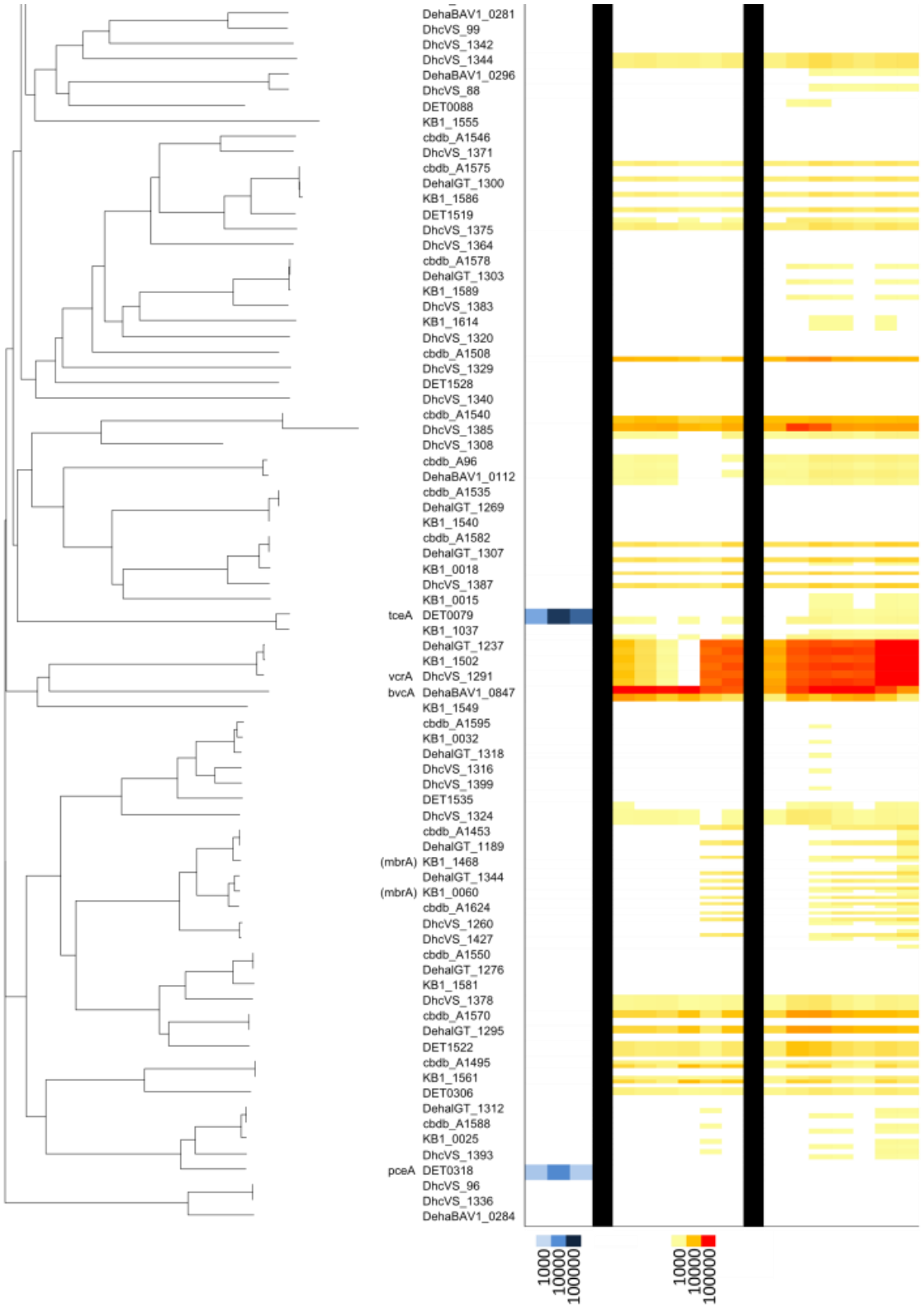

Figure 3.3 (Continued)

background) in the continuously fed TCE experiments (n = 6). The *tceA* transcript was the most dominant from an absolute intensity sense. KB-1-L metagenome (KB1_6; 17). The *bvcA* homolog appeared to have an inverse relationship with respiration displaying higher microarray intensity at lower respiration rates. In the time course TCE batch fed experiment (chloroethene concentrations versus time for the 70 hour experiment is presented in Appendix Figure A2.2), the *bvcA* homolog was detected with the highest intensity in the 8 to 23 hour sample with a notable decline after 28 hours. Both of these findings for *bvcA* directly contrasted the third highest intensity RDases, KB1_1502 (a *vcrA* homolog) which increased in abundance during higher respiration in the continuous fed experiment and displayed high intensities in the 28 and 70 hour batch fed samples. The second highest detected transcript for an RDase was a homolog of DET1545which directly contrasted the low abundance of the transcript in D2 under similar TCE feeding rates. In the KB-1® samples, DET1545 microarray fluorescence intensity increased with dehalorespiration rate.

The detection of multiple probes designed to target the same RDase but displaying distinct intensity patterns (Figure 3.3) highlighted the fact that the pangenome array was able to detect the behavior of homologous but non-identical genes. Focusing on the heatmap for all DET1545 homlogs (Figure 3.3 where DET1545 = DMC1488, marked with arrow), variability was seen within the seven probes designed to target the homologous cluster. The probes gi147689941, panDhc_506_RC, pan_Dhc_506, and KB1_0072 absolute intensity values were linearly correlated ($r > 0.93$ for all relationships across all samples). These four probes targeted the DET1545 homolog in the genomes of DMC BAV1, CBDB1, GT, and KB1. With the exception of pan_Dhc_506 which targeted all DET1545 homologs, these probes were not

Table 3.5. RDase interactions in KB-1®'s network ensemble. Black outlined boxes group variables that represent homologous RDases. The score presented in the 1-to-1 and 2-to-1 columns represent summed frequencies greater than 100 in the respective network model, with at least one of the two network ensembles predicting f > 500. Connected nodes are highlighted blue (RDase catalytic units), purple (RDase catalytic units), gold (putative regulators or redoxin type proteins), and red (the putative S-layer).

Table 3.5. (Continued)

Node1	1to1	2to1	Node2
DMC0076 *tceA*	607	-	DMC0819 hypothetical protein
	1000	964	DMC0942 acetyltransferase
	957	930	DMC1239 gamma-glutamyl kinase
DMC0173 RDase	1000	974	DMC0174 RDase anchoring protein
DMC0228 (1) RDase	-	990	DMC0824 ABC transporter, permease protein
	-	994	DMC0228 RDase
DMC0228 (2) RDase	709	217	DMC0041 Methyltransferase type 11
	-	775	DMC0756 tRNA -methyltransferase
	-	772	DMC1629 hypothetical protein
DMC0299 RDase	-	862	DMC0132 methylglyoxal synthase
	643	-	DMC1242 serine protease, DegP/HtrA family
	918	620	DMC1315 twitching mobility protein
DMC1462 (1) RDase	937	895	DMC2086 CRISPR-associated helicase Cas3
DMC1462 (2) RDase	-	696	DMC0698 phosphoribosylglycinamide transformylase
	788	928	DMC0751 metallopeptidase, M50 family
	934	549	DMC1038 tail tape measure protein
DMC1465 (1) RDase	980	955	DMC1315 twitching mobility protein
DMC1465 (2) RDase	116	643	DMC0014 hypothetical protein
	540	405	DMC0607 hypothetical protein
	753	142	DMC1976 SpoVT/AbrB domain protein
DMC1465 (3) RDase	725	552	DMC1812 DNA-binding response regulator
DMC1478 RDase	-	533	DMC0053 alcohol dehydrogenase
	567	133	DMC0428cell divisionFtsK/SpoIIIE
	632	613	DMC2369 addiction module toxin,
DMC1488 (1) RDase	1000	990	DMC1487 RDase anchoring protein
DMC1488 (2) RDase	-	933	DMC0199 phosphate kinase
	-	728	DMC1328 dihydroorotate dehydrogenase
	999	1000	DMC1487 RDase anchoring protein
DMC1488 (3) RDase	1000	986	DMC1487 RDase anchoring protein
	966	479	DMC2158 RDase
DMC1501 RDase	637	607	DMC0608 hypothetical protein
	325	688	DMC1102 hypothetical protein
DMC1590 RDase	996	823	DMC1292 hypothetical protein
DMC1612 RDase	924	901	DMC1732 ABC-type oligopeptide transport
	554	823	DMC2057adenine-specific DNA methylase

Table 3.5. (Continued)

Node1	1to1	2to1	Node2
DMC1612 RDase	924	901	DMC1732 ABC-type oligopeptide transport
	554	823	DMC2057adenine-specific DNA methylase
DMC1775 RDase	949	427	DMC0110 ABC transporter, type 2
	-	616	DMC0667 hypothetical protein
DMC1808 RDase	-	530	DMC0062 virulence-related protein
	-	858	DMC1024 sensor histidine kinase
	559	160	DMC2064 4Fe-4S ferredoxin
	593	-	DMC1096 hypothetical protein
	806	752	DMC1806 sensor histidine kinase
DMC1843 RDase	-	884	DMC0300 RDase anchoring protein
	923	971	DMC0863 hypothetical protein
	-	937	DMC1542 protein translocase TatA/TatE
DMC1867 RDase	-	553	DMC1468 transcriptional regulator
DMC1875 RDase	597	-	DMC0494 50S ribosomal protein L13
	694	266	DMC055416S rRNA processing protein RimM
	-	505	DMC1296 ABC transporter, permease protein
DMC1894 RDase	458	666	DMC0110 ABC-2 type transporter
	-	665	DMC1335 GH3 auxin-responsive promoter
	-	733	DMC1400 hypothetical protein
	-	512	DMC1402 ribosomal protein L25 (Ctc)
	-	713	DMC1893 RDase anchoring protein
DMC1894 RDase	974	559	DMC0191 glutaredoxin family protein
	712	569	DMC1312 hypothetical protein
DMC1900 RDase	892	909	DMC1894 panDhc_606 RDase
DMC2072 RDase	996	919	DMC0955 acetyltransferase, GNAT family
	997	997	DMC1361 S-layer
DMC2110 RDase	1000	923	DMC0807 translation factor SUA5
DMC2154 RDase	914	845	DMC0292 transcriptional regulator
DMC2169 RDase	508	637	DMC0339 hypothetical protein
	836	711	DMC0385 hypothetical protein
	788	-	DMC1675 acetyltransferase, GNAT family
DMC2177 RDase-frag	542	739	DMC0905 endonuclease III
DMC2179 RDase	980	-	DMC2086 CRISPR-associated helicase Cas3
DMC2241 RDase	918	775	DMC0662 cyclase
DMC2379 RDase	984	869	DMC1487 RDase anchoring protein
	0.918	0.572	DMC2382 transposase

predicted to target DMC195 or VS homologs. The pan_Dhc_506 probe appeared as the outlier in intensity values for both the DMC195 and VS homologs. The remaining three probes (panDHC_502, panDHC_502_RC, and panDHC_422) in the 1545 cluster displayed positive linear correlation with each other ($r > 0.62$ for all relationships across all samples) to the exclusion of the first cluster (the maximum linear correlation between any of these three probes with any of the other 4 probes was $r = 0.19$) and were predicted to target DET1545 homologs in DMC195 and VS. This was indicative of at least two distinct DET1545 homologs being captured by the KB-1® pangenome array.

3.D.9. KB-1® ensemble of networks reductive dehalogenase nearest neighbors:

The network inference ensembles for the KB-1® cultures predicted several key RDase relationships. Table 3.5 displays the interactions that were detected in at least 500 of the ensemble of 1000 networks for either the 1-to-1 or 2-to-1 constructions. As in the D2 model, of the 33 probes for RDase catalytic subunits' interactions exceeding a frequency cutoff of $f = 500$, 5 probes were connected to an RDase anchor subunit. These probes represented 11 of the 35 RDase catalytic homologs that were detected on the pangenome array (at an intensity greater than 1000 pfu). This finding was expected as they were putatively expressed on the same polycistronic transcript. Of all the relationships, the putative S-layer protein (in this case identified as DMC1361) maintained a strong summed frequency ($f_{11} = 1000, f_{21} = 996$) to DMC2072, the homolog of the abundant RDase *vcrA* in the KB-1® community. This was surprisingly analogous to the D2 model wherein the S-layer protein was connected to DET0079, *tceA* (f_{11} and $f_{21} = 1000$), the highest expressed RDase in the D2 community.

3.D.10. KB-1® strain identification in the REFS™ ensemble of 1000 networks

The ability of the pangenome microarray to detect multiple DMC strains in the commercially available KB-1® culture was checked by comparing the results of two DNA microarrays (previously published (17)) to the predictions made by the KB-1® ensemble of 1000 networks. The two DNA microarrays compared DNA extracted from the D2 culture (Cornell strain) in the Cy5 (red) channel and the KB-1-L lab maintained culture (Pinellas strain) in the Cy3 (green) channel. Figure 3.4 (a) displays the D2 DNA intensity versus the KB-1-L DNA intensity for all panDHC probes on the microarray. The panDHC probe-set was one of seven probe-sets designed on the microarray and described by Hug *et al.* 2011 and targeted the consensus sequences between all DMC strains (17). If all probes in their design captured DNA from the D2 and KB-1-L community equally, the expected relationship would be a linear one-to-one relationship that would fall along the plotted red-line. However, the data-points were predominantly split into two main groups. A subset of the panDHC probes displayed a higher intensity (greater than 6-fold ratio) when hybridized with D2 DNA rather than KB-1-L DNA and another subset a greater than 2 fold affinity to capture KB-1-L DNA rather than D2 DNA. These two regions are demarcated by the blue and yellow triangles respectively, selected so that the members cluster together and the respective standard error does not cross the 1:1 red line. Regions outside of these triangles were considered to be non-specific for either culture. These cutoffs were assigned to determine whether a probe is representative of the D2 or KB-1-L cultures or non-specific to either culture (from Figure 3.4, these regions were considered to be greater than 6, less than 0.5, and in-between both values when considering the D2 to KB-1-L DNA intensity ratio). The difference in ratio cutoffs was due to the D2 DNA Cy5 signal having a higher overall average microarray intensity on the DNA microarrays as compared to the KB-1-L

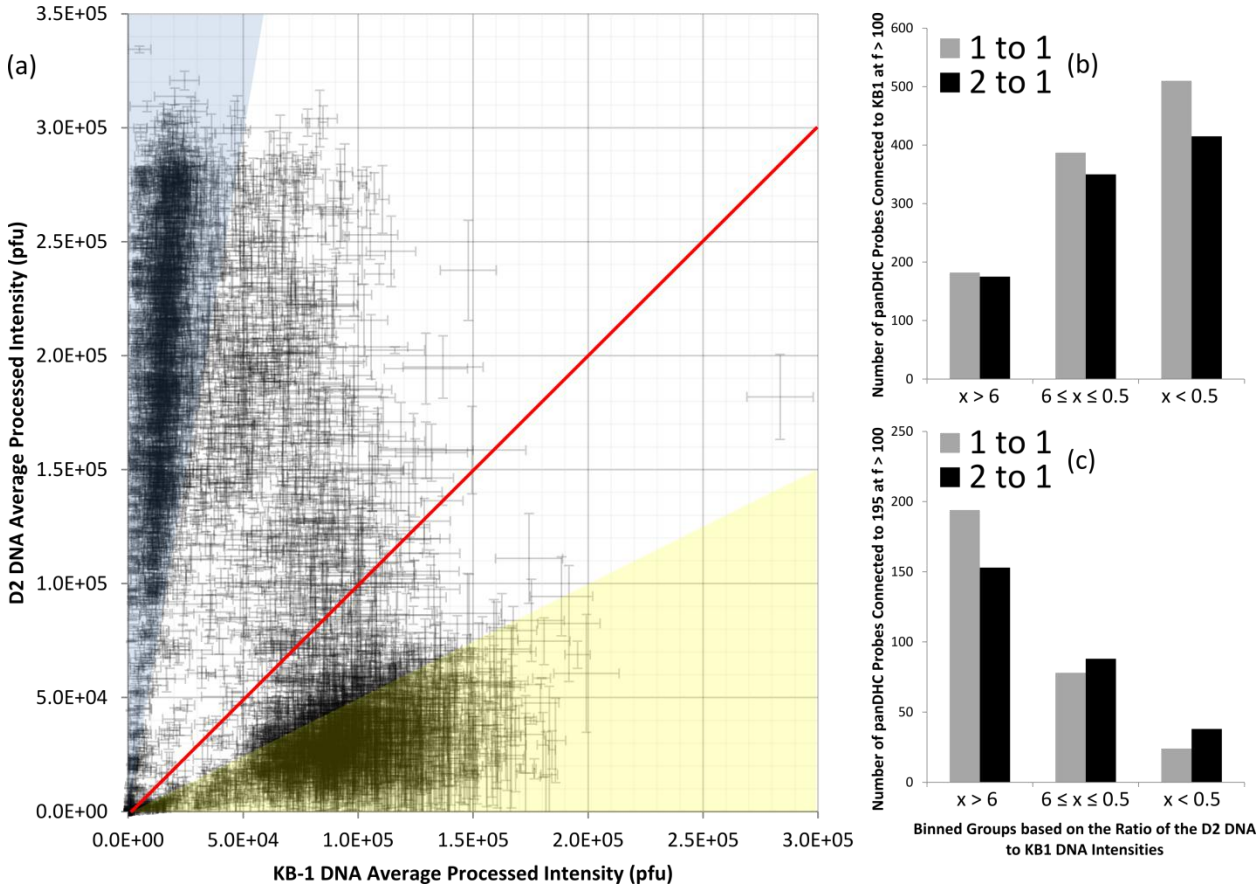

Figure 3.4. Detection of strain variation on the pangenome microarrays. (a) The DNA microarray intensity from the D2 culture is plotted against the DNA microarray intensity for the lab grown KB-1-L community for the panDHC probe set. Error bars indicate standard error about the average intensity. The red line is the one-to-one line. The blue and yellow triangle highlights the probes selected to uniquely represent the DMC195 in the D2 culture and the KB-1-L unique genome in the KB-1-L culture, respectively. The bar-charts represent the number of probes that are selected in the ensemble of 1000 networks to interact with DMC195 ($x > 6$), cross-hybridization ($6 \leq x \leq 0.5$), or KB-1-L specific probes ($x > 0.5$) for the (b) KB-1-L specific and (c) DMC195-specific probe sets on the pangenome microarray.

DNA Cy3. Additionally, the selection of these two cutoffs was based on the physical performance of the DNA pangenome microarray, rather than a predicted statistical filter.

The current pangenome microarray also contained specific probes designed using the genomes of only strain DMC195 (the sole DMC member of the D2 community) and KB-1 (the predicted dominant DMC strain of the KB-1® commercially available mixed culture). These two probes sets were used to filter the KB-1® 1-to-1 and 2-to-1 ensemble of 1000 networks. Interactions between the DMC195/panDHC or DMC KB-1/panDHC probesets that exceeded f = 100 (a lower frequency was selected to introduce more variability) were binned based off of the DNA cutoffs illustrated in Figure 3.4 (a). For example, if a DMC KB-1 probe was connected to a panDHC probe in the network ensemble and that panDHC probe displayed a D2/KB-1-L DNA ratio of less than 0.5, it would be considered KB-1 specific and therefore located in the rightmost column of Figure 3.4 (b). The DMC KB-1 probe-set displayed the highest number of interactions for panDHC probes that recovered the lab strain KB-1-L DNA at a ratio greater than 2 as compared to D2 DNA (Figure 3.4 (b)). Turning to the potential alternate strain, the DMC195 specific probes displayed the highest number of interactions with those panDHC probes that recovered D2 DNA at a ratio greater than 6 as compared to KB1 DNA (Figure 3.4 (c)).

3.E. Discussion

In applying a machine-learning approach to the analysis of two transcriptomic datasets for DMC, the intent was to apply an unbiased tool to comprehend the most confidently predicted relationships. To test the validity of the predictions, the first biological question asked was whether the network ensemble was successfully recapturing the polycistronic structure of the

mRNA transcripts. As shown from the operon analysis, the selected ratios at all frequency cutoffs of the final ensemble of 1000 networks displayed a significant over-sampling of interactions between operon members. One of the most surprising results of the operon analysis was the successful recapture of one of the longest polycistronic mRNAs predicted in DMC195's genome. The 37 gene stretch between DET0469-0506 encodes primarily short (510 ± 115 nucleotides) ribosomal proteins or ribosomal related proteins. This stretch displayed a per-gene normalized frequency (the sum of the frequency of all within operon interactions divided by the total number of genes on the operon) of 785 and 760 for the 1-to-1 and 2-to-1 models respectively. These findings displayed that the network ensemble was predicting biologically supported interactions.

With confidence that the network ensemble was enriching for true interactions, attention was turned to elucidate key edges involving experimental conditions and growth linked enzymes. When analyzing the interactions between the variables and the experimental parameters modeled, the connection of the PCE respiration rate to two histidine kinase receptors (DET0315 and DET1530), putatively described as being involved in the transcriptional regulation of RDases, proved to be the most compelling prediction. Both histidine kinase receptor genes' expression display an inverted trend to PCE respiration rate (higher at lower respiration rates) indicating these transcripts are undergoing regulation in expression in response to reductive dehalogenation rates. The DET0315 histidine kinase DNA binding response regulator is the *cis*-regulatory element of the PceA RDase on DMC195's genome. Previous lower computationally powered analysis (K-means and correlation analysis, Chapter 2) did not highlight a substantial relationship for this regulator. In the network ensembles for D2, DET0315 was predicted to

strongly interact with its neighboring DET0316 histidine kinase (f_{11} = 993, f_{12} = 996) in addition to the PCE respiration. Therefore, a strong relationship of the predicted *cis*-transcriptional regulatory elements for *pceA* was successfully captured in the network ensemble but was not previously noted in other statistical treatments of the dataset.

Turning to the variables that were directly connected to a RDase catalytic subunit, the putative cell wall S-Layer protein was connected to highly expressed RDases in the D2 and KB-1® network ensembles (f_{11} = f_{12} = 1000 and 997 to *tceA* and *vcrA* respective to the D2 and KB-1® cultures). The relationship was shown previously to be positively linearly correlated (Chapter 3) suggesting that this transcript is either co-regulated with the dominant RDase or that it responds positively to higher respiration rates as do the dominant RDases. Additionally, 7 of 12 and 4 of 26 RDases in the D2 and KB-1 models respectively were connected to an anchoring protein at f > 500.

Looking at *tceA*, it was surprising to note that neither of the regulators DET1531 nor DET1525 shared an edge with this RDase. Previous work showed that two regulators displayed the highest inverse correlation of *tceA*'s expression (Chapter 2). Instead, the network ensembles for D2 predicted that the DNA binding response regulator DET1531 interacts with the putative S-layer DET1407 (f11 = 784, f21 = 581). Appendix Figure A2.1 highlights the fact that DET1531 (as well as an additional regulator, DET1525) is connected to *tceA* indirectly through the DET1407 S-Layer. There is no direct link due to the fact that the ensemble cannot display cyclic relationships. Therefore, the tight relationship of the S-layer and *tceA* is actually precluding the interaction of DET1531 or 1525 to the RDase. However, the abundance of a

specific transcript encoding for a histidine kinase response regulator is not indicative of the binding state of that regulator, and therefore potential regulation pattern, of the final enzyme. At the very least, the predicted relationships indicate that when *tceA* transcript abundance is high in D2, DET1525 and 1531 are low. Unlike the tight S-layer and dominant RDase relationship, these two regulators do not display a predicted relationship in the KB-1® network ensemble as compared to the D2 ensemble. Future upstream promoter assays may help clarify the regulators involved (if any) in RDase regulation.

Investigating the specific expression pattern of the RDases under similar TCE continous feeding conditions found multiple RDases expressed. This expression of multiple RDases under similar phenotypic respiration of chlorinated organic compounds has been noted previously (1,13,18). This research extended the current literature by comparing two mixed microbial communities fed under similar continuous TCE feed rates. As expected, the fingerprint of RDase expression between D2 and KB-1® was different. DMC195 in D2 expressed 7 of the 17 encoded RDases across the entire dataset (> 1000 pfu), with tceA as the dominant RDase in most conditions. The commercially available KB-1® expressed 28 RDases confidently with a *bvcA* and DET1545 homolog displaying the highest intensities. Detection of a DET1545 homolog in KB-1® during high rates of TCE respiration was in direct contrast to DMC195 in D2. The D2 culture has shown DET1545 to be a minor RDase expressed primarily under low electron acceptor availability. The number of RDases expressed or transcripts detected in the KB-1® culture was surprising considering all experiments performed on this community provided TCE as the sole electron acceptor. Additionally, RDases that were not predicted to be on the laboratory strain KB-1-L's genome were detected. This could be indicative of either partial

coverage of the KB-1-L metagenome, or more likely, divergence between the commercially available KB-1® cultures used in this study and the laboratory maintained KB-1-L.

The networks, as a hypothesis generating platform, provided a possible explanation as to why a DET1545 homolog's transcript abundance is higher in the KB-1® culture as compared to the D2 culture. The bifurcating behavior between the two cultures is especially perplexing considering the fact the immediate genomic region surrounding the DMC1488 cluster is almost syntenous in all strains. DMC195 does maintain two small hypothetical proteins (DET1542 and DET1546) that could potentially play a role as to the difference in behavior. Both of these transcripts are detected at levels less than 300 pfu on the DMC195 specific microarrays.

If instead the existence of another RDase, DET1559, is considered in this analysis, an alternate hypothesis was displayed in the network ensembles. DET1559 was inserted into and interrupts part of the region between the DET1545 and *hyc* homologs in DMC195 as compared to the strains GT, CBDB1, and KB-1. The hypothetical protein that should be identified as DET1552 was shifted away from DET1545 to become DET1562. The homolog of DET1562 in KB-1 (KB1_0077) remained in the initial adjacent position (Figure 3.5). Turning to the Bayesian inference platform, DET1562 is not expressed highly and displayed no significant interactions in the D2 network ensembles. However, KB1_0077 was expressed confidently on the pangenome microarray. Additionally, the KB1_0077 transcript was connected to KB1_0029 (f11 = 922, f21 = 740) in the commercially available KB-1®'s network ensemble. This transcript encodes for a histidine kinase receptor near the DET1535 RDase homolog in KB-1 absent from DMC195's

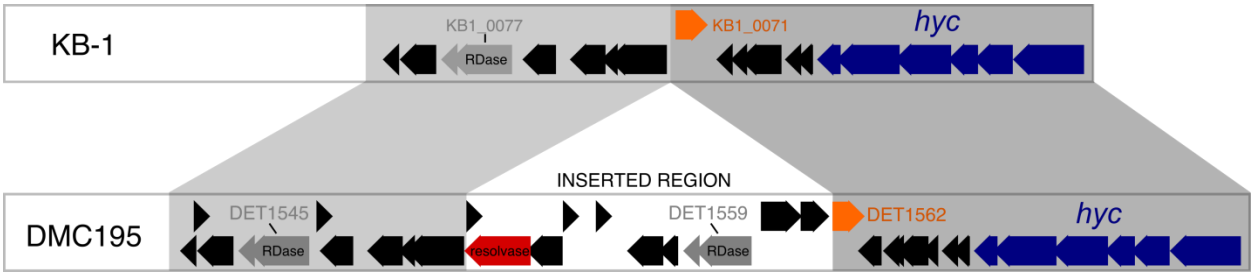

Figure 3.5. Diagram of the RDase DET1559 gene insertion between DET1545 (KB1_0077) and *hyc*. Both strain 195 and KB-1 are displayed to note the shift of KB1_0071 (orange, becomes DET1562 in DMC195) away from the RDase DET1545/KB1_0077.

genome. Additionally, the 2-to-1 network ensemble linked the KB1_0077 transcript to the KB1_0071 RDase anchoring protein (f21 = 523; the anchoring protein of the DET1545 homolog) and KB1_0430 (f21 = 523, a corrin/porphyrin methyltransferase involved in the vitamin B12 modification pathway).

While the KB1_0077 transcript is not genomically located directly next to the RDase KB1_0072, the network ensemble indicates it is linked to key RDase related transcripts. Therefore, future work should investigate whether the differential expression of the DMC1488 (DET1545) RDase between the D2 and commercially available KB-1® cultures is a result of the inclusion of the DET1559 RDase in DMC195's genome causing this single hypothetical protein to have a greater genomic distance. This analysis displayed the general utility of the hypothesis-generating network ensemble as a pipeline to develop numerous testable scientific questions. For example, if KB1_0077 small enzyme is a regulatory element for DET1545 or DET1525/1531 is a regulatory element for *tceA*, we potentially could heterologously express these regulators in model organisms. Then, a subsequent gel shift assay indicates (if folded properly) whether these enzymes are capable of binding to the promoter regions of the respective targets.

The DET1545 homolog in KB-1® itself behaved even more surprisingly within the KB-1® community by displaying transcript specific strain behavior. Probes that target the homologous sequences for this RDase in DMC VS and 195 (Cornell group) displayed confident intensity in the microarray dataset and behaved independently (linear correlation $r < 0.2$) to the probes designed for the homologs in the Pinellas group (BAV1, CBDB1, GT, and KB-1). If the

probes for 195 and VS were displaying signal due to cross-hybridization, a positively correlated relationship would have been detected.

The strong interaction conserved across D2 and KB-1® for the putative S-layer and the major RDase was mirrored by a well conserved behavior in the hydrogenases. Within the predicted respiration chain elements, the hydrogenase *hup* and the formate dehydrogenase *fdh* were positively and confidently related in the D2 network ensemble. The KB-1® network ensemble reaffirms this relationship (a *hup* probe targeted by panDHC1241_RC was connected to a *fdh* probe in 963 out of the 1000 models of the 2-to-1 network, in the 1-to-1 the *fdh* and *hup* are connected through *hym*, an alternate hydrogenase). The connection of these two respiratory linked enzymes is perplexing in that the active site of Fdh maintains a mutation that prevents the organism from utilizing formate as an electron donor (35). Recent studies in *E. coli* have shown that a formate dehydrogenase similar to that found in DMC (but lacking the specific point mutation) maintains hydrogen : benzyl-viologen redox activity, fulfilling the role of a hydrogenase (44). Although the study analyzed an Fdh without the authentic mutation, the study predicted that the hydrogenase behavior should be conserved for DMC-type organisms. Therefore, with high levels of Fdh being detected at the protein level (1), DMC may be generating this enzyme to provide additional hydrogenase activity for the cell. In addition, *hup* and *fdh* also displayed connections with the predicted NADH-ubiquinone oxidoreductase *nuo* (Table 3.3). The Nuo encoded in DMC strains is missing the NADH receiver domain on the same main operon (the genome encodes an NADH receiver domain in other locations (43)), therefore, it is possible that this enzyme is still used in respiratory process but its specific

electron donor *in vivo* is not NADH. Additionally, the KB-1® model predicted strain specific behavior for all of these oxidoreductases.

In general, the KB-1® network ensemble successfully connected probes designed specifically for DMC195 or KB-1 with representative panDHC probes of either the Cornell or Pinellas groups of DMC, respectively (Figure 3.4, i.e. a known probe that was designed to specifically target DMC195 was more likely to be connected to a panDHC probe that specifically targeted Cornell/DMC195). Although there is a chance this is indicative of a probe-set bias, there are numerous cases of inverse relationships between probes of the same homologous group. Together, this suggests that multiple DMC strains were present and actively transcribing mRNA under the feeding conditions considered in the current KB-1® dataset. However, we are currently limited on the array to primarily discern the differences between the Cornell and Pinellas type organisms. Care must be taken for cultures that fall outside of these two subsets as the best hitting probe would not be previously known. As the KB-1® community is divergent to the laboratory maintained community KB-1-L, this paper thus outlines a method to appropriately run, filter, and analyze a (poorly) characterized mixed community on the pangenome microarray. From this analysis, the pangenome array should serve as a useful tool to monitor the behavior of both well characterized and mixed unknown communities of DMC organisms.

3.F. Acknowledgements

We would like to thank Phil Dennis, Jennifer Webb, and SiREM Labs (Guelph; Ontario) for providing the commercially available mixed community KB-1®. Additionally, we would like to thank our funding sources, the Department of Defense Army Research Office (W911NF-07-1-0249), the National Science Foundation CBET Program (CBET-0731169), the NSF- IGERT funded Biogeochemistry and Environmental Biocomplexity small grant program (DGE 0221658), and the NSF Graduate Research Fellowship Program for funding Cresten Mansfeldt in this research.

REFERENCES:

1. Adrian, L., Szewzyk, U., Wecke, J., & Görisch, H. (**2000**). Bacterial dehalorespiration with chlorinated benzenes. *Nature*, 408: 580-583.

2. Adrian, L., Rahnenführer, J., Gobom, J., & Hölscher, T. (**2007**). Identification of a chlorobenzene reductive dehalogenase in *Dehalococcoides* sp. strain CBDB1. *Applied & Environmental Microbiology*, 73: 7717-7724.

3. Cheng, D., & He, J. (**2009**). Isolation and characterization of "*Dehalococcoides*" sp. strain MB, which dechlorinates tetrachloroethene to trans-1, 2-dichloroethene. *Applied & Environmental Microbiology*, 75: 5910-5918.

4. Chow, W. L., Cheng, D., Wang, S., & He, J. (**2010**). Identification and transcriptional analysis of trans-DCE-producing reductive dehalogenases in *Dehalococcoides* species. *The ISME Journal*, 4: 1020-1030.

5. Cupples, A. M., Spormann, A. M., & McCarty, P. L. (**2003**). Growth of a *Dehalococcoides*-like microorganism on vinyl chloride and cis-dichloroethene as electron acceptors as determined by competitive PCR. *Applied & Environmental Microbiology*, 69: 953-959.

6. Darling, A. C., Mau, B., Blattner, F. R., & Perna, N. T. (**2004**). Mauve: multiple alignment of conserved genomic sequence with rearrangements. *Genome Research*, 14: 1394-1403.

7. DiStefano, T. D., Gossett, J. M., & Zinder, S. H. (**1991**). Reductive dechlorination of high concentrations of tetrachloroethene to ethene by an anaerobic enrichment culture in the absence of methanogenesis. *Applied & Environmental Microbiology*, 57: 2287-2292.

8. Duhamel, M., & Edwards, E. A. (**2006**). Microbial composition of chlorinated ethene-degrading cultures dominated by *Dehalococcoides*. *FEMS Microbiology Ecology*, 58: 538-549.

9. Fennell, D. E., Gossett, J. M., & Zinder, S. H. (**1997**). Comparison of butyric acid, ethanol, lactic acid, and propionic acid as hydrogen donors for the reductive dechlorination of tetrachloroethene. *Environmental Science & Technology*, 31: 918-926.

10. Friedman, N., Linial, M., Nachman, I., & Pe'er, D. (**2000**). Using Bayesian networks to analyze expression data. *Journal of Computational Biology*, 7: 601-620.

11. Fung, J. M., Morris, R. M., Adrian, L., & Zinder, S. H. (**2007**). Expression of reductive dehalogenase genes in *Dehalococcoides ethenogenes* strain 195 growing on tetrachloroethene, trichloroethene, or 2, 3-dichlorophenol. *Applied & Environmental Microbiology*, 73: 4439-4445.

12. Gull, S. F. (**1988**). Bayesian inductive inference and maximum entropy. *Maximum Entropy and Bayesian Methods in Science and Engineering*, 1: 53-74.

13. He, J., Ritalahti, K. M., Yang, K. L., Koenigsberg, S. S., & Löffler, F. E. (**2003**). Detoxification of vinyl chloride to ethene coupled to growth of an anaerobic bacterium. *Nature*, 424: 62-65.

14. He, J., Sung, Y., Krajmalnik-Brown, R., Ritalahti, K. M., & Löffler, F. E. (**2005**). Isolation and characterization of *Dehalococcoides* sp. strain FL2, a trichloroethene (TCE)-and 1, 2-dichloroethene-respiring anaerobe. *Environmental Microbiology*, 7: 1442-1450.

15. Heavner, G. L., Mansfeldt, C. B., Hellerstedt, S. T., Dennis, P. C., Edwards, E. A., Richardson, R. E. (**2013**). Biomarkers of reductive dechlorination in bioaugmentation culture KB-1®. Submitted for review.

16. Heavner, G. L., Rowe, A. R., Mansfeldt, C. B., Pan, J. K., Gossett, J. M., & Richardson, R. E. (**2013**). Molecular biomarker-based biokinetic modeling of a PCE-dechlorinating and methanogenic mixed culture. Submitted for review.

17. Hug, L. A., Salehi, M., Nuin, P., Tillier, E. R., & Edwards, E. A. (**2011**). Design and verification of a pangenome microarray oligonucleotide probe set for *Dehalococcoides* spp. *Applied & Environmental Microbiology*, 77: 5361-5369.

18. Hug, L. A., Beiko, R. G., Rowe, A. R., Richardson, R. E., & Edwards, E. A. (**2012**). Comparative metagenomics of three *Dehalococcoides*-containing enrichment cultures: the role of the non-dechlorinating community. *BMC Genomics*, 13: 327.

19. Islam, M. A., Edwards, E. A., & Mahadevan, R. (**2010**). Characterizing the Metabolism of *Dehalococcoides* with a Constraint-Based Model. PLoS Computational Biology, 6(8).

20. Johnson NL, Kotz S, Kemp AW. (**1992**). Univariate discrete distributions, 2nd ed. Wiley, New York.

21. Johnson, D. R., Brodie, E. L., Hubbard, A. E., Andersen, G. L., Zinder, S. H., & Alvarez-Cohen, L. (**2008**). Temporal transcriptomic microarray analysis of "*Dehalococcoides ethenogenes*" strain 195 during the transition into stationary phase. *Applied & Environmental Microbiology*, 74: 2864-2872.

22. Johnson, D. R., Nemir, A., Andersen, G. L., Zinder, S. H., & Alvarez-Cohen, L. (**2009**). Transcriptomic microarray analysis of corrinoid responsive genes in *Dehalococcoides ethenogenes* strain 195. *FEMS Microbiology Letters*, 294: 198-206.

23. Kube, M., Beck, A., Zinder, S. H., Kuhl, H., Reinhardt, R., & Adrian, L. (**2005**). Genome sequence of the chlorinated compound–respiring bacterium *Dehalococcoides* species strain CBDB1. *Nature Biotechnology*, 23: 1269-1273.

24. Lee, P. K., He, J., Zinder, S. H., & Alvarez-Cohen, L. (**2009**). Evidence for nitrogen fixation by "*Dehalococcoides ethenogenes*" strain 195. *Applied & Environmental Microbiology*, 75: 7551-7555.

25. Lee, P. K., Cheng, D., Hu, P., West, K. A., Dick, G. J., Brodie, E. L., ... & Alvarez-Cohen, L. (**2011**). Comparative genomics of two newly isolated *Dehalococcoides* strains and an enrichment using a genus microarray. *The ISME Journal*, 5: 1014-1024.

26. Lee, P. K., Dill, B. D., Louie, T. S., Shah, M., VerBerkmoes, N. C., Andersen, G. L., ... & Alvarez-Cohen, L. (**2012**). Global transcriptomic and proteomic responses of *Dehalococcoides ethenogenes* strain 195 to fixed nitrogen limitation. *Applied & Environmental Microbiology*, 78: 1424-1436.

27. Löffler, F. E., Yan, J., Ritalahti, K. M., Adrian, L., Edwards, E. A., Konstantinidis, K. T., ... & Spormann, A. M. (**2012**). *Dehalococcoides mccartyi* gen. nov., sp. nov., obligate organohalide-respiring anaerobic bacteria, relevant to halogen cycling and bioremediation, belong to a novel bacterial class, *Dehalococcoidetes* classis nov., within the phylum *Chloroflexi*. *International Journal of Systematic and Evolutionary Microbiology*.

28. Magnuson, J. K., Romine, M. F., Burris, D. R., & Kingsley, M. T. (**2000**). Trichloroethene reductive dehalogenase from *Dehalococcoides* ethenogenes: Sequence of tceA and substrate range characterization. *Applied & Environmental Microbiology*, 66: 5141-5147.

29. Major, D., McMaster, M. L., Cox, E. E., Edwards, E. A., Dworatzek, S. M., Hendrickson, E. R., ... & Buonamici, L. W. (**2002**). Field demonstration of successful bioaugmentation to achieve dechlorination of tetrachloroethene to ethene. *Environmental Science & Technology*, 36: 5106-5116.

30. Maphosa, F., de Vos, W. M., & Smidt, H. (**2010**). Exploiting the ecogenomics toolbox for environmental diagnostics of organohalide-respiring bacteria. *Trends in Biotechnology*, 28: 308-316.

31. Maymo-Gatell, X., Chien, Y. T., Gossett, J. M., & Zinder, S. H. (**1997**). Isolation of a bacterium that reductively dechlorinates tetrachloroethene to ethene. *Science*, 276: 1568-1571.

32. Maymó-Gatell, X., Anguish, T., & Zinder, S. H. (**1999**). Reductive dechlorination of chlorinated ethenes and 1, 2-dichloroethane by "*Dehalococcoides ethenogenes*" 195. *Applied & Environmental Microbiology*, 65: 3108-3113.

33. Maymó-Gatell, X., Nijenhuis, I., & Zinder, S. H. (**2001**). Reductive dechlorination of cis-1, 2-dichloroethene and vinyl chloride by "*Dehalococcoides ethenogenes*". *Environmental Science & Technology*, 35: 516-521.

34. McMurdie, P. J., Behrens, S. F., Müller, J. A., Göke, J., Ritalahti, K. M., Wagner, R., ... & Spormann, A. M. (**2009**). Localized plasticity in the streamlined genomes of vinyl chloride respiring *Dehalococcoides*. *PLoS Genetics*, 5: e1000714.

35. Morris, R. M., Fung, J. M., Rahm, B. G., Zhang, S., Freedman, D. L., Zinder, S. H., & Richardson, R. E. (**2007**). Comparative proteomics of *Dehalococcoides* spp. reveals strain-specific peptides associated with activity. *Applied & Environmental Microbiology*, 73: 320-326.

36. Müller, J. A., Rosner, B. M., Von Abendroth, G., Meshulam-Simon, G., McCarty, P. L., & Spormann, A. M. (**2004**). Molecular identification of the catabolic vinyl chloride reductase from Dehalococcoides sp. strain VS and its environmental distribution. *Applied & Environmental Microbiology*, 70: 4880-4888.

37. Neumann, A., Wohlfarth, G., & Diekert, G. (**1998**). Tetrachloroethene dehalogenase from Dehalospirillum multivorans: cloning, sequencing of the encoding genes, and expression of the pceA gene in Escherichia coli. *Journal of Bacteriology*, 180: 4140-4145.

38. Rahm, B. G., Morris, R. M., & Richardson, R. E. (**2006**). Temporal expression of respiratory genes in an enrichment culture containing *Dehalococcoides ethenogenes*. *Applied & Environmental Microbiology*, 72: 5486-5491.

39. Rahm, B. G., & Richardson, R. E. (**2008**). *Dehalococcoides*' gene transcripts as quantitative bioindicators of tetrachloroethene, trichloroethene, and cis-1, 2-dichloroethene dehalorespiration rates. *Environmental Science & Technology*, 42: 5099-5105.

40. Rowe, A. R., Heavner, G. L., Mansfeldt, C. B., Werner, J. J., & Richardson, R. E. (**2012**). Relating Chloroethene Respiration Rates in Dehalococcoides to Protein and mRNA Biomarkers. *Environmental Science & Technology*.

41. Rowe, A. R., Mansfeldt, C. B., Heavner, G. L., Richardson, R. E. (**2013**). *Methanospirillum* respiratory biomarkers correlate with hydrogenotrophic methanogenesis rate during drowth in competition for hydrogen in an organochlroine-respiring mixed culture. *Environmental Science Technology*.

42. Scheutz, C., Durant, N. D., Dennis, P., Hansen, M. H., Jørgensen, T., Jakobsen, R., ... & Bjerg, P. L. (**2008**). Concurrent ethene generation and growth of *Dehalococcoides* containing vinyl chloride reductive dehalogenase genes during an enhanced reductive dechlorination field demonstration. *Environmental Science & Technology*, 42: 9302-9309.

43. Seshadri, R., Adrian, L., Fouts, D. E., Eisen, J. A., Phillippy, A. M., Methe, B. A., ... & Heidelberg, J. F. (**2005**). Genome sequence of the PCE-dechlorinating bacterium *Dehalococcoides ethenogenes*. *Science*, 307: 105-108.

44. Soboh, B., Pinske, C., Kuhns, M., Waclawek, M., Ihling, C., Trchounian, K., ... & Sawers, G. (**2011**). The respiratory molybdo-selenoprotein formate dehydrogenases of *Escherichia coli* have hydrogen: benzyl viologen oxidoreductase activity. *BMC Microbiology*, 11: 173.

45. Sung, Y., Ritalahti, K. M., Apkarian, R. P., & Löffler, F. E. (**2006**). Quantitative PCR confirms purity of strain GT, a novel trichloroethene-to-ethene-respiring *Dehalococcoides* isolate. *Applied & Environmental Microbiology*, 72: 1980-1987.

46. Tang, Y. J., Yi, S., Zhuang, W. Q., Zinder, S. H., Keasling, J. D., & Alvarez-Cohen, L. (**2009**). Investigation of carbon metabolism in "*Dehalococcoides ethenogenes*" strain 195 by use of isotopomer and transcriptomic analyses. *Journal of Bacteriology*, 191: 5224-5231.

47. Waller, A. S., Krajmalnik-Brown, R., Löffler, F. E., & Edwards, E. A. (**2005**). Multiple reductive-dehalogenase-homologous genes are simultaneously transcribed during dechlorination by *Dehalococcoides*-containing cultures. *Applied & Environmental Microbiology*, 71: 8257-8264.

CHAPTER 4:

Identification of Stress Responses in the Transcriptome and Proteome of *Dehalococcoides mccartyi*

4.A. Abstract

As mixed cultures containing *Dehalococcocides mccartyi* are commonly applied to treat chlorinated organic contaminants in environmental systems, these organisms are often exposed to a wide range of environmental stressors. The objective of this study was to subject *Dehalococcoides* strains in two mixed cultures (Cornell University's D2 and the commercial strain KB-1®) to a wide range of potential stress conditions and infer response pathways through high-throughput mRNA and protein expression data. The specific conditions analyzed in this study were electron donor limitation, solvent stress (toxic levels of 1,1,1-trichloroethane, cis-dichloroethene, or tetrachloroethene), oxygen stress, and pH stress. These studies successfully captured transcripts that have been previously related to stress (such as a methylglyoxal synthase (DET0137) and a small *hymC* subunit (DET0446). Under the majority of conditions, the DnaJ/HspR chaperones (DET1411-1412) displayed significant differential expression, suggesting they may serve as potential biomarkers for a general stress response. Unique stress responses occurred for the specific conditions. In feeding high rates of cis-dichloroethene to D2, four members of an operon encoding for a putative drug transporter (DET1616-1619) displayed a fold change of 2.8±1.1 to 3.9±1.5. Regulation of this pathway may be a response to either solvent accumulation, chloroform contamination, or the presence of cis-dichlorothene. In the cultures recovering from oxygen stress, the operon surrounding the superoxide dismutase (DET0953-0956 a.k.a. DMC0923-0925) displayed significantly higher abundance in D2's

protein pool (2.0±1.1) and in KB-1®'s transcriptome (26±21). Additionally, this transcript served as a potential indicator of a minor DMC member turning on a specific stress pathway and replacing the dominant DMC member of the community (in RNA abundance detected). This study serves as a first step to develop a wide range of prescriptive field site bioindicators by narrowing the potential pool of specific proteins or mRNAs to characterize in more detail.

4.B. Introduction

While chlorinated organic compounds, such as the chloroethenes and chlorobenzenes, are common groundwater contaminants and detrimental to human (37) and ecosystem health (4), bacteria of the *Dehalococcoides* genus respire these same molecules (26). Strains of *Dehalococcoides mccartyi* (DMC) also require hydrogen as an electron donor (23). This ability of dehalorespiration, and the unique ability to completely reductively dechlorinate tetrachloroethene (PCE) to ethene (ETH) (26) with some strains gaining energy from the critical vinyl chloride (VC) to ETH step, have prompted the application of these organisms in field-site bioremediation applications (39). Several case studies have noted successful application of DMC communities in on-site remediation (17,31,39). Additionally, commercial cultures of reductively dechlorinating mixed communities containing DMC are available for purchase.

The increased application of DMC in field sites exposes the organism to a broad range of environmental conditions, including conditions that can be stressful or lethal (3). This study classifies stressful conditions as any change to the culture state that causes the DMC strain in the mixed community to display slow, limited, or no respiration of chloroethenes. An improved understanding into the stress response of DMC is required for more designed and optimized

applications of the organism (3). Previous research monitoring specific respiratory responses of the organism focused on characterizing DMC strains under oxygen stress (2,21), 1,1-di- and 1,1,1-tri-chloroethane (DCA and TCA) stress (6), temperature stress (13), high sulfate concentrations (15), and electron acceptor saturation causing potential solvent toxicity (1). Screens for genome wide behavior under stressful conditions have also recently been reported for DMC grown under nitrogen limitation (25). Each of these field-relevant stress conditions impact the rate of reductive dechlorination. A few of these studies have suggested that stressful conditions can also alter traditional respiration biomarkers (2,13). Being able to assess stress in these organisms is critical to monitoring and ensuring effective remediation practices in the field.

This study looks to extend the insights of DMC stress through analyzing high-throughput data for specific stressful conditions. Datasets previously used to model DMC's global trasncriptomic behavior of DMC195 in D2 (Chapter 2 and 3) and the commercially available KB-1® community (Chapter 3) contains various conditions that challenged the organism. The D2 culture was selected for study because it provides a single strain of DMC in a mixed microbial community that has been previously well studied and characterized. In contrast, the SiREM KB-1® culture maintains multiple populations of DMC targeting the two major lineages (Cornell and Pinelles; Chapter 3). This provides an opportunity to detect DMC genus- and strain-specific responses to stress conditions. These conditions included exposure to oxygen, 1,1,1-trichloroethane, low pH, toxic or saturating levels of chlorinated electron acceptors, and electron donor limitation.

Understanding the impact of each of these potential stressors is important for optimized application of reductive dechlorination. Oxygen is introduced to DMC-type organisms in field site settings as shifting groundwater levels or infiltration of surface waters contaminate anaerobic environments with oxygenated water. To DMC-type organisms, oxygen is highly toxic in that it attacks the organism non-specifically through general oxidative pressures but also inhibits the metal cofactors that are essential for its main respiration linked hydrogenases (21). 1,1,1-trichloroethane (TCA), a common co-contaminant found with chloroethenes in field sites, has been shown to inhibit the crucial reductive dechlorination step of VC to ETH (6). At chlorinated organic saturating conditions, often found in groundwaters with non-aqueous phase liquids pooling at the base of aquifers, *Dehalococcoides* actually has been shown to be unable to reductively dechlorinate (1). Though these stressors generally inhibit dehalorespiration, they likely cause different physiological responses in the organism.

The objective of this work is to discover stress responses in DMC using transcriptomic and proteomic techniques. Understanding how DMC responds in an attempt to survive in these challenging conditions potentially uncovers biomarkers of general and specific stress that could be used diagnostically to understand reasons for stalled bioremediation.

4.C. Materials and Methods

This section describes the general culturing techniques required to maintain and explore the D2 and SiREM KB-1® communities, the experimental setups designed to target specific stress conditions, the different high-throughput approaches taken to analyze the cultures, and the subsequent data handling and management required to draw conclusions.

4.C.1. Electron acceptor and donor chemicals

The electron acceptors for DMC in this study were PCE (99+%, ACROS Organics), TCE (99+%, ACROS Organics), cis-DCE (99+%, TCIAmerica), and 1,1,1-TCA (99+%, ACROS Organics). The electron donors were either hydrogen (AIRGas), butyrate (99+%, ACROS Organics), and/or yeast extract (bacteriological grade, Mo Bio Laboratories). Cultures receiving hydrogen as an electron donor were fed acetic acid (99.7%, Fisher Scientific) as a carbon source.

4.C.2. Culture maintenance

This study investigated two liquid mixed microbial cultures: the Donna II (D2) Cornell laboratory strain and the commercially available KB-1® culture (SiREM Laboratories). The KB-1® culture was shown to have multiple species of DMC from the Cornell and Pinellas lineages whereas the D2 culture contains a sole DMC195 from the Cornell cluster. In addition to the respective DMC strains present in both mixed communities, both cultures contain populations of syntrophic fermenters and methanogenic Archaea (36). The KB-1® culture also contains strains of *Geobacter* (an organism capable of reductive dechlorination) and organisms from the *Spirochetes* (19). The D2 culture was maintained as previously described (11). The commercially available KB-1® was provided by SiREM Labs Guelph, Ontario. After receipt, the culture was stored at 4°C for under one week. Experiments for both the D2 and KB-1® cultures were conducted with 100 mL of liquid culture.

4.C.3. Gas chromatographic monitoring

Chlorinated ethene levels were monitored using gas chromatography (GC) flame ionization detection (FID), methane and high levels of hydrogen were monitored using a thermal

conductivity detector (TCD), and low levels of hydrogen was monitored using a reduction gas detector (RGD) as previously described (7,8,12,32). Oxygen for the KB-1® oxidative stress experiment was measured by GC TCD with a 3-ft × 1/8-in. column packed with 60/80 Molecular Sieve 5A (Supelco, Inc.), held isothermally at 30 °C as previously described (14).

4.C.4. Continuous feed rate apparatus setup

For all continuously fed experiments outlined in this study, the precise setup has been previously described (34,35, Chapter 2). In brief, 160-mL glass serum bottles were filled with 100 mL of anaerobic D2 or KB-1®. Varying combinations of Pressure Lok® syringes (VICI Precision Sampling) were loaded on a Cole Palmer 74900 Syringe Pump to deliver the electron acceptor and donor at an desired rates.

4.C.5. Experimental setup of the stress investigations

An overview of all experiments run and data collected is presented in Table 4.1. The specific experimental summary setup for each condition is presented in Appendix IV.

4.C.6. RNA extraction and reverse transcription:

RNA for the microarray studies was extracted from 50 mL of mixed community culture as described previously (Chapters 2 and 3). The extraction protocol was a modified form of the RNeasy© Mini Kit (Qiagen) (33,34,35, Chapters 2 and 3). The RNA was reverse transcribed into cDNA utilizing the Superscript II (Invitrogen) reverse transcriptase (42,Chapter 2 and 3). During the reverse transcription step, an amino-allyl dUTP was added to be polymerized into the final

Table 4.1. Summary of the stress experimental conditions run for the KB-1and D2 cultures, including stress type, culture type, number of replicates (n), culturing method (Batch vs. Continuous) and data types analyzed. Indications of stress observed in the metabolite data are listed: yes, no, or not conclusive (NC).. Underneath proteomic sequencing, Yes indicates analysis performed on all data sets, and (1) indicates one of the experimental samples was run. Complete descriptions of these experiments are provided in Appendix IV.

Stress Type	Mixed Culture Type	Number of Cultures Stressed	Batch or Continous	Stress Displayed in Metabolite Data?	Proteomic Sequencing	Microarray Data
TCA	KB-1™	4	Batch	No	-	Yes
Oxygen	KB-1™	4	Batch	Yes	Yes	Yes
	D2	4	Continous	Yes	Yes	-
Low pH	KB-1™	4	Continous	NC	Yes	-
	D2	4	Continous	Yes	Yes	-
DCE High	D2	3	Continous	Yes	(1)	Yes
Solvent	D2	2	Continous	Yes	(1)	Yes
No Donor	D2	2	Continous	Yes	(1)	Yes

complementary DNA (cDNA) in order that the NHS-ester cyanine-3 or -5 dye molecule (Cy3 or Cy5, GE Healthcare) would attach to the transcript of interest. The procedure for labeling and purifying the sample is detailed in Chapter 2.

4.C.7. Microarray platforms, hybridization, and scan:

Microarray samples for D2 were run on the Agilent 8x15 K 2-Color Microarray platform designed specifically for the community, as previously described (GSE26288; Chapter 2 and 3). The commercially available KB-1® samples were run on an Agilent 4x44 K 2-Color Microarray designed to target the pangenome of DMC195, BAV1, CBDB1, GT, KB-1, and VS as detailed in Hug *et al.* 2011 (20). The hybridization, washing, and scanning of the samples were performed by the Cornell University Microarray Core Facility (http://cores.lifesciences.cornell.edu/brcinfo/) and followed the methods outlined by the manufacturer (Chapter 2).

4.C.8. Microarray data processing

In brief, microarray image analysis was conducted using Agilent Feature Extraction 10.5 Image Analysis Software. The Feature Extraction Software was also utilized to perform a within-array modified LOESS normalization. Replicate spots for the same probe (ranging from 4-20 spots/probe) were geometrically averaged. The raw and normalized data have been uploaded and is freely available at the NCBI GEO database (reference series ID number GSE26288 and GSE42136).

4.C.9. Proteomic analysis

All protein samples were based on cell pellets of 50 mL culture (14,000×*g*, 10 minutes). These cell pellets were shipped on dry ice to the Environmental Molecular Sciences Laboratory (EMSL) at the Pacific National Northwest Laboratories (PNNL) following the method detailed below. All Shotgun and TMT Multiplex proteomic samples were processed by EMSL. The complete sample preparation and analysis method is presented in Appendix III.

4.C.10. Proteomic and transcriptomic data normalization

The values reported through the proteomic and transcriptomic analysis were normalized by dividing each detected value by the sum of all values detected for DMC in the individual experiment. This provided a global normalization to the total amount of DMC specific proteins or transcripts that were detected in the proteomic sequencing or microarray analysis, respectively. Both the proteomic sequencing and microarray analysis analyzed a total quantity of material (25 µg of extracted protein and 400 (for D2) or 800 ng (for KB-1®) reverse transcribed and labeled cDNA, respectively). Both KB-1® and D2 contain other organisms in the community that could potentially introduce a bias in the percentage of material that is DMC specific. This normalizing step was employed to circumvent potential global biases.

Significant differentially detected proteins of probe intensities were determined by an unpaired student t-test of the sum-normalized intensity values. The threshold was set at $p = 0.05$. For transcripts detected on microarrays, the processed fluorescence intensity had to exceed 1000 pfu in one of the analyzed samples to be reported (significantly above background hybridization

signal for both the pangenome and DMC195 specific microarrays) and display a ratio change greater than two.

4.D. Results

The results are broken into subsections looking at the response of the KB-1® culture to the addition of 1,1,1-TCA, of both D2 and KB-1® to the addition of oxygen, of both D2 and KB-1® to low pH, of D2 to high feed rates of DCE, of D2 to saturating PCE levels, and of D2 to no exogenous electron donor provided. Table 4.1 shows a summary of experiments and types of responses monitored for each.

4.D.1 KB-1®'s transcriptomic response to the presence of 1,1,1-TCA

Prior to 1,1,1-TCA addition, the KB-1® cultures were batch fed 220 µM TCE. After 22 hours, these cultures reductively dechlorianted the TCE to predominantly VC and ETH (Appendix Figure A5.1). At this time point, all cultures were refed and 22 µM 1,1,1-TCA was added to four cultures (Figure A5.1.c-f). Reductive dechlorination continued in all cultures without a significant detection of slowing chloroethene respiration. Intriguingly, two of the 1,1,1-TCA amended cultures (Figure A5.1.c,e) reductively dechlorinated TCE to ETH while the other two cultures (Figure A5.1.d,f) only reductively dechlorinated to VC even though these four cultures were established from the same parent culture.

Although stress was not evident from the reductive dechlorination patterns, the pangenome microarray detected differential transcript abundance including some probes that resolved unique DMC strain behaviors in the 1,1,1-TCA-amended KB-1® commercial cultures.

Table 4.2. Top and bottom 20 differentially detected transcripts for the KB-1® 17 hours post 1,1,1-TCA addition to the controls. The full list of is presented in Appendix Table A5.1.

DMC#	Probe ID	Strain	Description	Ratio of 17 hour Post TCA Added versus Controls	17 hour Post TCA Added Average Intensity (pfu)	Controls Average Intensity (pfu)
DMC1887	KB1_0047	-	hypothetical protein	48 ± 12	132122 ± 32441	2741 ± 3
DMC1260	panDhc_3290_RC	Pinellas	fasciclin domain protein	35 ± 7.5	30300 ± 5594	876 ± 100
DMC0924	KB1_0941	-	heat shock protein Hsp20	26 ± 21	53068 ± 8478	2049 ± 1592
DMC0924	gi147669481	Pinellas	heat shock protein Hsp20	25 ± 20	52967 ± 8874	2139 ± 1698
DMC1736	panDhc_346	Pinellas	extracellular solute-binding protein family 5	24 ± 23	18549 ± 2564	774 ± 721
DMC1264	panDhc_4045_RC	Pinellas	hypothetical protein	24 ± 13	17324 ± 3626	723 ± 359
DMC1264	VS1089	Pinellas	hypothetical protein	24 ± 6.7	8865 ± 2384	376 ± 35
DMC1264	panDhc_4120_RC	Pinellas	hypothetical protein	23 ± 10	16254 ± 3125	707 ± 280
DMC1207	panDhc_4028_RC	Pinellas	hypothetical protein	21 ± 13	26670 ± 4361	1256 ± 742
DMC1894	panDhc_606_RC	Pinellas	putative reductive dehalogenase	21 ± 8.9	28089 ± 7979	1339 ± 423
DMC1748	panDhc_1475_RC	Pinellas	hypothetical protein	18 ± 5.5	7168 ± 1351	390 ± 91
DMC1207	panDhc_4028	Pinellas	hypothetical protein	16 ± 11	30638 ± 5765	1890 ± 1197
DMC1523	KB1_0098	-	antioxidant, AhpC	16 ± 3.3	60515 ± 9531	3735 ± 472
DMC1264	panDhc_4120	Pinellas	protein of unknown function DUF1508	14 ± 8.0	25383 ± 7497	1834 ± 906
DMC1260	panDhc_3290	Pinellas	fasciclin domain protein	13 ± 4.7	24844 ± 2955	1968 ± 701
DMC0925	panDhc_1808	Pinellas	Rubrerythrin	13 ± 4.0	34251 ± 5101	2734 ± 776
DMC1523	panDhc_2442_RC	Unassigned	antioxidant, AhpC	11 ± 3.3	34682 ± 8127	3101 ± 550
DMC1210	VS1037	Unassigned	hypothetical protein	11 ± 9.2	32242 ± 1238	3041 ± 2651
DMC1487	panDhc_3740_RC	Unassigned	reductive dehalogenase anchoring protein	10 ± 5.0	38237 ± 3654	3666 ± 1731
DMC1488	panDhc_506_RC	Pinellas	putative reductive dehalogenase	10 ± 6.9	134473 ± 32755	13156 ± 8314
⋮	⋮	⋮	⋮	⋮	⋮	⋮
DMC0361	panDhc_1290	Unassigned	membrane-associated zinc metalloprotease	0.41 ± 0.064	499 ± 22	1231 ± 186
DMC0973	panDhc_1860	Cornell	hypothetical protein	0.41 ± 0.16	560 ± 227	1383 ± 26
DMC0994	KB1_1021	-	AMP-dependent synthetase and ligase	0.40 ± 0.084	895 ± 184	2255 ± 102
DMC1199	panDhc_2842_RC	Cornell	peptide methionine sulfoxide reductase MsrA	0.39 ± 0.14	468 ± 156	1202 ± 121
DMC0411	panDhc_1750_RC	Unassigned	DegV family protein	0.39 ± 0.11	6635 ± 1648	17133 ± 1966
DMC1561	panDhc_717_RC	Cornell	hypothetical protein	0.38 ± 0.013	1574 ± 3	4172 ± 142
DMC0553	VS504	Unassigned	ATP synthase F1, epsilon subunit	0.35 ± 0.007	1721 ± 14	4937 ± 91
DMC0196	panDhc_1387_RC	Cornell	glycosyl transferase, group 2 family protein	0.34 ± 0.061	1952 ± 218	5687 ± 793
DMC0553	KB1_0608	-	ATP synthase F1, epsilon subunit	0.34 ± 0.013	3198 ± 88	9447 ± 252
DMC1561	panDhc_717	Cornell	hypothetical protein	0.32 ± 0.095	1055 ± 310	3288 ± 116
DMC0550	panDhc_496	Pinellas	ATP synthase F1, alpha subunit	0.30 ± 0.078	510 ± 128	1678 ± 90
DMC0197	panDhc_1500	Cornell	NAD-dependent epimerase/dehydratase	0.28 ± 0.064	331 ± 2	1173 ± 268
DMC0547	GT_460801	-	ATP synthase F0, C subunit	0.28 ± 0.063	4174 ± 809	14878 ± 1654
DMC0178	VS174	Unassigned	formate dehydrogenase accessory protein	0.28 ± 0.18	962 ± 608	3450 ± 472
DMC0549	panDhc_2797_RC	Unassigned	ATP synthase F1, delta subunit	0.27 ± 0.075	3367 ± 612	12396 ± 2562
DMC0552	panDhc_645	Unassigned	ATP synthase subunit B	0.27 ± 0.088	4102 ± 1353	15336 ± 260
DMC0547	KB1_0602	-	ATP synthase F0, C subunit	0.27 ± 0.057	4163 ± 753	15571 ± 1757
DMC0547	gi147669178	Unassigned	ATP synthase F0, C subunit	0.27 ± 0.063	4176 ± 883	15683 ± 1686
DMC1235	panDhc_3190_RC	Unassigned	N utilization substance protein B	0.22 ± 0.042	1069 ± 173	4911 ± 500
DMC0201	panDhc_1571	Cornell	glycosyl transferase, group 2 family protein	0.18 ± 0.058	656 ± 157	3610 ± 755

Comparing the cultures that were sampled 17 hours after 1,1,1-TCA addition (Figure A5.1.c and d) to both the controls (Figure A5.1.a and b) revealed transcripts responding to the initial exposure to 1,1,1-TCA. This comparison detected 154 and 33 probes with significantly higher and lower absolute intensities corresponding to 87 and 29 unique proteins, respectively. Significance was determined by assigning a t-test p-value to the comparison of the average intensities. The highest and lowest 20 ratios are presented in Table 4.2 with the full list provided in Appendix Table A5.1. The highest ratios listed multiple homologous transcripts for the putative stress response proteins Hsp20 (26±21, DMC0924), rubrerythrin (13±4, DMC0925), and AhpC (16±3.3, DMC1523). Additional transcripts for putative stress response genes were detected to be higher in the 17 hour post 1,1,1-TCA addition cultures. These included transcripts encoding for a ribosomal general stress protein Ctc (6.7±4.1,DMC1402). In addition to the stress response transcripts, the top 20 ratios also listed two reductive dehalogenases (21±8.9 and 10±6.9 for DMC1894 and DMC1488, respectively) with the list of all significant ratios containing one more (6.2±1.9, DMC1900). DMC1488 is the DET1545 homolog in KB-1 (KB1_0072). The transcripts that displayed lower intensities in the cultures that were added 1,1,1-TCA primarily encoded for ATP synthase subunits (eight out of the bottom twenty).

To detect those transcripts that respond to prolonged exposure to 1,1,1-TCA, duplicate cultures sampled 48 hours after the addition of 1,1,1-TCA (Figure A5.1.e and f) were compared to the duplicate cultures sampled 17 hours after the addition of 1,1,1-TCA (Figure A5.1.c and d). This comparison detected 112 and 64 significantly higher and lower absolute intensities corresponding to 92 and 44 unique proteins, respectively. The highest and lowest 20 ratios are presented in Table 4.3. Of note, multiple probes for DMC0435, a putative *hymA*/*nuoE* type

Table 4.3. Top and bottom 20 differentially detected transcripts for the KB-1® 48 hour post TCA addition to the 17 hour post TCA addition. The full list of differentially regulated transcripts is presented in Appendix Table A5.2.

DMC#	Probe ID	Strain Group	Description	Ratio of 48 hour to 17 hour Post TCA Addition	48 hour Post TCA Added Average Intensity (pfu)	17 hour Post TCA Added Average Intensity (pfu)
DMC1264	panDhc_4041	Cornell	hypothetical protein	42 ± 14	30774 ± 5489	726 ± 204
DMC0014	panDhc_2210	Cornell	hypothetical protein	14 ± 2.3	3389 ± 434	245 ± 25
DMC0435	panDhc_3072	Unassigned	HymA and NuoE type Fe-S cluster protein	14 ± 2.6	20888 ± 3540	1529 ± 130
DMC0435	panDhc_3078	Cornell	HymA and NuoE type Fe-S cluster protein	9 ± 2.6	2402 ± 640	261 ± 26
DMC1488	panDhc_502	Cornell	reductive dehalogenase, putative	8 ± 0.8	18257 ± 85	2360 ± 252
DMC1887	panDhc_3169_RC	Cornell	hypothetical protein	7 ± 1.3	23480 ± 741	3147 ± 558
DMC1199	panDhc_2842_RC	Cornell	peptide methionine sulfoxide reductase MsrA	7 ± 2.7	3321 ± 599	468 ± 156
DMC0925	panDhc_1804_RC	Cornell	bacterioferritin domain protein	6 ± 1.3	2583 ± 491	408 ± 36
DMC0435	gi147669068	Cornell	HymA and NuoE type Fe-S cluster protein	6 ± 2.1	6112 ± 1235	972 ± 266
DMC1277	panDhc_1885	Cornell	acetyltransferase, GNAT family	6 ± 0.80	1625 ± 106	273 ± 32
DMC1398	gi57233747	Unassigned	hypothetical protein	6 ± 1.1	2464 ± 72	428 ± 77
DMC0827	panDhc_922_RC	Cornell	ABC transporter, permease protein, putative	6 ± 2.4	1241 ± 24	220 ± 93
DMC1524	panDhc_3906	Cornell	hypothetical protein	6 ± 0.89	44092 ± 478	7936 ± 1267
DMC2350	gi147668747	Cornell	Resolvase, N-terminal domain	5 ± 1.9	1525 ± 283	307 ± 100
DMC1153	panDhc_328	Cornell	DNA mismatch repair protein, MutL/HexB	5 ± 1.4	3131 ± 179	640 ± 185
DMC1561	panDhc_718	Cornell	cell wall/surface repeat protein	5 ± 1.9	2746 ± 151	568 ± 218
DMC1557	gi57233590	Unassigned	hypothetical protein	5 ± 1.0	10702 ± 1985	2233 ± 237
DMC1271	panDhc_1288	Cornell	radical SAM domain protein	5 ± 0.80	4588 ± 523	985 ± 126
DMC0435	panDhc_3072_RC	Cornell	HymA and NuoE type Fe-S cluster protein	5 ± 2.1	11472 ± 506	2468 ± 1112
DMC0014	panDhc_2210_RC	Cornell	hypothetical protein	5 ± 1.0	2431 ± 441	526 ± 66
⋮	⋮	⋮	⋮	⋮	⋮	⋮
DMC1089	panDhc_2029	Unassigned	imidazoleglycerol phosphate synthase, cyclase	0.21 ± 0.094	1307 ± 561	6197 ± 757
DMC1433	panDhc_2001	Unassigned	tryptophan synthase, alpha subunit	0.21 ± 0.11	228 ± 119	1089 ± 157
DMC1372	gi147669866	Unassigned	hypothetical protein	0.20 ± 0.17	570 ± 480	2801 ± 155
DMC1372	KB1_1410	Pinellas	hypothetical protein	0.20 ± 0.18	575 ± 502	2869 ± 330
DMC0549	panDhc_2797_RC	Unassigned	ATP synthase F1, delta subunit	0.20 ± 0.047	664 ± 104	3367 ± 612
DMC1433	KB1_1466	Unassigned	tryptophan synthase, alpha subunit	0.19 ± 0.14	265 ± 183	1362 ± 307
DMC1372	GT_1079521	Unassigned	hypothetical protein	0.19 ± 0.17	555 ± 477	2890 ± 274
DMC1283	panDhc_3978	-	ribosomal protein L31	0.19 ± 0.077	2976 ± 1207	15808 ± 484
DMC1091	panDhc_761_RC	-	pyridine nucleotide-disulfide oxidoreductase	0.18 ± 0.020	1098 ± 79	5950 ± 498
DMC1372	VS1201	Unassigned	transcriptional regulator, AbrB family	0.18 ± 0.060	227 ± 77	1286 ± 59
DMC1475	panDhc_3315_RC	Unassigned	nitrogenase Fe-Mo cofactor maturation	0.17 ± 0.15	234 ± 204	1383 ± 78
DMC1372	gi57233797	Unassigned	transcriptional regulator, AbrB family	0.16 ± 0.12	224 ± 158	1367 ± 205
DMC1090	panDhc_1102_RC	Unassigned	glutamine amidotransferase, class II	0.15 ± 0.10	689 ± 435	4485 ± 909
DMC0097	KB1_0242	-	*mod* oxidoreductase Fe4S4 region	0.14 ± 0.10	140 ± 95	994 ± 246
DMC0716	KB1_0740	Unassigned	short-chain dehydrogenase/reductase SDR	0.14 ± 0.083	2403 ± 1339	17525 ± 4290
DMC1092	panDhc_2525	Unassigned	imidazole glycerol phosphate synthase	0.13 ± 0.049	545 ± 194	4086 ± 339
DMC1736	panDhc_346	Pinellas	extracellular solute-binding protein family 5	0.12 ± 0.11	2164 ± 2066	18549 ± 2564
DMC1092	panDhc_2525_RC	-	imidazole glycerol phosphate synthase	0.11 ± 0.083	404 ± 303	3684 ± 477
DMC0098	KB1_0243	Cornell	*mod* molybdopterin oxidoreductase	0.11 ± 0.11	543 ± 539	5130 ± 47
DMC0176	panDhc_341_RC	Cornell	ATP-dependent RNA helicase, DEAD/DEAH	0.07 ± 0.052	238 ± 165	3426 ± 995

transcript was positively regulated (the greatest fold change displayed was 14±2.6). Conversely, probes recapturing transcripts for multiple subunits of *hym*, *mod*, and *atpase* were all significantly down regulated in the cultures sampled 48 hours after as compared to the cultures sampled 6 hours after 1,1,1-TCA addition.

Inspecting the GC data for the cultures sampled 48 hours after 1,1,1-TCA addition revealed that the two cultures were not behaving as biological duplicates. 1,1,1-TCA 48 [1] (Appendix Figure 5.1.e) was reductively dechlorinating TCE to ETH while 1,1,1-TCA 48 [2] (Appendix Figure 5.1.f) was reductively dechlorinating TCE to VC. This difference in reductive dechlorination pattern was reflected in the transcriptomic pool as the microarrays for these two cultures displayed a low linear correlation coefficient on a log-log plot of $r = 0.76$ (compared to the 1,1,1-TCA seven hours duplicate cultures $r = 0.97$). The variation noted in the microarray expression as well as the metabolite concentrations may be due to a specific strain response. Previous work identified multiple strains of DMC in KB-1® and established good indicator probes for the Pinelles and Cornell subclasses (Chapter 3). To discern if one of the multiple populations of DMC in KB-1® was responsible for reductively dechlorinating TCE to ETH, the average intensity was taken across all probes designed to target the differing subclasses of DMC. Binning these probes and taking the average intensity resulted in the bar chart comparison presented in Figure 4.1. The overall intensity of the probe subset specific to the Pinellas/KB-1-type strain decreased to a level that was significantly below the Cornell/195-type probe subset. This alteration in the dominance of DMC strains can be seen in Table 4.3 with Cornell/195-type probes highly enriched in the top 20 differentially expressed transcripts.

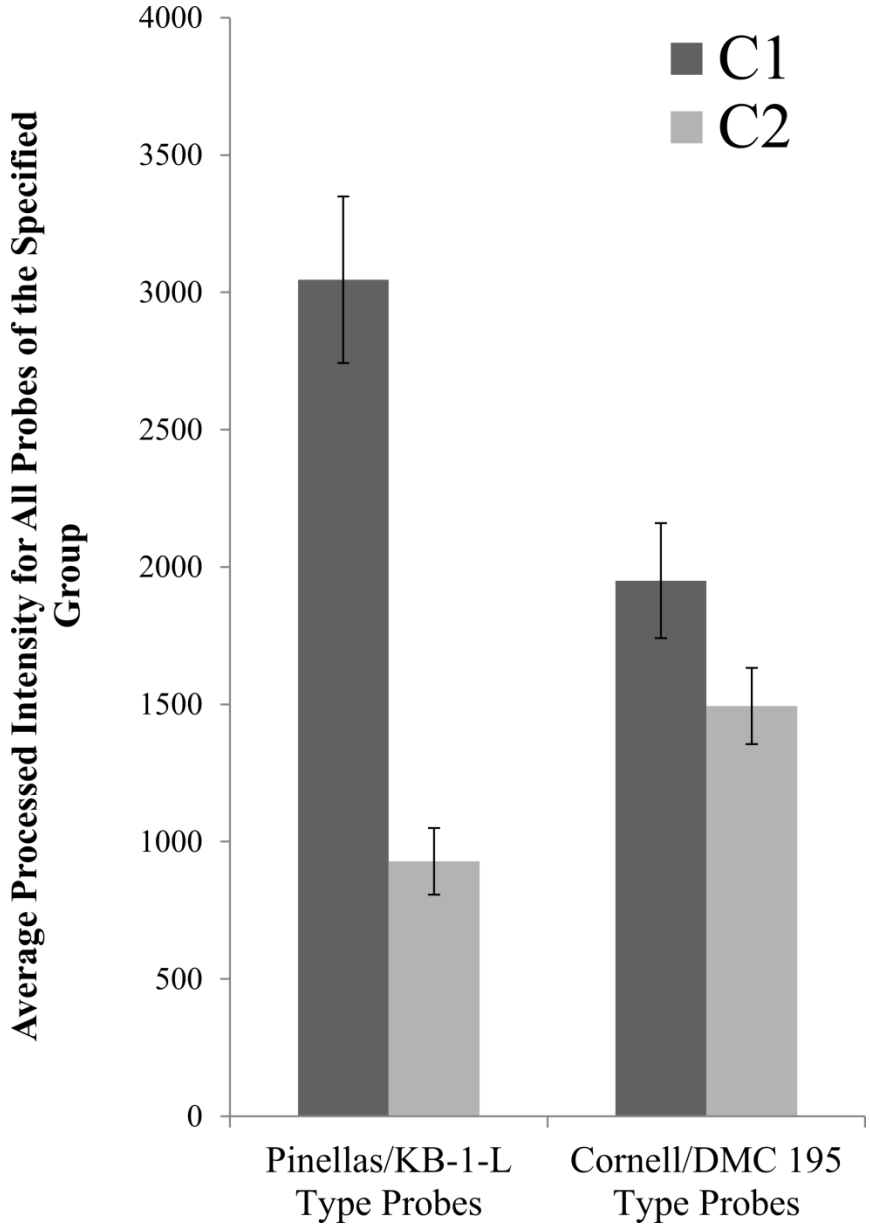

Figure 4.1. Average intensity of the Pinellas/KB-1-L and Cornell/195 specific probes in the panDHC set for the 1,1,1-TCA C1 (ethene generating) and C2 (non-ethene generating) cultures. Error bars represent the 95% confidence interval.

4.D.2 D2's proteomic response to the presence of oxygen

Cultures of D2 that had been respiring PCE for 20 hours at a continuous rate of 0.5 μmole/(L-hr) were challenged with a dose of 3.4 mg oxygen. The addition of oxygen caused a temporary cessation of complete reductive dechlorination in these cultures as evident by the slowing of ETH production and the buildup of PCE (Appendix Figure A5.2.c-f). Reductive dechlorination recovered to the initial state as evident by the PCE dropping back to non-detectable levels and ETH formation resuming (Figure A5.2.e and f, final time point).

To determine the response of the proteome to the initial stress of oxygen addition in D2, the cultures sampled 6 hours after the addition of oxygen (Figure A5.2.c and d) were compared to the control cultures (Figure A5.2.a and b). This comparison detected 11 and 4 significantly higher and lower protein scores, respectively, when compared to both controls, (Table 4.4.a). The protein that displayed the highest ratio change was a HisH imidazole glycerol phosphate synthase (4.08 ± 0.42), a protein involved in glutamine biosynthesis. In addition, a TatA twin arginine translocation protein displayed a 1.98 ± 0.42 fold change.

Cultures sampled 48 hours after the addition of oxygen (Figure A5.2.e and f) were compared to the control cultures (Figure A5.2.a and b) to determine the shifts in the proteome during the culture's recovery from oxygen exposure. Prior to 48 hours, DMC dechlorinated the PCE that accumulated in the oxygen exposed cultures to below detectable values. During this dechlorination, ETH was formed. The comparison of these two conditions detected 23 and 4 significantly higher and lower protein scores, respectively, presented in Table 4.4.b. The significantly higher protein scores in the oxygen recovery cultures included enzymes

Table 4.4. Differentially detected D2 proteins for the (a) 6 hours after oxygen addition to controls and(b) 48 hours after oxygen addition. Highlighted transcripts are putative chaperones or stress response proteins

(a) 6 Hours Exposed to Oxygen

DMC#	DET#	Description	Ratio of 6 Hour to Post Stress to 6 Hour Control	Ratio of 6 Hour to 48 Hour Post Stress	Average Protein Score 6hr Oxygen
DMC1092	DET1132	HisH imidazole glycerol phosphate synthase	4.08 ± 0.42	0.84 ± 0.29	7.5 ± 0.77
DMC0953	DET0985	NusA transcription elongation factor	2.53 ± 0.24	0.65 ± 0.18	14 ± 1.3
DMC1251	DET1294	DNA binding response regulator	2.35 ± 0.24	0.68 ± 0.10	19 ± 2.0
DMC1263	DET1306	hypothetical protein	2.32 ± 0.14	0.96 ± 0.36	62 ± 3.7
DMC0516	DET0527	TldD/PmbA family protein	2.31 ± 0.21	0.50 ± 0.05	8.5 ± 0.78
DMC1285	DET1329	HisI phosphoribosyl AMP cyclohydrolase	2.31 ± 0.17	0.43 ± 0.08	8.5 ± 0.64
DMC1407	DET1459	ribosomal subunit interface protein, putative	2.10 ± 0.27	0.80 ± 0.15	15 ± 2.0
DMC1542	DET1602	TatA twin arginine translocation protein	1.98 ± 0.18	2.44 ± 0.77	26 ± 2.3
DMC0423	DET0434	SecA translocase	1.97 ± 0.080	0.85 ± 0.11	29 ± 1.2
DMC0576	DET0589	GTPase domain, tubulin/FtsZ family protein	1.69 ± 0.014	1.43 ± 0.81	14 ± 0.11
DMC1490	DET1547	PheA prephenate dehydratase	1.58 ± 0.089	0.71 ± 0.15	15 ± 0.82
DMC1402	DET1454	5S rRNA E loop binding protein Ctc/L25/TL5	0.72 ± 0.006	1.00 ± 0.96	6.0 ± 0.05
DMC0551	DET0563	AtpG ATP synthase F1, gamma subunit	0.71 ± 0.006	0.72 ± 0.08	15 ± 0.12
DMC0732	DET0753	ThrS threonyl tRNA synthetase	0.691 ± 0.022	0.61 ± 0.09	31 ± 0.95
DMC0944	DET0976	PurA adenylosuccinate synthetase	0.543 ± 0.004	0.25 ± 0.01	8.0 ± 0.06

(b) 48 Hours After Exposure to Oxygen, Reductive Dechlorination Resuming

DMC#	DET#	Description	Ratio of 48 Hour Post Stress to 48 Hour Control	Ratio of 48 Hour to 6 Hour Post Stress	Average Protein Score 48hr Oxygen
DMC0516	DET0527	TldD/PmbA family protein	13 ± 0.44	2.0 ± 0.19	17 ± 0.56
DMC0644	DET0657	CobT-1 phosphoribosyltransferase	9.0 ± 0.41	2.8 ± 0.99	11 ± 0.52
DMC1329	DET1373	DnaK suppressor protein, putative	8.6 ± 0.92	3.6 ± 1.7	11 ± 1.2
DMC0534	DET0545	amidohydrolase family protein	7.9 ± 0.89	2.5 ± 1.8	9.9 ± 1.1
DMC0290	DET0297	hypothetical protein	7.4 ± 1.2	1.7 ± 0.91	19 ± 3.1
DMC0186	DET0193	ProC pyrroline 5 carboxylate reductase	5.2 ± 0.82	2.4 ± 0.50	13 ± 2.1
DMC1285	DET1329	HisI phosphoribosyl AMP cyclohydrolase	3.9 ± 0.61	2.3 ± 0.40	20 ± 3.1
DMC1251	DET1294	DNA binding response regulator	2.9 ± 0.33	1.5 ± 0.23	29 ± 3.3
DMC1407	DET1459	ribosomal subunit interface protein, putative	2.5 ± 0.32	1.2 ± 0.23	19 ± 2.5
DMC1380	DET1427	GroES chaperonin	2.5 ± 0.22	1.2 ± 0.25	137 ± 12
DMC0335	DET0343	FtsZ-1 cell division protein	2.5 ± 0.04	1.5 ± 0.23	44 ± 0.7
DMC1384	DET1431	HypB hydrogenase accessory protein	2.3 ± 0.03	1.5 ± 0.27	12 ± 0.13
DMC1557	DET1617	hypothetical protein	2.3 ± 0.42	1.8 ± 0.45	15 ± 2.7
DMC0720	DET0740	DapF diaminopimelate epimerase	2.3 ± 0.03	2.3 ± 0.34	20 ± 0.26
DMC1091	DET1131	pyridine nucleotide disulfide oxidoreductase	2.2 ± 0.10	2.8 ± 1.2	36 ± 1.6
DMC1366	DET1413	ClpB chaperone	2.1 ± 0.25	1.7 ± 0.26	92 ± 11
DMC0924	DET0954	Hsp20/alpha crystallin family protein	2.0 ± 0.27	1.7 ± 0.34	15 ± 2.0
DMC1215	DET1258	ArgD acetylornithine aminotransferase	2.0 ± 0.08	2.7 ± 0.39	15 ± 0.64
DMC0944	DET0976	PurA adenylosuccinate synthetase	1.9 ± 0.05	3.9 ± 0.10	32 ± 0.78
DMC0947	DET0979	Myo inositol 1 phosphate synthase	1.9 ± 0.04	2.0 ± 0.16	113 ± 2.2
DMC0543	DET0554	PpsA phosphoenolpyruvate synthase	1.8 ± 0.08	1.6 ± 0.29	96 ± 4.3
DMC0789	DET0816	SufB/SufD domain protein	1.6 ± 0.03	1.4 ± 0.17	81 ± 1.7
DMC0550	DET0562	AtpA ATP synthase subunit A	1.5 ± 0.00	1.3 ± 0.13	123 ± 0.32
DMC0386	DET0396	conserved hypothetical protein	0.78 ± 0.008	0.94 ± 0.26	12 ± 0.13
DMC0479	DET0490	RplR ribosomal protein L18	0.38 ± 0.12	0.28 ± 0.19	2.4 ± 0.78
DMC1313	DET1357	hypothetical protein	0.37 ± 0.017	0.34 ± 0.05	3.8 ± 0.17
DMC1527	DET1586	lemA family protein	0.36 ± 0.050	0.35 ± 0.05	11 ± 1.5

involved in protein folding and oxidative stress response (DET1373 DnaK 8.6±0.92; DET1427 GroES 2.5±0.22; DET1413 ClpB 2.1±0.25; DET0954 Hsp20 2.0±0.27).

4.D.3 Proteomic and transcriptomic response to the presence of oxygen for the KB-1® community

An oxygen stress study also was performed on the KB-1® community. Cultures of KB-1® that had reductively dechlorinated a batch pulse of 200 µmoles/L of TCE to DCE, VC, and ETH were purged, re-fed, and spiked with 3.1 mg of O_2 after 20 hours (Appendix Figure A5.3). The cultures sampled 10 hours after oxygen addition showed variability in the TCE to DCE reductive dechlorination step (Figure A5.3.c vs. d). This reductive dechlorination step can be performed by the *Geobacter* species in the community. Therefore, even with the detection of DCE, the DMC species were still inhibited as reductive dechlorination to VC or ETH was absent. These cultures were sacrificed to detect proteins and transcripts responding to the initial shock of oxygen. After 48 hours, the oxygen was completely scavenged (data not shown) and reductive dehalogenation resumed in the two remaining cultures (at around 30 hours after oxygen addition). The final time point at 70 hours after oxygen addition displayed a small but detectable quantity of VC and ETH building in the culture, indicating the DMC population is resuming reductive dechlorination. These cultures were sacrificed to detect proteins and transcripts involved in the cultures' recovery.

To determine the response of KB-1®'s proteome and transcriptome to the initial stress of oxygen addition, cultures sampled 10 hours after the spike (Figure A5.3.c and d) were compared to the control cultures (Figure A5.3.a and b). Eight proteins displayed confident differential

detection with three proteins higher in fold change (KB1_0054 RDase 1.21 ± 0.04; KB1_0866 hypothetical protein 1.15 ± 0.04; KB1_0743 aspartate aminotransferase 1.10 ± 0.02) and 5 proteins lower (KB1_0522 50S ribosomal protein 0.81 ± 0.04; KB1_603 ATP synthase 0.81 ± 0.04; KB1_0595 RpoD 0.81 ± 0.04; KB1_0425 pyridoxine biosynthesis 0.81 ± 0.04) in the 10 hours post oxygen amended culture. Applying this comparison of the cultures 10 hours post oxygen addition to the controls to the corresponding microarray transcriptomic data revealed 20 and 33 probes displaying higher and lower intensities, respectively (Table 4.5). The probes displaying higher intensities in the 10 hour post oxygen addition cultures were dominated by ribosomal protein targeting probes (16 out of the 20). In addition, the highest positive fold change was noted for a nicotinate-nucleotide-dimethylbenzimidazole (DMC1695, 20 ± 4.1). Surprisingly, probes targeting general stress and chaperon transcripts populated the list of the significant lower intensity probes at the 10 hour sampling point. These included *groES* (DMC1380, 0.25 ± 0.06), *ctc* (DMC1402, 0.31 ± 0.18), and a superoxide dismutase (DMC0926, 0.25 ± 0.06).

As the oxygen was scavenged by the KB-1® culture (below detection 48 hours after added), reductive dechlorination resumed (Appendix Figure 5.3.e-f). Comparing the duplicate cultures 70 hours after oxygen addition to the duplicate cultures 10 hours after oxygen addition revealed proteins and transcripts potentially involved in the recovery of DMC from oxidative stress. The proteomic survey revealed 24 and 9 proteins with higher and lower intensities, respectively (Appendix Table A5.5). Of note, the VcrA RDase, a RDase capable of coupling energy generation with reductive dechlorination of VC to ETH, displayed a substantially lower intensity with a ratio of 0.36 ± 0.03. In the corresponding transcriptomic data for the comparison

Table 4.5. Differentially detected KB-1® transcripts for the 10 hours after oxygen addition compared to the controls

DMC#	Probe ID	Strain	Description	Ratio of 10 Hour Post Oxygen Stress to Controls	Average Intensity of 10 Hour Oxygen Stress (pfu)	Average Intensity of Control Cultures (pfu)
DMC1695	KB1_0699	-	dimethylbenzimidazole phosphoribosyltransferase	20 ± 4.7	3547 ± 835	177 ± 1
DMC1695	panDhc_1257	Pinellas	dimethylbenzimidazole phosphoribosyltransferase	8.4 ± 3.5	2198 ± 555	262 ± 86
DMC0390	panDhc_1170_RC	Pinellas	3-dehydroquinate synthase family protein	3.9 ± 2.0	4067 ± 110	1041 ± 520
DMC0461	panDhc_180_RC	Unassigned	translation elongation factor G	3.2 ± 0.49	1912 ± 166	588 ± 73
DMC0958	gi147669523	Unassigned	ribosomal protein L7/L12	3.0 ± 1.1	11044 ± 1522	3736 ± 1237
DMC0964	GT_c801167	-	ribosomal protein L33	2.9 ± 0.06	7823 ± 75	2735 ± 47
DMC0964	gi147669529	Unassigned	ribosomal protein L33	2.8 ± 0.18	7349 ± 294	2635 ± 133
DMC0489	panDhc_3332	Unassigned	30S ribosomal protein S11	2.7 ± 0.59	9284 ± 1753	3392 ± 343
DMC0471	gi147669104	Unassigned	ribosomal protein L29	2.7 ± 0.55	9127 ± 1458	3394 ± 437
DMC0467	VS421	Unassigned	ribosomal protein S19	2.6 ± 0.64	7491 ± 701	2874 ± 652
DMC0471	GT_395950	-	ribosomal protein L29	2.6 ± 0.60	9136 ± 1529	3530 ± 569
DMC0471	KB1_0527	-	ribosomal protein L29	2.6 ± 0.61	9090 ± 1757	3517 ± 470
DMC0477	KB1_0532	-	ribosomal protein S8	2.3 ± 0.57	3928 ± 45	1723 ± 433
DMC0477	VS430	Unassigned	ribosomal protein S8	2.2 ± 0.48	3652 ± 184	1627 ± 338
DMC0477	gi147669110	Unassigned	ribosomal protein S8	2.2 ± 0.59	3775 ± 40	1690 ± 446
DMC0477	GT_397900	-	ribosomal protein S8	2.2 ± 0.59	3705 ± 235	1686 ± 438
DMC0469	panDhc_1764	Pinellas	ribosomal protein S3	2.1 ± 0.30	5935 ± 334	2775 ± 357
DMC0461	panDhc_179	Unassigned	translation elongation factor G	2.1 ± 0.21	5480 ± 352	2614 ± 205
DMC0490	gi147669123	Unassigned	30S ribosomal protein S4	2.0 ± 0.50	9484 ± 393	4699 ± 1155
DMC0163	panDhc_2202_RC	Cornell	DNA-binding response regulator	0.50 ± 0.11	436 ± 70	881 ± 124
DMC0611	panDhc_1365	Unassigned	response regulator	0.49 ± 0.07	4489 ± 346	9222 ± 1018
DMC0626	panDhc_2240	Cornell	hypothetical protein	0.47 ± 0.11	328 ± 76	693 ± 38
DMC1884	panDhc_3832	Unassigned	sensor histidine kinase/response regulator	0.47 ± 0.16	536 ± 177	1146 ± 29
DMC1308	panDhc_955_RC	Unassigned	pilin biogenesis protein, putative	0.46 ± 0.09	1295 ± 220	2790 ± 225
DMC1527	VS1470	Unassigned	lemA family protein	0.46 ± 0.11	2011 ± 468	4358 ± 50
DMC0513	panDhc_1469_RC	Cornell	PBS lyase HEAT-like repeat domain protein	0.46 ± 0.15	2399 ± 801	5234 ± 155
DMC0212	panDhc_2963_RC	Cornell	PBS lyase HEAT-like repeat domain protein	0.44 ± 0.01	1345 ± 42	3046 ± 34
DMC0990	gi57234218	Unassigned	hypothetical protein	0.44 ± 0.10	3992 ± 613	9078 ± 1540
DMC1268	gi57233985	Cornell	hypothetical protein	0.44 ± 0.11	1366 ± 353	3125 ± 58
DMC0754	gi57234427	Unassigned	R3H domain protein	0.43 ± 0.14	987 ± 310	2272 ± 131
DMC1331	panDhc_1597	Cornell	ribosomal large subunit pseudouridine synthase, RluD	0.43 ± 0.05	910 ± 78	2126 ± 188
DMC0212	panDhc_2963	Cornell	PBS lyase HEAT-like repeat domain protein	0.42 ± 0.09	537 ± 103	1274 ± 142
DMC0823	panDhc_1606	Cornell	sodium extrusion protein NatA, putative	0.42 ± 0.13	478 ± 149	1150 ± 21
DMC0755	VS684	Cornell	thymidylate kinase	0.40 ± 0.12	782 ± 236	1949 ± 44
DMC0954	panDhc_470_RC	Cornell	Mg chelatase-like protein	0.40 ± 0.07	401 ± 72	1011 ± 38
DMC0399	panDhc_863_RC	Cornell	polyA polymerase family protein	0.40 ± 0.04	900 ± 13	2275 ± 212
DMC0976	panDhc_3861	Cornell	hypothetical protein	0.39 ± 0.16	1148 ± 461	2911 ± 176
DMC1309	panDhc_3099	Cornell	type II secretion system protein, GspI/GspJ family	0.39 ± 0.08	649 ± 62	1650 ± 319
DMC0682	panDhc_1062	Cornell	thioredoxin	0.38 ± 0.08	849 ± 180	2205 ± 39
DMC0456	panDhc_1197	Cornell	3-dehydroquinate synthase	0.38 ± 0.16	574 ± 243	1511 ± 103
DMC1474	panDhc_2364	Cornell	DNA-binding response regulator, LuxR family	0.36 ± 0.16	208 ± 88	569 ± 78
DMC0884	panDhc_2188	Cornell	hypothetical protein	0.35 ± 0.15	1200 ± 512	3453 ± 363
DMC0923	panDhc_101_RC	Cornell	copper-translocating P-type ATPase	0.34 ± 0.04	511 ± 33	1498 ± 123
DMC1380	panDhc_3611	Unassigned	chaperonin GroES	0.34 ± 0.03	9545 ± 68	28342 ± 2723
DMC1306	panDhc_2285	Cornell	DNA-binding response regulator, LuxR family	0.33 ± 0.04	969 ± 56	2971 ± 339
DMC0610	panDhc_266_RC	Cornell	ribonucleotide reductase	0.32 ± 0.11	611 ± 178	1883 ± 353
DMC1347	panDhc_2649_RC	Cornell	hypothetical protein	0.31 ± 0.18	816 ± 458	2595 ± 216
DMC1402	panDhc_2383_RC	Cornell	ribosomal 5S rRNA E-loop binding protein Ctc/L25/TL5	0.31 ± 0.18	1838 ± 1008	5854 ± 742
DMC0612	panDhc_90	Cornell	sensory box sensor histidine kinase	0.30 ± 0.03	1919 ± 132	6354 ± 419
DMC0926	panDhc_2651_RC	Cornell	superoxide dismutase	0.25 ± 0.06	299 ± 65	1174 ± 150
DMC1380	panDhc_3611_RC	Cornell	chaperonin GroES	0.25 ± 0.06	8763 ± 1478	35451 ± 6231
DMC0094	panDhc_3588	Cornell	hypothetical protein	0.23 ± 0.02	4182 ± 63	17849 ± 1388
DMC0827	panDhc_922_RC	Cornell	ABC transporter, permease protein, putative	0.21 ± 0.04	158 ± 18	741 ± 126

between the KB-1® 70 and 10 hours after oxygen addition, 185 and 106 probes on the microarray displayed significantly higher or lower intensity, respectively. The top and bottom 20 ratios are presented in Table 4.6 with the full list detailed in Appendix Table 5.3. Members of the oxidative stress operon (DMC0923-0926) displayed higher intensity in the cultures 70 hours after oxygen addition (3.4 ± 0.083 to 13 ± 4.1 fold). An additional suite of RDase catalytic and anchoring subunits were also more abundant in the 70 hour cultures. Ribosomal protein encoding transcripts were the majority of the significantly lower intensity transcripts when comparing the cultures 70 hours to six hours after oxygen addition, reversing the up-regulation seen when comparing the six-hour cultures to the control.

Up until this point in the oxygen investigation, the pangenome microarrays were treated as if they were targeting a dominant single-strain in the KB-1® culture. However, previous work has shown that at least two strains of DMC were present in the KB-1® mixed community and are detectable using the pangenome platform (Chapter 3). Therefore, the tables are labeled to indicate the respective DMC type (Pinellas, Cornell, or unassigned) that the probe was both designed to target and on a previous DNA/DNA hybridization, displayed specific affinity for recapturing sequences from one mixed microbial community over the other (20). By coding the tables, it was noted a high fraction of the significantly up-regulated genes in the 10 hours after oxygen exposed cultures were Pinellas/KB-1-L type. The down-regulated probe set all targeted genes for Cornell/DMC195. An inverse relationship was seen when the transcripts for 70 hours after were compared to the 10 hours after oxygen exposure. The majority of transcripts indicating significant up-regulation, including the oxygen stress related transcripts encoding for a superoxide dismutase and Hsp20, were dominated by Cornell/195-type probes (150 probes

Table 4.6. Differentially detected KB-1® transcripts for the 70 hours after oxygen addition compared to 10 hours after oxygen addition. Full list is presented in Appendix Table A5.8.

DMC#	Probe ID	Strain	Description	Ratio of 70 Hour to 10 Hour Post Oxygen Stress	Average Intensity of 70 Hour Oxygen Stress (pfu)	Average Intensity of 10 Hour Oxygen Stress (pfu)
DMC1264	panDhc_4041	Cornell	hypothetical protein	44 ± 21	32331 ± 8725	739 ± 295
DMC0517	panDhc_793	Pinellas	Phosphoglucosamine mutase	34 ± 7.1	260120 ± 40503	7737 ± 1093
DMC1207	gi57233993	Cornell	hypothetical protein	26 ± 5.9	7759 ± 1685	293 ± 13
DMC1022	gi57234153	Cornell	hypothetical protein	19 ± 8.4	4294 ± 1081	224 ± 80
DMC1017	panDhc_2869	Unassigned	hypothetical protein	13 ± 3.2	33300 ± 8183	2578 ± 8
DMC0924	panDhc_2985	Cornell	Hsp20/alpha crystallin family	13 ± 4.1	6326 ± 1645	494 ± 95
DMC1009	panDhc_1509	Cornell	HD domain protein	9.1 ± 1.1	2443 ± 196	267 ± 22
DMC0435	panDhc_3072_RC	Cornell	[Fe] hydrogenase HymA	8.2 ± 2.9	9140 ± 1905	1109 ± 315
DMC1487	panDhc_3708_RC	Cornell	reductive dehalogenase anchoring	7.7 ± 2.0	86376 ± 12104	11267 ± 2511
DMC0926	panDhc_2651_RC	Cornell	superoxide dismutase	7.3 ± 1.6	2191 ± 83	299 ± 65
DMC1277	panDhc_1885_RC	Cornell	acetyltransferase GNAT family	7.3 ± 2.3	3481 ± 784	475 ± 102
DMC0926	panDhc_2651	Cornell	superoxide dismutase	6.9 ± 1.3	1663 ± 296	242 ± 12
DMC1488	panDhc_502_RC	Cornell	reductive dehalogenase putative	6.1 ± 1.9	47301 ± 11292	7713 ± 1608
DMC1149	panDhc_2017_RC	Cornell	lipoprotein putative	6.0 ± 2.5	1586 ± 80	265 ± 110
DMC2158	panDhc_482	Pinellas	putative reductive dehalogenase	5.9 ± 1.8	15832 ± 1272	2679 ± 797
DMC1678	panDhc_1554	Pinellas	hypothetical protein	5.9 ± 1.9	1133 ± 81	193 ± 63
DMC1474	panDhc_2364	Cornell	DNA-binding response regulator LuxR	5.2 ± 2.3	1088 ± 133	208 ± 88
DMC1106	panDhc_3280_RC	Cornell	transcriptional regulator Fur family	5.2 ± 1.8	1110 ± 111	213 ± 71
DMC1104	panDhc_2088	Cornell	DNA-binding response regulator	5.2 ± 4.1	1713 ± 379	330 ± 248
DMC1013	panDhc_737	Cornell	chromosome segregation ATPase	5.0 ± 1.5	1444 ± 383	7287 ± 1016
⋮	⋮	⋮	⋮	⋮	⋮	⋮
⋮	⋮	⋮	⋮	⋮	⋮	⋮
DMC0478	KB1_0533	-	50S ribosomal protein L6	0.14 ± 0.050	1852 ± 600	13690 ± 2376
DMC0477	VS430	Unassigned	ribosomal protein S8	0.12 ± 0.055	455 ± 198	3652 ± 184
DMC0959	VS863	Unassigned	ribosomal protein L10	0.12 ± 0.028	1694 ± 348	13795 ± 1276
DMC0471	gi147669104	Unassigned	ribosomal protein L29	0.12 ± 0.027	1099 ± 173	9127 ± 1458
DMC0471	GT_395950	-	ribosomal protein L29	0.12 ± 0.028	1090 ± 185	9136 ± 1529
DMC0467	panDhc_3673_RC	Unassigned	ribosomal protein S19	0.12 ± 0.035	1153 ± 215	9682 ± 2169
DMC0477	GT_397900	-	ribosomal protein S8	0.12 ± 0.053	439 ± 196	3705 ± 235
DMC0471	KB1_0527	-	ribosomal protein L29	0.12 ± 0.034	1075 ± 227	9090 ± 1757
DMC1372	KB1_1410	-	hypothetical protein	0.12 ± 0.036	218 ± 62	1847 ± 188
DMC1372	gi147669866	Pinellas	hypothetical protein	0.11 ± 0.029	201 ± 38	1757 ± 286
DMC0958	KB1_0978	-	ribosomal protein L7	0.11 ± 0.032	1721 ± 339	15254 ± 3113
DMC1372	GT_1079521	-	hypothetical protein	0.11 ± 0.030	195 ± 34	1754 ± 357
DMC0477	KB1_0532	-	ribosomal protein S8	0.11 ± 0.054	427 ± 211	3928 ± 45
DMC0477	gi147669110	Unassigned	ribosomal protein S8	0.11 ± 0.051	407 ± 192	3775 ± 40
DMC0920	GT_c760143	-	hypothetical protein	0.10 ± 0.019	230 ± 41	2272 ± 117
DMC0920	KB1_0937	-	hypothetical protein	0.094 ± 0.018	207 ± 31	2194 ± 267
DMC0922	gi147669479	Pinellas	hypothetical protein	0.091 ± 0.042	104 ± 43	1140 ± 211
DMC0922	KB1_0939	-	hypothetical protein	0.085 ± 0.044	93 ± 44	1093 ± 228
DMC0958	gi147669523	Pinellas	ribosomal protein L7	0.075 ± 0.022	827 ± 211	11044 ± 1522
DMC1695	KB1_0699	-	phosphoribosyltransferase	0.057 ± 0.014	201 ± 18	3547 ± 835

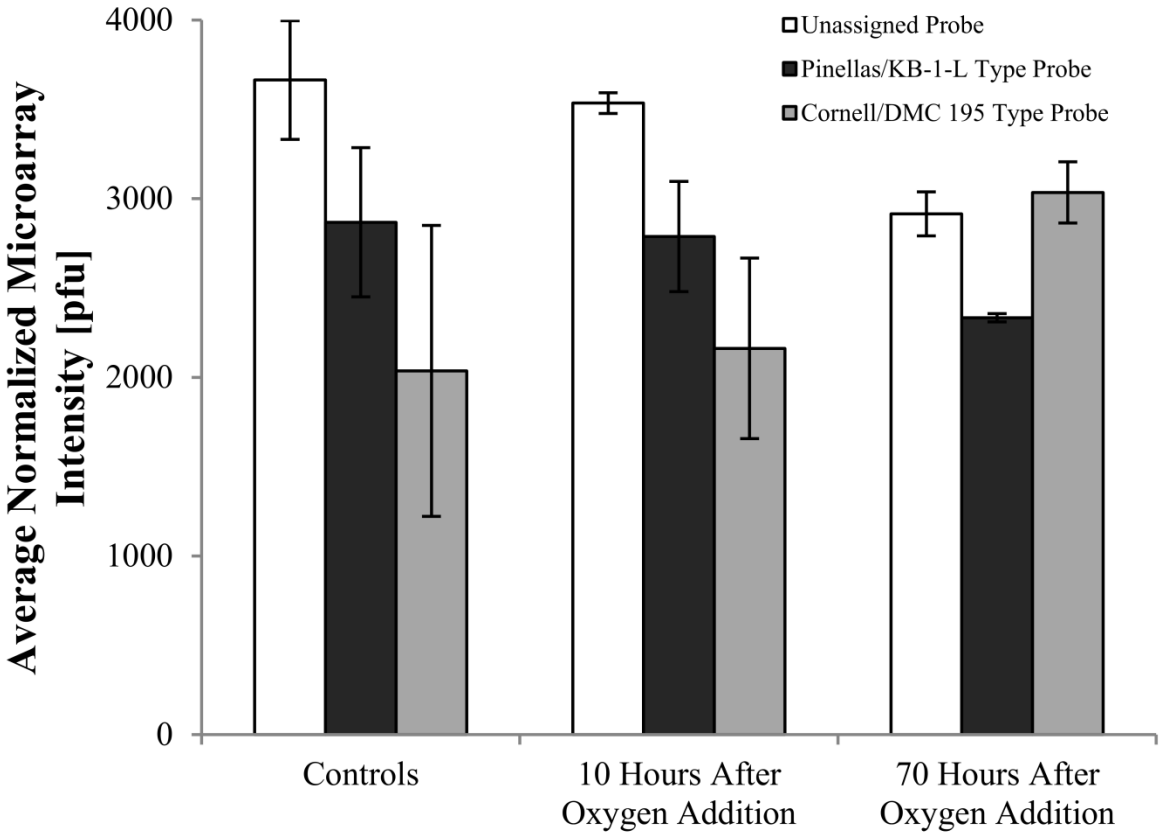

Figure 4.2. Average normalized microarray intensities for the three probe groups across dupicate cultures. Probes were binned based off of the technique established in Chapter 3. Error bars represent the standard error across duplicate cultures.

targeted Cornell/195, 10 targeted Pinellas/KB-1, and 19 did not fall into either group). The down-regulated transcript set was overrepresented for Pinellas/KB-1 (19 probes) as compared to the Cornell/195 (1 probe). Applying a more broad scale analysis of taking the average frequency across each individual probe group displayed the general trend that probes targeting a Cornell/195 type strain became more intense while those targeting a Pinellas type strain lessened in intensity (Figure 4.2). At the 70-hour time point after oxygen exposure, the Cornell type probe set had a significantly higher average intensity than the Pinellas type probe set (unpaired t-test value of $p = 0.03$).

4.D.4. DMC195 in D2's proteomic response to acid stress:

Lowering the pH from 7 to 5.3 for continuously fed D2 experiments identified the response of growth linked enzymes to and putative proteomic biomarkers of acid stress. The chloroethene and ethene concentrations over the course of the experiment are presented in Figure 5 for the D2 culture. The GC analysis detected that low pHs inhibited the production of ethene and displayed an accumulation of DCE. The proteomic samples included D2 cultures 24 and 48 hours after lowering the pH with appropriate controls. The results of a similar KB-1® study were inconclusive as to whether a stress was achieved and therefore will not be discussed here.

Focusing on the growth linked enzymes for DMC, Figure 4.3 lists the detected proteins involved in respiration or growth for the D2 culture. Surprisingly, the D2 cultures displayed a substantial reduction in the major hydrogenase Hup (0.36 ± 0.06 fold change) for the first time point post acid addition. The D2 mixed community displayed an increase of the RDase DET1545 homolog (3.7 ± 1.87 fold change). Two other major RDases in the D2 culture

DMC#	DET#	Description	Control 16 Hour	Acid (1) 24 Hour	Acid (2) 24 Hour	Ratio of 24 Hour Acid to Control	Control 48 Hour	Acid (1) 48 Hour	Acid (2) 48 Hour	Ratio of 48 Hour Acid to Control
DMC0076	DET0079	TceA trichloroethene reductive dehalogenase				0.55 ± 0.029				0.50 ± 0.034
DMC0097	DET0101	Mod molybdopterin oxidoreductase				1.3 ± 0.047				0.69 ± 0.18
DMC0106	DET0110	Hup [Ni/Fe] hydrogenase, group 1, large subunit, putative				0.41 ± 0.082				0.64 ± 0.010
DMC0108	DET0112	Hup [Ni/Fe] hydrogenase, iron-sulfur cluster-binding subunit				0.36 ± 0.062				0.65 ± 0.021
DMC0140	DET0145	[Fe] hydrogenase, HymA subunit				1.4 ± 0.45				0.90 ± 0.089
DMC0141	DET0146	[Fe] hydrogenase, HymB subunit				0.91 ± 0.32				1.0 ± 0.18
DMC0142	DET0147	[Fe] hydrogenase, HymC subunit				1.1 ± 0.077				0.84 ± 0.087
DMC0180	DET0187	Fdh formate dehydrogenase, alpha subunit				1.0 ± 0.19				0.86 ± 0.10
DMC0311	DET0318	PceA reductive dehalogenase, putative				2.0 ± 0.048				1.2 ± 0.012
DMC0335	DET0343	cell division protein FtsZ				1.0 ± 0.15				1.2 ± 0.11
DMC0550	DET0562	ATP synthase subunit A				1.4 ± 0.15				1.0 ± 0.046
DMC0551	DET0563	ATP synthase F1, gamma subunit				0.93 ± 0.25				1.0 ± 0.016
DMC0552	DET0564	ATP synthase subunit B				1.2 ± 0.071				1.0 ± 0.30
DMC0601	DET0614	hydrogenase, VhuG subunit, putative				1.3 ± 0.087				1.1 ± 0.10
DMC0602	DET0615	hydrogenase, VhuA subunit, putative				1.1 ± 0.37				1.2 ± 0.009
DMC0895	DET0925	proton-translocating NADH-quinone oxidoreductase, C subunit				0.90 ± 0.45				0.95 ± 0.12
DMC0896	DET0926	proton-translocating NADH-quinone oxidoreductase, D subunit				1.2 ± 0.12				0.90 ± 0.11
DMC0898	DET0928	proton-translocating NADH-quinone oxidoreductase, I subunit				1.4 ± 0.048				0.95 ± 0.11
DMC1361	DET1407	BNR/Asp-box repeat domain protein, S-Layer				0.75 ± 0.200				1.1 ± 0.15
DMC1488	DET1545	reductive dehalogenase, putative				3.7 ± 1.87				1.4 ± 0.28
DMC1501	DET1559	reductive dehalogenase, putative				0.94 ± 0.06				0.83 ± 0.078

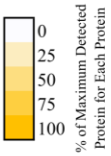

Figure 4.3. Respiration and growth linked enzymes response to lower pH in the D2 culture (yellow values). The color scale display the abundance of a specific protein in a sample divided by the maximum abundance of the specific protein across the 6 samples. Standard error accompanies the average ratio.

were differentially regulated. The major RDase, TceA, displayed about a two-fold decrease in ion intensity (0.55 ± 0.02) while the RDase PceA displayed a two fold increase (2.0 ± 0.048).

Turning to genome-wide proteomic bioindicators of low pH stress, Table 4.7 lists the proteins that were significantly regulated in the D2 culture for the varied stressed time points compared to the indicated controls. Of note, the proteome screen detected higher intensities of cobalamin transport and modification proteins (DMC0637 and DMC0654) with an additional Thioredoxin type carrier protein (DMC0648) in the D2 culture. Also, the chaperone DnaK was significantly up-regulated in the D2 cultures 24 hours and 48 hours post acid addition, albeit at a low fold change (1.2± 0.07). Considering that the DnaK TMT Ion intensity of 1393357 ± 23823 accounts for 4.8% of the total ions detected for DMC in D2, a 1.2-fold shift was actually quite significant.

4.D.5. DMC195 in D2's transcriptomic response to high cis-DCE feeding rates

DMC195 in D2 cultures continuously fed neat cis-DCE at a rapid rate of 31.1 μmoles/(L-hr) ceased reductive dechlorination after 48 hours (the GC results for these experiments are presented in Appendix Figure A5.6.a-c). This was unusual in that D2 fed similar rates of PCE and TCE regularly dechlorinate to ETH without displaying inhibition (Chapter 2). When the microarray values for the three cis-DCE inhibited cultures were compared against D2 cultures continuously fed cis-DCE at slower rates (Figure A5.6.d-i), 31 and 23 probes displayed significantly higher and lower intensities, respectively (Table 4.7). Of the 31 probes detected at significantly higher intensities, two targeted the general stress response proteins DnaJ and HspR (16±14 and 14±9.1 fold change, respectively). Four members of an operon encoding for a

Table 4.7. Differentially detected proteins for the D2 cultures with low pH

DMC#	DET#	Description	D2 24 hours Post Acid Addition Compared to Control	D2 24 hours Post Acid TMT Normalized Ion Intensity Average
DMC0648	DET0661	Thioredoxin	4.2 ± 0.31	123159 ± 14527
DMC0951	DET0983	translation initiation factor IF-2	2.7 ± 0.068	13491 ± 519
DMC0311	DET0318	PceA reductive dehalogenase	2.0 ± 0.038	333843 ± 7823
DMC0420	DET0431	sensory box sensor histidine kinase	1.9 ± 0.20	70961 ± 8641
DMC0488	DET0499	30S ribosomal protein S13	1.7 ± 0.041	105750 ± 3101
DMC1353	DET1399	chaperone protein DnaK	1.4 ± 0.024	1393357 ± 23823
DMC0552	DET0564	ATP synthase subunit B	1.2 ± 0.071	603527 ± 34271
DMC0637	DET0650	ABC-type cobalamin/Fe3+-siderophores transport	1.2 ± 0.010	433810 ± 3209
DMC0654	DET0667	acetyl-CoA decarbonylase/synthase complex	1.2 ± 0.035	60389 ± 1840
DMC0451	DET0462	chorismate synthase	0.82 ± 0.054	35664 ± 2430
DMC0076	DET0079	TceA trichloroethene reductive dehalogenase	0.55 ± 0.029	2186127 ± 115974
DMC0818	DET0846	histidyl-tRNA synthetase, putative	0.52 ± 0.12	130609 ± 27650
DMC0106	DET0110	Hup [Ni/Fe] hydrogenase, group 1, large subunit	0.41 ± 0.096	1404927 ± 281305

DMC#	DET#	Description	D2 48 hours Post Acid Addition Compared to Control	D2 48 hours Post Acid TMT Normalized Ion Intensity Average
DMC0648	DET0661	thioredoxin	2.5 ± 0.13	117568 ± 6176
DMC1264	DET1307	hypothetical protein	2.3 ± 0.13	204562 ± 11754
DMC1185	DET1227	DNA polymerase III, beta subunit	1.9 ± 0.17	327181 ± 29108
DMC1353	DET1399	chaperone protein DnaK	1.3 ± 0.039	1316052 ± 38933
DMC0602	DET0615	hydrogenase, group 3, VhuA subunit, putative	1.2 ± 0.009	912978 ± 6579
DMC0421	DET0432	DNA-binding response regulator, LuxR family	1.2 ± 0.036	32143 ± 972
DMC0451	DET0462	chorismate synthase	0.87 ± 0.023	39283 ± 1043
DMC0818	DET0846	histidyl-tRNA synthetase, putative	0.76 ± 0.020	171835 ± 4503
DMC0106	DET0110	Hup [Ni/Fe] hydrogenase, group 1, large subunit	0.64 ± 0.010	1891852 ± 30466
DMC0076	DET0079	TceA trichloroethene reductive dehalogenase	0.50 ± 0.034	2024675 ± 137116

putative drug resistance ABC transporter (DET1616-1619 a.k.a. DMC1556-1560) displayed a 2.75±1.1 to 3.9±1.5 fold change between the cis-DCE inhibited and respiring cultures. In addition, an associated RDase histidine kinase regulator, DET1529 (a.k.a. DMC1472), displayed a fold change of 6.1 ± 5.2. The most notable significantly lower intensity probes for the cis-DCE inhibited cultures encoded for the *pceA* RDase (DET0318-0319 a.k.a. DMC0311-0312) and putative regulators for RDases (DET1559-1560 a.k.a. DMC1502-1503).

4.D.6. DMC195 in D2's transcriptomic response to potential solvent stress

DMC195 in D2 ceased reductive dechlorination after 48 hours of being continuously fed neat PCE at a rate of 64.5 µmoles/(L-hr) (Appendix Figure A5.7.a-b). Additionally, methanogenesis halted in these cultures as well (data not presented). Accompanying the cessation of reductive dechlorination, saturation levels of PCE were detected in the culture suggesting free phase NAPL formation. However, due to a headspace purge every 24 hours, levels of PCE were not above saturation throughout the entire course experiment but instead varied (Appendix Figure A5.7). The microarray transcriptomic profile of these PCE high rate inhibited cultures were compared against data from other PCE high- and mid-rate experiments (GC data omitted, displaying standard reductive dechlorination of PCE to ETH) to discern potential biomarkers of solvent stress. This analysis identified 10 and 41 probes displaying significantly higher and lower intensities, respectively (Table 4.9). The probe targeting the DET0137 methylglyoxal synthase (DMC0132) displayed the highest fold change (39±15). Additional up-regulated genes in the PCE-Satruated cultures included the general stress response DET1411-1413 transcript encoding for DnaJ, HspR, and ClpB (4.1±0.31 to 7.4±1.1). Common growth linked transcripts were detected as significantly down-regulated transcripts in the PCE

Table 4.8. DCE inhibited differentially detected transcripts.

DMC#	DET#	Description	Ratio of DCE Inhibited to DCE Respiring	Average Intensity of DCE Inhibited (pfu)	Average Intensity of DCE Respiring (pfu)
DMC1364	DET1411	DnaJ family protein	16 ± 14	32693 ± 5163	2012 ± 1687
-	DET1509	(Authentic Point Mutation)	16 ± 19	904 ± 129	56 ± 65
DMC1365	DET1412	HspR protein, putative	14 ± 9.1	11105 ± 2630	794 ± 479
DMC1449	DET1504	ferrous iron transport protein A, putative	12.2 ± 6.0	5725 ± 943	468 ± 214
DMC1450	DET1505	transcriptional regulator, Fur family	8.1 ± 4.7	5569 ± 251	690 ± 397
-	DETCys1	DET tRNA Cysteine 1	6.6 ± 3.2	4404 ± 1466	664 ± 231
DMC1472	DET1529	sensory box protein, putative	6.1 ± 5.2	9108 ± 1274	1498 ± 1268
DMC1384	DET1431	hydrogenase accessory protein HypB	4.7 ± 2.1	2985 ± 733	634 ± 230
-	DETGly1	DET tRNA Glycine 3	4.7 ± 1.8	10955 ± 2741	2331 ± 667
-	DETSer1	DET tRNA Serine 1	4.3 ± 3.0	2811 ± 209	649 ± 455
DMC1092	DET1132	imidazole glycerol phosphate synthase	4.2 ± 2.6	2134 ± 327	510 ± 302
DMC1271	DET1314	radical SAM domain protein	4.1 ± 2.7	3529 ± 858	855 ± 520
DMC1556	DET1616	transcriptional regulator, AbrB family	3.9 ± 1.5	10325 ± 1853	2625 ± 918
DMC1475	DET1532	dinitrogenase iron-molybdenum cofactor	3.89 ± 2.1	2130 ± 443	548 ± 277
DMC1557	DET1617	hypothetical protein	3.86 ± 1.4	11089 ± 1585	2873 ± 986
DMC1093	DET1133	iron-sulfur cluster-binding protein	3.81 ± 1.8	2022 ± 523	531 ± 211
DMC1420	DET1475	hypothetical protein	3.71 ± 1.8	2388 ± 87	644 ± 320
-	DET1242	(Authentic Point Mutation)	3.53 ± 1.6	6683 ± 1300	1893 ± 785
DMC1331	DET1375	ribosomal large subunit pseudouridine synthase	3.32 ± 2.5	1195 ± 131	360 ± 266
DMC0099	DET0103	*mod,* iron-sulfur binding subunit	3.12 ± 1.1	3832 ± 793	1230 ± 372
DMC1301	DET1345	tagatose 1,6-diphosphate aldolase	3.11 ± 1.3	1419 ± 78	457 ± 185
DMC1559	DET1619	ABC transporter, ATP-binding protein	3.07 ± 1.4	2527 ± 442	824 ± 346
DMC1576	DET1638	hypothetical protein	2.95 ± 1.3	2161 ± 285	733 ± 298
DMC1052	DET1092	DNA methylase	2.94 ± 1.9	1542 ± 253	524 ± 332
DMC0145	DET0150	hypothetical protein	2.94 ± 1.4	4749 ± 931	1615 ± 677
DMC1400	DET1452	hypothetical protein	2.79 ± 0.91	5033 ± 982	1807 ± 472
DMC1199	DET1241	peptide methionine sulfoxide reductase	2.78 ± 1.1	2530 ± 435	909 ± 312
DMC1558	DET1618	hypothetical protein	2.75 ± 1.1	3080 ± 436	1119 ± 415
DMC1573	DET1634	hypothetical protein	2.47 ± 0.71	3248 ± 124	1317 ± 374
DMC0936	DET0968	hypothetical protein	2.36 ± 1.0	3739 ± 554	1586 ± 637
DMC0002	DET0002	GTP-binding protein, GTP1/OBG family	2.16 ± 0.63	3266 ± 618	1511 ± 336
DMC0825	DET0854	hypothetical protein	0.47 ± 0.17	2097 ± 576	4439 ± 1078
DMC0338	DET0346	hypothetical protein	0.41 ± 0.13	716 ± 131	1737 ± 437
DMC1445	DET1500	hypothetical protein	0.39 ± 0.093	899 ± 159	2319 ± 375
DMC0715	DET0734	hypothetical protein	0.37 ± 0.21	1193 ± 646	3184 ± 467
DMC1542	DET1602	twin-arginine translocation protein	0.36 ± 0.072	1315 ± 20	3630 ± 724
DMC1396	DET1448	hypothetical protein	0.33 ± 0.15	9313 ± 2499	28194 ± 10483
DMC1527	DET1586	lemA family protein	0.32 ± 0.11	725 ± 80	2271 ± 718
DMC1219	DET1262	ribosomal protein L28	0.31 ± 0.15	993 ± 172	3240 ± 1528
DMC0185	DET0192	cvpA family protein	0.30 ± 0.073	1570 ± 171	5236 ± 1131
DMC0028	DET0028	universal stress protein family	0.26 ± 0.12	477 ± 192	1853 ± 498
DMC0436	DET0447	acyl CoA carboxyltransferase	0.23 ± 0.085	289 ± 49	1284 ± 435
DMC0455	DET0466	3-dehydroquinate dehydratase, type I	0.22 ± 0.10	183 ± 70	833 ± 204
DMC1502	DET1560	sensory box sensor histidine kinase	0.22 ± 0.12	317 ± 149	1450 ± 377
DMC1258	DET1301	ISDet4, transposase	0.21 ± 0.095	341 ± 107	1612 ± 515
DMC0182	DET0189	methyltransferase, putative	0.20 ± 0.10	477 ± 213	2350 ± 531
DMC1503	DET1561	DNA-binding response regulator, LuxR family	0.20 ± 0.097	150 ± 61	765 ± 214
DMC0990	DET1029	hypothetical protein	0.19 ± 0.071	368 ± 111	1916 ± 405
DMC1104	DET1144	DNA-binding response regulator	0.15 ± 0.065	129 ± 37	838 ± 258
DMC0948	DET0980	hypothetical protein	0.11 ± 0.048	433 ± 168	3848 ± 662
DMC1312	DET1356	hypothetical protein	0.10 ± 0.082	196 ± 148	1897 ± 482
DMC0820	DET0848	SPFH domain/band 7 family domain protein	0.085 ± 0.025	187 ± 43	2212 ± 420
DMC0311	DET0318	*pceA* reductive dehalogenase	0.077 ± 0.022	562 ± 86	7265 ± 1682
DMC0312	DET0319	*pceA* anchoring protein	0.015 ± 0.005	154 ± 38	10486 ± 2221

Table 4.9. PCE solvent stress differentially detected transcripts.

DMC#	DET#	Description	Ratio of PCE Overfed to PCE High & Mid Respiration	Average Normalized Intensity for the PCE Overfed Cultures (pfu)	Average Normalized Intensity for the PCE High Cultures (pfu)	Average Normalized Intensity for the PCE Mid Cultures (pfu)
DMC0132	DET0137	methylglyoxal synthase	39 ± 15	13181 ± 1110	276 ± 28	396 ± 142
DMC0575	DET0588	hypothetical protein	21 ± 6.6	11578 ± 1064	564 ± 156	525 ± 76
DMC0573	DET0586	hypothetical protein	14 ± 3.5	1265 ± 642	62 ± 7	123 ± 29
DMC1365	DET1412	HspR protein, putative	7.4 ± 1.1	2834 ± 498	314 ± 36	453 ± 42
DMC1364	DET1411	DnaJ family protein	6.9 ± 1.8	4375 ± 1371	665 ± 75	600 ± 142
DMC1450	DET1505	transcriptional regulator, Fur family	5.1 ± 2.2	3471 ± 1629	697 ± 70	658 ± 280
DMC1366	DET1413	chaperone ClpB	4.1 ± 0.31	877 ± 200	132 ± 7	291 ± 13
DMC1063	DET1103	hypothetical protein	4.0 ± 1.4	1763 ± 42	329 ± 43	560 ± 183
DMC1305	DET1349	DNA-binding protein, excisionase family	3.4 ± 0.88	6075 ± 1437	2181 ± 448	1419 ± 230
DMC0361	DET0370	membrane-associated zinc metalloproteas	2.7 ± 1.2	11214 ± 1482	3734 ± 1461	4623 ± 900
DMC1170	DET1212	translation elongation factor G	0.43 ± 0.093	528 ± 202	1141 ± 127	1300 ± 235
-	DETThr1	tRNA Threonine 1	0.43 ± 0.054	4461 ± 1882	12566 ± 1389	8189 ± 487
DMC0899	DET0929	*nuo* , J subunit	0.39 ± 0.057	531 ± 118	1373 ± 50	1376 ± 194
DMC0976	DET1011	hypothetical protein	0.35 ± 0.056	3182 ± 2500	9426 ± 1080	8705 ± 952
DMC1339	DET1384	preprotein translocase, YajC subunit	0.34 ± 0.075	534 ± 426	1479 ± 188	1642 ± 288
DMC1571	DET1632	NifU-like protein	0.33 ± 0.051	877 ± 195	3016 ± 393	2243 ± 178
DMC0031	DET0031	hypothetical protein	0.32 ± 0.048	353 ± 211	1108 ± 146	1078 ± 64
DMC1541	DET1601	twin-arginine translocation protein, TatA/E	0.31 ± 0.078	634 ± 356	1920 ± 411	2166 ± 271
DMC0444	DET0455	HIT domain protein	0.31 ± 0.058	312 ± 287	1045 ± 58	974 ± 166
DMC0580	DET0593	enolase	0.30 ± 0.066	253 ± 208	906 ± 115	769 ± 131
DMC1544	DET1604	pyrophosphokinase	0.29 ± 0.080	1272 ± 1004	3576 ± 598	5210 ± 1149
DMC0604	DET0617	hypothetical protein	0.28 ± 0.061	290 ± 101	1281 ± 251	770 ± 61
DMC0611	DET0624	response regulator	0.28 ± 0.080	206 ± 200	828 ± 170	648 ± 121
DMC0210	DET0217	oxidoreductase, aldo/keto reductase	0.27 ± 0.067	223 ± 171	804 ± 109	873 ± 179
DMC0097	DET0101	*mod*	0.26 ± 0.083	546 ± 122	2637 ± 682	1518 ± 274
DMC0741	DET0764	hypothetical protein	0.26 ± 0.057	901 ± 908	4195 ± 690	2849 ± 424
DMC0549	DET0561	ATP synthase F1, delta subunit	0.26 ± 0.057	653 ± 500	2976 ± 437	2142 ± 354
DMC0440	DET0451	malate dehydrogenase, NAD-dependent	0.25 ± 0.034	297 ± 287	1203 ± 99	1189 ± 110
DMC1486	DET1543	hypothetical protein	0.22 ± 0.065	317 ± 246	1412 ± 197	1466 ± 374
DMC1502	DET1560	sensory box sensor histidine kinase	0.22 ± 0.041	224 ± 269	1272 ± 157	764 ± 89
DMC0424	DET0435	ribose-phosphate pyrophosphokinase	0.21 ± 0.029	149 ± 157	948 ± 69	460 ± 35
DMC0582	DET0595	peptidyl-tRNA hydrolase	0.21 ± 0.059	199 ± 209	954 ± 64	946 ± 249
DMC1358	DET1404	conserved hypothetical protein, truncation	0.21 ± 0.055	227 ± 218	1453 ± 337	731 ± 79
DMC0552	DET0564	ATP synthase subunit B	0.21 ± 0.070	347 ± 422	1664 ± 320	1700 ± 468
DMC0743	DET0766	V-type H(+)-translocating pyrophosphatase	0.20 ± 0.037	367 ± 467	2298 ± 176	1348 ± 210
DMC1002	DET1041	PQQ enzyme repeat domain protein	0.20 ± 0.031	295 ± 251	1915 ± 157	1044 ± 125
DMC0631	DET0644	transketolase	0.20 ± 0.044	173 ± 181	1146 ± 207	621 ± 67
DMC0411	DET0421	degV family protein	0.18 ± 0.029	1101 ± 995	8358 ± 743	3707 ± 484
DMC0901	DET0931	*nuo* , L subunit	0.18 ± 0.040	154 ± 138	963 ± 125	752 ± 125
DMC0001	DET0001	chromosomal replication initiator protein	0.17 ± 0.032	1332 ± 1813	8063 ± 1060	7793 ± 1072
DMC0548	DET0560	ATP synthase F0, B subunit	0.17 ± 0.026	758 ± 987	5854 ± 839	3320 ± 180
DMC0641	DET0654	cobalamin biosynthesis protein CobD	0.16 ± 0.063	130 ± 123	905 ± 208	731 ± 229
DMC1236	DET1279	acyl carrier protein	0.16 ± 0.058	362 ± 395	2326 ± 660	2262 ± 524
DMC0759	DET0782	thiamine-phosphate pyrophosphorylase	0.16 ± 0.047	149 ± 117	1224 ± 169	692 ± 178
DMC0140	DET0145	*hymA* , hydrogenase	0.15 ± 0.035	668 ± 796	4675 ± 917	3949 ± 422
DMC0391	DET0401	octaprenyltransferase	0.15 ± 0.050	322 ± 341	2808 ± 485	1363 ± 364
DMC0550	DET0562	ATP synthase subunit A	0.15 ± 0.020	482 ± 627	3683 ± 165	2713 ± 309
DMC0142	DET0147	*hymC* , hydrogenase	0.15 ± 0.025	833 ± 809	7062 ± 352	4036 ± 626
DMC0546	DET0558	ATP synthase F0, A subunit	0.15 ± 0.029	198 ± 241	1824 ± 289	874 ± 80
DMC0143	DET0148	*hymD* , hydrogenase	0.14 ± 0.043	374 ± 367	2170 ± 303	3292 ± 897
DMC0141	DET0146	*hymB* , hydrogenase	0.11 ± 0.018	160 ± 146	1107 ± 168	1906 ± 40

over-fed cultures. These transcripts included *hym* (DET0145-0148), *atpase* (DET0580,0560-0562,0564), and *nuo* (DET0929,0931).

4.D.7. DMC195 in D2's transcriptomic response to electron donor starvation

Subcultures of the D2 mixed community were fed at a low continuous rate of PCE (0.8µM/hr) with no electron donor provided. DMC195 in D2 reductively dechlorinated much of the PCE presumably utilizing hydrogen released from endogenous decay of biomass (Appendix Figure A5.9.a-b). However, the concentration of PCE began to build in these cultures indicating DMC195 was electron donor limited. The transcriptomic profile of these electron donor limited cultures were compared against those of cultures that were fed at a low electron acceptor rate with an electron donor provided that did not display electron donor limitation (these cultures were fed fermented yeast extract (Figure A5.9.c-d.; FYE) yeast extract (Figure A5.9.e-f.; YE), and butyrate (Figure A5.9.g-i). This comparison for the no donor culture found 5 and 8 transcripts to be significantly higher or lower in intensity, respectively. The probes displaying significantly higher intensity included those that targeted transcripts for the general stress response DnaJ/HspR (DET1411-12; 12±7.1 and 12±9.5 fold change), a transcript for an operon containing an iron-sulfur cluster-binding protein (DET1507, 5.4±2.9 fold), a hypothetical protein (DET1568, 4.2±1.6), and a hydrogenase accessory protein (DET1433, 3.4±2.1) (Appendix Table A5.6).

4.E Discussion

The overarching goal of this study was to detect specific biomarkers of DMC cellular stress by challenging the D2 and commercially available KB-1® cultures to a wide range of

known and field-relevant, stress-inducing conditions. The application of proteomic and transcriptomic studies allowed a screen for and detection of multiple putative biomarkers of cellular stress. An exploration of the specific biomarkers associated with the conditions that challenged the cultures follows. Unexpectedly, in the KB-1® community we observed strain variability to survive or recover from a specific stressed condition. Even with this variation, the generation of numerous screens elucidated a few overarching genes or proteins that may be further explored as general stress response biomarkers. The last portion of this discussion will highlight those and explore potential future utility.

4.E.1. General stress biomarkers

As was noted through many of the surveys, DnaJ and Hsp20 were detected to be up-regulated under stressful environmental conditions, often times in the top 20 highest fold changes. Even in stressed cultures where they did not display the top fold change, such as the TCA culture, these transcripts displayed positive and significant up-regulation (2.4±0.1 for cultures 48 hours after 1,1,1-TCA addition compared to the controls). Both of these enzymes serve as molecular chaperones, with DnaJ binding to misfolded enzymes to encourage proper folding and prevent the aggregation of misfolded enzymes. In doing so, DnaJ interacts with DnaK (another chaperone protein that was shown to be upregulated during times of stress) and creates a weak alternative ATPase generating pathway (41).

DnaJ is also widely distributed in bacteria. However, strains of DMC maintain an amino acid stretch (starting at the 75th amino acid in position and terminating at the 107th, 5'-QYGEQ FEKARASQQQTQGNPFGGYDFSFGGSEG-3') which is unique for *Dehalococcoides* type

organisms. This provides a substantial region to screen for unique peptides in complex samples or design primers for field site detection with quantitative reverse transcriptase PCR (qRTPCR). In addition to the potential application of utilizing the DnaJ/HspR transcript as a useful biomarker of cellular stress, focus should be placed on investigating these chaperones in the proper folding of other enzymes within DMC. Slightly modified chaperones may explain why certain DMC enzymes, such as RDases, are not currently overexpressed in model organisms (30). Previous studies have noted that co-translation of complex proteins, such as a cyclohexanone monooxygenase, with their strain-specific chaperones improve the assembly of these enzymes (24).

4.E.2. KB-1®'s fluctuation of dominant DMC strain

In the KB-1® stress experiments, cultures that were established from the same source material behaved differently in reductive dechlorination and transcriptomic profiles. In the 1,1,1-TCA experiment, cultures exposed to 1,1,1-TCA for 48 hours either dechlorinated TCE to VC or ETH. If ethene generation was detected, the average of the Pinelles/KB-1-L specific probes on the pangenome microarray displayed a significantly higher intensity than if only VC generation was detected. The Cornell/195 specific probes on the pangenome became dominant in average intensity for the culture dechlorinating to VC. This indicated that ETH generation is linked to the presence and transcriptional activity of a Pinellas/KB-1 strain. This is not surprising, as the Pinellas/KB-1-L strain has been shown to maintain and express a VcrA homolog, an RDase that generates energy from the VC to ETH reductive dechlorination step (43). Therefore, it is possible one DMC population in the culture was reductively dechlorinating DCE to VC and did not display inhibition in the 1,1,1-TCA experiments while an additional population was responsible

for the VC to ETH step. This may explain the relatively unchanged average transcript levels for Cornell/DMC195 type probes on the pangenome microarray and the divergence in dechlorination profiles in KB-1®.

The KB-1® batch oxygen stress experiment also recaptured DMC strain-specific fluctuations. We qualitatively noted that the differentially expressed probes (Table 4.5 and 4.6) grouped significantly up- or down-regulated probes primarily into one of the three strain types (Pinelles/KB-1-L-type, Cornell/195 type, or unassigned). For example, in the 70 hours after oxygen addition culture, low but detectable amounts of VC were noted. This resumption of dechlorination of TCE to VC was accompanied by an up-regulation of oxidative stress response genes (the operon surrounding the superoxide dismutase DMC0923-0926). The probes encoding for these stress response genes all targeted the Cornell/195-type strain. On a more quantitative approach, we averaged the probe intensity for each group in the controls, 6 hours after, and 70 hours after oxygen addition (Figure 4.4). After 70 hours, the Pinellas/KB-1-L-type strain is significantly less in abundance than the Cornell/195-type. Taken together, this links a specific strain, the Cornell/195 type, with becoming dominant in RNA intensity after recovering from oxygen exposure and could be linked to the resumption of reductive dehalogenation. Additionally, numerous members of the putative oxidative stress response operon (DET0956 aka DMC0926) were positively differentially expressed. This would appear to be a good biomarker for recovery from oxygen exposure.

4.E.3. DMC's proteomic response to the presence of oxygen

The inspection of DMC's response to oxygen addition revealed strain-specific lists of responses of the proteomes of both D2 and KB-1®. In both cultures, the addition of oxygen had an initial effect of slowing the rate of reductive dechlorination. This was followed by a recovery phase of at least partial reductive dechlorination. The continuously fed PCE D2 cultures exposed to oxygen for six hours displayed enzymes that were expressed at an intensity upwards of three to four fold greater than in the base control cultures. This was surprising in of itself as these cultures were sampled a mere six hours after the addition of oxygen. These D2 cultures grew at low respiration and cell turnover rates. Substantial changes in protein detection highlight a critical investment the organism is making to up-regulate a protein under slow growth conditions. Additionally, more proteins were identified as significantly up-regulated rather than down which probably indicates the degradation of rates for these cultures due to the presence of oxygen was slower than the rate of protein formation in response to the stress. The proteins significantly up-regulated when comparing the 6-hours of oxygen exposed cultures to the control cultures include DET1132 (a.k.a DMC1092 a HisH imidazole glycerol phosphate synthase, 4.08±0.42 fold), DET1329 (a.k.a DMC1285 a HisI phosphoribosyl AMP cyclohydrolase, 2.31±0.21 fold), DET1602 (a.k.a DMC1542, TatA twin arginine translocation protein, 1.98±0.18 fold), and DET0434 (a.k.a. DMC0423, SecA translocase, 1.97±0.08 fold). The HisI and HisH are predicted members of the histidine/glutamine biosynthetic pathway. Why this metabolic process is linked to oxygen stress is currently unclear. The TatA and SecA proteins, which were more abundantly detected than the HisHI proteins, are enzymes involved in the secretion of proteins across the membrane. This potentially resulted from more oxidative damage outside the cell than within.

As the oxygen is scavenged in the D2 culture, DMC resumes complete dechlorination to ETH, no PCE is subsequently detected. The proteins differentially detected between the cultures 48 hours after oxygen was added to the controls identified general stress or chaperone proteins (DnaK, GroES, ClpB, and Hsp20) as significantly up-regulated. The presence of the Hsp20/alpha crystallin family protein (DET0954 a.k.a DMC0924) is a good indicator that the transcript region surrounding this enzyme (DET0953-0956) is annotated correctly as an oxidative stress response operon. Across all proteins detected, the highest up-regulation (albeit at modest protein detection) was DET0527 (DMC0516) a TldD/PmbA family protein (13±0.44) that was also significantly up-regulated in the 6 hour oxygen exposed cultures. This enzyme is a potential zinc-dependent metelloprotease whose class was recently characterized (18). Displaying a protease with significant up-regulation may be indicative of DMC attempting to recycle their own or other community member peptides in the culture.

4.E.4. D2's proteomic response to low pH conditions.

A surprising finding from exposing D2 to low pHs was the substantial lower abundance of the highly expressed hydrogenase (Hup) and the RDase TceA. The D2 culture displayed a corresponding pause in chloroethene respiration. The culture displaying such a drastic down-regulation of enzymes could suggest a potential physical activity either stripped or destroyed the RDases and hydrogenase. However, in the D2 culture, an accompanying up-regulation of PceA was detected. It is possible that the RDases may be themselves pH-optimized or the cell maintains a tight protease network to transform the protein pool faster than expected.

4.E.5. ABC-transporter's differential regulation in response to high rates of DCE

DMC195 ceasing reductive dechlorination when fed high rates of neat cis-DCE was a perplexing development. Both PCE and TCE were fed at similar rates in previous studies (Chapter 1) and did not display the same inhibition. Intriguingly, four members of an operon encoding for a putative drug resistance ABC transporter (DET1616-1619) displayed higher intensity in the inhibited cultures as compared to the respiring DCE cultures. Commercially available DCE is listed at 99+% purity, but is stabilized by ~0.2% 4-methoxyphenol (also called mequinol) to prevent polymerization. Additionally, chloroform, which inhibits reductive dehalogenation, has previously been noted to be a common contaminant of cis-DCE (27). Therefore, future studies should investigate whether monomethyl ether of hydroquinone is inhibitory to DMC species or chloroform is still present in the commercially available cis-DCE.

4.E.5. Methylglyoxyl synthase's differential expression in PCE saturating conditions

In the screen for transcripts differentially expressed between the inhibited PCE saturating cultures and the other higher respiring cultures in the experimental dataset, we noted a methylglyoxal synthase/phosphate transporter (DET0137) to be significantly higher in intensity (39±15 fold). This was surprising as an additional methylglyoxal synthase encoding gene, DET1576, was seen to be significantly up-regulated under nitrogen limitation conditions (25). A methylglyoxal synthase was also significantly up-regulated (2.5±0.31 fold) in the 17 hour post TCA addition culture versus the control. As this gene synthesizes methylglyoxyl, a highly toxic electrophile it is quizzical that this gene would be up-regulated in stress conditions. However, methylglyoxyl synthase abundance in model organisms (such as *E. coli*) was related to the loss

of carbon-source transport regulation, especially in conditions of switching from carbon starved to overfed (40). In these experiments, high rates of butyrate addition accompanied the PCE. Additionally, the culture was purged every 24 hours and did not actually experience saturating PCE during the entire course of the experiment (Appendix Figure A5.8). It is possible that the entire culture of D2 (methanogenesis ceased as well) was inhibited by the overabundance of a carbon-source (butyrate).

The screen of multiple high-throughput datasets successfully highlighted transcripts and proteins linked to stress. These specific relationships require further in-culture monitoring and biochemical characterization to strengthen the utility of the macromolecules as a potential field-site bioindicators.

4.F. Acknowledgements:

We would like to thank our funding sources, the Department of Defense Army Research Office (W911NF-07-1-0249), the National Science Foundation CBET Program (CBET-0731169), and the NSF- IGERT funded Biogeochemistry and Environmental Biocomplexity small grant program (DGE 0221658). Additionally, we would like to thank the NSF Graduate Research Fellowship Program for funding Cresten Mansfeldt in this research.

Portions of this work were performed at the Environmental Molecular Sciences Laboratory, a DOE national scientific user facility located at the Pacific Northwest National Laboratory.

REFERENCES:

1. Aktaş, Ö., Schmidt, K. R., Mungenast, S., Stoll, S., & Tiehm, A. (**2011**). Effect of chloroethene concentrations and granular activated carbon on reductive dechlorination rates and growth of *Dehalococcoides* spp. *Bioresource Technology*, 103: 286–292.

2. Amos, B. K., Ritalahti, K. M., Cruz-Garcia, C., Padilla-Crespo, E., & Löffler, F. E. (**2008**). Oxygen effect on *Dehalococcoides* viability and biomarker quantification. *Environmental Science & Technology*, 42: 5718-5726.

3. Aulenta, F., Majone, M., & Tandoi, V. (**2006**). Enhanced anaerobic bioremediation of chlorinated solvents: environmental factors influencing microbial activity and their relevance under field conditions. *Journal of Chemical Technology and Biotechnology*, 81: 1463-1474.

4. Bankston, J. L., Sola, D. L., Komor, A. T., & Dwyer, D. F. (**2002**). Degradation of trichloroethylene in wetland microcosms containing broad-leaved cattail and eastern cottonwood. *Water Research*, 36: 1539-1546.

5. Battesti, A., & Bouveret, E. (**2006**). Acyl carrier protein/SpoT interaction, the switch linking SpoT-dependent stress response to fatty acid metabolism. *Molecular Microbiology*, 62: 1048-1063.

6. Chan, W. W., Grostern, A., Löffler, F. E., & Edwards, E. A. (**2011**). Quantifying the effects of 1, 1, 1-trichloroethane and 1, 1-dichloroethane on chlorinated ethene reductive dehalogenases. *Environmental Science & Technology*, 45: 9693-9702.

7. DiStefano, T. D., Gossett, J. M., & Zinder, S. H. (**1991**). Reductive dechlorination of high concentrations of tetrachloroethene to ethene by an anaerobic enrichment culture in the absence of methanogenesis. *Applied & Environmental Microbiology*, 57: 2287-2292.

8. DiStefano, T. D., Gossett, J. M., & Zinder, S. H. (**1992**). Hydrogen as an electron donor for dechlorination of tetrachloroethene by an anaerobic mixed culture. *Applied & Environmental Microbiology*, 58: 3622-3629.

9. Duhamel, M., & Edwards, E. A. (**2006**). Microbial composition of chlorinated ethene-degrading cultures dominated by *Dehalococcoides*. *FEMS Microbiology Ecology*, 58: 538-549.

10. Darling, A. C., Mau, B., Blattner, F. R., & Perna, N. T. (**2004**). Mauve: multiple alignment of conserved genomic sequence with rearrangements. *Genome Research*, 14: 1394-1403.

11. Fennell, D. E., Gossett, J. M., & Zinder, S. H. (**1997**). Comparison of butyric acid, ethanol, lactic acid, and propionic acid as hydrogen donors for the reductive dechlorination of tetrachloroethene. *Environmental Science & Technology*, 31: 918-926.

12. Freedman, D. L., & Gossett, J. M. (**1989**). Biological reductive dechlorination of tetrachloroethylene and trichloroethylene to ethylene under methanogenic conditions. *Applied & Environmental Microbiology*, 55: 2144-2151.

13. Friis, A. K., Heimann, A. C., Jakobsen, R., Albrechtsen, H. J., Cox, E., & Bjerg, P. L. (**2007**). Temperature dependence of anaerobic TCE-dechlorination in a highly enriched *Dehalococcoides*-containing culture. *Water Research*, 41: 355-364.

14. Gossett, J. M. (**2010**). Sustained aerobic oxidation of vinyl chloride at low oxygen concentrations. *Environmental Science & Technology*, 44: 1405-1411.

15. Heimann, A. C., Friis, A. K., & Jakobsen, R. (**2005**). Effects of sulfate on anaerobic chloroethene degradation by an enriched culture under transient and steady-state hydrogen supply. *Water Research*, 39: 3579-3586.

16. Holliger, C., Wohlfarth, G., & Diekert, G. (**2006**). Reductive dechlorination in the energy metabolism of anaerobic bacteria. *FEMS Microbiology Reviews*, 22: 383-398.

17. Hood, E. D., Major, D. W., Quinn, J. W., Yoon, W. S., Gavaskar, A., & Edwards, E. A. (**2008**). Demonstration of enhanced bioremediation in a TCE source area at Launch Complex 34, Cape Canaveral Air Force Station. *Ground Water Monitoring & Remediation*, 28: 98-107.

18. Hu, Y., Peng, N., Han, W., Mei, Y., Chen, Z., Feng, X., ... & She, Q. (**2012**). An archaeal protein evolutionarily conserved in prokaryotes is a zinc-dependent metalloprotease. *Bioscience Reports*.

19. Hug, L. A., Beiko, R. G., Rowe, A. R., Richardson, R. E., & Edwards, E. A. (**2012**). Comparative metagenomics of three *Dehalococcoides*-containing enrichment cultures: the role of the non-dechlorinating community. *BMC Genomics*, 13: 327.

20. Hug, L. A., Salehi, M., Nuin, P., Tillier, E. R., & Edwards, E. A. (**2011**). Design and verification of a pangenome microarray oligonucleotide probe set for *Dehalococcoides* spp. *Applied & Environmental Microbiology*, 77: 5361-5369.

21. Jayachandran, G., Görisch, H., & Adrian, L. (**2004**). Studies on hydrogenase activity and chlorobenzene respiration in *Dehalococcoides* sp. strain CBDB1. *Archives of Microbiology*, 182: 498-504.

22. Kube, M., Beck, A., Zinder, S. H., Kuhl, H., Reinhardt, R., & Adrian, L. (**2005**). Genome sequence of the chlorinated compound–respiring bacterium *Dehalococcoides* species strain CBDB1. *Nature Biotechnology*, 23: 1269-1273.

23. Löffler, F. E., Yan, J., Ritalahti, K. M., Adrian, L., Edwards, E. A., Konstantinidis, K. T., Fullerton, H., Zinder, S. H., & Spormann, A. M. (**2012**). *Dehalococcoides mccartyi* gen. nov., sp. nov., obligate organohalide-respiring anaerobic bacteria, relevant to halogen cycling and bioremediation, belong to a novel bacterial class, *Dehalococcoidetes* classis

nov., within the phylum Chloroflexi. *International Journal of Systematic and Evolutionary Microbiology*.

24. Lee, D. H., Kim, M. D., Lee, W. H., Kweon, D. H., & Seo, J. H. (**2004**). Consortium of fold-catalyzing proteins increases soluble expression of cyclohexanone monooxygenase in recombinant *Escherichia coli*. *Applied Microbiology and Biotechnology*, 63: 549-552.

25. Lee, P. K., Dill, B. D., Louie, T. S., Shah, M., VerBerkmoes, N. C., Andersen, G. L., Zinder, S. H. & Alvarez-Cohen, L. (**2012**). Global transcriptomic and proteomic responses of *Dehalococcoides ethenogenes* strain 195 to fixed nitrogen limitation. *Applied & Environmental Microbiology*, 78: 1424-1436.

26. Maymo-Gatell, X., Chien, Y. T., Gossett, J. M., & Zinder, S. H. (**1997**). Isolation of a bacterium that reductively dechlorinates tetrachloroethene to ethene. *Science*, 276: 1568-1571.

27. Maymó-Gatell, X., Nijenhuis, I., & Zinder, S. H. (**2001**). Reductive dechlorination of cis-1, 2-dichloroethene and vinyl chloride by "*Dehalococcoides ethenogenes*". *Environmental Science & Technology*, 35: 516-521.

28. McMurdie, P. J., Behrens, S. F., Müller, J. A., Göke, J., Ritalahti, K. M., Wagner, R., Goltsman, E., & Spormann, A. M. (**2009**). Localized plasticity in the streamlined genomes of vinyl chloride respiring *Dehalococcoides*. *PLoS Genetics*, 5: e1000714.

29. Men, Y., Feil, H., VerBerkmoes, N. C., Shah, M. B., Johnson, D. R., Lee, P. K., ... & Alvarez-Cohen, L. (**2011**). Sustainable syntrophic growth of *Dehalococcoides ethenogenes* strain 195 with *Desulfovibrio vulgaris Hildenborough* and *Methanobacterium congolense*: global transcriptomic and proteomic analyses. *The ISME Journal*, 6: 410-421.

30. Neumann, A., Wohlfarth, G., & Diekert, G. (**1998**). Tetrachloroethene dehalogenase from *Dehalospirillum multivorans*: cloning, sequencing of the encoding genes, and expression of the pceA gene in *Escherichia coli*. *Journal of Bacteriology*, 180: 4140-4145.

31. Okutsu, N., Tamura, W., Mizumoto, M., Ueno, T., Ishida, H., & Iizumi, T. (**2012**). Field demonstration of bioaugmentation in trichloroethene-contaminated groundwater. *Water Practice & Technology*, 7.

32. Rahm, B. G., Morris, R. M., & Richardson, R. E. (**2006**). Temporal expression of respiratory genes in an enrichment culture containing *Dehalococcoides ethenogenes*. *Applied & Environmental Microbiology*, 72: 5486-5491.

33. Rahm, B. G., & Richardson, R. E. (**2007**). Correlation of respiratory gene expression levels and pseudo-steady-state PCE respiration rates in *Dehalococcoides ethenogenes*. *Environmental Science & Technology*, 42: 416-421.

34. Rahm, B. G., & Richardson, R. E. (**2008**). *Dehalococcoides*' gene transcripts as quantitative bioindicators of tetrachloroethene, trichloroethene, and cis-1, 2-

dichloroethene dehalorespiration rates. *Environmental Science & Technology*, 42: 5099-5105.

35. Rowe, A. R., Heavner, G. L., Mansfeldt, C. B., Werner, J. J., & Richardson, R. E. (**2012**). Relating Chloroethene Respiration Rates in *Dehalococcoides* to Protein and mRNA Biomarkers. *Environmental Science & Technology*.

36. Rowe, A. R., Lazar, B. J., Morris, R. M., & Richardson, R. E. (**2008**). Characterization of a dechlorinating mixed culture: community structure and comparisons of gene expression in planktonic and biofloc-associated *Dehalococcoides* and *Methanospirillum*. *Applied & Environmental Microbiology.*

37. Rowe, B. L., Toccalino, P. L., Moran, M. J., Zogorski, J. S., & Price, C. V. (**2007**). Occurrence and potential human-health relevance of volatile organic compounds in drinking water from domestic wells in the United States. *Environmental Health Perspectives*, 115: 1539.

38. Seshadri, R., Adrian, L., Fouts, D. E., Eisen, J. A., Phillippy, A. M., Methe, B. A., ... & Heidelberg, J. F. (**2005**). Genome sequence of the PCE-dechlorinating bacterium *Dehalococcoides ethenogenes*. *Science*, 307: 105-108.

39. Scheutz, C., Durant, N. D., Dennis, P., Hansen, M. H., Jørgensen, T., Jakobsen, R., Cox, E. E., & Bjerg, P. L. (**2008**). Concurrent ethene generation and growth of *Dehalococcoides* containing vinyl chloride reductive dehalogenase genes during an enhanced reductive dechlorination field demonstration. *Environmental Science & Technology*, 42: 9302-9309.

40. Tötemeyer, S., Booth, N. A., Nichols, W. W., Dunbar, B., & Booth, I. R. (**2002**). From famine to feast: the role of methylglyoxal production in *Escherichia coli*. *Molecular Microbiology*, 27: 553-562.

41. Vorob'eva, L. I. (**2004**). Stressors, stress reactions, and survival of bacteria: a review. *Applied Biochemistry & Microbiology*, 40: 217-224.

42. Waller, A. (**2010**). Molecular investigation of chloroethene reductive dehalogenation by the mixed microbial community KB1. Ph.D. Theis. Toronto University.

43. Waller, A. S., Krajmalnik-Brown, R., Löffler, F. E., & Edwards, E. A. (**2005**). Multiple reductive-dehalogenase-homologous genes are simultaneously transcribed during dechlorination by *Dehalococcoides*-containing cultures. *Applied & Environmental Microbiology*, 71: 8257-8264.

44. West, K. A., Johnson, D. R., Hu, P., DeSantis, T. Z., Brodie, E. L., Lee, P. K., Feil, Helene, Andersen, G. L., & Alvarez-Cohen, L. (**2008**). Comparative genomics of "*Dehalococcoides ethenogenes*" 195 and an enrichment culture containing unsequenced "*Dehalococcoides*" strains. *Applied & Environmental Microbiology*, 74: 3533-3540.

45. Zhang, W., Culley, D. E., Hogan, M., Vitiritti, L., & Brockman, F. J. (**2006**). Oxidative stress and heat-shock responses in *Desulfovibrio vulgaris* by genome-wide transcriptomic analysis. *Antonie Van Leeuwenhoek,* 90: 41-55.

CHAPTER 5

Summary and Future Directions

5.A. Summary of research objectives

The overarching theme of this research dissertation was generating and analyzing high-throughput data to predict mRNA transcript and protein relationships for *Dehalococcoides mccartyi* (DMC). This was to further the inferred characterization of key biological processes and discover potential useful strain specific biomarkers of cellular state. Additionally, high-throughput studies allow the DMC research community to interrogate a genetically intractable organism. With this work, we set out to address two important emerging issues for DMC in the fields of microbiology, systems biology, and bioremediation: 1) do cost-effective high-throughput surveys of DMC provide an alternate route to predict gene or protein functions or behaviors; and 2) are data-driven hypotheses able to identify useful biomarkers of stable and stressed cellular state to begin to be developed for field site monitoring? Data-driven hypothesis modeling for the mixed microbial cultures D2 and KB-1^{TM} involved the following workflow.

1) Design and/or implement microarrays targeting DMC specific genes across a wide range of experimental conditions to manipulate the pool of mRNA transcripts (using in-house DMC 195 specific microarrays and the pangenome microarray (1)).
2) Infer interaction networks composed of genes, metabolites, and phenotypes by constructing Bayesian inference ensembles on microarray data using the Reverse Engineering/Forward Simulation^{TM} platform.
3) Screen for stress response relationships by detecting differential expression in the transcriptomic and available proteomic datasets.

The investigation of transcriptomic behavior across two mixed community network ensembles allowed for comparison of strain biology identifying conserved and strain specific relationships.

5.B. Summary of data-driven hypothesis generation

5.B.1. Development of the main transcriptomic dataset with simple analyses

Applications of microarrays to monitor DMC's transcriptome were previously concerned with targeted experimental studies such as monitoring the mRNA pool with the presence or absence of a particular experimental variable (4,7,9), primarily in batch-fed form. By sampling continuously fed D2 cultures, we were able to more closely tie the stable level of transcript abundance to the observed experimental conditions and responses of the culture (10). Covering a wider range of electron acceptors, electron donors, and feed rates within the same dataset challenged the culture over a more continuous distribution of respiration rates and responses. This allowed a greater dynamic range over which we could detect co-expression relationships. The data generated in this way is unique within the DMC research community.

Applying established and computationally less intense statistical techniques (such as K-means and hierarchical clustering) to this dataset highlighted several key relationships for D2. We showed that five main clusters existed for transcript behavior and responded either positively, negatively, or indifferently to DMC's respiration rate. The group that responded positively included transcripts for the RDases *tceA* and *pceA*; the hydrogenases *hupL* and *hymA*; and other respiration and growth linked enzymes such as *atpase*, the NADH:Ubiquinone oxidoreductase *nuo*, and the non-formate oxidizing formate dehydrogenase *fdh*. The wider cluster group contained 409 total transcripts. These transcripts potentially encode for enzymes

that fulfill functions in the respiration chain that are known to occur but have yet been completely annotated.

Considering specific relationships rather than transcriptome-wide responses, we noted the DET0079 *tceA* transcript displayed an inverse relationship with the putative RDase transcriptional regulators DET1525 and DET1531. Although conformational state of the final protein determines the nature of these transcriptional regulators, DET1531 displayed the lowest negative correlation to *tceA* ($r = -0.93$) out of any transcript. If this relationship is causal and not just correlated, this finding raises the possibility that the regulation of RDases in the DMC genome may not be simply limited to predicted cis-regulatory elements.

Additional investigations on the commercially available KB-1^{TM} culture used a pangenome array that targeted all protein encoding genes collectively found in the *Dehalococcoides* genus (3). This was the first application of a pangenome array to monitor the transcriptome of any DMC species (previous work of validation and characterization investigated genomic DNA only (3,6)). Surprisingly, the pangenome array recaptured unique signals for multiple DMC populations in the KB-1^{TM} culture. Therefore, this pangenome platform is a useful first tool for monitoring mixed microbial communities that potentially contain more than one strain.

5.B.2. Data-driven hypothesis discovery

The utility of the transcriptomic datasets lay in the range of experimental conditions run and the variability of the individual transcript's response. The size of our dataset allowed us to

apply a more computational intense data mining technique to discover novel relationships. We ran these datasets through a Bayesian network inference platform (Reverse Engineering/Forward Simulation™) to predict a sparse set of confident gene-to-gene and gene-to-response interactions and their likelihood of existence in an ensemble (n = 1000) of networks. We created separate network ensembles for the independent D2 and KB-1™ datasets to allow for cross-comparisons between two microarray platforms and two mixed microbial communities. This comparison allowed us to highlight extremely well conserved interactions in DMC. The relationships predicted in both the D2 and KB-1™ models connected transcripts of the *hup, nuo,* and *fdh* operons to each other. This suggests two oxidoreductases with questions surrounding their function (the operon for *nuo* lacks the *nuoEFG* receiver domain which is encoded elsewhere on the genome (11); *fdh* maintains an authentic point mutation in its active site preventing formate oxidation) may actually participate in the hydrogen-to-chloroethene electron transport chain or other respiration linked processes. Additionally, both models connected a key RDase (*tceA* in D2 and *vcrA* in KB-1™) to the transcript for the putative S-layer protein. If the relationship of connecting an RDase transcript to the S-layer holds true for all strains of DMC, the S-layer may be under the same regulatory pathway as that of a major RDase. By co-regulating the final enzyme required for reductive dechlorination with the proteinaceous cell wall, DMC may be employing a survival mechanism that every instance it senses opportunities for growth, it will also express an RDase. This may begin to explain the success and survival of DMC in enrichment cultures.

5.B.3. Identified stress related biomarkers

The proteomic and transcriptomic dataset contained experiments that caused a stress response in the DMC species prompting reductive dechlorination to either slow or cease. Learning from these conditions potentially provide a useful understanding of the basic biology of DMC stress response and can highlught biomarkers of stress for DMC. In Chapter 1, we identified the RDase DET1559 as potentially involved in the reductive dechlorination of chlorinated aromatics due to the fact it was up-regulated significantly when the culture was fed chlorobenzenes or chlorophenols. This simple differential regulation screen provides useful and future testable hypotheses for the stressed cultures as well. When applied to the dataset comprised of the stress inducing conditions of adding trichloroethane (TCA), spiking in oxygen, lower pH, saturating the culture with PCE, overfeeding of DCE, and providing no exogenous donor, many individual stress related transcripts and proteins were connected to these conditions. Two in particular, DnaJ and HspR (DET1411-1412), are genes predicted to encode proteins that might participate in a general stress-reduction pathway and were significantly up-regulated in varied proteomic and transcriptomic samples. These two transcripts may therefore provide useful biomarkers of general stress to monitor in field-site settings.

In addition to enzymes and transcripts potentially involved in general stress response, we also identified putative biomarkers specifically for solvent saturation/carbon overabundance and oxidative stress. A methylglyoxyl synthase (DET0137) displayed 39±15 fold higher intensity (with significant expression intensity greater than 10,000 pfu) when saturating conditions of PCE with a high concentration of butyrate was sensed in the cell. It has been noted in model organisms that methylglyoxyl synthase and methylglyoxyl build and become toxic to the cell

when the organism loses control over carbon assimilation (15). However, future focus should still be placed to see if DMC is using a methylglyoxal synthase (or methylglyoxyl itself) to either combat cellular stress or regulate the characteristics of other proteins. In the oxygen experiments preformed on KB-1™, we noted that the dominant member in average absolute RNA intensity recaptured by a pangenome microarray switched from one lineage of DMC (Pinellas) to a second (Cornell). The Cornell type strain in KB-1™ that overtook the Pinellas displayed significantly higher transcripts surrounding and including the superoxide dismutase (maximum of 13 ± 4.1 fold chain). This suggests the superoxide dismutase operon (DET0954-0957 in DMC195) serves as a good indicator of DMC recovering from oxygen exposure.

5.C. Methodological future directions

5.C.1. Direct RNA sequencing of DMC transcriptomes

A major gap in the current literature for the DMC research field and reductive dechlorination in general is the lack of any published or publicly available results directly sequencing the RNA pool. The community of researchers investigating DMC is incorporating RNA sequencing techniques as the Alameda Naval Air Station (ANAS) culture's metatranscriptome has been sequenced (but currently is unpublished and is listed but unavailable in public repositories). Although microarrays are still lower in cost, the expense associated with next-generation sequencing technologies, such as RNA-seq, considerably lowers each year (16). This method of RNA detection allows the DMC research community to avoid several of the major limitations of using microarrays (1). Probes for microarrays must be designed with a reference genome or metagenome. One of the major limitations associated with requiring an annotated genome as a basis for probe design is that we are dependent on open reading frame

prediction across the organism and may lose ability to detect novel biology. Additionally, as more strains of DMC are identified, cultured, and sequenced, probe sets designed to target the entire *Dehalococcoides* genus would need to be redesigned. This could confound comparisons between one probe set design to the next, complicating cross-analysis between future and past experiments. Finally, the application of DMC-specific microarrays to mixed communities such as D2 and KB-1^{TM} does not observe significant portions of relevant data as the RNA from community members is lost. This provides a significant oversight of informative data as it has been shown in the literature that DMC maintains incomplete biosynthetic pathways for crucial amino acids and coenzymes (such as cobalamin Vitamin B12)(2,17). Thus, the full metatranscriptomic interaction network for key biological processes would be unable to be described, missing key complete biosynthesis pathways.

5.C.2. Modify proteomic analysis to detect strain-specific peptides in DMC co-cultures

The tandem mass spectrometry tagged (TMT) multiplex data (14) discussed in Chapter 4 may be used to further characterize the strain variation detected in the KB-1^{TM} mixed microbial community. During the investigation of stress response, we reported whole protein ion intensity scores. These scores were a result of multiple distinct peptides being detected for a single protein. However, due to strain variation, some of these peptides would be shared across strains of DMC while others would be unique for a specific strain. Rather than looking at whole protein relative concentrations, specific peptide ions that uniquely match a specific strain's homolog should be monitored. This will provide a more nuanced understanding of the specific strain's

protein pool responses to various experimental conditions and also cross-validate transcriptomic results obtained from pangenome arrays.

5.D. Suggested future directions of research

5.D.1. Natural chlorinated organic matter as an electron acceptor

In altering the electron acceptor from chlorinated ethenes to chlorinated benzenes, the transcript for the DET1559 RDase was most differentially regulated. However, no new RDase transcript was detected out of the pool of 17. This suggests alternative electron acceptors should be explored to potentially turn on alternative RDases. An informative study would be monitoring DMC exposed to chlorinated natural organic matter with micorarrays. Recently, the reductive dechlorination of natural chlorinated organics was noted (5). This potentially describes a natural niche for dehalorespiring organisms. In the process, the study developed a method capable of synthesizing a mixed pool of chlorinated organic matter. This provides an exciting opportunity to provide a type of chlorinated electron acceptor that not has been fed previously to the well-characterized D2 community. Monitoring DMC195 transcriptomically would then screen for the expression of a varied subclass of the 17 RDases present on the genome. The immediate goal of this experiment is to transcriptomically express previously non-detected RDases. Future studies separating the chlorinated-compounds by column fractionation would then determine the specific response of individual RDases.

5.D.2. Update the network ensembles for D2 and KB-1™ with additional experiments and new analyses

By creating a pipeline to analyze transcriptomic data through a Bayesian network inference platform, a priority for future work should be placed on challenging the culture to an even wider range of conditions in order to update the ensemble. The Bayesian inference method predicts more confident interactions with the greater number of samples analyzed. The Reverse Engineering/Forward Simulation™ platform, in particular, maintains the ability to conduct *in silico* experiments. The user sets the appropriate experimental conditions in the network ensemble and the platform predicts a numeric level for all variables in the network with confidence intervals. What is useful about this function is that a specific state could be set prior to analysis and then subsequent transcriptomic data from the experiment could be used to either confirm or deny the prediction. Each time this is preformed, the network ensemble is updated with the new data. Repeated iterations converges towards a very confident network more accurately modeling the interaction of genes.

The investigations presented in the text primarily were concerned with selected relationships of interest, such as the connection of an RDase with neighboring elements. One of the powers of network inference is the ability to detect and model large scale organizations in the cell such as metabolic pathways. Therefore, the model will be extended to determine if key cycles or pathways are able to be described through network inference.

What is currently missing from this modeling approach is a concrete cutoff to ascertain the difference between significant and non-significant interactions. In order to establish this

baseline case, the platform will be used to construct a shuffled dataset. The resulting networks that the REFS model predicts will be b+ased on background noise of the model prediction. Establishing a cutoff above this will greatly strengthen our ability to confidently portray our results and hypotheses.

5.D.3. Biochemically test data-driven hypotheses

Hypotheses discovered during the course of this research provide a mechanism to select biochemical assays to investigate the behavior of putative or misannotated enzymes.

Whole cell extracts. Previous investigations have used whole-cell extracts of proteins to characterize the substrate range of key reductive dehalogenases (1,8). We made an attempt to enrich DMC195 in D2 for the lower expressed RDase DET1545 by growing the culture at low PCE feed-rates for 40 days. Subsequent activity assays did display reductive dechlorination, but the dominant protein in these samples was TceA followed by DET1559 and PceA. One of the challenges surrounding RDase enzymatic assays is the ability to separate similar molecular weight and charged proteins. For example, DET1559 and PceA co-migrated with each other in a protein gradient gel. With advances in protein column separation, similar sized RDases such as PceA and DET1559 potentially can be separated and further biochemically characterized.

One of the exciting things about the initial investigations into biochemically characterized RDases was that the extracted protein from the cell was able to reductively dehalogenate chlorobenzene congeners. This indicates one of the traditional RDases DMC 195

expresses under PCE feeding and that has been monitored in the D2 culture is capable of chloroaromatic dehalorespiration (and from the work presented in this text, DET0318 and DET1559 are likely candidates). Reattempting a capture and characterization of DET1545 or switching to DET1559 would be natural extension of this work.

Heterologous expression of proteins. One of the consistently perplexing themes in the body of knowledge for DMC is the detection of significant amounts of transcripts and proteins for formate dehydrogenase (Fdh). In DMC, this enzyme maintains an authentic point mutation that substitutes a selenocysteine for a cysteine at one of the active sites, hindering the enzymes ability to oxidize formate (11). However, as was seen in Chapters 2 and 3, this enzyme is up-regulated under states of higher cellular respiration and shares neighbors in the Bayesian inference network ensemble with hydrogenases (Hup and Hym). A recent paper investigating a similar Fdh in *E. coli* found that the enzyme was capable of acting as a hydrogenase for the cell when the other hydrogenases were suppressed (13). Due to the similarity of the enzyme architecture, Fdh would be a prime candidate to over-express in model organisms and determine if it is capable of acting as a hydrogenase for the DMC strains, which would explain both its high expression and connection to other hydrogenases in the network ensembles.

5.D.4. Test potential biomarkers of stress in additional cultures and field-site applications

The high-throughput data for DMC cultures challenged with a wide variety of stress inducing conditions highlighted the chaperone DnaJ and HspR (DET1411-1412) as a general cell stress response. A recommended extension from this finding would be to design primers

targeting these transcripts for quantitative reverse transcriptase PCR (qRTPCR) to quantifiably monitor *dnaJ* and *hspR* in even wider ranges of varied forms of stress. If these transcripts still appear to be general biological indicators for most forms of stress, quantifying and detecting DnaJ and HspR in the field would be the next natural extension. However, due to the basal high level of expression for these two enzymes, quantifiable shifts may be difficult to discern in complex settings. A potential solution to the problem would be to identify within sample normalization techniques that note the quantifiable shift of the abundance of the protein of interest to a stable translated protein. However, as both DnaJ and HspR are considered housekeeping genes, their abundance may not vary considerably even when the ratio is considered.

5.D.5. Combine reductively-dechlorinating, mixed-community cultures to optimize ethene generation

Through the KB-1^{TM} experiments, the complete reduction to ethene was often disrupted by culturing practices. Attention should be paid to increase the robustness of this key step. In preliminary studies, combining the mixed community cultures D2 and KB-1^{TM} produced a stable culture that was able to reductively dechlorinate 110 µM PCE to ethene (>95%) in under 10 hours. Investigations should be made into mixing the current culture collection to provide an optimal dechlorinating community. Additionally, the oxygen and TCA stress studies displayed a strain-to-strain variation in the response of DMC. Ethene generation and resilience to TCA stress was linked to the presence of a Pinellas type DMC. We also noted that what appeared as a minor Cornell type DMC member of the population overtook the Pinellas type after oxygen exposure

and, to a lesser extent, after TCA exposure (in average total RNA). Therefore, we could test if the combined culture is more resilient to certain stress types than the individual cultures.

5.E. Closing Statement

The application of various omic techniques allows us as a microbial and environmental engineering community to query and monitor bioremediating natural and engineered systems. The tools we now have to investigate these complex systems have also generated sizable datasets that are difficult to fully comprehend and are subjected to individual biases. This work looked at uniting the fields of environmental engineering, environmental microbiology, and systems biology to produce a pathway to efficiently go from data to hypothesis generation. It is our continued hope that this system-wide view of *Dehalococcoides* will lead to a process of data-to-hypothesis-to-data generation that will rapidly and more fully characterize this important organism ultimately leading to field-deployed diagnostic assays for site management.

REFERENCES:

1. Adrian, L., Rahnenführer, J., Gobom, J., & Hölscher, T. (**2007**). Identification of a chlorobenzene reductive dehalogenase in *Dehalococcoides* sp. strain CBDB1. *Applied & Environmental Microbiology*, 73: 7717-7724.

2. Hug, L. A., Beiko, R. G., Rowe, A. R., Richardson, R. E., & Edwards, E. A. (**2012**). Comparative metagenomics of three *Dehalococcoides*-containing enrichment cultures: the role of the non-dechlorinating community. *BMC Genomics*, 13: 327.

3. Hug, L. A., Salehi, M., Nuin, P., Tillier, E. R., & Edwards, E. A. (**2011**). Design and verification of a pangenome microarray oligonucleotide probe set for *Dehalococcoides* spp. *Applied & Environmental Microbiology*, 77: 5361-5369.

4. Johnson, D. R., Nemir, A., Andersen, G. L., Zinder, S. H., & Alvarez-Cohen, L. (**2009**). Transcriptomic microarray analysis of corrinoid responsive genes in *Dehalococcoides ethenogenes* strain 195. *FEMS Microbiology Letters*, 294: 198-206.

5. Krzmarzick, M. J., Crary, B. B., Harding, J. J., Oyerinde, O. O., Leri, A. C., Myneni, S. C., & Novak, P. J. (**2012**). Natural niche for organohalide-respiring *Chloroflexi*. *Applied & Environmental Microbiology*, 78: 393-401.

6. Lee, P. K., Cheng, D., Hu, P., West, K. A., Dick, G. J., Brodie, E. L., ... & Alvarez-Cohen, L. (**2011**). Comparative genomics of two newly isolated *Dehalococcoides* strains and an enrichment using a genus microarray. *The ISME Journal*, 5: 1014-1024.

7. Lee, P. K., Dill, B. D., Louie, T. S., Shah, M., VerBerkmoes, N. C., Andersen, G. L., ... & Alvarez-Cohen, L. (**2012**). Global transcriptomic and proteomic responses of *Dehalococcoides ethenogenes* strain 195 to fixed nitrogen limitation. *Applied and Environmental Microbiology*, 78: 1424-1436.

8. Magnuson, J. K., Romine, M. F., Burris, D. R., & Kingsley, M. T. (**2000**). Trichloroethene reductive dehalogenase from *Dehalococcoides ethenogenes*: Sequence of tceA and substrate range characterization. *Applied & Environmental Microbiology*, 66: 5141-5147.

9. Men, Y., Feil, H., VerBerkmoes, N. C., Shah, M. B., Johnson, D. R., Lee, P. K., ... & Alvarez-Cohen, L. (**2011**). Sustainable syntrophic growth of *Dehalococcoides ethenogenes* strain 195 with *Desulfovibrio vulgaris Hildenborough* and *Methanobacterium congolense*: global transcriptomic and proteomic analyses. *The ISME Journal*, 6: 410-421.

10. Rahm, B. G., & Richardson, R. E. (**2007**). Correlation of respiratory gene expression levels and pseudo-steady-state PCE respiration rates in *Dehalococcoides ethenogenes*. *Environmental Science & Technology*, 42: 416-421.

11. Seshadri, R., Adrian, L., Fouts, D. E., Eisen, J. A., Phillippy, A. M., Methe, B. A., ... & Heidelberg, J. F. (**2005**). Genome sequence of the PCE-dechlorinating bacterium *Dehalococcoides ethenogenes*. *Science*, 307: 105-108.

12. Shendure, J. (**2008**). The beginning of the end for microarrays? *Nature Methods*, 5: 585-587.

13. Soboh, B., Pinske, C., Kuhns, M., Waclawek, M., Ihling, C., Trchounian, K., ... & Sawers, G. (**2011**). The respiratory molybdo-selenoprotein formate dehydrogenases of Escherichia coli have hydrogen: benzyl viologen oxidoreductase activity. *BMC Microbiology*, 11: 173.

14. Thompson, A., Schäfer, J., Kuhn, K., Kienle, S., Schwarz, J., Schmidt, G., ... & Hamon, C. (**2003**). Tandem mass tags: a novel quantification strategy for comparative analysis of complex protein mixtures by MS/MS. *Analytical Chemistry*, 75: 1895-1904.

15. Tötemeyer, S., Booth, N. A., Nichols, W. W., Dunbar, B., & Booth, I. R. (**2002**). From famine to feast: the role of methylglyoxal production in Escherichia coli. *Molecular Microbiology*, 27: 553-562.

16. Wang, Z., Gerstein, M., & Snyder, M. (**2009**). RNA-Seq: a revolutionary tool for transcriptomics. *Nature Reviews Genetics*, 10: 57-63.

17. Yi, S., Seth, E. C., Men, Y. J., Stabler, S. P., Allen, R. H., Alvarez-Cohen, L., & Taga, M. E. (**2012**). Versatility in corrinoid salvaging and remodeling pathways supports the corrinoid-dependent metabolism of *Dehalococcoides mccartyi*. *Applied and Environmental Microbiology*.

APPENDIX I

Supporting Figures and Tables for Chapter 2

Table A1.1 Full table of significantly differentially expressed transcripts between the continuous and batch fed cultures.

ID	Description	Regulation	Ratio	ID	Description	Regulation	Ratio
DET0014	hypothetical protein	UP	2.7 ± 0.77	DET1021	hypothetical protein	DOWN	0.20 ± 0.08
DET0035	*gmk* guanylate kinase	DOWN	0.42 ± 0.12	DET1031	hypothetical protein	DOWN	0.40 ± 0.10
DET0036	hypothetical protein	DOWN	0.44 ± 0.03	DET1035	tryptophan synthase subunit	UP	3.2 ± 0.39
DET0108	endonuclease/exonuclease	UP	2.2 ± 0.43	DET1038	ileS isoleucyl tRNA synthetase	UP	2.5 ± 0.39
DET0137	*mgsA* methylglyoxal synthase	DOWN	0.31 ± 0.11	DET1051	hypothetical protein	UP	3.8 ± 0.61
DET0180	RDase	UP	5.5 ± 4.10	DET1057	hypothetical protein	UP	2.3 ± 0.28
DET0181	RDase anchor	UP	5.1 ± 0.91	DET1063	DNA binding regulator, LuxR	UP	2.7 ± 0.81
DET0297	hypothetical protein	UP	4.9 ± 3.03	DET1068	recombinase, phage integrase	DOWN	0.30 ± 0.09
DET0298	hypothetical protein	UP	4.5 ± 4.12	DET1092	DNA methylase	DOWN	0.41 ± 0.07
DET0322	hypothetical protein	DOWN	0.35 ± 0.11	DET1105	hypothetical protein	DOWN	0.27 ± 0.21
DET0368	*proS* prolyl tRNA synthetase	UP	2.7 ± 0.24	DET1106	hypothetical protein	DOWN	0.33 ± 0.06
DET0420	hypothetical protein	DOWN	0.25 ± 0.16	DET1107	hypothetical protein	DOWN	0.29 ± 0.04
DET0423	hypothetical protein	UP	4.2 ± 5.13	DET1146	hypothetical protein	DOWN	0.36 ± 0.07
DET0485	rplX ribosomal protein L24	DOWN	0.43 ± 0.07	DET1173	*fwdE* family protein	UP	2.6 ± 0.74
DET0558	*atpB* ATP synthase F0	DOWN	0.21 ± 0.04	DET1186	hypothetical protein	UP	2.9 ± 1.12
DET0560	*atpF* ATP synthase F0	DOWN	0.33 ± 0.07	DET1206	*metM* dehydrogenase	DOWN	0.34 ± 0.09
DET0561	*atpH* ATP synthase F1	DOWN	0.33 ± 0.05	DET1224	*cobA* adenosyltransferase	DOWN	0.43 ± 0.04
DET0562	*atpA* ATP synthase	DOWN	0.41 ± 0.04	DET1278	*nusB* N utilization substance	DOWN	0.25 ± 0.06
DET0673	hypothetical protein	UP	3.6 ± 0.14	DET1284	hypothetical protein	DOWN	0.38 ± 0.06
DET0721	hypothetical protein	DOWN	0.36 ± 0.04	DET1285	serine protease, DegP/HtrA	UP	2.9 ± 0.58
DET0736	oxidoreductase, dehydrogenase	UP	2.7 ± 0.42	DET1286	serine protease, DegP/HtrA	UP	3.9 ± 1.28
DET0754	hypothetical protein	UP	2.7 ± 1.12	DET1300	universal stress protein	DOWN	0.27 ± 0.06
DET0755	hypothetical protein	UP	3.8 ± 0.57	DET1377	hypothetical protein	UP	3.0 ± 0.69
DET0861	hydrogenase, EchB subunit	DOWN	0.37 ± 0.07	DET1379	auxin responsive GH3 protein	UP	3.7 ± 0.28
DET0862	*echC* hydrogenase	DOWN	0.35 ± 0.10	DET1419	transcriptional regulator, AbrB	DOWN	0.29 ± 0.15
DET0864	*ech* hydrogenase subunit	DOWN	0.37 ± 0.08	DET1448	hypothetical protein	UP	2.8 ± 0.62
DET0908	arsenical pump membrane	UP	7.8 ± 2.81	DET1511	hypothetical protein	DOWN	0.14 ± 0.12
DET0909	hypothetical protein	UP	2.8 ± 0.35	DET1544	RDase anchoring protein	UP	3.5 ± 0.59
DET0945	ABC transporter, permease	DOWN	0.43 ± 0.04	DET1545	RDase	UP	3.3 ± 0.69
DET0964	*recJ* DNA exonuclease	DOWN	0.38 ± 0.08	DET1569	hypothetical protein	UP	3.0 ± 0.65
DET1021	hypothetical protein	DOWN	0.20 ± 0.08	DET1624	hypothetical protein	UP	2.6 ± 0.39
DET1031	hypothetical protein	DOWN	0.40 ± 0.10				

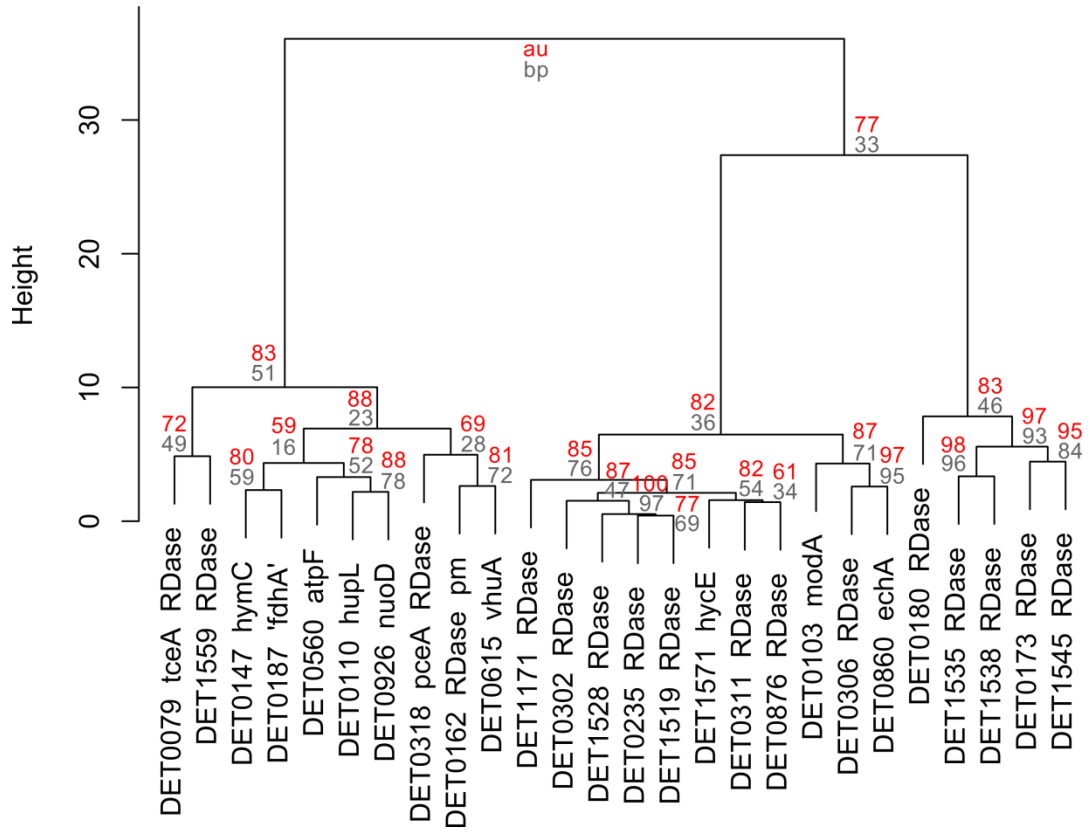

Figure A1.1 Hierarchial cluster dendogram of respiration linked oxidoreductases for the microarray dataset described in Chapter 1. The approximated unbiased (au) and the bootstrap probability (bp) is located above each intersection

Table A1.2. The 20 most positive and negative linear correlations for redoxin type electron carriers

DET0661 Thioredoxin			DET1623 Desulforedoxin			DET0198 Glutaredoxin		
ID	Gene Description	Corr	ID	Gene Description	Corr	ID	Gene Description	Corr
DET1430	*hypA* hydrogenase nickel insertion	0.898	DET1051	hypothetical protein	0.811	DET0813	ABC transporter, ATP-binding protein	0.832
DET1506	SsrA-binding protein	0.896	DET0987	acetyltransferase, GNAT family	0.772	DET1589	divalent cation tolerance protein CutA	0.822
DET1531	response regulator, LuxR family	0.884	DET0098	hypothetical protein	0.720	DET1186	hypothetical protein	0.809
DET1468	hypothetical protein	0.880	DET0017	hypothetical protein	0.689	DET1253	hypothetical protein	0.809
DET0220	hypothetical protein	0.853	DET0626	hypothetical protein	0.674	DET1459	ribosomal subunit interface protein	0.800
DET1529	sensory box protein, putative	0.845	DET0363	hypothetical protein	0.672	DET0877	hypothetical protein	0.800
DET0347	hypothetical protein	0.841	DET0130	response regulator	0.662	DET1324	hypothetical protein	0.799
DET0951	nifU domain protein	0.837	DET1585	hypothetical protein	0.655	DET1250	hypothetical protein	0.798
DET1525	transcriptional regulator, putative	0.834	DET0018	hypothetical protein	0.653	DET1580	transcription regulator, TetR family	0.793
DET0179	hypothetical protein	0.829	DET1217	acetyltransferase, GNAT family	0.652	DET1303	fasciclin domain protein	0.793
DET1431	hydrogenase accessory protein HypB	0.821	DET0189	methyltransferase, putative	0.642	DET1545	reductive dehalogenase, putative	0.792
DET0060	cyclodiphosphate synthase	0.809	DET1360	general secretion family protein	0.639	DET1049	HD domain protein	0.790
DET1505	transcriptional regulator, Fur family	0.801	DET0959	Smr domain protein	0.632	DET1307	hypothetical protein	0.790
DET0044	hypothetical protein	0.801	DET1250	hypothetical protein	0.628	DET0083	ISDet1, transposase orfA	0.787
DET0150	hypothetical protein	0.799	DET0734	hypothetical protein	0.622	DET0014	hypothetical protein	0.786
DET0387	hypothetical protein	0.793	DET0755	hypothetical protein	0.621	DET0133	hypothetical protein	0.784
DET1411	DnaJ family protein	0.790	DET1357	hypothetical protein	0.620	DET0765	hypothetical protein	0.783
DET0821	hypothetical protein	0.788	DET0416	hypothetical protein	0.602	DET0312	reductive dehalogenase anchoring protein	0.780
DET1452	hypothetical protein	0.786	DET0446	[Fe] hydrogenase, HymA subunit, putative	0.601	DET1449	membrane protein, MarC family	0.779
DET1013	hypothetical protein	0.780	DET1053	hypothetical protein	0.597	DET0955	bacterioferritin domain protein	0.777
⋮			⋮			⋮		
DET1595	ApbE/NosX family protein	-0.734	bactKB12	Community Sequence 16S rRNA	-0.505	DET0402	methyltransferase, UbiE/COQ5 family	-0.701
DET0332	protein-export membrane protein SecF	-0.735	DET1502	major facilitator family protein	-0.513	DET0470	30S ribosomal protein S12	-0.702
DET0478	ribosomal protein S19	-0.735	DET0542	thioredoxin-disulfide reductase	-0.517	DET0591	hypothetical protein	-0.711
DET0560	ATP synthase F0, B subunit	-0.738	DET1629	radical SAM domain protein	-0.517	DET0438	metallo-beta-lactamase family	-0.712
DET0595	peptidyl-tRNA hydrolase	-0.740	DET0438	metallo-beta-lactamase family protein	-0.518	DET1279	acyl carrier protein	-0.712
DET1417	IMP cyclohydrolase	-0.742	DET0593	enolase	-0.520	DET0400	3-dehydroquinate synthase family	-0.721
DET0112	*hup* , iron-sulfur cluster-binding subunit	-0.746	Luciferase	Control	-0.520	DET0562	ATP synthase subunit A	-0.724
DET0110	*hup,* large subunit	-0.749	DET1002	glycosyl transferase, group 1 family protein	-0.536	DET0185	*fdh* accessory protein FdhE	-0.729
DET0652	cobalamin/Fe3+-siderophores transport	-0.752	DET0128	cobyrinic acid a,c-diamide synthase	-0.546	DET0628	radical SAM domain protein	-0.734
DET1040	inner membrane protein, 60 kDa	-0.753	DET1402	hypothetical protein	-0.549	DET0840	adenylosuccinate lyase	-0.735
DET1283	hypothetical protein	-0.758	DET0454	fumarate hydratase, beta subunit	-0.552	DET0474	ribosomal protein L3	-0.737
DET1407	putative S-layer	-0.761	DET0449	isopropylmalate isomerase small subunit	-0.564	DET1039	SpoIIIJ-associated protein Jag	-0.738
DET0559	ATP synthase F0, C subunit	-0.769	DET0728	[Fe] hydrogenase, HymA subunit	-0.564	DET0476	ribosomal protein L23	-0.739
DET0078	*tceA* anchoring protein	-0.770	DET0183	ATP-dependent RNA helicase	-0.566	DET1284	hypothetical protein	-0.751
DET1381	GGDEF domain/HD domain protein	-0.771	DET0561	ATP synthase F1, delta subunit	-0.588	DET1260	argininosuccinate synthase	-0.759
DET1225	hypothetical protein	-0.778	DET0727	pyruvic-ferredoxin oxidoreductase	-0.606	DET1240	peptidyl-prolyl cis-trans isomerase	-0.763
DET0653	hypothetical protein	-0.781	DET1335	glutamyl-tRNA(Gln) amidotransferase	-0.611	DET0371	reductoisomerase	-0.763
DET0186	*fdh* , membrane subunit	-0.783	DET0506	ribosomal protein S9	-0.621	DET0870	translation elongation factor P	-0.779
DET0079	*tceA*	-0.793	DET1383	-	-0.621	DET1327	ribosomal protein L31	-0.785
DET0997	translation elongation factor Tu	-0.824	DET1130	glutamine amidotransferase, class II	-0.646	DET0993	ribosomal protein L11	-0.793

DET0406 Rubredoxin			DET1501 Flavoredxin		
ID	Gene Description	Corr	ID	Gene Description	Corr
DET1036	serine protease, DegP/HtrA family	0.793	DET0947	indolepyruvate ferredoxin oxidoreductase	0.833
DET1631	TPR domain protein	0.750	DET0973	dihydrodipicolinate synthase	0.803
DET0842	imidazoleglycerol-phosphate dehydratase	0.741	DET0134	hypothetical protein	0.799
DET0404	dimethyladenosine transferase	0.692	DET1624	hypothetical protein	0.778
DET0429	cysteine ligase	0.670	DET0829	membrane protein, MgtC / SapB family	0.777
DET1136	hypothetical protein	0.665	DET0827	3-isopropylmalate dehydratase	0.775
DET1367	hypothetical protein	0.647	DET0636	cell division protein FtsZ	0.744
DET1423	peptidase, M48 family	0.646	DET1064	sensory box sensor histidine kinase	0.742
DET1579	mechanosensitive ion channel family	0.645	DET0972	aspartate-semialdehyde dehydrogenase	0.735
DET0911	aminopeptidase protein	0.640	DET1053	hypothetical protein	0.731
DET1387	hypothetical protein	0.634	DET0199	ferredoxin-thioredoxin reductase	0.728
DET1317	hypothetical protein	0.622	DET0762	hypothetical protein	0.727
DET0381	iron-sulfur cluster-binding, Rieske	0.620	DET0980	hypothetical protein	0.722
DET1514	hypothetical protein	0.619	DET1118	acetyltransferase, GNAT family	0.720
DET1052	endoribonuclease L-PSP, putative	0.612	DET1364	hypothetical protein	0.716
DET1376	hypothetical protein	0.610	DET0622	radical SAM domain protein	0.712
DET1018	hypothetical protein	0.608	DET1273	hypothetical protein	0.704
DET1630	DNA gyrase, A subunit	0.607	DET1285	serine protease, DegP/HtrA	0.704
DET0792	hypoxanthine phosphoribosyltransferase	0.606	DET0416	hypothetical protein	0.702
DET1246	hypothetical protein	0.601	DET1372	dihydroorotate dehydrogenase	0.701
⋮			⋮		
DET0087	hypothetical protein	-0.448	DET1219	DNA mismatch repair protein	-0.631
DET0164	hypothetical protein	-0.450	DET1385	thiotransferase enzyme MiaB	-0.632
DET0629	D-ala D-ala ligase	-0.450	DET0087	hypothetical protein	-0.632
DET1356	hypothetical protein	-0.451	DET0656	hypothetical protein	-0.632
DET1074	hypothetical protein	-0.472	DET1221	hypothetical protein	-0.638
DET0544	BadF/BadG/BcrA/BcrD ATPase	-0.477	DET1073	hypothetical protein	-0.643
DET0593	enolase	-0.491	DET0073	hypothetical protein	-0.644
DET1076	hypothetical protein	-0.493	DET0771	hypothetical protein	-0.645
DET0204	NAD-dependent epimerase/dehydratase	-0.499	DET0239	radical SAM domain protein	-0.650
DET1119	hypothetical protein	-0.507	DET0152	hypothetical protein	-0.650
DET0439	FtsK/SpoIIIE family protein	-0.508	DET0208	glycosyl transferase, group 2 family protein	-0.653
DET0783	translin family protein	-0.509	DET0241	radical SAM domain protein	-0.655
DET0244	ribonucleotide reductase	-0.511	DET1554	hypothetical protein	-0.657
DET0596	DNA ligase, NAD-dependent	-0.514	DET1076	hypothetical protein	-0.664
DET1155	nitrogenase molybdenum-iron alpha	-0.520	DET1006	permease, putative	-0.674
COM06	*Clostridia* 16S rRNA	-0.521	DET1477	hypothetical protein	-0.681
COM12	*Clostridia* 16S rRNA	-0.526	DET1239	hypothetical protein	-0.698
DETLys1	tRNA Lysine 1	-0.566	DET0964	single-stranded-DNA-specific exonuclease Rec	-0.726
DET0170	DNA-binding response regulator	-0.571	DET1158	nitrogenase iron protein	-0.734
DET1609	Ser/Thr protein phosphatase	-0.588	DET1443	hypothetical protein	-0.761

APPENDIX II

Supporting Figures and Tables for Chapter 3

Appendix Table A2.1 Continuous experimental setup conditions and responses for the D2 mixed community data series.

	EARATE	EARATE (last 48 hours)	EDRATE (as H2)	EDRATE (total ED)	aaeq (total from YE)	Duration (hrs)	EDRATE Total (YE and ED)	Total eeq Respired	Hydraulic Residence Time (days)	ED/EA eeq ratio (does not include YE)	ED/EA eeq ratio (includes YE)	SSPCE (mM)	SSTCE (mM)	SSDCE (mM)	SSDCP (mM)	SSMCP (mM)	RespnRate	RespnRate (last 48 hours)	PCEresp	TCEresp	DCEresp	DCPresp	Acetate	Butyrate	H2levelAvg	Methanogenesis
NoDonA	0.5	0.0	0.0	0.0	0.0	168.0	0.0	22.0	40.0	0.0	0.0	26700.0	2040.0	851.0	0.0	0.0	1.3	0.7	0.2	0.2	0.2	0.0	1.8	10.0	0.0	0.1
NoDonB	0.5	0.0	0.0	0.0	0.0	168.0	0.0	25.3	40.0	0.0	0.0	22900.0	3570.0	3620.0	0.0	0.0	1.3	0.9	0.3	0.3	0.3	0.0	2.1	10.0	0.0	0.1
FYE_A	0.8	0.3	0.0	0.0	300.0	168.0	17.9	74.3	40.0	0.0	3.2	4120.0	483.0	1410.0	0.0	0.0	4.1	5.5	0.7	0.7	0.7	0.0	2.6	10.0	0.0	4.8
FYE_B	0.9	0.5	0.0	0.0	300.0	168.0	17.9	86.3	40.0	0.0	2.5	6150.0	995.0	560.0	0.0	0.0	4.9	8.3	0.8	0.8	0.8	0.0	2.2	10.0	0.0	6.5
YE_A	0.8	0.7	0.0	0.0	300.0	168.0	17.9	79.4	40.0	0.0	2.8	4480.0	368.0	264.0	0.0	0.0	4.5	6.5	0.8	0.8	0.8	0.0	3.4	10.0	0.0	5.3
YE_B	0.8	0.3	0.0	0.0	300.0	168.0	17.9	75.2	40.0	0.0	2.8	3980.0	376.0	234.0	0.0	0.0	4.3	5.2	0.7	0.7	0.7	0.0	1.7	10.0	0.0	4.9
HighAINHIB	72.5	79.9	1040.0	5200.0	1050.0	168.0	5262.5	1279.1	10.0	1.8	1.9	########	3660.0	4210.0	0.0	0.0	82.3	20.0	13.9	13.9	13.9	0.0	1858.2	9446.5	0.2	5.0
HighBINHIB	80.2	66.9	1040.0	5200.0	1050.0	168.0	5262.5	772.6	10.0	1.6	1.7	########	2600.0	447.0	0.0	0.0	45.1	45.8	7.5	7.5	7.5	0.0	1648.5	10371.9	0.2	6.1
Lact1	8.0	7.9	40.0	120.0	1050.0	168.0	182.5	772.6	10.0	0.8	2.1	13700.0	2600.0	1610.0	0.0	0.0	45.1	45.8	7.5	7.5	7.5	0.0	1.0	10.0	0.0	64.5
Lact2	6.6	8.0	40.0	120.0	1050.0	168.0	182.5	605.4	10.0	0.5	1.3	4620.0	236.0	400.0	0.0	0.0	37.1	43.1	6.2	6.2	6.2	0.0	1.0	10.0	0.0	44.7
LowA	0.8	0.6	8.6	43.2	300.0	168.0	61.1	81.9	40.0	1.4	4.1	64.6	696.0	400.0	0.0	0.0	4.9	3.8	0.8	0.8	0.8	0.0	3.1	10.0	0.0	11.8
LowB	0.8	0.4	8.6	43.2	300.0	168.0	61.1	77.9	40.0	1.4	4.1	48.7	0.0	70.0	0.0	0.0	4.8	2.5	0.8	0.8	0.8	0.0	1.9	10.0	0.1	11.6
LowC	1.0	1.2	8.6	43.2	300.0	168.0	61.1	105.8	40.0	1.1	3.3	32.9	27.5	52.0	0.0	0.0	5.9	7.0	1.0	1.0	1.0	0.0	1.4	10.0	0.1	14.9
But2	10.1	9.4	288.8	1444.0	1050.0	168.0	1506.5	998.6	10.0	1.5	1.8	18000.0	200.0	228.0	0.0	0.0	55.3	38.6	9.2	9.2	9.2	0.0	8429.7	4484.8	0.0	99.4
DCEAINHIB	59.5	66.8	240.0	1200.0	1050.0	168.0	1262.5	584.9	10.0	1.6	2.0	0.0	0.0	625000.0	0.0	0.0	37.4	6.2	0.0	0.0	18.7	0.0	11023.3	8623.0	0.2	1.1
DCEBINHIB	56.9	73.3	240.0	1200.0	1050.0	168.0	1262.5	581.7	10.0	1.4	1.8	0.0	0.0	550000.0	0.0	0.0	35.6	7.8	0.0	0.0	17.8	0.0	11432.3	8584.9	0.3	0.9
DCECINHIB	63.7	61.8	240.0	1200.0	1050.0	168.0	1262.5	723.4	10.0	1.4	2.7	0.0	0.0	599000.0	0.0	0.0	46.4	2.4	0.0	0.0	23.2	0.0	12655.3	9824.6	0.3	1.0
HalfbutA	17.4	26.8	40.0	200.0	1050.0	168.0	262.5	1522.1	11.1	0.3	0.7	40400.0	561.0	1590.0	0.0	0.0	84.6	145.0	14.2	14.2	14.2	0.0	755.8	10.0	0.0	48.4
HalfbutB	7.6	8.5	40.0	200.0	1050.0	168.0	262.5	673.9	11.1	0.7	1.7	15000.0	195.0	1230.0	0.0	0.0	39.3	50.6	6.6	6.6	6.6	0.0	208.2	10.0	0.0	58.2
HalfbutC	17.7	25.3	40.0	200.0	1050.0	168.0	262.5	1700.6	11.1	0.3	0.7	19500.0	481.0	3120.0	0.0	0.0	97.2	144.0	16.3	16.3	16.3	0.0	494.0	10.0	0.0	48.6
But1	4.9	4.7	160.0	800.0	1050.0	168.0	862.5	444.2	10.0	1.1	1.5	0.0	0.0	237.0	0.0	0.0	29.0	27.0	4.8	4.8	4.8	0.0	1027.4	10.0	0.0	92.0
PCEHigh2A	43.2	43.2	1040.0	5200.0	300.0	24.0	5325.0	348.3	1.2	3.0	3.4	77527.4	577.8	2363.2	0.0	0.0	141.0	141.0	23.7	23.7	23.7	0.0	1507.6	453.7	0.1	15.5
PCEHigh2B	38.5	38.5	1040.0	5200.0	300.0	24.0	5325.0	330.4	1.2	3.4	3.8	66725.7	751.2	777.9	0.0	0.0	133.0	133.0	22.3	22.3	22.3	0.0	1562.0	443.7	0.1	15.9
PCEHigh2C	46.5	46.5	1040.0	5200.0	300.0	24.0	5325.0	426.5	1.2	2.8	3.1	75049.9	724.3	3908.9	0.0	0.0	167.0	167.0	28.2	28.2	28.2	0.0	1636.8	398.5	0.1	21.4
TCEA	8.6	7.8	163.3	816.6	300.0	96.0	847.8	326.8	10.0	3.2	3.8	0.0	0.0	0.0	0.0	0.0	34.2	31.1	0.0	8.5	8.5	0.0	2224.5	17.8	0.0	59.1
TCEB	1.7	1.6	34.7	173.4	150.0	96.0	189.1	66.6	10.0	3.5	5.1	0.0	0.0	0.0	0.0	0.0	6.9	6.3	0.0	1.7	1.7	0.0	234.4	10.0	0.0	21.1
TCEC	0.4	0.4	8.1	40.4	150.0	96.0	56.0	13.9	10.0	3.9	11.4	0.0	0.0	0.0	0.0	0.0	1.5	1.5	0.0	0.4	0.4	0.0	14.9	10.0	0.0	9.2
TCED	5.9	1.7	163.3	816.6	300.0	96.0	847.8	222.8	10.0	2.7	3.2	0.0	0.0	0.0	0.0	0.0	23.5	6.8	0.0	5.9	5.9	0.0	1369.6	12.9	0.0	46.0
TCEE	1.8	1.8	34.7	173.4	150.0	96.0	189.1	71.8	10.0	3.3	4.8	0.0	0.0	0.0	0.0	0.0	7.4	7.1	0.0	1.8	1.8	0.0	210.9	10.0	0.0	25.6
TCEF	0.3	0.4	8.1	40.4	150.0	96.0	56.0	13.6	10.0	4.1	11.9	0.0	0.0	0.0	0.0	0.0	1.4	1.5	0.0	0.3	0.3	0.0	32.7	10.0	0.0	11.6
DCE2A	14.9	14.9	163.3	816.6	150.0	48.0	847.8	141.6	10.0	2.2	2.6	0.0	0.0	0.0	0.0	0.0	36.8	36.8	0.0	0.0	14.9	0.0	1131.1	10.0	0.2	23.1
DCE2B	4.4	4.8	34.7	173.4	150.0	96.0	189.1	85.7	10.0	2.0	3.0	0.0	0.0	0.0	0.0	0.0	8.9	9.6	0.0	0.0	4.4	0.0	308.4	10.0	0.1	20.6
DCE2C	1.1	1.1	8.1	40.4	150.0	96.0	56.0	20.8	10.0	1.9	5.5	0.0	0.0	0.0	0.0	0.0	2.3	2.3	0.0	0.0	1.1	0.0	29.6	10.0	0.0	7.3
DCE2D	16.2	13.2	163.3	816.6	300.0	96.0	847.8	320.4	10.0	2.6	3.0	0.0	0.0	0.0	0.0	0.0	32.4	26.3	0.0	0.0	16.2	0.0	3667.3	152.6	0.2	12.6
DCE2E	4.1	3.8	34.7	173.4	150.0	96.0	189.1	82.3	10.0	2.2	3.2	0.0	0.0	0.0	0.0	0.0	8.2	7.6	0.0	0.0	4.1	0.0	197.7	10.0	0.1	19.8
DCE2F	1.2	1.2	8.1	40.4	150.0	96.0	56.0	21.9	10.0	1.8	5.4	0.0	0.0	0.0	0.0	0.0	2.3	2.3	0.0	0.0	1.2	0.0	11.4	10.0	0.1	10.2
PCEA	4.2	4.4	49.2	246.2	300.0	96.0	277.5	226.6	10.0	1.5	2.5	886.0	92.6	142.5	0.0	0.0	25.1	26.3	4.2	4.2	4.2	0.0	4120.4	43.5	0.3	58.6
PCEB	0.7	0.9	10.5	52.3	150.0	96.0	67.9	42.2	10.0	1.9	4.8	915.2	104.6	0.0	0.0	0.0	4.4	5.2	0.7	0.7	0.7	0.0	3618.0	14.8	0.4	41.4
PCEC	0.1	0.2	2.4	12.2	150.0	96.0	27.8	9.2	10.0	2.3	17.1	975.6	0.0	0.0	0.0	0.0	1.0	1.3	0.2	0.2	0.2	0.0	4943.8	9.3	0.3	41.1
PCED	3.8	2.7	49.2	246.2	300.0	96.0	277.5	208.6	10.0	1.7	2.8	765.6	0.0	0.0	0.0	0.0	22.7	16.4	3.8	3.8	3.8	0.0	6825.2	82.1	0.5	49.2
PCEE	0.8	0.8	10.5	52.3	150.0	96.0	67.9	46.1	10.0	1.7	4.2	624.9	0.0	0.0	0.0	0.0	4.9	4.8	0.8	0.8	0.8	0.0	3810.0	13.5	0.5	44.6
PCEF	0.1	0.2	2.4	12.2	150.0	96.0	27.8	8.8	10.0	2.2	16.1	402.0	2.4	0.0	0.0	0.0	0.9	1.0	0.2	0.2	0.2	0.0	2849.3	8.8	0.5	39.6
H2B	1.7	1.7	10.0	10.0	0.0	36.0	10.0	34.8	12.0	0.7	0.7	148.0	1215.2	806.0	0.0	0.0	9.7	9.7	1.7	1.7	1.7	0.0	1.0	10.0	0.1	0.3
H2D	1.5	1.5	10.0	10.0	0.0	36.0	10.0	25.3	12.0	0.9	0.9	1823.9	4913.6	2768.4	0.0	0.0	7.3	7.3	1.4	1.4	1.4	0.0	1.0	10.0	0.1	0.3
CPA	0.3	0.4	4.0	20.0	150.0	72.0	40.8	0.0	28.6	1.5	9.2	0.0	0.0	14960.0	0.0	0.0	0.0	0.0	0.0	0.0	0.0	0.0	3.9	10.0	0.1	12.2
CPB	0.5	0.6	8.0	40.0	150.0	72.0	60.8	3.9	28.6	1.9	6.8	0.0	0.0	110000.0	13300.0	0.4	0.4	0.0	0.0	0.0	0.0	0.4	3.1	10.0	0.1	13.7
CPC	0.3	0.3	4.0	20.0	150.0	72.0	40.8	4.3	28.6	1.6	9.9	0.0	0.0	1760.0	12600.0	0.4	0.4	0.0	0.0	0.0	0.0	0.4	3.4	10.0	0.0	11.1
CPD	0.5	0.6	8.0	40.0	150.0	72.0	60.8	4.3	28.6	1.9	6.8	0.0	0.0	110000.0	12600.0	0.4	0.4	0.0	0.0	0.0	0.0	0.4	4.6	10.0	0.1	11.0

Appendix Table A2.2. Discrete experimental setup conditions and responses for the D2 mixed community data series. The Censoring Switches are highlighted grey when Cens = 1. The EA_Type (1=PCE, 2=TCE, 3=DCE, 4=Chlorophenol) and ED_Type (0=none, 1=Butyrate, 2= Lactacte, 3=Hydrogen, 4=Yeast Extract) are highlighted to represent the different conditions.

CPD	CPC	CPB	CPA	H2D	H2B	PCEF	PCEE	PCED	PCEC	PCEB	PCEA	DCE2F	DCE2E	DCE2D	DCE2C	DCE2B	DCE2A	TCEF	TCEE	TCED	TCEC	TCEB	TCEA		PCEHigh2C	PCEHigh2B	PCEHigh2A	But1	HalfbutC	HalfbutB	HalfbutA	DCECINHIB	DCEBINHIB	DCEAINHIB	But2	LowC	LowB	LowA	Lact2	Lact1	HighBINHIB	HighAINHIB	YE_B	YE_A	FYE_B	FYE_A	NoDonB	NoDonA	
1	1	1	1	1	1	1	1	1	1	1	1	1	1	1	1	1	1	1	1	1	1	1	1	CensEDRATE	1	1	1	1	1	1	1	1	1	1	1	1	1	1	1	1	1	1	1	1	1	1	0	0	CensEDRATE
0	0	0	0	1	1	1	1	1	1	1	1	0	0	0	0	0	0	0	0	0	0	0	0	CensSSPCE	1	1	1	0	1	1	1	0	0	0	1	1	1	1	1	1	1	1	1	1	1	1	1	1	CensSSPCE
0	0	0	0	1	1	1	0	0	0	1	1	0	0	0	0	0	0	0	0	0	0	0	0	CensSSTCE	1	1	1	0	1	1	1	0	0	0	1	1	0	1	1	1	1	1	1	1	1	1	1	1	CensSSTCE
0	0	0	0	1	1	0	0	0	0	0	1	0	0	0	0	0	0	0	0	0	0	0	0	CensSSDCE	1	1	1	1	1	1	1	1	1	1	1	1	1	1	1	1	1	1	1	1	1	1	1	1	CensSSDCE
1	1	1	0	1	1	1	1	1	1	1	1	1	1	1	1	1	1	1	1	1	1	1	1	CensRespnRate	1	1	1	1	1	1	1	1	1	1	1	1	1	1	1	1	1	1	1	1	1	1	1	1	CensRespnRate
0	0	0	0	1	1	1	1	1	1	1	1	0	0	0	0	0	0	0	0	0	0	0	0	CensPCErespn	1	1	1	1	1	1	1	0	0	0	1	1	1	1	1	1	1	1	1	1	1	1	1	1	CensPCErespn
0	0	0	0	1	1	1	1	1	1	1	1	0	0	0	0	0	0	1	1	1	1	1	1	CensTCErespn	1	1	1	1	1	1	1	0	0	0	1	1	1	1	1	1	1	1	1	1	1	1	1	1	CensTCErespn
0	0	0	0	1	1	1	1	1	1	1	1	1	1	1	1	1	1	1	1	1	1	1	1	CensDCErespn	1	1	1	1	1	1	1	1	1	1	1	1	1	1	1	1	1	1	1	1	1	1	1	1	CensDCErespn
1	1	1	1	0	0	1	1	1	1	1	1	1	1	1	1	1	1	1	1	1	1	1	1	CensAcetate	1	1	1	1	0	0	0	1	1	1	1	1	1	1	0	0	1	1	1	1	1	1	1	1	CensAcetate
0	0	0	0	0	0	1	1	1	1	1	1	0	0	1	0	0	0	0	0	1	0	0	1	CensButyrate	1	1	1	0	0	0	0	1	1	1	1	0	0	0	0	0	1	1	0	0	0	0	0	0	CensButyrate
1	1	1	1	0	0	0	0	0	0	0	0	0	0	0	0	0	0	0	0	0	0	0	0	CensSSDCP	0	0	0	0	0	0	0	0	0	0	0	0	0	0	0	0	0	0	0	0	0	0	0	0	CensSSDCP
1	1	1	0	0	0	0	0	0	0	0	0	0	0	0	0	0	0	0	0	0	0	0	0	CensSSMCP	0	0	0	0	0	0	0	0	0	0	0	0	0	0	0	0	0	0	0	0	0	0	0	0	CensSSMCP
0	0	0	0	0	0	0	0	0	0	0	0	0	0	0	0	0	0	0	0	0	0	0	0	CensSaturation	0	0	0	0	0	0	0	0	0	0	0	0	0	0	0	0	1	1	0	0	0	0	0	0	CensSaturation
0	0	0	0	0	0	0	0	0	0	0	0	0	0	0	0	0	0	0	0	0	0	0	0	CensINHIB	0	0	0	0	0	0	0	1	1	1	0	0	0	0	0	0	1	1	0	0	0	0	0	0	CensINHIB
0	0	0	0	0	0	0	0	0	0	0	0	0	0	0	0	0	0	0	0	0	0	0	0	CensDCEINHIB	0	0	0	0	0	0	0	1	1	1	0	0	0	0	0	0	0	0	0	0	0	0	0	0	CensDCEINHIB
1	1	1	1	0	0	0	0	0	0	0	0	0	0	0	0	0	0	0	0	0	0	0	0	CensDCPRespn	0	0	0	0	0	0	0	0	0	0	0	0	0	0	0	0	0	0	0	0	0	0	0	0	CensDCPRespn
4	4	4	4	1	1	1	1	1	1	1	1	3	3	3	3	3	3	2	2	2	2	2	2	EA_Type	1	1	1	1	1	1	1	3	3	3	1	1	1	1	1	1	1	1	1	1	1	1	1	1	EA_Type
1	1	1	1	3	3	1	1	1	1	1	1	1	1	1	1	1	1	1	1	1	1	1	1	ED_Type	1	1	1	1	1	1	1	1	1	1	1	1	1	1	2	2	1	1	4	4	4	4	0	0	ED_Type

Appendix Table A2.3. Network inference variation types run on the datasets.

Dataset	Inputted Data	Allowed Parent	Priors Run
D2	AI	1-to-1	BID
	AI	1-to-1	Gull
	AI1PC	1-to-1	BIC
	AI1PC	1-to-1	Gull
	Ratio	1-to-1	BIC
	Ratio	1-to-1	Gull
	AI	2-to-1	Gull
	AI1PC	2-to-1	Gull
	Ratio	2-to-1	Gull
KB-1™	Ratio	1-to-1	Gull
	Ratio	2-to-1	Gull

Appendix Table A2.4. Connection of discrete experimental setup modifiers to other variables in the D2 1-to-1 and 2-to-1 ensemble at a frequency > 500 for both ensembles

Discrete Variable	Probe Name	Probe Description	1-to-1 Frequency	2-to-1 Frequency
CensAcetate	COM02	*Syntrophomonas* 16S rRNA	968	900
	COM22	*Clostridia* 16S rRNA	968	900
	COM38	*Nitrospira* 16S rRNA	1000	999
CensDCEINHIB	DET0073	hypothetical protein	995	995
	DET0102	*mod* molybdopterin oxidoreductase, membrane subunit	569	855
	DET0103	*mod* molybdopterin oxidoreductase, iron-sulfur binding subunit	808	855
	DET0922	twitching mobility protein	999	847
CensDCErespn	DETtRNA	tRNA-Thr-1	1129	989
	DET0076	resolvase domain protein	847	905
	DET0077	hypothetical protein	1648	907
	DET0150	hypothetical protein	896	519
	DET0315	sensory box sensor histidine kinase	947	928
	DET0381	iron-sulfur cluster-binding protein, Rieske family	888	988
	DET0499	30S ribosomal protein S13	1157	1002
	DET0530	glucose-1-phosphate thymidylyltransferase	891	701
	DET0542	thioredoxin-disulfide reductase	678	962
	DET0590	glyceraldehyde-3-phosphate dehydrogenase, type I	916	759
	DET1034	hypothetical protein	882	985
	DET1035	tryptophan synthase subunit beta	915	977
	DET1085	major capsid protein, HK97 family	963	906
	DET1090	hypothetical protein	699	514
	DET1225	hypothetical protei	923	765
	DET1330	acetyltransferase, GNAT family	1852	1613
	DET1365	glutamyl-tRNA synthetase	918	863
	DET1417	phosphoribosylaminoimidazolecarboxamide formyltransferase/IMP cyclohydrolase	940	766
	DET1606	RecA	576	618
	DET1607	regulatory protein RecX	916	995
CensEDRATE	DET0616	hydrogenase maturation protease	998	978
	DET0750	50S ribosomal protein L20	625	544
	DET1002	glycosyl transferase, group 1 family protein	1011	983
	DET1005	transcriptional regulator, ArsR family	974	587
	DET1106	hypothetical protein	1000	642
	DET1214	hypothetical protein	760	621
	DET1534	reductive dehalogenase anchoring protein, putative	830	551
	DET1535	reductive dehalogenase, putative	830	549
	DET1570	*hyc* hydrogenase	1001	645
CensINHIB	COM24	*Clostridia* 16S rRNA	991	541
	COM47	*Bacteroides* 16S rRNA	994	747
	DET0097	iron dependent repressor, putative	1136	1809
	DET0111	*hup* [Ni/Fe] hydrogenase, group 1, small subunit	924	685
	DET0112	*hup* [Ni/Fe] hydrogenase, iron-sulfur cluster-binding subunit	923	691
	DET0115	ABC transporter, permease protein	945	610
	DET0451	malate dehydrogenase, NAD-dependent	910	591
CensPCErespn	COM36	*Spirochete* 16S rRNA	967	538
	DET0351	hypothetical protein	998	614
CensRespnRate	DET0867	*ech* hydrogenase	510	721
	DET0960	imidazoleglycerol phosphate synthase, cyclase subunit	924	844
	DET1082	hypothetical protein	844	992
	DET1116	sugar fermentation stimulation protein, putative	992	966
	DET1366	hypothetical protein	873	827
	DET1508	ISDet3, transposase orfA	624	627
	DET1509	(authentic point mutation)	623	646
CensSSDCE	DET0439	FtsK/SpoIIIE family protein	856	518
	DET0981	tRNA pseudouridine synthase B	943	1009
	DET1133	iron-sulfur cluster-binding protein	989	548
	DET1476	DNA binding domain, excisionase family	751	966
CensTCErespn	DET0657	nicotinate-nucleotide-dimethylbenzimidazole phosphoribosyltransferase	997	996

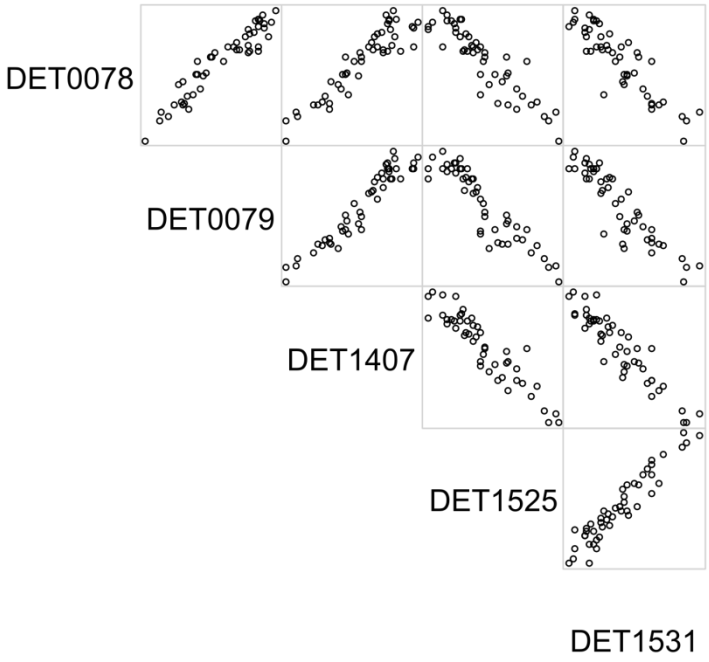

Appendix Figure A2.1. Scatterplot matrix displaying the similarity in relationships across transcripts. Values plotted are average intensities for the given transcript across (n = 49) microarray samples.

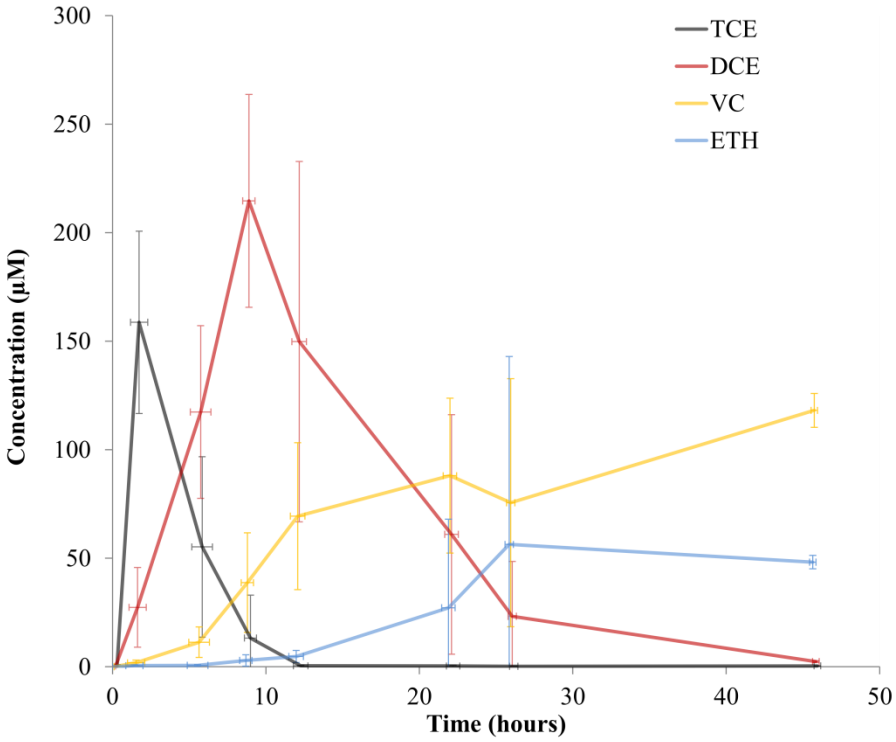

Appendix Figure A2.2. Chloroethene metabolite concentration for the KB-1™ time course experiment. Error bars represent the range across all cultures sampled at that time point.

APPENDIX III

Summary of Proteomic Analysis Methods

KB-1® Oxygen, Acid, and D2 Acid Series:

Urea Sample Digestion. Three groups of six samples (including D2 Acid Stress. (A1,A2,B1,B2,C1,C2), KB1 Acid Exposure (A1,A2,B1,B2,C1,C2), and KB1 O2 Stress (A1,A2,B1,B2,C1,C2)) were prepared for isobaric tag labeling. Cell pellets were resuspended in 9 M urea and vortexed into solution. Each sample was added to a barocycle pulse tube (Pressure Biosciences Inc., South Easton, MA) and barocycled for 10 cycles (20 seconds at 35,000 psi back down to ambient pressure for 10 seconds) for cell lysis. The sample was transferred to a centrifuge tube and spun at 5000 x g for 5 minutes to collect debris, transferred to a fresh tube and assayed with Bicinchoninic acid (BCA) (Thermo Scientific, Rockford, IL) to determine the protein concentration. The sample was then reduced with 10mM Dithiothreitol (DTT) (Sigma, St. Louis, MO) with incubation at 60˚C for 30 min with constant shaking at 800 rpm. Samples were then diluted 10-fold for preparation for digestion with 100 mM NH_4HCO_3 ; 1 mM $CaCl_2$ and sequencing-grade modified porcine trypsin (Promega, Madison, WI) was added to all protein samples at a 1:50 (w/w) trypsin-to-protein ratio for 3 h at 37˚C. The samples were cleaned using Discovery C18 50 mg/1 mL solid phase extraction tubes (Supelco, St.Louis, MO), using the following protocol: 3 mL of methanol was added for conditioning followed by 2 mL of 0.1% TFA in H2O. The samples were then loaded onto each column followed by 4mL of 95:5: H2O:ACN, 0.1% TFA. Samples were eluted with 1mL 80:20 ACN:H2O. The samples were concentrated down to ~30 µL using a Speed Vac and a final assay was performed to determine

the peptide concentration. An equal mass of each sample was aliquoted into fresh centrifuge tubes.

TMT Isobaric Tag labeling. Each set of 6 samples was labeled using amine-reactive Thermo Scientific Tandem Mass Tag (TMT) Isobaric Mass Tagging Kits (Thermo Scientific, Rockford, IL) according to the manufacture's instructions. Briefly, 41µL of anhydrous acetonitrile was added to each reagent (TMT 126 to 131), vortexed and allowed to dissolve for 5 minutes with occasional vortexing. Reagents were then added to the samples and incubated for 1 hour at room temperature. The reaction was quenched by adding 8µL of 5% hydroxylamine to the sample with incubation for 15 minutes at room temperature. The samples within each set were then combined and dried in the speed vac to volatilize the organics. Each of the 4 samples were then cleaned using Discovery C18 50 mg/1 mL solid phase extraction tubes as described above and once again assayed with Bicinchoninic acid to determine the final peptide concentration.

2D-LC-MS/MS analysis. The 2D-LC system was custom built using two Agilent 1200 nanoflow pumps and one 1200 capillary pump (Agilent Technologies, Santa Clara, CA), various Valco valves (Valco Instruments Co., Houston, TX), and a PAL autosampler (Leap Technologies, Carrboro, NC). Full automation was made possible by custom software that allows for parallel event coordination providing near 100% MS duty cycle through use of two trapping and analytical columns. All columns were manufactured at EMSL by slurry packing media into fused silica (Polymicro Technologies Inc., Phoenix, AZ) using a 1 cm sol-gel frit for media retention. First dimension SCX column; 5-µm PolySULFOETHYL A (PolyLC Inc.,

Columbia, MD), 15-cm x 360 µm outer diameter (o.d.) x 150 µm inner diameter (i.d.) Trapping columns; 5-µm Jupiter C18 (Phenomenex, Torrence, CA), 4 cm x 360 µm o.d. x 150 µm i.d. Second dimension reversed-phase columns; 3-µm Jupiter C18 (Phenomenex, Torrence, CA), 35-cm x 360 µm o.d. x 75 µm i.d. Mobile phases consisted of 0.1 mM NaH_2PO_4 (A) and 0.3 M NaH_2PO_4 (B) for the first dimension and 0.1% formic acid in water (A) and 0.1% formic acid in acetonitrile (B) for the second dimension.

MS analysis was performed using a LTQ Orbitrap Velos ETD mass spectrometer (Thermo Scientific, San Jose, CA) fitted with a custom electrospray ionization (ESI) interface. Electrospray emitters were custom made using 150 µm o.d. x 20 µm i.d. chemically etched fused silica (2). The heated capillary temperature and spray voltage were 275°C and 2.2 kV, respectively. Data was acquired for 100 min, beginning 65 min after sample injection and 15 min into gradient. Orbitrap spectra (AGC 1x106) were collected from 400-2000 m/z at a resolution of 60k followed by data dependent ion trap CID MS/MS (collision energy 35%, AGC 3x104) of the ten most abundant ions. A dynamic exclusion time of 60 sec was used to discriminate against previously analyzed ions.

Data Analysis. MS/MS data was searched using SEQUEST against a peptide database constructed from a series of isolate genomes and metagenomic datasets, using relatively conservative filters [Xcorr values of 1.9 (+1), 2.2 (+2), and 3.5 (+3)]. The following genomic data was used in these searches: *Dehalococcoides* sp. CBDB1, *Dehalococcoides mccartyi* 195, *Dehalococcoides* str. KB-1, *Geobacter lovleyi*, *Methanoregula boonei*, *Methanosaeta thermophila*, *Methanospirillum hungatei*, PCEDH *Dehalococcoides* metagenome from D2,

PCEOT others metagenome from D2, *Spirochaeta thermophila*, *Sporomusa* str. KB1, *Syntrophomonas wolfei,* and *Syntrophus aciditrophicus*. Resulting peptide identifications were filtered using an MSGF cutoff value to 1 e-10 (3). TMT ion intensities, acquired using the tool MASIC (MS/MS Automated Selected Ion Chromatogram), were used to measure relative peptide abundance. The intensity associated with each reporter ion is proportional to the contribution of each of the component samples to the total peptide abundance. Aggregation of the relative abundance measurements can be used to measure the regulation of each of the identified proteins.

D2 Oxygen Series:

Urea Sample Digestion. Six D2 samples (including two controls with no O2 stress (1A and 1B), two with 6 hours of O2 exposure (2A and 2B) and two at 48 hours post O2 exposure (recovered) (3A and 3B) were prepared for digestion and fractionation. The cell pellets were resuspended in 9M urea and vortexed into solution. Each sample was added to a barocycle pulse tube (Pressure Biosciences Inc., South Easton, MA) and barocycled for 10 cycles (20 seconds at 35,000 psi back down to ambient pressure for 10 seconds) for cell lysis. The samples were then transferred to a centrifuge tubes and spun at 5000xg for 5 minutes to collect debris, transferred to a fresh tube and assayed with bicinchoninic acid (BCA) (Thermo Scientific, Rockford, IL) to determine the protein concentration. The samples were then reduced with 10mM dithiothreitol (DTT) (Sigma, St. Louis, MO) with incubation 60˚C for 30 minutes with constant shaking at 800rpm. Samples were then diluted 10-fold for preparation for digestion with 100mM NH_4HCO_3 ; 1mM $CaCl_2$ and sequencing-grade modified porcine trypsin (Promega, Madison, WI) was added to all protein samples at a 1:50 (w/w) trypsin-to-protein ratio for 3 h at 37˚C. The samples

were cleaned using Discovery C18 50 mg/1 mL solid phase extraction tubes (Supelco, St.Louis, MO), using the following protocol: 3 mL of methanol was added for conditioning followed by 2 mL of 0.1% TFA in H_2O. The samples were then loaded onto each column followed by 4mL of 95:5: H_2O:ACN, 0.1% TFA. Samples were eluted with 1mL 80:20 ACN:H_2O. The samples were concentrated down to ~30µL using a Speed Vac and a final BCA assay was performed to determine the peptide concentration.

HPLC fractionation. Each sample was diluted to a volume of 930 µL with 10 mm ammonium formate buffer (pH 10.0), and resolved on a XBridge C18, 250x4.6 mm, 5 µM with 4.6x20 mm guard column (Waters, Milford, MA). Separations were performed at 0.5 mL/min using an Agilent 1100 series HPLC system (Agilent Technologies, Santa Clara, CA) with mobile phases (A) 10 mM Ammonium Formate, pH 10.0 and (B) 10 mM Ammonium Formate, pH 10.0/acetonitrile (10:90). The gradient was adjusted from at 100% A to 95% A over the first 10 min, 95% A to 65% A over minutes 10 to 70, 65% A to 30% A over minutes 70 to 85, maintained at 30% A over minutes 85 to 95, re-equilibrated with 100% A over minutes 95 to 105, and held at 100% A until minute 120. Fractions were collected every 1.25 minutes (96 fractions over the entire gradient) and every 24th fraction was combined for a total of 24 samples (each with n=4 fractions pooled) for each of the 6 LC runs. All fractions were dried under vacuum and 35 µL of 25 mM ammonium bicarbonate, pH 8.0 was added to each fraction for storage at -20°C until LC-MS/MS analysis.

From each collected fraction, peptides were analyzed by reversed phase high-performance LC separation coupled with the use of a Velos Orbitrap mass spectrometer

(ThermoFisher Scientific, San Jose, CA, USA) operated in a data-dependent MS-MS mode.

Additional information for Data Analysis section. Peptide relative abundances were inferred from spectral counts. Raw spectral counts were normalized using the NSAF technique that accounts for differences in protein length and protein loading biases (1).

REFERENCES

1. Kelly RT, Page JS, Luo Q, Moore RJ, Orton DJ, et al. (2006) Chemically Etched Open Tubular and Monolithic Emitters for Nanoelectrospray Ionization Mass Spectrometry. Anal Chem 78: 7796-7801.

2. Kim S, Gupta N, Pevzner PA (2008) Spectral Probabilities and Generating Functions of Tandem Mass Spectra: A Strike against Decoy Databases. J Prot Res 7: 3354-3363.

3. Zybailov, B., Mosley, A.L., Sardiu, M.E., Coleman, M.K., Florens, L., Washburn, M.P. (2006). Statistical analysis of membrane proteome expression changes in *Saccharomyces cerevisiae*. J. Proteome Research 5: 2339–2347

APPENDIX IV

Summary of Stressed Experimental Series

High Rate D2 continuous PCE fed. A total of nine 100 mL subcultures of D2 were established for PCE high feeding rate comparisons. Butyrate was provided in an excess amount needed for PCE reduction to serve as the electron donor and carbon source. Three sets of triplicate cultures were continuously fed 64.5 µM/hr PCE (neat) with 260.1 µM/hr butyrate, 10.0 µM/hr PCE (neat) with 10.0 µM/hr butyrate, and 45.0 µM/hr PCE (in saturated media) with 260 µM/hr butyrate via syringe pump. The first set of triplicates fed at the high rate was purged every 24 hours. The triplicate sets were sacrificed for analysis at 166, 166, and 24 hours, respectively.

High Rate D2 continuously cis-DCE fed. Three 100 mL subcultures of D2 were continuously fed 31.1 µM/hr cis-DCE (neat) and 60.1 µM/hr butyrate (to serve as the electron donor and carbon source) via syringe pump. After 48 hours, cultures were purged every 24 hours to remove accumulating cis-DCE. The three cultures were sacrificed at 165 hours for analysis.

No electron donor added to D2 continuous PCE fed. Six 100 mL subcultures of D2 were continuously fed 0.8 µM/hr PCE (in saturated media). Two cultures did not receive an electron donor, two received a 100 µl pulse of 5 g/L yeast extract every 120 hours, and two received a 100 µl pulse of 5 g/L fermented yeast extract every 100 hours. Three additional cultures were continuously fed 1.2 µM/hr PCE (in saturated media) and 2.16 µM/hour butyrate. The nine cultures were sacrificed at 166 hours for analysis.

Oxygen addition to D2 continuously fed PCE. Six 100 mL subcultures of D2 were continuously fed 0.50 µM/hr PCE (in saturated media) and 6.48 µM/hr butyrate (to serve as the carbon source and electron donor). After 24 hours, 3.42 mg of oxygen (99+% AIRGas) was added to four out of the six cultures. One culture with no oxygen added (to serve as control) was sacrificed for nucleic acid and protein extraction. At 30 hours, two of the cultures treated with oxygen were sacrificed. After 74 hours, the remaining two oxygen exposed cultures and one non-oxygen exposed control-culture were sacrificed for analysis.

Acid amendment to D2 continuously fed PCE. Six 100 mL subcultures of D2 were continuously fed 0.20 µM/hr PCE-saturated media with 3.5 µM/hr acetate (acetate serves as the carbon source). Additionally, 6 mL of hydrogen gas (AirGas) was added to serve as the electron donor and re-spiked throughout the experiment to maintain the concentration of hydrogen above detectable levels on the TCD. After 13 hours, 1.25 mL of 5 mM of HCl was added to four out of the six cultures to lower the pH from 7 to ~5.3. At 17 hours, two of the low pH cultures and one neutral pH culture (to serve as control) were sacrificed for nucleic acid and protein extraction. At 22 hours, the remaining cultures had to be vented to release excess pressure built. After 72 hours, the final three cultures (1 control and 2 HCl low pH) were sacrificed for analysis.

Acid addition to KB-1^{TM} continuously fed TCE. Six 100 mL subcultures of KB-1^{TM} were continuously fed 0.60 µM/hr TCE with 19.3 µM/hr acetate and batch fed 6 mL hydrogen as previously described (Heavner *et al.* 2012, in review). Approximately 20 hours after establishing the continuous feed, HCl (12N, Fisher Scientific) was added to lower the pH from 7 to ~5.3 to four out of the six cultures. One culture was sacrificed for nucleic acid and protein extraction to

serve as the first control. Approximately 10 hours later, at the 34 hour total experimental time mark, two low pH cultures were sacrificed. Approximately 14 hours later, at the 48 hour total experimental time mark, the final two low pH cultures and the remaining neutral culture (serving as the full experimental control) were sacrificed for analysis.

Oxygen addition to KB-1^{TM} batch TCE fed. Six 100 mL subcultures of KB-1^{TM} were batch-fed 220 µM TCE, 4 mM acetate, and 6 mL hydrogen as previously described (Heavner *et al.* 2012, in review). Approximately 24 hours later, the cultures were purged, re-fed with the same dose as the starter, and 3.14 mg of oxygen was added to four of the six cultures. One culture was sacrificed for nucleic acid and protein extraction to serve as the first control. Approximately 6 hours later, at the 30 hour total experimental time mark, two oxygen exposed cultures were sacrificed for analysis. Approximately 60 hours later, at the 92 hour total experimental time mark (70 hours post oxygen addition), the final two cultures that received a spike of oxygen and the remaining no oxygen added control culture (serving as the full experimental control) were sacrificed for analysis.

1,1,1-Trichloroethane addition to KB-1^{TM} batch TCE fed. Six 100 mL subcultures of KB-1^{TM} were batch-fed 220 µM TCE, 4 mM acetate acetate, and 6 mL hydrogen. Approximately 24 hours later, one culture was sacrificed for nucleic acid and protein extraction to serve as the first control. The remaining 5 cultures were purged, re-fed with the same dose as the starter, and 220 uM 1,1,1-trichloroethane (TCA) was added to 4 out of 5 remaining cultures. Approximately 6 hours later, at the 30 hour total experimental time mark, two cultures that were spiked with 1,1,1-TCA were sacrificed for analysis. Approximately 42 hours later, at the 72 hour total

experimental time mark, the final two cultures spiked with 1,1,1-TCA and the remaining no 1,1,1-TCA added culture (serving as the full experimental control) were sacrificed for analysis.

APPENDIX V

Supporting Figures and Tables for Chapter 4

Figure A5.1. Dechlorination profiles showing chloroethenes' (TCE, DCE, VC) and ethene's (ETH) total amount detected normalized to liquid culture volume for the KB-1^{TM} cultures batch fed 220 µM TCE for the entire experiment. Experiment titles for the samples indicate the time the cultures were sacrificed after the TCA stressor was added. Cultures sampled at 24 hours and 40 hours as a control (a,b); 17 hours post trichloroethane (TCA) amendment (c,d), and 48 hour post TCA addition (e,f). Data labels indicate the specific metabolites. The red bar denotes the time of 22 µM TCA addition (added to the stress cultures after 20 hours from start of experiment).

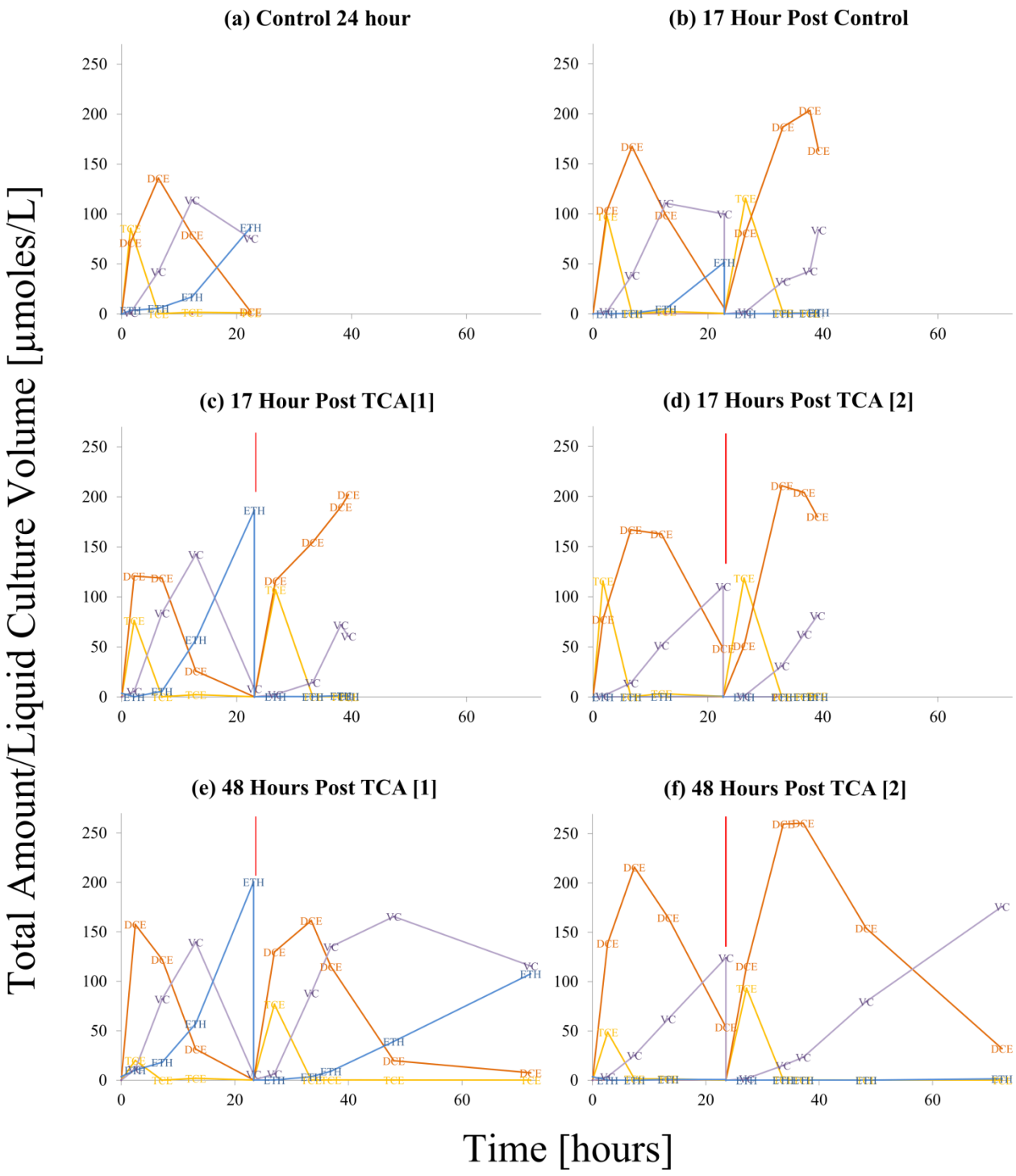
(a) Control 24 hour
(b) 17 Hour Post Control
(c) 17 Hour Post TCA[1]
(d) 17 Hours Post TCA [2]
(e) 48 Hours Post TCA [1]
(f) 48 Hours Post TCA [2]
Total Amount/Liquid Culture Volume [µmoles/L]
Time [hours]
DCE
TCE
VC
ETH
0
20
40
60
50
100
150
200
250

Table A5.1. Full table of all transcripts differentially regulated in the TCA 17 hour versus

Table A5.1 (Continued)

DMC#	Probe ID	Strain	Description	Ratio of 17 hour Post TCA Added versus	17 hour Post TCA Added Average Intensity (pfu)	Controls Average Intensity (pfu)
DMC1887	KB1_0047	-	hypothetical protein	48 ± 12	132122 ± 32441	2741 ± 3
DMC1260	panDhc_3290_RC	Pinellas	fasciclin domain protein	35 ± 7.5	30300 ± 5594	876 ± 100
DMC0924	KB1_0941	-	heat shock protein Hsp20	26 ± 21	53068 ± 8478	2049 ± 1592
DMC0924	gi147669481	Pinellas	heat shock protein Hsp20	25 ± 20	52967 ± 8874	2139 ± 1698
DMC1736	panDhc_346	Pinellas	extracellular solute-binding protein family 5	24 ± 23	18549 ± 2564	774 ± 721
DMC1264	panDhc_4045_RC	Pinellas	hypothetical protein	24 ± 13	17324 ± 3626	723 ± 359
DMC1264	VS1089	Pinellas	hypothetical protein	24 ± 6.7	8865 ± 2384	376 ± 35
DMC1264	panDhc_4120_RC	Pinellas	hypothetical protein	23 ± 10	16254 ± 3125	707 ± 280
DMC1207	panDhc_4028_RC	Pinellas	hypothetical protein	21 ± 13	26670 ± 4361	1256 ± 742
DMC1894	panDhc_606_RC	Pinellas	putative reductive dehalogenase	21 ± 8.9	28089 ± 7979	1339 ± 423
DMC1748	panDhc_1475_RC	Pinellas	hypothetical protein	18 ± 5.5	7168 ± 1351	390 ± 91
DMC1207	panDhc_4028	Pinellas	hypothetical protein	16 ± 11	30638 ± 5765	1890 ± 1197
DMC1523	KB1_0098	-	antioxidant, AhpC	16 ± 3.3	60515 ± 9531	3735 ± 472
DMC1264	panDhc_4120	Pinellas	protein of unknown function DUF1508	14 ± 8.0	25383 ± 7497	1834 ± 906
DMC1260	panDhc_3290	Pinellas	fasciclin domain protein	13 ± 4.7	24844 ± 2955	1968 ± 701
DMC0925	panDhc_1808	Pinellas	Rubrerythrin	13 ± 4.0	34251 ± 5101	2734 ± 776
DMC1523	panDhc_2442_RC	Unassigned	antioxidant, AhpC	11 ± 3.3	34682 ± 8127	3101 ± 550
DMC1210	VS1037	Unassigned	hypothetical protein	11 ± 9.2	32242 ± 1238	3041 ± 2651
DMC1487	panDhc_3740_RC	Unassigned	reductive dehalogenase anchoring protein	10 ± 5.0	38237 ± 3654	3666 ± 1731
DMC1488	panDhc_506_RC	Pinellas	putative reductive dehalogenase	10 ± 6.9	134473 ± 32755	13156 ± 8314
DMC0128	VS141	Pinellas	hypothetical protein	9.9 ± 2.9	1269 ± 258	128 ± 27
DMC1243	panDhc_1744	Pinellas	peptidase S1 and S6 chymotrypsin/Hap	9.7 ± 2.7	2862 ± 745	297 ± 31
DMC1488	panDhc_506	Pinellas	putative reductive dehalogenase	9.5 ± 5.6	132030 ± 34076	13943 ± 7340
DMC1407	gi147669899	Pinellas	putative ribosomal subunit interface protein	9.3 ± 5.0	9466 ± 1899	1019 ± 513
DMC1893	panDhc_3729	Pinellas	putative reductive dehalogenase anchoring protein	9.3 ± 4.6	8005 ± 2202	863 ± 359
DMC1482	panDhc_1026	Pinellas	sensor histidine kinase	9.2 ± 4.8	3854 ± 830	420 ± 199
DMC1487	KB1_0071	-	putative reductive dehalogenase anchoring protein	9.1 ± 5.8	204127 ± 46745	22429 ± 13419
DMC0877	KB1_0894	-	hypothetical protein	9.1 ± 4.0	7584 ± 2114	836 ± 282
DMC1561	panDhc_781	Pinellas	hypothetical protein	9.0 ± 6.5	7638 ± 1332	851 ± 594
DMC1407	KB1_1446	-	putative ribosomal subunit interface protein	8.9 ± 5.1	9527 ± 1663	1076 ± 587
DMC1872	panDhc_29_RC	Pinellas	sensor histidine kinase/response regulator	8.8 ± 3.5	11055 ± 3000	1263 ± 373
DMC0877	gi147669435	Pinellas	hypothetical protein	8.5 ± 3.4	7162 ± 1879	840 ± 249
DMC0877	GT_c720662	-	hypothetical protein	8.4 ± 3.3	7424 ± 1952	879 ± 254
DMC0716	KB1_0740	-	short-chain dehydrogenase/reductase SDR	8.1 ± 3.6	17525 ± 4290	2173 ± 799
DMC1722	panDhc_2312	Pinellas	phosphoribosyltransferase	7.8 ± 3.5	7228 ± 1703	932 ± 360
DMC0973	panDhc_1864_RC	Pinellas	hypothetical protein	7.4 ± 3.9	5067 ± 1113	681 ± 323
DMC1306	panDhc_2290_RC	Pinellas	DNA-binding response regulator, LuxR family	7.4 ± 5.1	3071 ± 258	414 ± 282
DMC0892	panDhc_1190_RC	Pinellas	twitching motility protein	7.3 ± 4.3	5599 ± 344	770 ± 456
DMC1210	KB1_1234	-	hypothetical protein	7.3 ± 3.2	44063 ± 4666	6062 ± 2604
DMC1403	panDhc_1712	Unassigned	hypothetical protein	7.2 ± 4.6	16251 ± 3779	2262 ± 1347
DMC0328	gi57234914	-	putative DNA-binding protein	7.2 ± 4.7	13828 ± 3670	1928 ± 1168
DMC0172	panDhc_2578_RC	Pinellas	hypothetical protein	7.1 ± 5.1	11145 ± 1234	1577 ± 1130
DMC1305	panDhc_3905_RC	Unassigned	DNA-binding protein, excisionase family	7.0 ± 3.8	11315 ± 1175	1618 ± 869
DMC1523	VS1460	Unassigned	peroxiredoxin-like protein	7.0 ± 1.9	9047 ± 2026	1296 ± 216
DMC1210	gi147669705	Unassigned	hypothetical protein	6.9 ± 3.1	45681 ± 5231	6592 ± 2829
DMC1306	panDhc_2290	Pinellas	DNA-binding response regulator, LuxR family	6.9 ± 3.9	2582 ± 371	374 ± 205
DMC0172	KB1_0304	-	hypothetical protein	6.8 ± 4.3	7423 ± 867	1086 ± 665
DMC0128	KB1_0276	-	hypothetical protein	6.8 ± 1.0	14043 ± 75	2078 ± 312
DMC1895	panDhc_2870	Pinellas	transcriptional regulator, MarR family	6.7 ± 4.0	1352 ± 145	201 ± 117
DMC1402	KB1_1441	-	ribosomal protein L25 (General stress protein Ctc)	6.7 ± 5.6	36888 ± 2456	5501 ± 4614
DMC0973	panDhc_1864	Pinellas	hypothetical protein	6.7 ± 4.1	3481 ± 503	520 ± 307
DMC1736	panDhc_346_RC	Pinellas	extracellular solute-binding protein family 5	6.6 ± 5.6	7866 ± 768	1185 ± 993
DMC1878	panDhc_4_RC	Pinellas	sensor histidine kinase/response regulator	6.6 ± 3.3	2418 ± 641	368 ± 155
DMC0716	panDhc_1914	Pinellas	short-chain dehydrogenase/reductase SDR	6.5 ± 2.4	13315 ± 3223	2045 ± 573
DMC1242	KB1_1265	-	serine protease, DegP	6.5 ± 4.2	10621 ± 2522	1637 ± 984
DMC0128	gi147668886	Pinellas	hypothetical protein	6.4 ± 0.86	15584 ± 369	2422 ± 320
DMC1024	panDhc_18_RC	Pinellas	sensor histidine kinase	6.4 ± 4.3	1809 ± 181	284 ± 187
DMC1402	panDhc_2386_RC	Pinellas	ribosomal protein L25 (General stress protein Ctc)	6.3 ± 5.4	23374 ± 2667	3702 ± 3159
DMC0094	KB1_0239	-	hypothetical protein	6.3 ± 5.1	38668 ± 8015	6126 ± 4738
DMC0112	panDhc_2375_RC	Pinellas	transcriptional regulator, TetR family	6.2 ± 1.3	2327 ± 90	373 ± 76
DMC2379	gi147669941	Unassigned	reductive dehalogenase related	6.2 ± 1.9	139773 ± 28188	22592 ± 5032
DMC0094	panDhc_3579	Pinellas	hypothetical protein	6.0 ± 3.9	5717 ± 1446	958 ± 572
DMC0821	panDhc_1908_RC	Pinellas	biotin-acetyl-CoA-carboxylase ligase	5.9 ± 4.2	2157 ± 402	366 ± 250
DMC2365	panDhc_2	Pinellas	hypothetical protein	5.8 ± 1.5	5895 ± 646	1012 ± 228
DMC0884	KB1_0901	-	hypothetical protein	5.8 ± 2.0	8630 ± 2083	1490 ± 376
DMC1900	KB1_1468	-	putative reductive dehalogenase	5.8 ± 3.4	3481 ± 446	605 ± 346
DMC0905	panDhc_2384_RC	Pinellas	endonuclease III	5.7 ± 4.3	1916 ± 281	334 ± 245
DMC1243	panDhc_1744_RC	Unassigned	peptidase S1 and S6 chymotrypsin/Hap	5.6 ± 1.2	4146 ± 835	740 ± 34
DMC2042	panDhc_2692_RC	Pinellas	hypothetical protein	5.4 ± 2.5	1907 ± 93	352 ± 160
DMC2127	panDhc_3283	Pinellas	ferric uptake regulator, Fur family	5.4 ± 3.2	1537 ± 97	285 ± 168

Table A5.1 (Continued)

DMC#	Probe ID	Strain	Description	Ratio of 17 hour Post TCA Added versus	17 hour Post TCA Added Average Intensity (pfu)	Controls Average Intensity (pfu)
DMC1736	KB1_1110	-	extracellular solute-binding protein family 5	5.4 ± 3.4	19612 ± 3192	3652 ± 2264
DMC1523	panDhc_2442	Pinellas	antioxidant, AhpC	5.3 ± 2.3	59312 ± 11230	11236 ± 4398
DMC1305	KB1_1335	-	DNA-binding protein, excisionase family	5.2 ± 1.7	9241 ± 1063	1765 ± 531
DMC0734	panDhc_632	Pinellas	hypothetical protein	5.2 ± 5.2	19353 ± 2333	3738 ± 3699
DMC1402	panDhc_2386	Pinellas	ribosomal protein L25 (General stress protein Ctc)	5.1 ± 4.4	3129 ± 228	609 ± 524
DMC2141	panDhc_3104	Pinellas	hypothetical protein	5.1 ± 3.6	2844 ± 603	554 ± 369
DMC2042	KB1_1299	-	hypothetical protein	5.0 ± 3.0	2374 ± 28	471 ± 282
DMC2365	KB1_1145	-	hypothetical protein	4.9 ± 3.2	1807 ± 78	370 ± 240
DMC1011	KB1_1096	-	hypothetical protein	4.9 ± 3.5	10973 ± 994	2260 ± 1598
DMC0905	panDhc_2384	Pinellas	endonuclease III	4.7 ± 3.7	1807 ± 309	383 ± 292
DMC1011	gi147669570	Unassigned	hypothetical protein	4.6 ± 3.3	10288 ± 589	2213 ± 1584
DMC1445	panDhc_2878	Unassigned	hypothetical protein	4.6 ± 2.7	3831 ± 254	827 ± 474
DMC1564	gi147670007	Unassigned	hypothetical protein	4.5 ± 1.0	13009 ± 662	2880 ± 637
DMC1018	panDhc_2262	Pinellas	two component transcriptional regulator	4.5 ± 2.2	1219 ± 55	270 ± 129
DMC1011	GT_843758	-	hypothetical protein	4.5 ± 3.3	11059 ± 918	2471 ± 1809
DMC1905	panDhc_1410_RC	Pinellas	hypothetical protein	4.3 ± 0.68	1174 ± 88	272 ± 38
DMC1446	KB1_1483	-	flavodoxin/nitric oxide synthase	4.3 ± 2.9	1085 ± 15	255 ± 175
DMC1305	panDhc_3905	Pinellas	DNA-binding protein, excisionase family	4.2 ± 1.4	3084 ± 90	728 ± 241
DMC1446	GT_1138048-1138482	-	flavodoxin/nitric oxide synthase	4.2 ± 2.9	971 ± 70	230 ± 155
DMC1307	panDhc_131_RC	Pinellas	type II secretion system protein GspE	4.2 ± 3.3	1895 ± 247	450 ± 344
DMC1400	panDhc_3305	Pinellas	hypothetical protein	4.2 ± 1.5	14584 ± 389	3500 ± 1286
DMC1193	panDhc_3425_RC	Pinellas	hypothetical protein	4.2 ± 2.3	2331 ± 498	561 ± 290
DMC0171	KB1_0303	-	histidine kinase	4.1 ± 2.0	1016 ± 158	246 ± 115
DMC1445	panDhc_2878_RC	Unassigned	hypothetical protein	4.1 ± 2.6	3611 ± 222	882 ± 563
DMC1446	gi147669930	Unassigned	flavodoxin/nitric oxide synthase	4.1 ± 3.0	1048 ± 35	257 ± 191
DMC2298	panDhc_2462	Pinellas	transcriptional regulator, XRE family	4.0 ± 2.6	1216 ± 29	301 ± 195
DMC1193	panDhc_3425	Pinellas	hypothetical protein	4.0 ± 2.2	2428 ± 500	605 ± 304
DMC0820	panDhc_1897_RC	Pinellas	band 7 protein	4.0 ± 0.28	1668 ± 92	416 ± 17
DMC1899	KB1_0059	-	reductive dehalogenase anchoring protein, putative	4.0 ± 2.5	1689 ± 158	423 ± 266
DMC1716	panDhc_2742_RC	Pinellas	hypothetical protein	4.0 ± 3.2	3907 ± 254	985 ± 785
DMC1765	panDhc_3076_RC	Pinellas	large conductance mechanosensitive channel protein	4.0 ± 0.83	1281 ± 47	324 ± 67
DMC1895	panDhc_2870_RC	Pinellas	transcriptional regulator, MarR family	3.9 ± 0.36	2104 ± 188	533 ± 10
DMC1487	panDhc_3708	Cornell	reductive dehalogenase anchoring protein, putative	3.9 ± 0.46	35080 ± 2292	8885 ± 854
DMC1561	panDhc_781_RC	Pinellas	hypothetical protein	3.9 ± 2.0	6138 ± 568	1555 ± 783
DMC1445	KB1_1482	-	hypothetical protein	3.9 ± 2.3	2670 ± 247	686 ± 397
DMC1905	panDhc_1404	Pinellas	hypothetical protein	3.9 ± 0.73	1006 ± 73	259 ± 45
DMC1564	VS1506	Unassigned	hypothetical protein	3.8 ± 0.39	8794 ± 398	2285 ± 207
DMC0125	panDhc_3396_RC	Pinellas	response regulator receiver protein	3.8 ± 2.9	5394 ± 352	1403 ± 1048
DMC2298	panDhc_2462_RC	Pinellas	transcriptional regulator, XRE family	3.8 ± 2.7	1575 ± 30	414 ± 298
DMC1242	panDhc_1001_RC	Unassigned	serine protease, DegP	3.8 ± 2.5	2924 ± 13	780 ± 525
DMC0820	KB1_0861	-	band 7 protein	3.7 ± 1.9	25292 ± 846	6745 ± 3324
DMC0222	gi147668777	Pinellas	hypothetical protein	3.6 ± 2.6	977 ± 105	270 ± 195
DMC0881	panDhc_1037_RC	Pinellas	peptidase M29, aminopeptidase II	3.6 ± 0.70	3615 ± 668	1017 ± 67
DMC2042	panDhc_2692	Pinellas	hypothetical protein	3.5 ± 1.4	1129 ± 25	319 ± 129
DMC1876	panDhc_2456_RC	Pinellas	hypothetical membrane protein	3.5 ± 2.2	4175 ± 5	1182 ± 720
DMC2186	KB1_0094	-	transcriptional regulator, TetR family	3.5 ± 1.2	912 ± 152	259 ± 77
DMC0222	GT_c255974-255717	-	hypothetical protein	3.5 ± 2.2	968 ± 78	276 ± 172
DMC1351	panDhc_1202_RC	Pinellas	glycerol-3-phosphate dehydrogenase,NAD-dependent	3.5 ± 0.55	20835 ± 992	5976 ± 906
DMC1095	KB1_1132	-	putative O-acetylserine(thiol)-lyase-A related protein	3.4 ± 2.2	1582 ± 131	459 ± 292
DMC1490	panDhc_1798	Pinellas	prephenate dehydratase	3.4 ± 1.7	7998 ± 911	2348 ± 1148
DMC0222	KB1_0342	-	hypothetical protein	3.4 ± 2.2	950 ± 73	281 ± 181
DMC1564	KB1_0142	-	hypothetical protein	3.4 ± 0.97	13153 ± 1286	3920 ± 1063
DMC1397	KB1_1437	-	membrane transporter, MarC family	3.3 ± 1.3	2135 ± 272	643 ± 235
DMC1563	VS1505	Unassigned	desulfoferrodoxin Dfx domain protein	3.3 ± 0.36	27144 ± 2269	8193 ± 557
DMC1616	panDhc_3413	Pinellas	hypothetical protein	3.3 ± 0.82	7885 ± 1590	2407 ± 354
DMC0133	panDhc_1697_RC	Pinellas	phosphate binding protein	3.2 ± 1.5	1080 ± 138	333 ± 149
DMC1372	GT_1079521-1079769	-	hypothetical protein	3.2 ± 0.60	2890 ± 274	894 ± 141
DMC1563	panDhc_4087_RC	Pinellas	putative desulforedoxin	3.2 ± 0.66	17818 ± 2469	5597 ± 870
DMC2186	gi147669964	Unassigned	transcriptional regulator, TetR family	3.2 ± 1.4	945 ± 176	297 ± 116
DMC1372	KB1_1410	-	hypothetical protein	3.1 ± 0.54	2869 ± 330	915 ± 118
DMC1372	gi147669866	Pinellas	hypothetical protein	3.1 ± 0.70	2801 ± 155	895 ± 195
DMC0112	panDhc_2375	Unassigned	transcriptional regulator, TetR family	3.1 ± 1.4	6424 ± 506	2075 ± 895
DMC1185	panDhc_1089	Unassigned	non-canonical purine NTP pyrophosphatase, RdgB	3.1 ± 1.3	15071 ± 1119	4884 ± 2020
DMC1306	KB1_1336	-	DNA-binding response regulator, LuxR family	3.0 ± 0.26	6111 ± 365	2037 ± 131
DMC0374	panDhc_1063_RC	Cornell	inositol-5-monophosphate dehydrogenase	2.9 ± 0.31	8533 ± 658	2897 ± 202
DMC1563	panDhc_4087	Pinellas	putative desulforedoxin	2.9 ± 0.39	13775 ± 1109	4697 ± 496
DMC2127	KB1_1146	-	transcriptional regulator, Fur family	2.9 ± 0.84	4185 ± 792	1435 ± 313
DMC0125	VS137	Pinellas	DNA-binding response regulator	2.9 ± 1.5	2184 ± 91	752 ± 386
DMC1563	gi57233584	-	desulforedoxin, putative	2.7 ± 0.27	21986 ± 1018	8015 ± 704
DMC0055	KB1_0213	-	ATP-dependent Clp protease, ATP-binding subunit	2.7 ± 1.3	4384 ± 355	1617 ± 745

Table A5.1 (Continued)

DMC#	Probe ID	Strain	Description	Ratio of 17 hour Post TCA Added versus	17 hour Post TCA Added Average Intensity (pfu)	Controls Average Intensity (pfu)
DMC1880	panDhc_3306	Pinellas	hypothetical protein	2.7 ± 0.61	9541 ± 775	3566 ± 754
DMC1373	panDhc_1766	Pinellas	SAM-dependent methyltransferase UbiE/COQ5	2.6 ± 1.0	1867 ± 138	709 ± 265
DMC1018	panDhc_2262_RC	Pinellas	two component transcriptional regulator	2.6 ± 0.52	1644 ± 90	636 ± 123
DMC0433	panDhc_2049	Unassigned	protein of unknown function DUF28	2.6 ± 0.46	9332 ± 1655	3642 ± 59
DMC1400	panDhc_3297	Unassigned	hypothetical protein	2.6 ± 0.33	9354 ± 1163	3659 ± 120
DMC0132	VS145	Unassigned	methylglyoxal synthase	2.5 ± 0.31	1221 ± 14	482 ± 60
DMC0734	panDhc_632_RC	Unassigned	hypothetical protein	2.5 ± 0.091	64778 ± 1969	25935 ± 528
DMC1208	KB1_1232	-	NADPH-dependent FMN reductase	2.4 ± 0.34	930 ± 100	386 ± 36
DMC1699	VS599	Unassigned	thioredoxin	2.4 ± 0.48	13056 ± 1613	5521 ± 890
DMC1554	panDhc_885	Unassigned	homocitrate synthase	2.3 ± 0.86	8677 ± 603	3714 ± 1349
DMC2122	KB1_1142	-	DNA-binding response regulator, LuxR family	2.3 ± 0.93	1339 ± 91	581 ± 230
DMC1373	panDhc_1786	Unassigned	methyltransferase, UbiE/COQ5 family	2.2 ± 0.30	11346 ± 1429	5099 ± 233
DMC0997	panDhc_1856_RC	Unassigned	serine protease, DegP	2.2 ± 0.31	5906 ± 626	2729 ± 267
DMC0734	panDhc_636_RC	Cornell	hypothetical protein	2.1 ± 0.52	12757 ± 532	5949 ± 1424
DMC1524	panDhc_3906	Cornell	hypothetical protein	0.50 ± 0.091	7936 ± 1267	15916 ± 1413
DMC0810	panDhc_818	Unassigned	phosphoribosylamine--glycine ligase	0.49 ± 0.058	1147 ± 103	2318 ± 170
DMC0902	panDhc_524_RC	Unassigned	proton-translocating NADH-quinone oxidoreductase	0.49 ± 0.077	743 ± 99	1519 ± 125
DMC1549	panDhc_1995	Unassigned	metallophosphoesterase	0.48 ± 0.069	770 ± 19	1602 ± 228
DMC0029	panDhc_588	Unassigned	Trk system potassium uptake protein, putative	0.48 ± 0.067	677 ± 19	1423 ± 195
DMC0955	panDhc_1643	Cornell	acetyltransferase, GNAT family	0.47 ± 0.029	1545 ± 93	3278 ± 42
DMC1426	panDhc_576_RC	Unassigned	anthranilate synthase component I	0.47 ± 0.023	733 ± 13	1558 ± 70
DMC0450	panDhc_1214	Unassigned	chorismate mutase / prephenate dehydratase	0.44 ± 0.097	656 ± 112	1496 ± 209
DMC0578	panDhc_1333_RC	Unassigned	2-hydroxyglutaryl-CoA dehydratase D-component	0.43 ± 0.042	430 ± 16	998 ± 89
DMC0453	panDhc_2849	Unassigned	Shikimate kinase	0.43 ± 0.061	1951 ± 53	4589 ± 647
DMC1152	VS977	Unassigned	hypothetical protein	0.41 ± 0.046	428 ± 34	1032 ± 80
DMC1170	panDhc_182	Cornell	translation elongation factor G	0.41 ± 0.051	409 ± 13	999 ± 120
DMC1580	KB1_0697	-		0.41 ± 0.11	2522 ± 659	6174 ± 291
DMC0361	panDhc_1290	Unassigned	membrane-associated zinc metalloprotease	0.41 ± 0.064	499 ± 22	1231 ± 186
DMC0973	panDhc_1860	Cornell	hypothetical protein	0.41 ± 0.16	560 ± 227	1383 ± 26
DMC0994	KB1_1021	-	AMP-dependent synthetase and ligase	0.40 ± 0.084	895 ± 184	2255 ± 102
DMC1199	panDhc_2842_RC	Cornell	peptide methionine sulfoxide reductase MsrA	0.39 ± 0.14	468 ± 156	1202 ± 121
DMC0411	panDhc_1750_RC	Unassigned	degV family protein	0.39 ± 0.11	6635 ± 1648	17133 ± 1966
DMC1561	panDhc_717_RC	Cornell	hypothetical protein	0.38 ± 0.013	1574 ± 3	4172 ± 142
DMC0553	VS504	Unassigned	ATP synthase F1, epsilon subunit	0.35 ± 0.007	1721 ± 14	4937 ± 91
DMC0196	panDhc_1387_RC	Cornell	glycosyl transferase, group 2 family protein	0.34 ± 0.061	1952 ± 218	5687 ± 793
DMC0553	KB1_0608	-	ATP synthase F1, epsilon subunit	0.34 ± 0.013	3198 ± 88	9447 ± 252
DMC1561	panDhc_717	Cornell	hypothetical protein	0.32 ± 0.095	1055 ± 310	3288 ± 116
DMC0550	panDhc_496	Pinellas	ATP synthase F1, alpha subunit	0.30 ± 0.078	510 ± 128	1678 ± 90
DMC0197	panDhc_1500	Cornell	NAD-dependent epimerase/dehydratase	0.28 ± 0.064	331 ± 2	1173 ± 268
DMC0547	GT_460801	-	ATP synthase F0, C subunit	0.28 ± 0.063	4174 ± 809	14878 ± 1654
DMC0178	VS174	Unassigned	formate dehydrogenase accessory protein	0.28 ± 0.18	962 ± 608	3450 ± 472
DMC0549	panDhc_2797_RC	Unassigned	ATP synthase F1, delta subunit	0.27 ± 0.075	3367 ± 612	12396 ± 2562
DMC0552	panDhc_645	Unassigned	ATP synthase subunit B	0.27 ± 0.088	4102 ± 1353	15336 ± 260
DMC0547	KB1_0602	-	ATP synthase F0, C subunit	0.27 ± 0.057	4163 ± 753	15571 ± 1757
DMC0547	gi147669178	Unassigned	ATP synthase F0, C subunit	0.27 ± 0.063	4176 ± 883	15683 ± 1686
DMC1235	panDhc_3190_RC	Unassigned	N utilization substance protein B	0.22 ± 0.042	1069 ± 173	4911 ± 500
DMC0201	panDhc_1571	Cornell	glycosyl transferase, group 2 family protein	0.18 ± 0.058	656 ± 157	3610 ± 755

Table A5.2. Full table of all transcripts differentially regulated in the TCA 48/17 hour

Table A5.2. (Continued)

DMC ID	Probe ID	Strain	DMC Description	Ratio of 48 Hour/17 Hour TCA Stress	Average Normalized Intensity of 48 Hour Stress	Average Normalized Intensity of 17 Hour Stress
DMC1264	panDhc_4041	Cornell	hypothetical protein	42 ± 14	726 ± 204	30774 ± 5489
DMC0014	panDhc_2210	Cornell	hypothetical protein	14 ± 2.3	245 ± 25	3389 ± 434
DMC0435	panDhc_3072	Unassigned	[Fe] hydrogenase, *hymA* subunit	14 ± 2.6	1529 ± 130	20888 ± 3540
DMC0435	panDhc_3078	Cornell	[Fe] hydrogenase, *hymA* subunit	9.2 ± 2.6	261 ± 26	2402 ± 640
DMC1488	panDhc_502	Cornell	RDase	7.7 ± 0.8	2360 ± 252	18257 ± 85
DMC1887	panDhc_3169_RC	Pinellas	hypothetical protein	7.5 ± 1.3	3147 ± 558	23480 ± 741
DMC1199	panDhc_2842_RC	Cornell	peptide methionine sulfoxide reductase *msrA*	7.1 ± 2.7	468 ± 156	3321 ± 599
DMC0925	panDhc_1804_RC	Cornell	bacterioferritin domain protein	6.3 ± 1.3	408 ± 36	2583 ± 491
DMC0435	gi147669068	Unassigned	[Fe] hydrogenase, *hymA* subunit	6.3 ± 2.1	972 ± 266	6112 ± 1235
DMC1277	panDhc_1885	Cornell	acetyltransferase, GNAT family	6.0 ± 0.8	273 ± 32	1625 ± 106
DMC1398	gi57233747	Cornell	hypothetical protein	5.8 ± 1.1	428 ± 77	2464 ± 72
DMC0827	panDhc_922_RC	Cornell	ABC transporter, permease protein, putative	5.6 ± 2.4	220 ± 93	1241 ± 24
DMC1524	panDhc_3906	Cornell	hypothetical protein	5.6 ± 0.9	7936 ± 1267	44092 ± 478
DMC2350	gi147668747	Unassigned	Resolvase, N-terminal domain	5.0 ± 1.9	307 ± 100	1525 ± 283
DMC1153	panDhc_328	Cornell	DNA mismatch repair protein	4.9 ± 1.4	640 ± 185	3131 ± 179
DMC1561	panDhc_718	Cornell	cell wall/surface repeat protein	4.8 ± 1.9	568 ± 218	2746 ± 151
DMC1557	gi57233590	Cornell	hypothetical protein	4.8 ± 1.0	2233 ± 237	10702 ± 1985
DMC1271	panDhc_1288	Cornell	radical SAM domain protein	4.7 ± 0.80	985 ± 126	4588 ± 523
DMC0014	panDhc_2210_RC	Cornell	hypothetical protein	4.6 ± 1.0	526 ± 66	2431 ± 441
DMC1561	panDhc_717_RC	Cornell	hypothetical protein	4.6 ± 0.18	1574 ± 3	7265 ± 281
DMC1024	panDhc_28	Cornell	sensory box sensor histidine kinase	4.5 ± 0.665	412 ± 18	1839 ± 263
DMC1270	panDhc_748	Cornell	hypothetical protein	4.4 ± 0.268	1047 ± 14	4639 ± 274
DMC1193	panDhc_3420	Cornell	hypothetical protein	4.3 ± 0.487	452 ± 51	1957 ± 6
DMC1524	panDhc_3906_RC	Cornell	hypothetical protein	4.2 ± 0.940	3952 ± 288	16691 ± 3510
DMC1355	panDhc_1298	Pinellas	heat-inducible transcription repressor	4.1 ± 1.107	1107 ± 193	4579 ± 930
DMC1556	gi57233591	-	transcriptional regulator, AbrB family	4.0 ± 0.946	1252 ± 128	5047 ± 1066
DMC1407	panDhc_2803	Unassigned	ribosome-associated protein Y (PSrp-1)	4.0 ± 0.820	6152 ± 99	24716 ± 5030
DMC0983	panDhc_2685_RC	Cornell	hypothetical protein	4.0 ± 1.083	239 ± 41	948 ± 200
DMC0557	panDhc_2339_RC	Cornell	endonuclease V	3.9 ± 0.723	350 ± 54	1361 ± 143
DMC0435	KB1_0491	-	[Fe] hydrogenase, *hymA* subunit	3.8 ± 1.546	1343 ± 518	5099 ± 662
DMC0922	panDhc_3840_RC	Cornell	hypothetical protein	3.7 ± 0.379	1977 ± 194	7374 ± 193
DMC1557	VS1499	Cornell	hypothetical protein	3.7 ± 0.85	1228 ± 53	4529 ± 1031
DMC0922	panDhc_3840	Cornell	hypothetical protein	3.7 ± 0.319	2008 ± 84	7374 ± 563
DMC0059	panDhc_669_RC	Cornell	cysteinyl-tRNA synthetase	3.6 ± 0.72	427 ± 15	1540 ± 302
DMC1522	panDhc_2615	Cornell	transcription regulator, TetR family	3.6 ± 0.533	1806 ± 250	6439 ± 360
DMC1472	panDhc_3098	Cornell	sensory box protein, putative	3.6 ± 0.561	467 ± 37	1660 ± 227
DMC1332	VS1157	Unassigned	hypothetical protein	3.5 ± 0.49	1098 ± 110	3892 ± 365
DMC1521	panDhc_686	Cornell	mechanosensitive ion channel family protein	3.4 ± 0.443	490 ± 23	1683 ± 202
DMC0093	panDhc_2147_RC	Cornell	iron dependent repressor	3.4 ± 0.067	483 ± 9	1658 ± 5
DMC0223	panDhc_3540_RC	Cornell	TM2 domain protein	3.2 ± 0.513	597 ± 29	1927 ± 291
DMC0185	panDhc_2988	Cornell	*cvpA* family protein	3.2 ± 0.843	771 ± 192	2483 ± 205
DMC1473	panDhc_2662_RC	Cornell	sensor histidine kinase	3.2 ± 0.759	774 ± 98	2487 ± 495
DMC1906	panDhc_3912	Cornell	hypothetical protein	3.1 ± 0.559	317 ± 40	991 ± 126
DMC1269	gi57233984	-	hypothetical protein	3.1 ± 0.701	655 ± 112	2002 ± 307
DMC0132	panDhc_3176	Cornell	methylglyoxal synthase	3.0 ± 0.735	365 ± 43	1113 ± 235
DMC1332	gi57233859	-	hypothetical protein	3.0 ± 0.539	1138 ± 98	3402 ± 538
DMC1751	panDhc_3812	Unassigned	hypothetical protein	3.0 ± 0.113	505 ± 14	1494 ± 39
DMC0196	panDhc_1387	Cornell	glycosyl transferase, group 2 family	2.9 ± 0.663	968 ± 99	2848 ± 571
DMC1917	GT_c58845-57931	-	hypothetical protein	2.9 ± 1.088	594 ± 204	1733 ± 255
DMC0197	panDhc_1500	Cornell	NAD-dependent epimerase/dehydratase family	2.9 ± 0.514	331 ± 2	948 ± 170
DMC0832	panDhc_1724_RC	Unassigned	hydrogenase, EchB subunit	2.9 ± 0.708	603 ± 111	1720 ± 286
DMC0059	panDhc_681	Cornell	cysteinyl-tRNA synthetase	2.8 ± 0.668	369 ± 71	1040 ± 145
DMC0892	panDhc_1176	Cornell	twitching mobility protein	2.8 ± 0.501	3551 ± 277	9800 ± 1604
DMC0923	panDhc_101	Cornell	copper-translocating P-type ATPase	2.7 ± 0.398	670 ± 31	1792 ± 253
DMC0136	panDhc_2047_RC	Unassigned	phosphate ABC transporter, ATP-binding	2.7 ± 0.311	372 ± 4	991 ± 115
DMC1139	panDhc_234_RC	Cornell	ABC transporter, ATP-binding/permease	2.6 ± 0.485	444 ± 5	1133 ± 215
DMC0807	panDhc_2438_RC	Cornell	Sua5/YciO/YrdC/YwlC family protein	2.5 ± 0.238	875 ± 61	2178 ± 142
DMC0793	panDhc_2602_RC	Cornell	hypothetical protein	2.5 ± 0.516	848 ± 132	2083 ± 293
DMC1556	VS1498	Unassigned	transcriptional regulator, *abrB*	2.5 ± 0.170	6819 ± 420	16724 ± 535
DMC0434	panDhc_3431	Unassigned	holo-(acyl-carrier protein) synthase	2.4 ± 0.396	918 ± 149	2220 ± 41
DMC0196	panDhc_1387_RC	Cornell	glycosyl transferase, group 2 family	2.4 ± 0.341	1952 ± 218	4714 ± 406
DMC0524	panDhc_1334_RC	Pinellas	DNA-directed DNA polymerase	2.4 ± 0.435	1368 ± 144	3290 ± 483
DMC1903	gi57233685	-	hypothetical protein	2.4 ± 0.244	38228 ± 1710	91631 ± 8381
DMC0817	panDhc_633_RC	Pinellas	ATP phosphoribosyltransferase	2.4 ± 0.752	430 ± 121	1026 ± 144
DMC1364	panDhc_1391	Cornell	DnaJ family protein	2.4 ± 0.077	445 ± 1	1057 ± 34

Table A5.2. (Continued)

DMC ID	Probe ID	Strain	DMC Description	Ratio of 48 Hour/17 Hour TCA Stress	Average Normalized Intensity of 48 Hour Stress	Average Normalized Intensity of 17 Hour Stress
DMC1564	panDhc_3967	Cornell	hypothetical protein	2.4 ± 0.234	5735 ± 540	13542 ± 421
DMC1578	panDhc_2420_RC	Unassigned	transcriptional repressor, *lexA*	2.3 ± 0.148	1388 ± 73	3253 ± 113
DMC0393	panDhc_2111	Cornell	Ser/Thr protein phosphatase family	2.3 ± 0.132	491 ± 21	1150 ± 42
DMC0992	KB1_1019	-	hypothetical protein	2.3 ± 0.517	1221 ± 276	2791 ± 32
DMC1014	panDhc_1082_RC	Unassigned	Tubulin/FtsZ GTPase	2.3 ± 0.304	3801 ± 506	8662 ± 65
DMC0957	panDhc_2427	Pinellas	protein of unknown function DUF502	2.2 ± 0.404	3526 ± 524	7827 ± 823
DMC0589	KB1_0647	-	riboflavin biosynthesis protein RibF	2.2 ± 0.388	907 ± 96	2003 ± 282
DMC1555	gi57233600	-	histidine triad (HIT) protein	2.2 ± 0.239	1636 ± 156	3609 ± 185
DMC0493	panDhc_2087_RC	Unassigned	tRNA pseudouridine synthase A	2.2 ± 0.619	1122 ± 304	2473 ± 181
DMC1301	panDhc_1349	Cornell	tagatose 1,6-diphosphate aldolase-like	2.2 ± 0.237	1551 ± 116	3414 ± 264
DMC0991	KB1_1018	-	Leucyl aminopeptidase	2.2 ± 0.281	6582 ± 833	14470 ± 251
DMC1533	KB1_0111	-	AIR synthase related protein domain	2.2 ± 0.431	1358 ± 258	2983 ± 145
DMC0662	panDhc_2491	Cornell	cyclase, putative	2.2 ± 0.328	1092 ± 93	2392 ± 294
DMC1193	panDhc_3420_RC	Cornell	hypothetical protein	2.2 ± 0.333	859 ± 23	1868 ± 281
DMC0215	panDhc_815	Unassigned	serine protease inhibitor	2.2 ± 0.433	1151 ± 231	2480 ± 16
DMC1762	panDhc_4152	Unassigned	hypothetical protein	2.1 ± 0.181	3179 ± 80	6802 ± 551
DMC1355	panDhc_1287_RC	Cornell	heat-inducible transcription repressor HrcA	2.1 ± 0.486	1699 ± 362	3605 ± 303
DMC0406	VS359	Unassigned	hypothetical protein	2.1 ± 0.271	27108 ± 3309	55940 ± 2678
DMC1087	panDhc_1993_RC	Pinellas	glutamate synthase, alpha subunit domain	2.1 ± 0.457	647 ± 143	1327 ± 38
DMC0822	panDhc_2743	Pinellas	hypothetical protein	2.0 ± 0.457	681 ± 146	1370 ± 105
DMC1170	panDhc_182_RC	Unassigned	translation elongation factor G	2.0 ± 0.153	2187 ± 5	4398 ± 334
DMC1475	panDhc_3325	Cornell	dinitrogenase iron-molybdenum cofactor family	2.0 ± 0.532	530 ± 138	1066 ± 50
DMC0722	panDhc_2035_RC	Pinellas	triosephosphate isomerase	0.49 ± 0.041	15248 ± 740	7512 ± 512
DMC0367	panDhc_2924	Unassigned	elongation factor Ts	0.49 ± 0.074	18960 ± 2340	9287 ± 805
DMC0140	panDhc_3063	Unassigned	[Fe] hydrogenase, *hymA* subunit	0.47 ± 0.060	3824 ± 454	1817 ± 83
DMC1387	KB1_1425	-	hydrogenase formation protein *hypD*	0.45 ± 0.069	2490 ± 203	1118 ± 147
DMC0037	KB1_0195	-	PyrK family protein	0.44 ± 0.110	1904 ± 187	844 ± 192
DMC0961	VS865	Unassigned	ribosomal protein L11	0.43 ± 0.075	3406 ± 248	1451 ± 232
DMC0810	panDhc_818	Unassigned	phosphoribosylamine--glycine ligase	0.42 ± 0.083	1147 ± 103	485 ± 84
DMC1373	panDhc_1738	Unassigned	methyltransferase, UbiE/COQ5 family	0.42 ± 0.080	3324 ± 615	1394 ± 69
DMC0542	panDhc_1292	Unassigned	deoxyguanosinetri-PO4 tri-PO4-hydrolase	0.42 ± 0.087	1888 ± 338	784 ± 84
DMC0707	panDhc_2670_RC	Cornell	pyruvic-ferredoxin oxidoreductase	0.39 ± 0.084	4332 ± 637	1672 ± 266
DMC1386	VS1215	Unassigned	hydrogenase assembly chaperone HypC	0.39 ± 0.131	1600 ± 43	617 ± 208
DMC1430	panDhc_2365	Unassigned	N-(5'phosphoribosyl)anthranilate isomerase	0.37 ± 0.069	932 ± 173	345 ± 6
DMC1325	KB1_1355	-	hypothetical protein	0.36 ± 0.035	5073 ± 36	1815 ± 176
DMC1253	GT_c988413	-	hypothetical protein	0.35 ± 0.067	118947 ± 22235	41631 ± 1486
DMC1219	panDhc_4040_RC	Cornell	ribosomal protein L28	0.34 ± 0.077	11094 ± 883	3727 ± 807
DMC0553	KB1_0608	-	ATP synthase F1, epsilon subunit	0.33 ± 0.075	3198 ± 88	1067 ± 237
DMC0458	gi57234697	-	hypothetical protein	0.32 ± 0.061	1005 ± 189	324 ± 5
DMC0553	VS504	Unassigned	ATP synthase F1, epsilon subunit	0.31 ± 0.057	1721 ± 14	532 ± 98
DMC1282	gi57233954	-	50S ribosomal protein L27	0.28 ± 0.073	26179 ± 2931	7310 ± 1726
DMC0097	panDhc_35	Pinellas	*mod* Fe4S4 region	0.26 ± 0.035	1324 ± 171	348 ± 14
DMC1089	panDhc_2036_RC	Unassigned	imidazoleglycerol phosphate synthase, cyclase	0.26 ± 0.060	5002 ± 1137	1314 ± 29
DMC0984	gi57234231	-	hypothetical protein	0.26 ± 0.086	3912 ± 132	1023 ± 334
DMC0547	gi147669178	Unassigned	ATP synthase F0, C subunit	0.23 ± 0.053	4176 ± 883	981 ± 75
DMC0547	KB1_0602	-	ATP synthase F0, C subunit	0.23 ± 0.047	4163 ± 753	955 ± 90
DMC0547	GT_460801	-	ATP synthase F0, C subunit	0.23 ± 0.048	4174 ± 809	939 ± 80
DMC0547	VS498	Unassigned	ATP synthase F0, C subunit	0.22 ± 0.080	4377 ± 962	959 ± 280
DMC0547	gi57234631	-	ATP synthase F0, C subunit	0.22 ± 0.080	4579 ± 912	989 ± 310
DMC1433	panDhc_2001	Unassigned	tryptophan synthase, alpha subunit	0.21 ± 0.113	1089 ± 157	228 ± 119
DMC0549	panDhc_2797_RC	Unassigned	ATP synthase F1, delta subunit	0.20 ± 0.047	3367 ± 612	664 ± 104
DMC1433	KB1_1466	-	tryptophan synthase, alpha subunit	0.19 ± 0.142	1362 ± 307	265 ± 183
DMC1091	panDhc_761_RC	Unassigned	pyridine nucleotide-disulfide oxidoreductase	0.18 ± 0.020	5950 ± 498	1098 ± 79
DMC1372	VS1201	Unassigned	transcriptional regulator, *abrB* family	0.18 ± 0.060	1286 ± 59	227 ± 77
DMC1475	panDhc_3315_RC	Pinellas	nitrogenase Fe-Mo cofactor maturation	0.17 ± 0.148	1383 ± 78	234 ± 204
DMC0097	KB1_0242	-	*mod* Fe4S4 region	0.14 ± 0.102	994 ± 246	140 ± 95
DMC1092	panDhc_2525	Cornell	imidazole glycerol phosphate synthase	0.13 ± 0.049	4086 ± 339	545 ± 194
DMC0176	panDhc_341_RC	Cornell	ATP-dependent RNA helicase	0.07 ± 0.052	3426 ± 995	238 ± 165

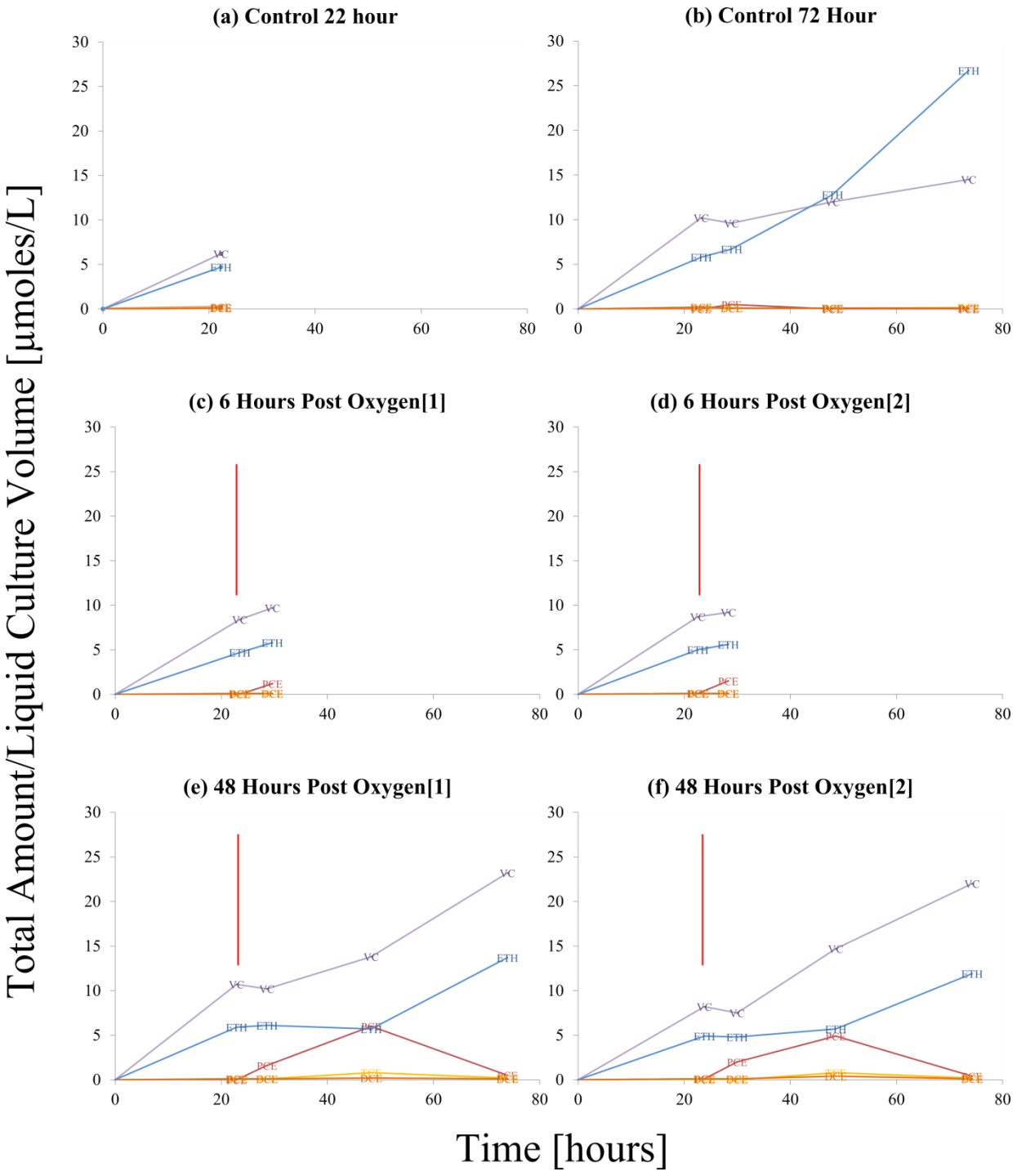

Figure A5.2. Dechlorination profiles showing nominal concentrations of chloroethenes (PCE, TCE, DCE, VC) and ethene (ETH) in D2 cultures continuously fed 0.5 µmoles/(L-hr) PCE sampled at 22 and 72 hours as a control (a,b); six hours post oxygen addition (c,d), and 48 hour post oxygen addition (e,f). Data labels indicate the specific metabolites. The red bar denotes the time of 3.42 mg oxygen addition (added to the stress cultures after 24 hours from start).

Table A5.3. Differentially detected D2 proteins for the 48 hours after oxygen addition compared to the 6 hours after oxygen addition

DMC#	DET#	Description	Ratio of 48 Hour to 6 Hour Post Stress	Average Protein Score (48hr Oxygen)
DMC0601	DET0614	hydrogenase, group 3, VhuG subunit, putative	4.22 ± 3.04	8 ± 0.9
DMC0944	DET0976	PurA adenylosuccinate synthetase	3.95 ± 0.10	32 ± 0.8
DMC1215	DET1258	ArgD acetylornithine aminotransferase	2.74 ± 0.39	15 ± 0.6
DMC0186	DET0193	ProC pyrroline 5 carboxylate reductase	2.39 ± 0.50	13 ± 2.1
DMC1285	DET1329	HisI phosphoribosyl AMP cyclohydrolase	2.32 ± 0.40	20 ± 3.1
DMC0657	DET0670	iron sulfur cluster binding protein	2.31 ± 0.35	23 ± 0.4
DMC0720	DET0740	DapF diaminopimelate epimerase	2.25 ± 0.34	20 ± 0.3
DMC0719	DET0739	aspartate aminotransferase	2.23 ± 0.29	12 ± 0.6
DMC1227	DET1270	ArgS arginyl tRNA synthetase	2.20 ± 0.37	10 ± 0.2
DMC0631	DET0644	Tkt 1 transketolase	2.04 ± 0.30	31 ± 3.3
DMC0419	DET0430	ValS valyl tRNA synthetase	2.03 ± 0.03	20 ± 0.3
DMC0516	DET0527	TldD/PmbA family protein	1.99 ± 0.19	17 ± 0.6
DMC0947	DET0979	myo inositol 1 phosphate synthase family protein	1.99 ± 0.16	113 ± 2.2
DMC1170	DET1212	FusA 2 translation elongation factor G	1.84 ± 0.20	23 ± 2.3
DMC0760	DET0783	translin family protein	1.76 ± 0.20	13 ± 0.7
DMC0040	DET0040	hypothetical protein	1.71 ± 0.14	89 ± 7.3
DMC1260	DET1303	fasciclin domain protein	1.55 ± 0.12	22 ± 1.7
DMC0624	DET0637	cell division protein FtsA	1.52 ± 0.17	26 ± 2.1
DMC0965	DET0997	Tuf translation elongation factor Tu	1.44 ± 0.03	172 ± 3.9
DMC0996	DET1035	tryptophan synthase subunit beta	1.43 ± 0.08	72 ± 1.9
DMC1370	DET1417	PurH formyltransferase/IMP cyclohydrolase	1.39 ± 0.06	98 ± 1.8
DMC0552	DET0564	AtpD ATP synthase subunit B	1.21 ± 0.05	360 ± 2.8
DMC0695	DET0709	Tig trigger factor	0.84 ± 0.05	58 ± 3.3
DMC0912	DET0942	lipoprotein, putative	0.81 ± 0.01	15 ± 0.0
DMC0428	DET0439	FtsK/SpoIIIE family protein	0.65 ± 0.06	11 ± 0.8
DMC1536	DET1596	transcriptional regulator, putative	0.49 ± 0.09	10 ± 1.5
DMC1213	DET1256	ArgJacetyltransferase/N acetylglutamate synthase	0.45 ± 0.06	4 ± 0.5
DMC0703	DET0717	TopA DNA topoisomerase I	0.42 ± 0.07	4 ± 0.2
DMC1527	DET1586	LemA family protein	0.35 ± 0.05	11 ± 1.5
DMC1313	DET1357	hypothetical protein	0.34 ± 0.05	4 ± 0.2

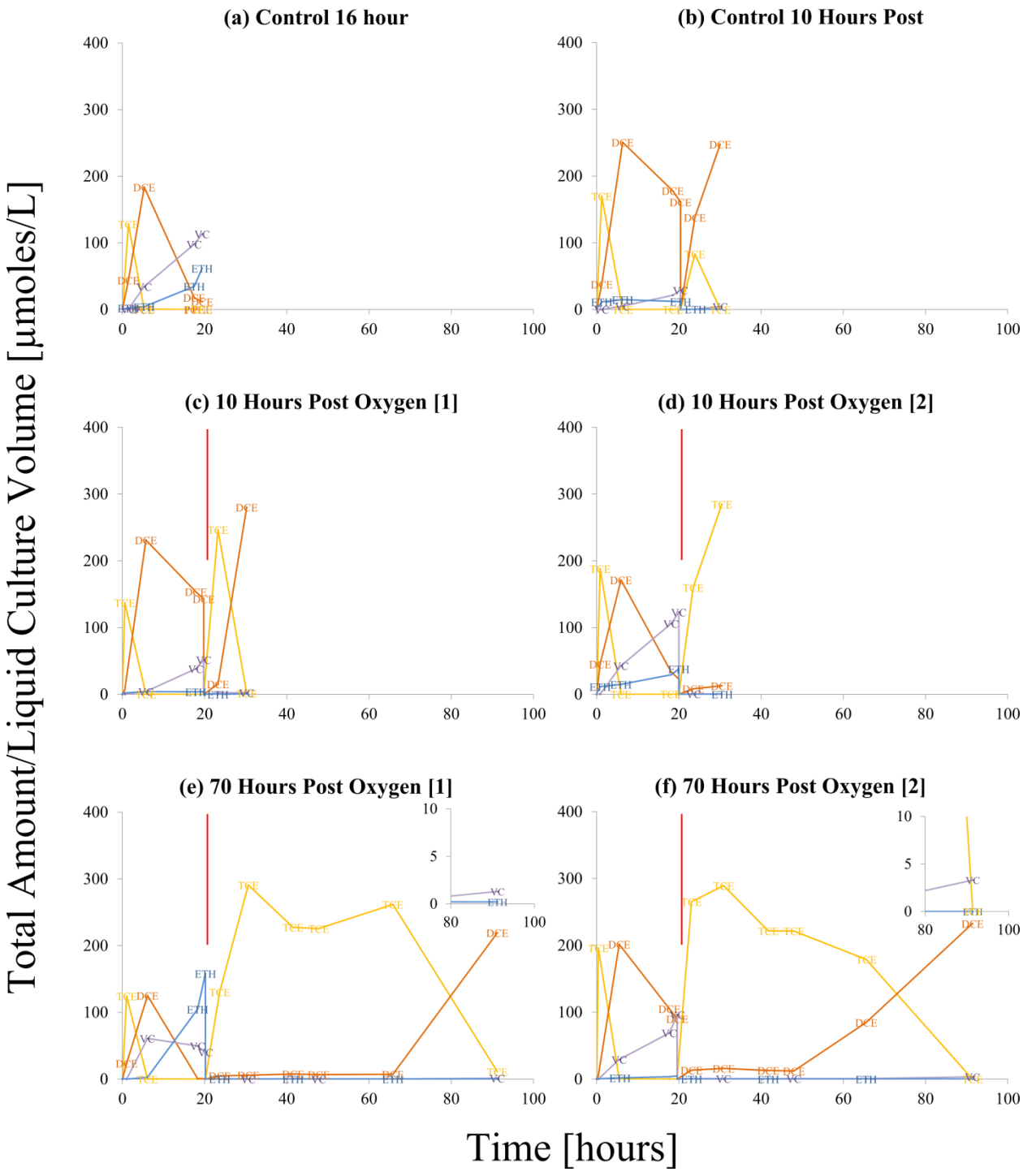

Figure A5.3. Dechlorination profiles showing nominal concentrations of chloroethenes (TCE, DCE, VC) and ethene (ETH) in KB-1™ batch fed TCE cultures sampled at 16 hours as a control (a); 6 hours post oxygen addition (c,d), 91 hour total/70 hour post as a control (b), and 70 hour post oxygen addition (e,f). Data labels indicate the specific metabolites. The red bar denotes the time of oxygen amendment (added to the stress cultures after 20 hours from start of experiment).

Table A5.4. Differentially detected KB-1™ transcripts for the 48 hr compared to 6 hr

Table A5.4. (Continued)

DMC#	Probe ID	Strain Type	Description	Ratio of 48 Hour to 6 Hour Post Oxygen Stress	Average Intensity of 48 Hour Oxygen Stress (pfu)	Average Intensity of 6 Hour Oxygen Stress (pfu)
DMC1264	panDhc_4041	Cornell	hypothetical protein	44 ± 21	739 ± 295	32331 ± 8725
DMC0517	panDhc_793	Pinelles	Phosphoglucosamine mutase	34 ± 7.1	7737 ± 1093	260120 ± 40503
DMC1207	gi57233993	Cornell	hypothetical protein	26 ± 5.9	293 ± 13	7759 ± 1685
DMC1022	gi57234153	Cornell	hypothetical protein	19 ± 8.4	224 ± 80	4294 ± 1081
DMC1017	panDhc_2869	Unassigned	hypothetical protein	13 ± 3.2	2578 ± 8	33300 ± 8183
DMC0924	panDhc_2985	Cornell	Hsp20/alpha crystallin family	13 ± 4.1	494 ± 95	6326 ± 1645
DMC1009	panDhc_1509	Cornell	HD domain protein	9.1 ± 1.1	267 ± 22	2443 ± 196
DMC0435	panDhc_3072_RC	Cornell	[Fe] hydrogenase HymA	8.2 ± 2.9	1109 ± 315	9140 ± 1905
DMC1487	panDhc_3708_RC	Cornell	reductive dehalogenase anchoring	7.7 ± 2.0	11267 ± 2511	86376 ± 12104
DMC0926	panDhc_2651_RC	Cornell	superoxide dismutase	7.3 ± 1.6	299 ± 65	2191 ± 83
DMC1277	panDhc_1885_RC	Cornell	acetyltransferase GNAT family	7.3 ± 2.3	475 ± 102	3481 ± 784
DMC0926	panDhc_2651	Cornell	superoxide dismutase	6.9 ± 1.3	242 ± 12	1663 ± 296
DMC1488	panDhc_502_RC	Cornell	reductive dehalogenase putative	6.1 ± 1.9	7713 ± 1608	47301 ± 11292
DMC1149	panDhc_2017_RC	Cornell	lipoprotein putative	6.0 ± 2.5	265 ± 110	1586 ± 80
DMC2158	panDhc_482	Pinelles	putative reductive dehalogenase	5.9 ± 1.8	2679 ± 797	15832 ± 1272
DMC1678	panDhc_1554	Pinelles	hypothetical protein	5.9 ± 1.9	193 ± 63	1133 ± 81
DMC1474	panDhc_2364	Cornell	DNA-binding response regulator LuxR	5.2 ± 2.3	208 ± 88	1088 ± 133
DMC1106	panDhc_3280_RC	Cornell	transcriptional regulator Fur family	5.2 ± 1.8	213 ± 71	1110 ± 111
DMC1104	panDhc_2088	Cornell	DNA-binding response regulator	5.2 ± 4.1	330 ± 248	1713 ± 379
DMC1013	panDhc_737	Cornell	chromosome segregation ATPase	5.0 ± 1.5	1444 ± 383	7287 ± 1016
DMC1104	panDhc_2088_RC	Cornell	DNA-binding response regulator	5.0 ± 2.1	415 ± 162	2077 ± 268
DMC0014	panDhc_2210	Cornell	hypothetical protein	4.9 ± 0.76	572 ± 89	2802 ± 11
DMC0986	panDhc_2154	Cornell	ribonuclease III	4.9 ± 1.2	527 ± 103	2574 ± 419
DMC0925	panDhc_1804	Cornell	bacterioferritin domain protein	4.7 ± 1.5	261 ± 63	1231 ± 259
DMC0794	panDhc_3244_RC	Cornell	hypothetical protein	4.5 ± 3.2	226 ± 156	1019 ± 100
DMC0728	panDhc_2868_RC	Cornell	hypoxanthine phosphoribosyltransferase	4.5 ± 0.73	231 ± 38	1033 ± 12
DMC1023	panDhc_2200_RC	Cornell	DNA-binding response regulator LuxR	4.4 ± 2.1	340 ± 155	1501 ± 163
DMC0922	panDhc_3840_RC	Cornell	hypothetical protein	4.4 ± 1.4	1357 ± 441	5949 ± 67
DMC1260	panDhc_3287	Cornell	fasciclin domain protein	4.3 ± 2.3	467 ± 223	2025 ± 456
DMC1199	panDhc_2842_RC	Cornell	peptide methionine	4.2 ± 1.3	793 ± 242	3351 ± 79
DMC1678	panDhc_1549	Pinelles	hypothetical protein	4.1 ± 1.6	321 ± 123	1325 ± 142
DMC0613	panDhc_3513	Cornell	hypothetical protein	4.1 ± 1.3	260 ± 80	1070 ± 66
DMC1557	gi57233590	Cornell	hypothetical protein	4.1 ± 1.5	1625 ± 584	6676 ± 126
DMC0922	panDhc_3840	Cornell	hypothetical protein	4.1 ± 0.99	1510 ± 346	6182 ± 473
DMC1524	panDhc_3906_RC	Cornell	hypothetical protein	4.1 ± 1.9	3034 ± 1407	12329 ± 816
DMC0925	panDhc_1804_RC	Cornell	bacterioferritin domain	4.0 ± 1.1	513 ± 144	2055 ± 22
DMC1390	panDhc_3876	Cornell	hypothetical protein	4.0 ± 0.28	547 ± 8	2188 ± 147
DMC0741	gi57234447	Cornell	hypothetical protein	4.0 ± 0.86	1556 ± 327	6211 ± 250
DMC0185	panDhc_2988	Cornell	cvpA family	3.9 ± 0.96	791 ± 177	3122 ± 294
DMC1190	KB1_1204		sensor histidine kinase	3.9 ± 0.90	251 ± 12	981 ± 222
DMC1309	panDhc_3099	Cornell	type II	3.9 ± 0.43	649 ± 62	2521 ± 140
DMC0212	panDhc_2963	Cornell	PBS lyase	3.8 ± 1.0	537 ± 103	2049 ± 387
DMC1561	panDhc_717	Cornell	hypothetical protein	3.8 ± 1.9	1584 ± 778	5978 ± 170
DMC0058	gi57233568	Cornell	2C-methyl-D-erythritol 24-cyclodiphosphate synthase	3.8 ± 1.1	635 ± 181	2384 ± 96
DMC1560	panDhc_2027_RC	Cornell	hypothetical protein	3.7 ± 1.5	635 ± 253	2369 ± 107
DMC1306	panDhc_2285	Cornell	DNA-binding response regulator LuxR	3.7 ± 0.82	969 ± 56	3598 ± 769
DMC1310	panDhc_2739_RC	Cornell	type II secretion system	3.7 ± 1.5	468 ± 185	1737 ± 218
DMC0786	panDhc_2075	Unassigned	ABC transporter ATP-binding protein	3.7 ± 1.1	425 ± 117	1561 ± 134
DMC0163	panDhc_2202_RC	Cornell	DNA-binding response regulator	3.7 ± 0.72	436 ± 70	1596 ± 188
DMC1335	panDhc_375_RC	Cornell	auxin-responsive GH3	3.7 ± 0.87	724 ± 12	2650 ± 629
DMC1270	panDhc_748	Cornell	hypothetical protein	3.6 ± 0.60	1388 ± 227	5040 ± 44
DMC1306	panDhc_2285_RC	Cornell	DNA-binding response regulator LuxR	3.6 ± 1.5	1211 ± 491	4318 ± 169
DMC1522	panDhc_2615_RC	Unassigned	transcription regulator TetR family	3.5 ± 1.2	490 ± 169	1732 ± 60
DMC0164	panDhc_492_RC	Cornell	sensory box sensor histidine	3.5 ± 0.72	323 ± 8	1135 ± 231
DMC0199	panDhc_1423	Cornell	D-glycero-D-manno-heptose 7-phosphate	3.5 ± 0.85	2570 ± 575	9031 ± 836
DMC0627	gi57234556	Cornell	universal stress protein family	3.5 ± 1.2	861 ± 276	3013 ± 307
DMC0661	gi57234556	Cornell	universal stress protein family	3.5 ± 1.2	861 ± 276	3013 ± 307
DMC0226	panDhc_257	Cornell	sensory box sensor histidine	3.5 ± 2.1	479 ± 278	1669 ± 267
DMC1280	VS1106	Cornell	NADH dehydrogenase-like protein	3.4 ± 0.47	704 ± 11	2416 ± 329
DMC1490	panDhc_1789	Unassigned	prephenate dehydratase	3.4 ± 0.49	483 ± 53	1653 ± 148
DMC1304	panDhc_2804_RC	Cornell	RNA polymerase sigma-70 factor	3.4 ± 1.0	521 ± 150	1781 ± 105
DMC1023	panDhc_2200	Cornell	DNA-binding response regulator LuxR	3.4 ± 1.0	940 ± 239	3209 ± 544
DMC0112	gi57235062	Cornell	transcriptional regulator TetR family	3.4 ± 0.46	768 ± 30	2622 ± 339
DMC0521	panDhc_3117_RC	Cornell	phosphatidylethanolamine-binding protein	3.4 ± 0.59	514 ± 30	1754 ± 287
DMC0930	panDhc_894_RC	Cornell	tRNA modification enzyme MiaB	3.4 ± 0.95	2073 ± 552	7064 ± 574
DMC0399	panDhc_863_RC	Cornell	polyA polymerase	3.4 ± 0.27	900 ± 13	3038 ± 243
DMC0923	panDhc_101_RC	Cornell	copper-translocating P-type ATPase	3.4 ± 0.25	511 ± 33	1714 ± 71
DMC0923	panDhc_101	Cornell	copper-translocating P-type ATPase	3.4 ± 0.63	605 ± 112	2028 ± 62
DMC1407	panDhc_2803	Unassigned	ribosome-associated protein Y (PSrp-1)	3.3 ± 1.3	3327 ± 1342	10928 ± 364
DMC1458	GT_1194681		putative transcriptional regulator	3.3 ± 0.45	505 ± 65	1658 ± 87
DMC1523	panDhc_2437_RC	Cornell	antioxidant AhpC/TSA	3.3 ± 1.3	7025 ± 2554	23029 ± 2669
DMC1269	gi57233984	Cornell	hypothetical protein	3.3 ± 0.21	862 ± 56	2825 ± 17
DMC0212	panDhc_2963_RC	Cornell	PBS lyase HEAT-like repeat	3.3 ± 0.61	1345 ± 42	4381 ± 809
DMC0612	panDhc_90	Cornell	sensory box sensor histidine	3.3 ± 0.70	1919 ± 132	6241 ± 1268
DMC0955	panDhc_1643	Cornell	acetyltransferase GNAT	3.2 ± 1.0	2438 ± 676	7875 ± 1059
DMC0786	panDhc_2075_RC	Unassigned	ABC transporter ATP-binding protein	3.2 ± 1.0	2492 ± 767	7965 ± 443
DMC0094	panDhc_3588	Cornell	hypothetical protein	3.2 ± 0.60	4182 ± 63	13336 ± 2517
DMC1391	panDhc_3537	Cornell	hypothetical protein	3.2 ± 0.23	501 ± 35	1580 ± 28
DMC1560	panDhc_2027	Cornell	hypothetical protein	3.1 ± 1.3	425 ± 168	1339 ± 60

Table A5.4. (Continued)

DMC#	Probe ID	Strain Type	Description	Ratio of 48 Hour to 6 Hour Post Oxygen Stress	Average Intensity of 48 Hour Oxygen Stress (pfu)	Average Intensity of 6 Hour Oxygen Stress (pfu)
DMC0755	VS684	Cornell	thymidylate kinase	3.1 ± 0.97	782 ± 236	2456 ± 174
DMC0593	panDhc_1272	Cornell	Holliday junction DNA helicase RuvB	3.1 ± 0.19	385 ± 3	1206 ± 72
DMC1398	gi57233747	Cornell	hypothetical protein	3.1 ± 0.18	586 ± 13	1833 ± 95
DMC0191	panDhc_3692_RC	Cornell	glutaredoxin family	3.1 ± 0.88	561 ± 117	1737 ± 337
DMC1018	panDhc_2256	Cornell	DNA-binding response	3.1 ± 0.62	6130 ± 27	18930 ± 3790
DMC0626	panDhc_2240	Cornell	hypothetical protein	3.0 ± 0.74	328 ± 76	994 ± 76
DMC0022	gi57233641	Cornell	hypothetical protein	3.0 ± 0.53	639 ± 15	1928 ± 336
DMC0219	panDhc_1078_RC	Cornell	hypothetical protein	3.0 ± 1.2	370 ± 144	1110 ± 17
DMC1458	KB1_1537		putative transcriptional regulator	3.0 ± 0.71	564 ± 93	1685 ± 287
DMC0164	panDhc_492	Cornell	sensory box	3.0 ± 0.63	589 ± 16	1757 ± 366
DMC0195	panDhc_906	Cornell	glycosyl transferase	3.0 ± 0.49	1337 ± 70	3988 ± 623
DMC1635	VS225	Pinelles	hypothetical protein	3.0 ± 0.67	1023 ± 80	3040 ± 637
DMC1977	VS225	Pinelles	hypothetical protein	3.0 ± 0.67	1023 ± 80	3040 ± 637
DMC1391	panDhc_3544_RC	Pinelles	hypothetical protein	3.0 ± 0.55	350 ± 1	1037 ± 192
DMC0892	panDhc_1176_RC	Cornell	twitching mobility	2.9 ± 0.66	519 ± 115	1530 ± 37
DMC1558	panDhc_4033	Unassigned	hypothetical protein	2.9 ± 1.5	524 ± 254	1541 ± 136
DMC0058	VS60	Cornell	24-cyclodiphosphate synthase	2.9 ± 0.15	1577 ± 77	4625 ± 84
DMC1561	panDhc_718	Cornell	cell wall/surface repeat protein	2.9 ± 0.14	985 ± 38	2886 ± 88
DMC1242	panDhc_999	Cornell	serine protease DegP/HtrA family	2.9 ± 0.08	1125 ± 31	3267 ± 21
DMC0375	gi57234817	Cornell	hypothetical protein	2.9 ± 0.30	1918 ± 53	5560 ± 552
DMC0202	panDhc_381	Cornell	hypothetical protein	2.9 ± 1.1	2900 ± 1054	8344 ± 1047
DMC0714	panDhc_563_RC	Cornell	mercuric reductase	2.9 ± 0.93	574 ± 158	1647 ± 276
DMC0130	panDhc_2229_RC	Cornell	DNA-binding response regulator	2.9 ± 1.2	461 ± 190	1318 ± 48
DMC1556	gi57233591	Cornell	transcriptional regulator AbrB family	2.8 ± 0.71	1281 ± 306	3644 ± 265
DMC0112	panDhc_2411	Cornell	transcriptional regulator TetR family	2.8 ± 0.60	1658 ± 336	4701 ± 295
DMC1458	panDhc_1271	Cornell	putative transcriptional regulator	2.8 ± 0.56	575 ± 108	1628 ± 96
DMC0095	panDhc_1049	Cornell	mobA family	2.8 ± 0.89	1965 ± 549	5496 ± 849
DMC0372	panDhc_3375	Cornell	iron-sulfur cluster-binding protein Rieske	2.8 ± 0.66	3528 ± 815	9832 ± 499
DMC0397	panDhc_3852_RC	Cornell	hypothetical protein	2.8 ± 0.51	343 ± 11	953 ± 171
DMC0820	panDhc_1887	Unassigned	SPFH domain/band 7 family	2.8 ± 0.66	1739 ± 393	4832 ± 347
DMC1561	panDhc_717_RC	Cornell	hypothetical protein	2.7 ± 0.24	2450 ± 180	6682 ± 334
DMC0197	panDhc_1500	Cornell	NAD-dependent epimerase/dehydratase	2.7 ± 0.43	1085 ± 59	2958 ± 442
DMC0068	panDhc_447	Cornell	SNF2 family helicase putative	2.7 ± 0.53	395 ± 76	1062 ± 56
DMC1149	panDhc_2017	Cornell	lipoprotein putative	2.7 ± 0.44	2084 ± 68	5572 ± 898
DMC1487	panDhc_3708	Cornell	reductive dehalogenase	2.7 ± 0.47	9903 ± 1296	26336 ± 3194
DMC0399	panDhc_863	Cornell	polyA polymerase	2.7 ± 0.68	517 ± 89	1374 ± 258
DMC1243	panDhc_1731	Cornell	serine protease DegP/HtrA family	2.6 ± 0.24	2282 ± 185	6002 ± 257
DMC0508	panDhc_1158_RC	Cornell	ABC transporter	2.6 ± 0.71	413 ± 88	1082 ± 182
DMC1335	panDhc_375	Cornell	auxin-responsive GH3	2.6 ± 0.34	1781 ± 71	4658 ± 584
DMC0434	panDhc_3431	Unassigned	holo-(acyl-carrier protein) synthase	2.6 ± 0.23	613 ± 31	1599 ± 114
DMC0387	panDhc_1350	Cornell	thiamine-monophosphate kinase	2.6 ± 1.2	674 ± 293	1741 ± 169
DMC0927	gi57234239	Cornell	Smr domain	2.6 ± 1.1	741 ± 304	1914 ± 4
DMC0843	gi57234349	Cornell	membrane protein MmpL family	2.6 ± 0.33	1334 ± 101	3430 ± 347
DMC0877	gi57234340	Unassigned	hypothetical protein	2.6 ± 0.33	1334 ± 101	3430 ± 347
DMC1309	panDhc_3099_RC	Cornell	type II secretion system	2.6 ± 0.27	2006 ± 65	5128 ± 525
DMC1305	gi57233908	Cornell	DNA-binding protein excisionase family	2.6 ± 0.15	7910 ± 451	20180 ± 348
DMC0195	panDhc_906_RC	Cornell	histidinol-phosphate phosphatase	2.5 ± 0.26	3983 ± 75	10156 ± 1015
DMC0755	gi57234426	Cornell	thymidylate kinase	2.5 ± 0.61	478 ± 113	1212 ± 61
DMC0111	panDhc_1255	Unassigned	ABC transporter type 2	2.5 ± 1.2	708 ± 327	1795 ± 53
DMC1307	panDhc_132	Cornell	type II secretion system	2.5 ± 0.51	3634 ± 735	9205 ± 59
DMC1328	panDhc_1517_RC	Cornell	dihydroorotate dehydrogenase	2.5 ± 0.81	1767 ± 553	4461 ± 277
DMC0295	panDhc_444_RC	Pinelles	putative reductive dehalogenase	2.5 ± 0.27	443 ± 45	1112 ± 34
DMC0734	panDhc_636_RC	Cornell	hypothetical protein	2.5 ± 0.75	5531 ± 1651	13856 ± 95
DMC0013	panDhc_1858_RC	Cornell	orotidine 5-prime-phosphate decarboxylase	2.5 ± 0.65	597 ± 156	1488 ± 33
DMC0815	panDhc_1208	Cornell	histidinol-phosphate aminotransferase	2.5 ± 0.89	1556 ± 545	3878 ± 223
DMC1564	panDhc_3967	Cornell	hypothetical protein	2.5 ± 0.46	3060 ± 131	7599 ± 1377
DMC0144	panDhc_1774_RC	Unassigned	hydrolase alpha/beta fold	2.5 ± 0.63	892 ± 189	2211 ± 303
DMC0326	panDhc_518	Unassigned	polynucleotide adenylyltransferase	2.5 ± 0.71	656 ± 179	1616 ± 154
DMC0434	panDhc_3432_RC	Unassigned	holo-acyl-carrier-protein synthase	2.5 ± 0.45	610 ± 90	1497 ± 167
DMC1308	panDhc_955_RC	Unassigned	pilin biogenesis protein putative	2.5 ± 0.57	1295 ± 220	3172 ± 511
DMC1403	panDhc_1718_RC	Cornell	hypothetical protein	2.4 ± 0.26	595 ± 63	1449 ± 0
DMC1212	panDhc_1207_RC	Cornell	twitching mobility	2.4 ± 0.30	1189 ± 128	2866 ± 169
DMC0144	panDhc_1774	Cornell	hydrolase alpha/beta fold family	2.4 ± 0.25	453 ± 12	1080 ± 108
DMC0954	panDhc_470_RC	Cornell	Mg chelatase-like	2.4 ± 0.53	401 ± 72	949 ± 126
DMC0201	panDhc_1571	Cornell	glycosyl transferase group 2	2.4 ± 0.35	2340 ± 219	5532 ± 637
DMC0201	panDhc_1537_RC	Cornell	glycosyl transferase family 2	2.4 ± 0.67	881 ± 208	2080 ± 326
DMC0983	panDhc_2685	Cornell	hypothetical protein	2.4 ± 0.51	413 ± 66	973 ± 139
DMC0196	panDhc_1387_RC	Cornell	glycosyl transferase group 2	2.4 ± 0.30	4052 ± 279	9530 ± 1034
DMC1271	panDhc_1288	Cornell	radical SAM domain protein	2.3 ± 0.17	1723 ± 9	4045 ± 300
DMC1557	VS1499	Cornell	hypothetical protein	2.3 ± 0.13	1364 ± 11	3198 ± 180
DMC0213	gi57234992	Cornell	hypothetical protein	2.3 ± 0.36	1453 ± 146	3401 ± 389
DMC0509	panDhc_1470	Cornell	daunorubicin resistance ABC transporter	2.3 ± 0.94	500 ± 200	1169 ± 61
DMC1193	panDhc_3420	Cornell	hypothetical protein	2.3 ± 0.77	732 ± 233	1702 ± 143
DMC1527	panDhc_2698_RC	Cornell	lemA family	2.3 ± 0.44	1814 ± 343	4178 ± 125
DMC1199	panDhc_2824_RC	Pinelles	peptide methionine sulfoxide reductase	2.3 ± 0.25	1128 ± 56	2574 ± 245
DMC0008	panDhc_2490	Cornell	hypothetical protein	2.3 ± 0.66	762 ± 209	1738 ± 156
DMC1243	panDhc_1744_RC	Unassigned	peptidase S1 and S6	2.3 ± 0.28	653 ± 58	1487 ± 123
DMC0145	VS158	Unassigned	hypothetical protein	2.3 ± 0.62	717 ± 168	1625 ± 228
DMC1277	panDhc_1885	Cornell	acetyltransferase GNAT	2.3 ± 0.85	669 ± 245	1514 ± 125

Table A5.4. (Continued)

DMC#	Probe ID	Strain Type	Description	Ratio of 48 Hour to 6 Hour Post Oxygen Stress	Average Intensity of 48 Hour Oxygen Stress (pfu)	Average Intensity of 6 Hour Oxygen Stress (pfu)
DMC0394	panDhc_1633	Cornell	dimethyladenosine transferase	2.3 ± 0.82	681 ± 242	1535 ± 136
DMC1095	panDhc_1454	Cornell	cysteine synthase A	2.2 ± 0.48	631 ± 125	1411 ± 124
DMC1324	panDhc_1363	Cornell	radical SAM	2.2 ± 0.52	709 ± 142	1577 ± 183
DMC0014	panDhc_2210_RC	Cornell	hypothetical protein	2.2 ± 0.10	1182 ± 51	2628 ± 46
DMC1361	panDhc_54	Cornell	hypothetical protein	2.2 ± 0.46	85889 ± 16459	189960 ± 15253
DMC0575	gi57234622	Cornell	hypothetical protein	2.2 ± 0.35	759 ± 18	1657 ± 263
DMC0417	panDhc_1971	Cornell	transcriptional activator	2.2 ± 0.38	2122 ± 366	4627 ± 120
DMC0741	panDhc_2319	Cornell	hypothetical protein	2.2 ± 0.64	746 ± 218	1619 ± 11
DMC1544	panDhc_2840	Unassigned	pyrophosphokinase	2.2 ± 0.16	794 ± 6	1711 ± 129
DMC0013	panDhc_1858	Unassigned	orotidine 5-prime-phosphate	2.2 ± 0.41	1443 ± 246	3105 ± 273
DMC1328	panDhc_1517	Cornell	dihydroorotate dehydrogenase	2.1 ± 0.39	1216 ± 218	2612 ± 82
DMC1523	panDhc_2437	Cornell	antioxidant AhpC/TSA	2.1 ± 0.59	7552 ± 2059	16204 ± 594
DMC0203	panDhc_1988_RC	Cornell	hypothetical protein	2.1 ± 0.31	3723 ± 358	7975 ± 864
DMC0197	panDhc_1500_RC	Cornell	NAD-dependent epimerase/dehydratase	2.1 ± 0.23	3729 ± 408	7870 ± 127
DMC1177	panDhc_87	Cornell	DNA mismatch repair protein	2.1 ± 0.55	927 ± 241	1955 ± 19
DMC0409	panDhc_1954_RC	Cornell	amino acid ABC transporter	2.1 ± 0.40	8843 ± 1371	18566 ± 2109
DMC1555	gi57233600	Cornell	histidine triad (HIT) protein	2.1 ± 0.16	1985 ± 117	4149 ± 218
DMC0791	panDhc_2392_RC	Cornell	thymidylate synthase	2.1 ± 0.54	2629 ± 687	5424 ± 90
DMC0520	panDhc_278_RC	Cornell	glucosamine--fructose-6-phosphate aminotransferase	2.1 ± 0.28	603 ± 73	1243 ± 71
DMC0948	KB1_0968		hypothetical protein	2.1 ± 0.26	7568 ± 190	15567 ± 1926
DMC1024	panDhc_28_RC	Cornell	sensory box sensor histidine	2.0 ± 0.30	3345 ± 385	6831 ± 636
DMC0196	panDhc_1387	Cornell	glycosyl transferase group 2	2.0 ± 0.12	2976 ± 97	6074 ± 295
DMC1682	panDhc_3835	Cornell	hypothetical protein	2.0 ± 0.35	516 ± 46	1052 ± 155
DMC1680	panDhc_3853	Pinelles	hypothetical protein	2.0 ± 0.27	701 ± 78	1415 ± 105
DMC0205	panDhc_2214	Cornell	hypothetical protein	2.0 ± 0.33	4877 ± 114	9847 ± 1614
DMC2382	KB1_0001	Pinelles	transposase	2.0 ± 0.16	3997 ± 304	8009 ± 195
DMC0978	panDhc_3819	Unassigned	hypothetical protein	0.49 ± 0.074	3421 ± 164	1691 ± 239
DMC0730	KB1_0753	Pinelles	ribosomal protein	0.48 ± 0.059	16743 ± 1969	7999 ± 317
DMC0053	panDhc_1071	Unassigned	alcohol dehydrogenase	0.47 ± 0.002	1242 ± 0	587 ± 3
DMC1373	panDhc_1766	Pinelles	SAM-dependent methyltransferase	0.47 ± 0.064	1493 ± 201	706 ± 14
DMC2494	KB1_1093	Pinelles	hypothetical protein	0.47 ± 0.15	1002 ± 6	472 ± 152
DMC0710	panDhc_1493	Unassigned	pyruvic-ferredoxin oxidoreductase	0.47 ± 0.14	4714 ± 241	2216 ± 635
DMC1535	panDhc_1250_RC	Unassigned	ApbE/NosX family	0.46 ± 0.12	1591 ± 193	728 ± 169
DMC0059	KB1_1605	Pinelles	cysteinyl-tRNA synthetase	0.46 ± 0.072	1662 ± 231	759 ± 56
DMC0951	panDhc_277	Unassigned	translation initiation	0.45 ± 0.047	4109 ± 215	1837 ± 169
DMC1088	panDhc_503	Unassigned	glutamate synthase	0.42 ± 0.047	12878 ± 1453	5386 ± 6
DMC0917	panDhc_241	Pinelles	thiamine pyrophosphate	0.40 ± 0.033	1087 ± 89	437 ± 4
DMC1373	panDhc_1786	Unassigned	methyltransferase UbiE/COQ5	0.39 ± 0.046	5648 ± 315	2228 ± 226
DMC1718	GT_699218	Pinelles	hypothetical protein	0.39 ± 0.075	1902 ± 192	749 ± 122
DMC1718	gi147669416	Unassigned	hypothetical protein	0.39 ± 0.051	1940 ± 140	760 ± 83
DMC1718	KB1_0867	Pinelles	hypothetical protein	0.39 ± 0.039	1951 ± 160	763 ± 42
DMC0461	panDhc_179	Unassigned	translation elongation	0.39 ± 0.046	5480 ± 352	2133 ± 213
DMC0730	KB1_0754	Pinelles	translation initiation	0.38 ± 0.12	15567 ± 2278	5942 ± 1587
DMC0731	KB1_0754	Pinelles	translation initiation	0.38 ± 0.12	15567 ± 2278	5942 ± 1587
DMC0940	panDhc_1340_RC	Unassigned	aspartate-semialdehyde dehydrogenase	0.38 ± 0.080	1363 ± 95	519 ± 103
DMC0732	panDhc_304	Unassigned	threonyl-tRNA synthetase	0.37 ± 0.11	2726 ± 426	1007 ± 249
DMC0485	panDhc_2050	Unassigned	methionine aminopeptidase	0.37 ± 0.079	6587 ± 1129	2410 ± 317
DMC0465	gi147669098	Unassigned	ribosomal protein	0.36 ± 0.053	34648 ± 845	12600 ± 1827
DMC0964	GT_c801167	Pinelles	ribosomal protein	0.36 ± 0.073	7823 ± 75	2809 ± 571
DMC0964	gi147669529	Unassigned	ribosomal protein	0.36 ± 0.070	7349 ± 294	2611 ± 504
DMC0542	panDhc_1292	Unassigned	putative deoxyguanosinetriphosphate	0.35 ± 0.17	3772 ± 340	1333 ± 611
DMC1619	panDhc_1303	Pinelles	putative threonine	0.35 ± 0.025	1456 ± 28	506 ± 36
DMC0465	KB1_0521	Pinelles	ribosomal protein	0.35 ± 0.040	35740 ± 3639	12409 ± 684
DMC0341	KB1_0396	Pinelles	GatB domain	0.34 ± 0.10	6930 ± 289	2356 ± 718
DMC0490	KB1_0545	Pinelles	30S ribosomal protein S4	0.34 ± 0.055	9275 ± 217	3137 ± 502
DMC0341	VS289	Unassigned	GatB domain	0.33 ± 0.11	6741 ± 349	2246 ± 722
DMC1535	KB1_0113	Pinelles	ApbE/NosX family	0.33 ± 0.11	2456 ± 313	807 ± 249
DMC0466	panDhc_1823_RC	Unassigned	ribosomal protein L2	0.33 ± 0.083	4436 ± 917	1456 ± 214
DMC0367	panDhc_2935	Unassigned	elongation factor Ts	0.33 ± 0.049	7690 ± 86	2518 ± 376
DMC0812	panDhc_702_RC	Pinelles	adenylosuccinate lyase	0.33 ± 0.17	1447 ± 187	473 ± 232
DMC0467	VS421	Unassigned	ribosomal protein S19	0.32 ± 0.076	7491 ± 701	2407 ± 527
DMC0341	gi147668974	Unassigned	GatB domain	0.32 ± 0.10	7303 ± 448	2323 ± 753
DMC0469	panDhc_1764_RC	Unassigned	ribosomal protein S3	0.32 ± 0.043	13187 ± 1637	4171 ± 235
DMC1353	panDhc_232_RC	Pinelles	chaperone protein	0.31 ± 0.049	2398 ± 372	744 ± 26
DMC1736	panDhc_346	Pinelles	extracellular solute-binding protein family	0.31 ± 0.047	1249 ± 63	387 ± 55
DMC0490	gi147669123	Unassigned	30S ribosomal	0.30 ± 0.033	9484 ± 393	2845 ± 285
DMC0388	panDhc_1968_RC	Unassigned	putative ubiquinone/menaquinone	0.30 ± 0.14	2284 ± 243	680 ± 318
DMC0374	panDhc_1063_RC	Cornell	inositol-5-monophosphate dehydrogenase	0.30 ± 0.057	2541 ± 412	750 ± 80
DMC0953	panDhc_558_RC	Unassigned	transcription termination	0.29 ± 0.15	1606 ± 259	473 ± 222
DMC1872	panDhc_29_RC	Pinelles	sensor histidine	0.29 ± 0.054	1501 ± 262	431 ± 31
DMC0368	VS321	Unassigned	ribosomal protein S2	0.28 ± 0.086	15814 ± 1085	4434 ± 1324
DMC0469	panDhc_1764	Pinelles	ribosomal protein S3	0.27 ± 0.048	5935 ± 334	1612 ± 271
DMC0961	gi147669526	Unassigned	ribosomal protein L11	0.27 ± 0.086	18178 ± 141	4826 ± 1562
DMC0443	panDhc_2678	Pinelles	putative fumarate hydratase beta	0.27 ± 0.019	4048 ± 282	1074 ± 25
DMC1002	panDhc_3962	Unassigned	protein of unknown function	0.26 ± 0.175	2571 ± 262	679 ± 445
DMC1731	panDhc_3962	Unassigned	protein of unknown function	0.26 ± 0.175	2571 ± 262	679 ± 445
DMC0125	panDhc_3396_RC	Pinelles	response regulator receiver protein	0.26 ± 0.082	2266 ± 535	596 ± 121
DMC0489	panDhc_3332	Unassigned	ribosomal protein S11	0.25 ± 0.051	9284 ± 1753	2357 ± 161
DMC1227	panDhc_350_RC	Unassigned	arginyl-tRNA synthetase	0.25 ± 0.11	2980 ± 393	755 ± 318

Table A5.4. (Continued)

DMC#	Probe ID	Strain Type	Description	Ratio of 48 Hour to 6 Hour Post Oxygen Stress	Average Intensity of 48 Hour Oxygen Stress (pfu)	Average Intensity of 6 Hour Oxygen Stress (pfu)
DMC0465	VS419	Unassigned	ribosomal protein L23	0.25 ± 0.077	24479 ± 5152	6124 ± 1384
DMC0729	VS656	Unassigned	ribosomal protein L20	0.25 ± 0.064	4319 ± 815	1079 ± 189
DMC1093	panDhc_3196_RC	Unassigned	iron-sulfur cluster domain protein	0.25 ± 0.011	4708 ± 62	1160 ± 48
DMC0368	gi147669004	Unassigned	ribosomal protein S2	0.24 ± 0.060	3526 ± 494	859 ± 175
DMC0459	gi57234696	Unassigned	ribosomal protein S12	0.24 ± 0.061	11348 ± 1972	2745 ± 505
DMC0459	VS413	Unassigned	ribosomal protein S12	0.23 ± 0.059	11631 ± 1638	2728 ± 568
DMC1325	KB1_1355	Pinelles	hypothetical protein sp.	0.23 ± 0.10	3463 ± 468	809 ± 336
DMC0695	panDhc_714	Unassigned	trigger factor	0.22 ± 0.075	2478 ± 181	551 ± 183
DMC0695	KB1_0718	Pinelles	trigger factor	0.22 ± 0.091	6676 ± 257	1468 ± 606
DMC1282	KB1_1310	Pinelles	ribosomal protein L27	0.21 ± 0.078	20995 ± 4898	4445 ± 1258
DMC1695	panDhc_1257	Pinelles	Nicotinate-nucleotide phosphoribosyltransferase	0.21 ± 0.054	2198 ± 555	459 ± 29
DMC0489	gi57234753	Unassigned	ribosomal protein S11	0.21 ± 0.082	18965 ± 3357	3957 ± 1395
DMC1282	GT_1011160	Pinelles	ribosomal protein L27	0.20 ± 0.084	22144 ± 5026	4519 ± 1545
DMC1282	gi147669776	Unassigned	ribosomal protein L27	0.20 ± 0.083	22243 ± 4876	4407 ± 1560
DMC1149	panDhc_2023	Pinelles	hypothetical periplasmic protein	0.20 ± 0.10	4330 ± 100	854 ± 433
DMC0482	gi147669115	Unassigned	ribosomal protein L15	0.20 ± 0.076	13129 ± 2571	2584 ± 856
DMC1722	panDhc_2312	Pinelles	phosphoribosyltransferase	0.20 ± 0.046	1511 ± 348	297 ± 16
DMC0482	KB1_0537	Pinelles	ribosomal protein L15	0.20 ± 0.068	12254 ± 2518	2402 ± 666
DMC0390	panDhc_1170_RC	Pinelles	3-dehydroquinate synthase	0.20 ± 0.016	4067 ± 110	797 ± 62
DMC0128	gi147668886	Pinelles	hypothetical protein	0.19 ± 0.019	2670 ± 122	513 ± 45
DMC0461	panDhc_180_RC	Unassigned	translation elongation factor G	0.19 ± 0.017	1912 ± 166	364 ± 2
DMC0732	panDhc_304_RC	Unassigned	threonyl-tRNA synthetase	0.19 ± 0.050	3929 ± 1019	748 ± 39
DMC0488	VS441	Unassigned	30S ribosomal protein S13	0.19 ± 0.060	11182 ± 376	2100 ± 664
DMC0469	panDhc_1762	Unassigned	ribosomal protein S3	0.18 ± 0.036	7408 ± 1098	1363 ± 170
DMC1260	panDhc_3290_RC	Pinelles	fasciclin domain	0.18 ± 0.051	1153 ± 259	208 ± 36
DMC0128	KB1_0276	Pinelles	hypothetical protein	0.18 ± 0.020	2426 ± 219	436 ± 28
DMC0328	KB1_0383	Pinelles	putative DNA-binding	0.17 ± 0.061	1378 ± 181	241 ± 78
DMC1091	panDhc_761_RC	Unassigned	pyridine nucleotide-disulfide oxidoreductase family	0.16 ± 0.043	4617 ± 929	737 ± 131
DMC0464	panDhc_2466	Unassigned	ribosomal protein L4/L1e	0.16 ± 0.062	6319 ± 1242	995 ± 338
DMC0460	KB1_0516	Pinelles	30S ribosomal protein S7	0.16 ± 0.070	12757 ± 3153	1999 ± 740
DMC0328	GT_c268694	Pinelles	putative DNA-binding	0.15 ± 0.070	907 ± 174	139 ± 58
DMC0473	gi57234668	Unassigned	ribosomal protein L14	0.15 ± 0.047	20337 ± 5516	3017 ± 490
DMC1228	panDhc_3885	Pinelles	hypothetical protein	0.14 ± 0.040	2234 ± 187	302 ± 86
DMC0478	KB1_0533	Pinelles	50S ribosomal protein L6	0.14 ± 0.050	13690 ± 2376	1852 ± 600
DMC0477	VS430	Unassigned	ribosomal protein S8	0.12 ± 0.055	3652 ± 184	455 ± 198
DMC0959	VS863	Unassigned	ribosomal protein L10	0.12 ± 0.028	13795 ± 1276	1694 ± 348
DMC0471	gi147669104	Unassigned	ribosomal protein L29	0.12 ± 0.027	9127 ± 1458	1099 ± 173
DMC0471	GT_395950	Pinelles	ribosomal protein L29	0.12 ± 0.028	9136 ± 1529	1090 ± 185
DMC0467	panDhc_3673_RC	Unassigned	ribosomal protein S19	0.12 ± 0.035	9682 ± 2169	1153 ± 215
DMC0477	GT_397900	Pinelles	ribosomal protein S8	0.12 ± 0.053	3705 ± 235	439 ± 196
DMC0471	KB1_0527	Pinelles	ribosomal protein L29	0.12 ± 0.034	9090 ± 1757	1075 ± 227
DMC1372	KB1_1410	Pinelles	hypothetical protein	0.12 ± 0.036	1847 ± 188	218 ± 62
DMC1372	gi147669866	Pinelles	hypothetical protein	0.11 ± 0.029	1757 ± 286	201 ± 38
DMC0958	KB1_0978	Pinelles	ribosomal protein L7	0.11 ± 0.032	15254 ± 3113	1721 ± 339
DMC1372	GT_1079521	Pinelles	hypothetical protein	0.11 ± 0.030	1754 ± 357	195 ± 34
DMC0477	KB1_0532	Pinelles	ribosomal protein S8	0.11 ± 0.054	3928 ± 45	427 ± 211
DMC0477	gi147669110	Unassigned	ribosomal protein S8	0.11 ± 0.051	3775 ± 40	407 ± 192
DMC0920	GT_c760143-759943	Pinelles	hypothetical protein	0.10 ± 0.019	2272 ± 117	230 ± 41
DMC0920	KB1_0937	Pinelles	hypothetical protein	0.094 ± 0.018	2194 ± 267	207 ± 31
DMC0922	gi147669479	Pinelles	hypothetical protein	0.091 ± 0.042	1140 ± 211	104 ± 43
DMC0922	KB1_0939	Pinelles	hypothetical protein	0.085 ± 0.044	1093 ± 228	93 ± 44
DMC0958	gi147669523	Unassigned	ribosomal protein L7	0.075 ± 0.022	11044 ± 1522	827 ± 211
DMC1695	KB1_0699	Pinelles	Nicotinate-nucleotide phosphoribosyltransferase	0.057 ± 0.014	3547 ± 835	201 ± 18

Table A5.5. Differentially detected KB-1 proteins for the 48 hours after oxygen addition compared to the 6 hours after oxygen addition

DMC#	KB1#	Description	Ratio of 48 Hours Post Oxygen to 6 Hours Post Oxygen
DMC1373	KB1_1411	methyltransferase, UbiE/COQ5 family	3.65 ± 2.22
DMC1017	KB1_1103	hypothetical protein	2.24 ± 0.41
DMC1873	KB1_0033	transcriptional regulator, MarR family	2.14 ± 0.21
DMC0392	KB1_0446	methyltransferase, UbiE/COQ5 family	1.84 ± 0.42
DMC0707	KB1_0730	pyruvic-ferredoxin oxidoreductase, gamma subunit	1.54 ± 0.01
DMC1183	KB1_1199	hypothetical protein	1.48 ± 0.13
DMC0734	KB1_0757	hypothetical protein	1.42 ± 0.11
DMC0535	KB1_0591	excinuclease ABC, A subunit	1.36 ± 0.09
DMC0466	KB1_0522	50S ribosomal protein L2	1.35 ± 0.11
DMC0944	KB1_0964	adenylosuccinate synthetase	1.35 ± 0.04
DMC0789	KB1_0830	sufB/sufD domain protein	1.33 ± 0.11
DMC0036	KB1_0194	hypothetical protein	1.33 ± 0.12
DMC0965	KB1_0984	translation elongation factor Tu	1.24 ± 0.09
DMC0703	KB1_0726	DNA topoisomerase I	1.22 ± 0.06
DMC0695	KB1_0718	trigger factor	1.21 ± 0.01
DMC0938	KB1_0958	polyribonucleotide nucleotidyltransferase	1.18 ± 0.06
DMC0577	KB1_0635	glyceraldehyde-3-phosphate dehydrogenase, type I	1.16 ± 0.04
DMC0820	KB1_0861	SPFH domain/band 7 family domain protein	1.15 ± 0.03
DMC0118	KB1_0265	pyridine nucleotide-disulphide oxidoreductase family protein	1.15 ± 0.04
DMC0527	KB1_0582	ATP-binding protein, DnaC family	1.14 ± 0.03
DMC0502	KB1_0557	S-adenosyl-L-homocysteine hydrolase	1.14 ± 0.04
DMC0960	KB1_0980	50S ribosomal protein L1	1.09 ± 0.01
DMC1381	KB1_1419	co-chaperonin GroEL	1.07 ± 0.02
DMC0719	KB1_0743	aspartate aminotransferase	1.06 ± 0.01
DMC1540	KB1_0118	twin-arginine translocation protein TatB, putative	0.93 ± 0.02
DMC0913	KB1_0930	lipoprotein, putative	0.82 ± 0.03
DMC0587	KB1_0645	soluble hydrogenase, tritium exchange subunit	0.82 ± 0.02
DMC0618	KB1_0674	cation ABC transporter, periplasmc-binding protein	0.80 ± 0.06
DMC1535	KB1_0113	ApbE/NosX family protein	0.38 ± 0.06
DMC2072	KB1_1502	reductive dehalogenase	0.36 ± 0.03
DMC0344	KB1_0400	hypothetical protein	0
DMC0460	KB1_0516	30S ribosomal protein S7	0
DMC0892	KB1_0909	twitching mobility protein	0

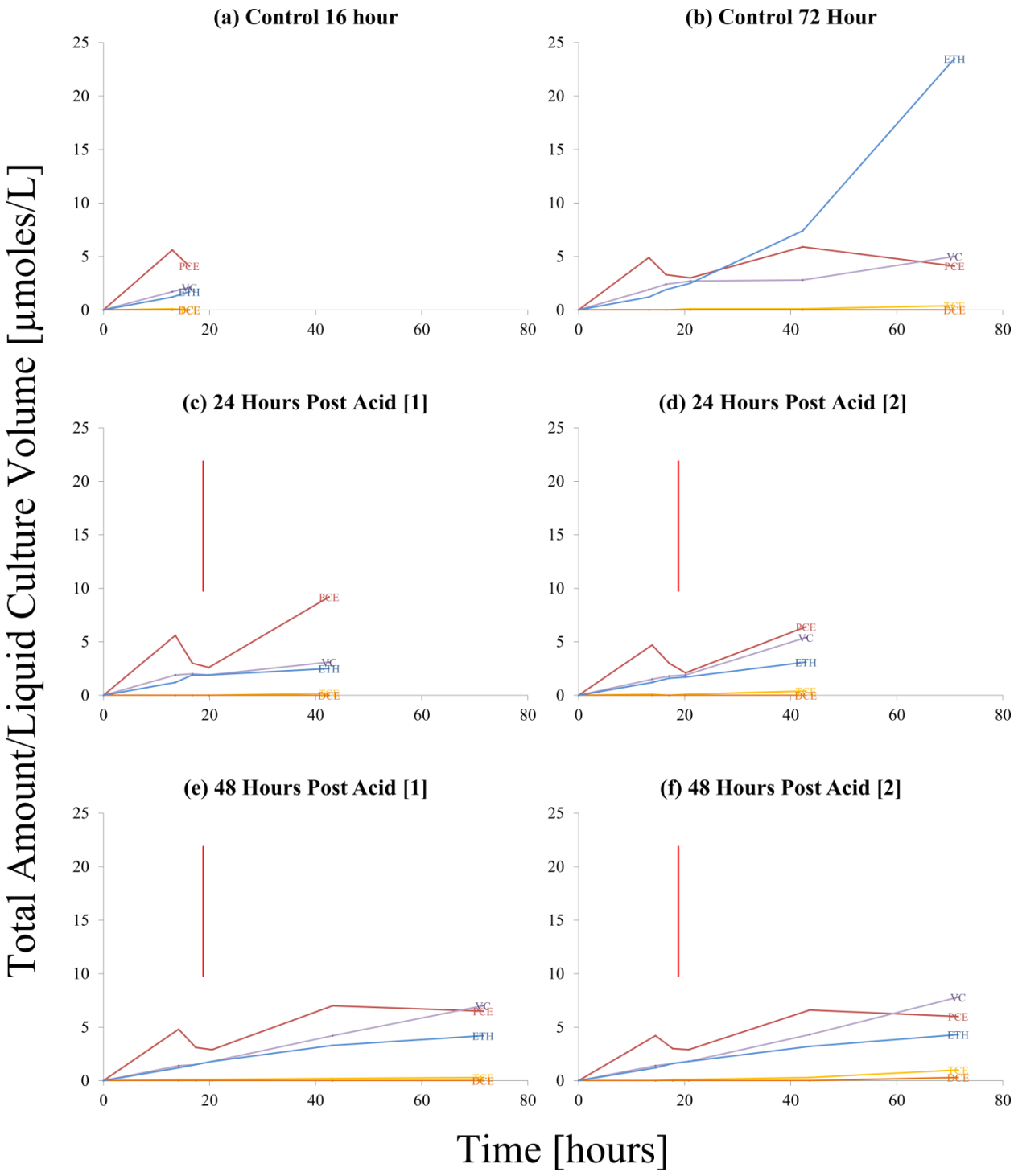

Figure A5.4. Dechlorination profiles showing nominal concentrations of chloroethenes (PCE, TCE, DCE, VC) and ethene (ETH) in D2 continuously fed 0.5 µM/hr PCE cultures sampled at 16 and 72 hours as a control (a,b); 24 hours post acid (HCl) addition (c,d), and 48 hour post acid (HCl) addition (e,f). Data labels indicate the specific metabolites. The red bar denotes the time of HCl addition and lowering of the pH to 5.3 (24 hours past the start of the experiment).

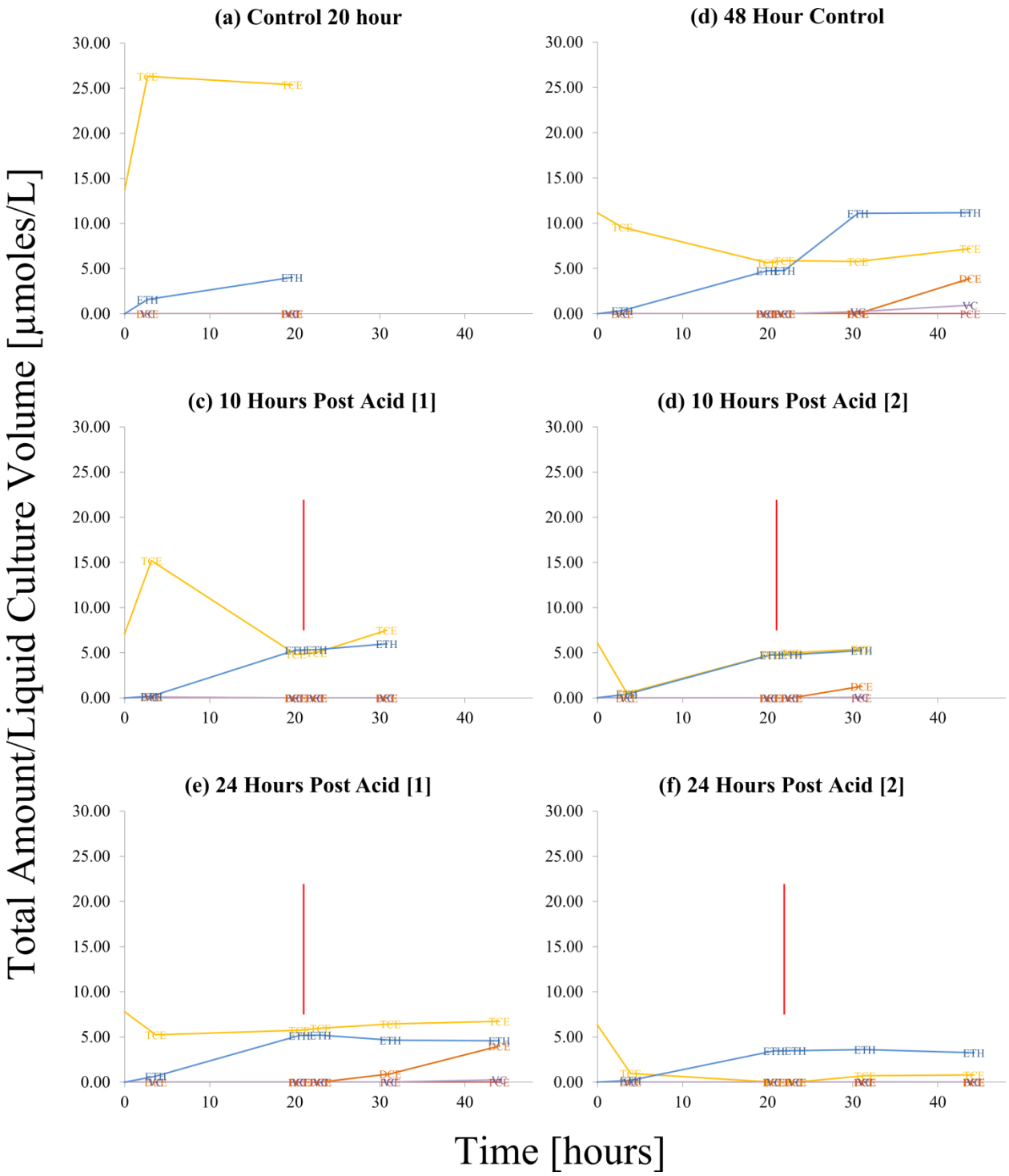

Figure A5.5. Dechlorination profiles showing nominal concentrations of chloroethenes (TCE, DCE, VC) and ethene (ETH) in KB-1™ continuously fed 0.5 µM/hr TCE cultures sampled at 10 hours as a control (a); 10 hours post acid (HCl) addition (b,c), 48 hours/24 hours post as a control (d), and 48 hour post acid (HCl) addition. Data labels indicate the specific metabolites. The red bar denotes the time of HCl addition.

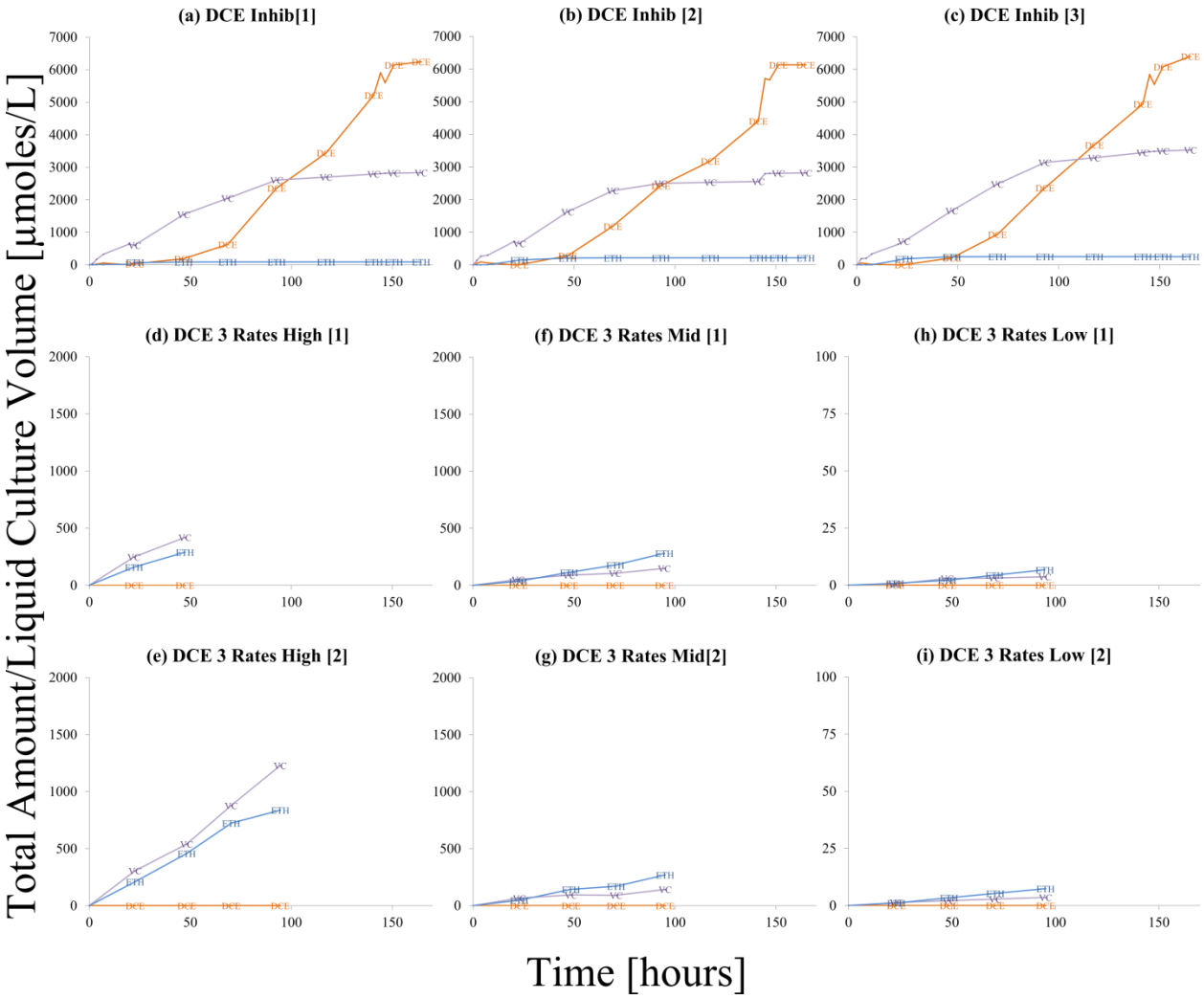

Figure A5.6. Dechlorination profiles showing nominal concentrations of chloroethenes (DCE, VC) and ethene (ETH) in D2 fed DCE cultures for high rates with inhibition (a,b,c), high-rate repeat (d,e), mid-rate (f,g), and low rate (h,i). Data labels indicate the specific metabolites. The y-axis data range was adjusted to allow visualization of the data.

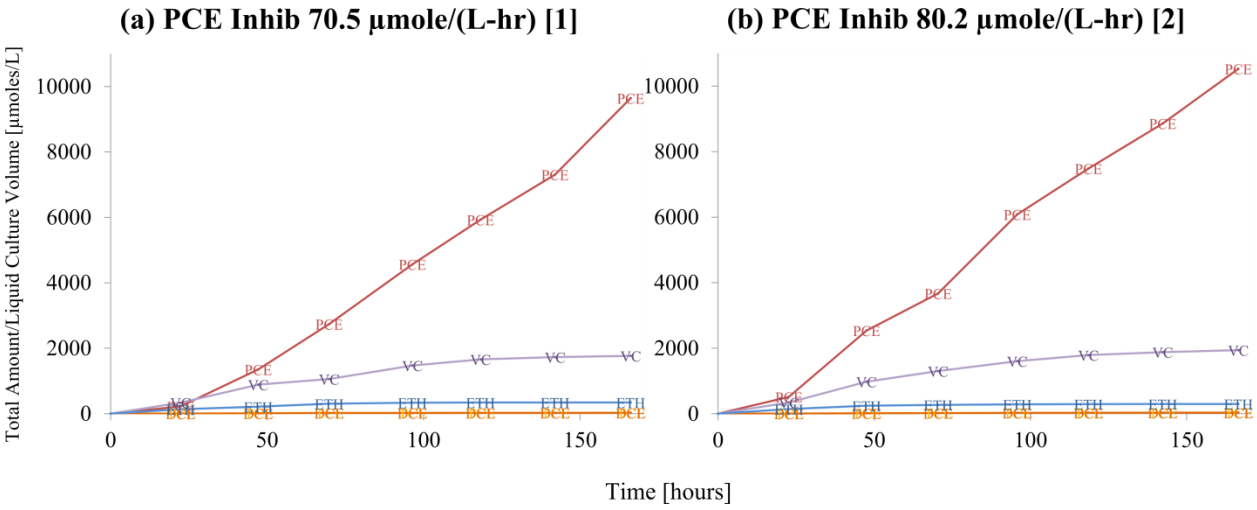

Figure A5.7. The chloroethenes (PCE, TCE, DCE, VC) and ethene (ETH) total amount detected normalized to liquid culture volume for D2 cultures continuously fed PCE at high rates displaying inhibition (a,b). Data labels indicate the specific metabolites.

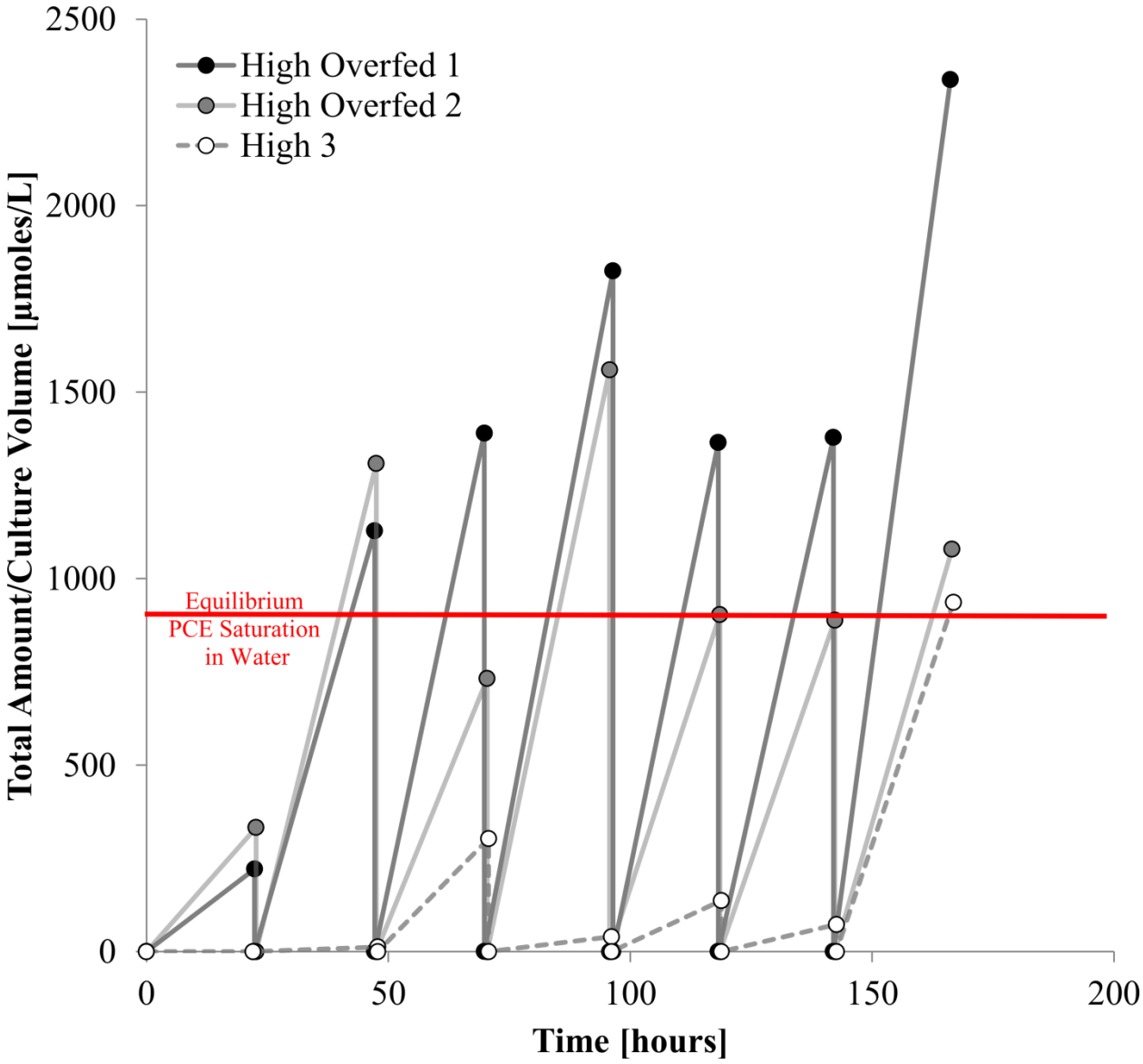

Figure A5.8. The non-cumulative PCE concentration for the D2 PCE Inhibited cultures displaying the impact of purges on the state of saturation.

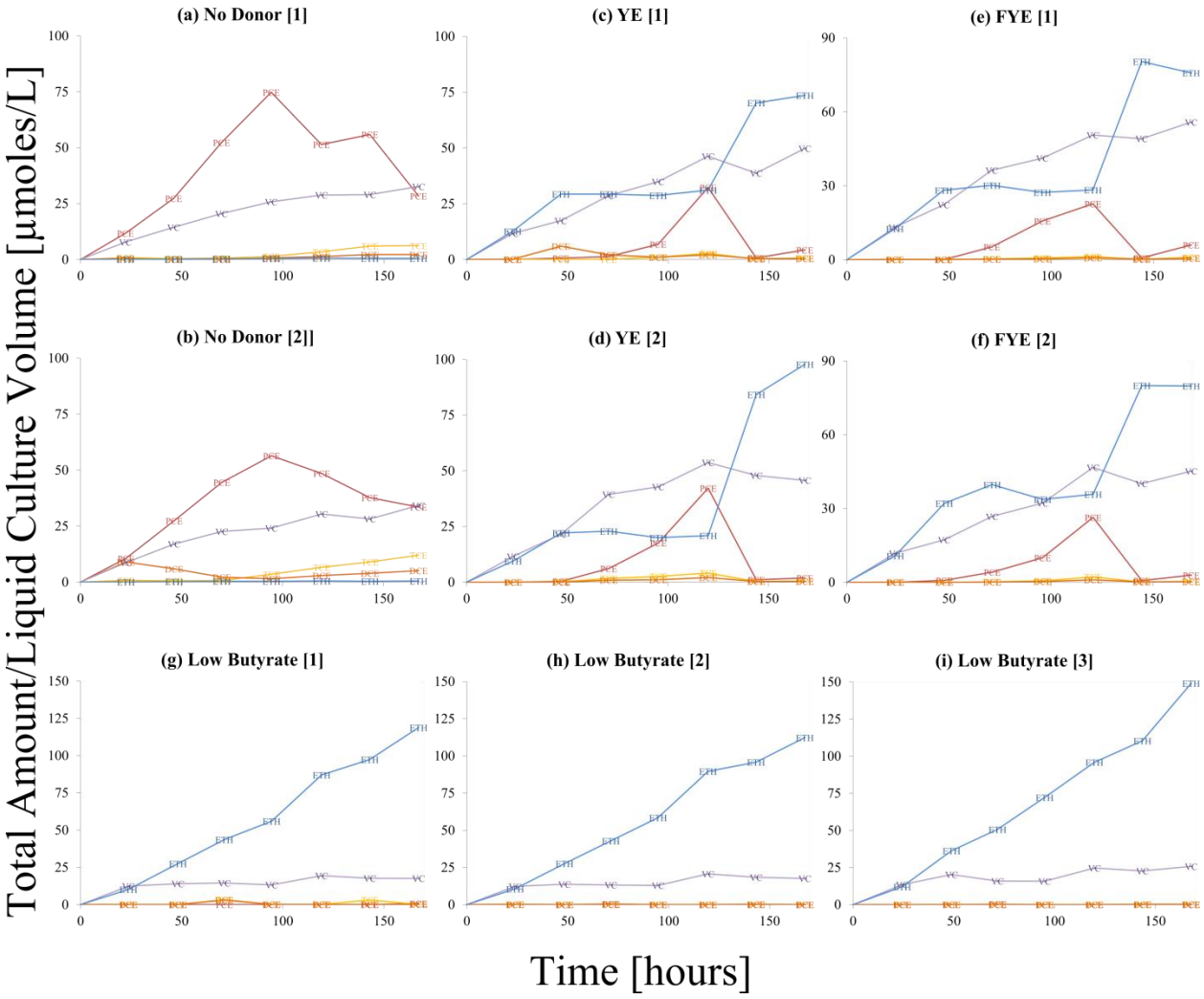

Figure A5.9. The chloroethenes (PCE, TCE, DCE, VC) and ethene (ETH) total amount detected normalized to liquid culture volume for the continuously fed PCE cultures with no electron donor (a,b), yeast extract (YE; c,d), fermented yeast extract (FYE; e,f), and butyrate (g-i). Data labels indicate the specific metabolites. The y-axis values were adjusted for the Low Butyrate cultures to visualize the data.

Table A5.6. Differentially detected transcripts for the no donor cultures

DMC#	DET#	Description	Ratio of No Donor to YE, FYE, and Butyrate Donors	No Donor Average Normalized Intensity (pfu)
DMC1365	DET1412	HspR protein, putative	12 ± 7.16	12753 ± 3291
DMC1364	DET1411	DnaJ family protein	12 ± 9.45	41936 ± 3232
DMC1507	DET1565	iron-sulfur cluster-binding protein	5.4 ± 2.92	475 ± 73
DMC1510	DET1568	hypothetical protein	4.2 ± 1.60	12178 ± 1236
DMC1386	DET1433	hydrogenase assembly chaperone	3.4 ± 2.13	1158 ± 77
DMC0125	DET0130	response regulator	0.24 ± 0.080	636 ± 63
DMC1095	DET1135	cysteine synthase A	0.23 ± 0.081	429 ± 26
DMC0964	DET0996	ribosomal protein L33	0.18 ± 0.066	372 ± 34
DMC1011	DET1051	hypothetical protein	0.10 ± 0.052	844 ± 83
DMC0182	DET0189	methyltransferase, putative	0.10 ± 0.032	127 ± 10
DMC1264	DET1307	hypothetical protein	0.086 ± 0.064	948 ± 545
DMC1396	DET1448	hypothetical protein	0.074 ± 0.033	1206 ± 158
DMC1207	DET1250	hypothetical protein	0.054 ± 0.045	84 ± 65